MICROALGAL-BACTERIAL FLOCS AND EXTRACELLULAR POLYMERIC SUBSTANCES FOR OPTIMUM FUNCTION OF INTEGRATED ALGAL POND SYSTEMS

A thesis submitted in fulfilment of the
requirements for the degree of

DOCTOR OF PHILOSOPHY
in
(Environmental Biotechnology)

at

RHODES UNIVERSITY

By

TAOBAT ADEKILEKUN JIMOH

February 2021

Abstract

Despite the dire state of sanitation infrastructures, water scarcity, and the dwindling reserve of natural resources due to ever-increasing population growth, implementation of a suitable technology that can provide a solution to all these issues continues to be ignored. The integrated algal pond system (IAPS) is a wastewater treatment technology that combines the processes of anaerobic digestion and photosynthetic oxygenation to achieve wastewater treatment and facilitate the recovery of treated water and resources in the form of biogas and microalgal-bacterial biomass. The natural process of bioflocculation through microalgal-bacterial mutualism and production of extracellular polymeric substances (EPS) in high rate algal oxidation ponds (HRAOPs) of an IAPS increases efficiency of wastewater treatment and potentially enhances harvestability and biomass recovery, which could contribute significantly to the successful establishment of a biorefinery. Using a 500 PE pilot-scale IAPS supplied domestic sewage coupled with laboratory experiments, this study investigated the importance and function of *in situ* EPS production and MaB-floc formation in HRAOP. A metagenomic study revealed the biological components of the biomass or mixed liquor suspended solids (MLSS) produced in HRAOP and showed that the suspended biomass is composed largely of eukaryotes that were dominated by the colonial microalgae *Pseudopediastrum* sp. and *Desmodesmus* sp., and a diverse range of prokaryotes including bacteria and cyanobacteria. Dominance, within the bacterial population, by a sulphur-oxidizing bacterium, *Thiothrix* which comprised up to 80% of the prokaryotes, coincided with a period of poor flocculation and was therefore rationalized to have contributed to bulking and poor biomass settleability. Otherwise, good flocs were formed in the MLSS with settleability up to 95% and, within 1 h. The formation of MaB-flocs appeared to be dependent on EPS concentration of the mixed liquor due to the observed positive correlation between soluble EPS (S-EPS), biomass concentration, and settleability. The contribution and role of MLSS components towards the formation and sustenance of MaB-flocs were further demonstrated in laboratory experiments using pure strains of microalgae, cyanobacteria, and bacteria. Results showed that pure cultures of dominant microalgae in MLSS, *Pseudopediastrum* sp. and *Desmodesmus* sp. achieved a rapid 92 and 75% settleability within 3 h. A self-flocculating filamentous cyanobacterium, *Leptolyngbya* strain ECCN 20BG was isolated, characterized, and shown to achieve 99% settleability within 5 min by forming large tightly aggregated flocs. In further experiments, this strain was found to improve the settleability of MLSS by an average of 20%. Bacterial strains identified as *Bacillus* strain ECCN 40b, *Bacillus* strain ECCN 41b, *Planococcus* strain ECCN

45b, and *Exiguobacterium* strain ECCN 46b were also observed to produce sticky EPS-like materials in pure cultures that could also contribute to the aggregation of cells in a mixed environment. Given these results, various factors and/or mechanisms that might enhance microbial aggregation and biomass recovery from HRAOP MLSS were identified in this study and include; (1) dominance by larger colonial microalgae prevents disintegration of MaB-flocs and enhances recovery of biomass from MLSS by gravity sedimentation, (2) presence of filamentous cyanobacteria species that can self-flocculate to form an interwoven network of filaments may play an important role in the structural stability and settleability of MaB-flocs in MLSS, and (3) production of EPS to form the matrix or scaffold whereon all microbial components aggregate to develop a microenvironment. Indeed, all forms of EPS, except for that produced by *Bacillus* strain ECCN 41b, showed bioflocculating property and were able to serve as flocculants for the recovery of *Chlorella*, an alga known for its poor settleability. A combination of biochemical analyses and FTIR spectroscopy revealed the importance of carbohydrate enrichment of these biopolymers. Carbohydrate concentration in all forms of EPS was between 12 and 41% suggesting that production of these compounds by microbes within the MLSS contributed to MaB-floc formation. EPS extracted from bulk MLSS and EPS produced by *Bacillus* strains possessed some surface-active properties that were comparable to Triton X-100, indicating potential application in bioremediation and recovery of oil from contaminated soil and water. In particular, EPS generated from *Bacillus* strain ECCN 41b displayed relatively distinct properties including the quantity produced (> 500 mg/L), increased viscosity, inability to flocculate microalgal cells, a rhamnolipid content of 32%, and a higher surface-activity. Based on these results, *Bacillus* strain ECCN 41b was rationalized to produce anionic EPS with potential application in metal or oil recovery. In addition to EPS production, the bacteria *Planococcus* strain ECCN 45b and *Exiguobacterium* strain ECCN 46b appeared pigmented. Based on partial characterization using UV/Vis spectrophotometry, thin-layer chromatography, FTIR, and NMR, the pigments produced by these two strains appeared to be identical and were tentatively identified as ketocarotenoids. This study successfully demonstrated the importance of EPS production and formation of MaB-flocs in the MLSS from HRAOP of an IAPS treating domestic sewage. It is evident that increased settleability of the biomass does contribute to the reported efficiency of wastewater treatment by IAPS and would reduce both total suspended solids (TSS) and chemical oxygen demand (COD). In addition, demonstration that this biomass contains products of value such as carotenoids and EPS with potential for commercial use strengthens the idea of using IAPS as a platform technology for innovation of the wastewater treatment process to a biorefinery.

Acknowledgements

I dedicate this thesis to Almighty Allah for seeing me through safely and making this study a reality.

My foremost and heartfelt appreciation goes to my supervisor, Prof. A. K. Cowan for his timely feedback and constructive criticism throughout the course of this study. Thank you, Prof., for the guidance, welfare, and academic support which facilitated the completion of this study. Time spent under your supervision has been invaluable and has made me a better scientist.

I am grateful for the funding provided by Water Research Commission (WRC) and Institute for Environmental Biotechnology (EBRU), without which this research would not have been possible. I also acknowledge the financial support from Rhodes University for the Postgraduate Scholarship awarded me towards the successful completion of this study.

To my better half and colleague, Olajide Keshinro, thank you for being my pillar throughout the period of study. Your invaluable contribution, affection and unwavering support were very much appreciated. I cherished our time as laboratory partners, helping with the herculean tasks contributed immensely to the successful completion of this study. I love you so much.

I extend my appreciation to EBRU staff, Xolisa Maganca, Richard Laubscher, Gila Eustace and Dr Yinka Titilawo, for their assistance and support, without which the completion of this study would have been very difficult. Thank you, Sis Xoli, for always ready to help with administrative issues. Thank you, Dr Yinka, for assisting with the molecular studies. I would also like to thank my colleagues, Wiya Leon Masudi, Linda Sibelo and Anele Dube for their contributions and making my PhD journey at EBRU a memorable one. I cannot forget to appreciate the technical assistance rendered by Mr Andile Magaba and Mr Norman Singapi when needed.

Special gratitude to my parents, Dr M. A. Jimoh and Mrs G. A. Jimoh for their, advice, prayers and encouraging words that kept me going even when things seem difficult. I also appreciate the words of encouragement and prayers from my in-laws, Keshinros and Har-Yusuphs, during the period of this study. Indeed, I have found a new and worthy family. I am also grateful for the regular moral support and concern from my siblings, Sis. Asiata, Sis. Basheerat, Kasirat, Taoheed and Sodiq, thanks for your sense of belonging at crucial times.

Table of Contents

List of Figures

List of Tables

List of Abbreviations

ACE	Abundance-based coverage estimator
AFP	Advanced facultative pond
AIWPS	Advanced integrated wastewater pond system
ANOVA	Analysis of variance
ASP	Algal settling pond
ATR	Attenuated total reflectance
B-EPS	Bound-Extracellular polymeric substances
BLAST	Basic local alignment search tool
BOD	Biological oxygen demand
BSA	Bovine serum albumin
CCM	CO_2 concentration mechanism
CFU	Colony forming unit
CO_2	Carbon dioxide
COD	Chemical oxygen demand
CRF	Controlled rock filtration
DAF	Dissolved air floatation
DB	Drying bed
DNA	Deoxyribonucleic acid
DO	Dissolved oxygen
DWA	Department of Water Affairs
EBRU	Institute for Environmental Biotechnology Rhodes University
ECCN	EBRU culture collection number
EPS	Extracellular polymeric substance
F/M	Food to microorganism ratio
FTIR	Fourier transformed infrared spectroscopy

HRAOP	High rate algal oxidation pond
HRT	Hydraulic retention time
IAPS	Integrated algal pond system
IPD	In-pond digester
LB	Luria broth
LCA	Life cycle assessment
MABA	Microalgal-bacterial aggregates
MaB-flocs	Microalgal-bacterial flocs
MIC	Minimum inhibitory concentration
MJ	Mega Joule
MLSS	Mixed liquor suspended solids
MP	Maturation pond
NCBI	National centre for biotechnology information
NGS	Next generation sequencing
NH_4^+-N	Ammonium nitrogen
NMR	Nuclear magnetic resonance
NO_3-N	Nitrate nitrogen
OTU	Operational taxonomic unit
PBS	Phosphate buffered saline
PE	Person equivalent
PFP	Primary facultative pond
PO_4^{-3}-P	Ortho-phosphate phosphorus
QS	Quorum sensing
RAB	Revolving algal biofilm
R_f	Retention factor
RT	Room temperature

Rubisco	Ribulose bisphosphate carboxylase oxygenase
SAIAB	South African Institute for Aquatic Biodiversity
SAURAN	Southern African Universities Radiometric Network
SE	Standard error
SEM	Scanning electron microscopy
S-EPS	Soluble-Extracellular polymeric substances
SPSS	Statistical package for the social sciences
SSF	Slow sand filtration
TLC	Thin layer chromatography
TSS	Total suspended solids
v/v	Volume/volume
v/v/v	Volume/volume/volume
VS	Volatile solids
w/v	Weight/volume
WSP	Waste stabilization pond
WRC	Water Research Commission
WWTW	Wastewater treatment works

Chapter 1: General introduction

1.1 Introduction

The search for an efficient, simple, cost-effective, and sustainable technology that provides a good quality effluent resulted in the development of algal pond technology for wastewater treatment (Gutzeit *et al*., 2005; Mambo *et al*., 2014a). The integrated algal pond system (IAPS) is a derivative of the advanced integrated wastewater pond system (AIWPS®) developed decades ago (Oswald *et al*., 1957). The technology relies on the combined activity of anaerobic fermentation, photosynthetic oxygenation by algae, and biological oxidation by bacteria to passively remediate wastewater. These combined activities result in the reclamation of treated water for recycle and reuse, and the production of methane-rich biogas and biomass as additional by-products (Cowan *et al*., 2016; Laubscher and Cowan, 2020). Apart from domestic wastewater treatment, IAPS has been used for remediation of acid mine decant, and piggery, dairy, and tannery effluents (Fallowfield and Garrett, 1985; Rose *et al*., 1996; Rose *et al*., 1998; Craggs *et al*., 2003a). More recently, many studies have also confirmed the use of this technology in the treatment of domestic, industrial, and agricultural wastes (Van Den Hende *et al*., 2014a and 2016b; Arashiro *et al*., 2019; Pham *et al*., 2020; Chambonniere *et al*., 2020).

IAPS as a wastewater treatment concept technology was proposed in the 1950s, and more than four decades later, a design was finalized for deployment of the technology in South Africa which occurred in late 1994 (Rose *et al*., 2007). Even so, the technology has yet to be implemented in a commercial setting in South Africa. Among the major limitations which have been highlighted include residual chemical oxygen demand (COD), and total suspended solids (TSS) in the final effluent (Meiring and Oellermann, 1995). These shortcomings were considered to be the result of residual microalgae escaping over the weir of the settlers thus affecting the quality of the final treated water (Mambo *et al*., 2014b). Furthermore, algal-based systems such as IAPS are easily influenced by vagaries of weather, changes in environmental and operational conditions, as well as organic loading rates, which usually bring about dynamic shifts in species composition and particularly in the population of microalgae (Sutherland *et al*., 2017). As such, certain conditions may favour the dominance of freely suspended small-sized species and the absence of flocs which would contribute to poor settleability and therefore poor effluent quality (Hu *et al*., 2017; De Godos *et al*., 2011). This is usually so for unicellular microalgae that hardly settle by gravity and consequently result in high TSS in the final effluent (Gutzeit *et al*., 2005; De Godos *et al*., 2011; Hu *et al*., 2017; Arcila and Buitrón, 2017).

One of the major successes of a wastewater treatment system is the ability of the sludge to show a good settling characteristic (De Schryver *et al*., 2008). Similarly, for IAPS, the operational success of the system depends on good settleability of the generated biomass. This allows for the reuse of the treated water and beneficiation of the resultant biomass. To achieve a cost-effective and sustainable settleability requires flocculation of biomass produced in high rate algal oxidation ponds (HRAOPs) of an IAPS. Flocculation is the aggregation of cells into flocs that can be easily separated from treated water by gravity (Vandamme *et al*., 2013). In an earlier study, research in our laboratory demonstrated the presence of microalgal-bacterial flocs (MaB-flocs) in the HRAOPs of an IAPS (Jimoh and Cowan, 2017). Formation of such flocs is believed to occur either autonomously or assisted by other microbes and may involve the production of extracellular polymeric substances (EPS) (Jimoh and Cowan, 2017; Ummalyma *et al*., 2017).

A MaB-floc is an aggregated, immobilized community of microalgae and bacteria embedded in a self-produced gel-like matrix and suspended in the growth medium or water column. It holds much environmental and biotechnological potential and has been shown as a promising step towards achieving a successful algal biorefinery if cultivated on wastewater (Van Den Hende *et al*., 2015; Zhu, 2015). MaB-flocs have been demonstrated to remove organic matter and nutrients from various laboratory-scale wastewater treatment systems (Gutzeit *et al*., 2005; Van Den Hende *et al*., 2011) and confirmed to be present during IAPS treatment of municipal sewage (Jimoh and Cowan, 2017). In addition, it is thought that this bio-interaction enhances microalgal harvesting and contributes to bioremediation by facilitating degradation of organic pollutants, detoxification of metal-contaminated water, control of harmful algal and bacterial blooms in freshwater, and may serve as feedstock in production of biofuels (Ramanan *et al*., 2016). Moreover, many studies have reported the potential of MaB-floc as a valuable resource in biogas production (Van Den Hende *et al*., 2015, 2016a; Wieczorek *et al*., 2015; Laubscher and Cowan, 2020), as fertilizer (Coppens *et al*., 2016; Laubscher and Cowan, 2020), and as aquaculture feeds (Van Den Hende *et al*., 2014b; Jung *et al*., 2020).

The self-produced gel matrix of MaB-flocs appears to be composed of extracellular molecules secreted by competent cells to provide structural and biochemical support to the surrounding cells. The interaction between these molecules often leads to the formation of gels, hence the name gel matrix (Sutherland, 2001). All living organisms produce gel matrices such as collagen fibres, reticular fibres, and blood plasma in animals; and cellulose and mucilage in plants (Brownlee, 2002; Theocharis *et al*., 2016). At the microbial level, a gel matrix is composed of

water and EPS in which cells are cocooned. In other words, EPS matrices can be regarded as an essential scaffold whereon microbial cells are anchored such that each relates with another in an organized life form (Flemming, 2011). EPS are polymers formed biosynthetically and are responsible for the constructive aggregation of flocs and biofilms (Flemming and Wingender, 2001a & 2001b).

From an environmental and biotechnological point of view, EPS matrices and the resulting floc or biofilm offer great advantages to microbes, especially in water treatment and purification, biomass recovery, and removal of heavy metals. These polymeric substances consist of macromolecules such as carbohydrates, proteins, lipids, nucleic acids; insoluble materials such as sheaths, condensed gel, attached organic materials, and other polymeric compounds that are either secreted by active transport or generated from cell lysis (Sheng *et al*., 2010; More *et al.*, 2014). The components together thus form a well-organized matrix that serves as a protective barrier from adverse environmental conditions such as desiccation, dehydration, and predation while providing intimate cell-cell communication, cell adhesion to surfaces, aggregation of cells, and formation of biofilms (Islam and Lam, 2014; Schlafer and Meyer, 2017). Thus, EPS enables cells to interact in a similar pattern as multicellular organisms whereby they can thrive and adapt to their surroundings, and protect themselves from eradication (Flemming and Wingender, 2001a & 2001b).

Apart from an environmental role in floc and biofilm formation, EPS can be efficiently harvested from the medium for a range of applications as an emulsifier, bioflocculant, biosurfactants, and heavy metal chelator etc. (Van Hille *et al*., 1999; Xiao and Zheng, 2016). Moreover, some polymers are specifically designed by genetic engineering to suit specific purposes (Schmid *et al*., 2015). This opens a range of emerging applications especially in the medical and industrial fields, as antiviral, antitumor, anti-inflammatories, and antibacterial agents (Xiao and Zheng, 2016). This makes EPS a valuable resource of commercial interest. Besides, there has been increasing demand for biopolymers to replace commercially available synthetics. Thus, if carefully extracted and purified, EPS is another potential by-product of industrial application from IAPS.

IAPS and its variations have been implemented globally to provide passive but effective and reliable remediation of wastewater for reuse and nutrient recycle for food production at a lower cost than existing systems (Oswald, 1991; Oswald, 1995). Indeed, the design of oxidation ponds (i.e. HRAOP of an IAPS) was developed as a simple and economical means of secondary

wastewater treatment (Ludwig *et al*., 1951; Oswald *et al*., 1953a). The fundamental principle involved in organic waste treatment in these ponds is the photosynthetic oxygenation and natural aeration of dissolved organic matter by microorganisms under conditions where oxygen does not become depleted (Oswald *et al*., 1953b & 1957). In this case, the oxygen needed for the decomposition of organic matter in HRAOP is produced by microalgae via photosynthesis. Contrary to the energy-intensive mechanical process of aeration employed in wastewater treatment systems such as activated sludge and trickling filters, where atmospheric oxygen is forced into the treatment system at an accelerated state, a natural process is employed in HRAOP and involves the dissociation of water molecules by microalgae (Cowan and Render, 2012). The oxygen is readily available for a swift decomposition of organic matter by bacteria and in the process, CO_2 and other metabolic products are progressively generated. It is this CO_2 from bacterial metabolism and the atmosphere that are fixed by microalgae in HRAOP.

In an ideal oxidation pond treatment process, the two phases of bacterial metabolism and microalgal photosynthesis may overlap forcing a symbiotic or mutualistic interaction. Both of these terms are used interchangeably in the literature to describe the association between microalgae and bacteria in a mixed culture system. In such interaction, the oxygen needed by bacteria is supplied through photosynthesis, and in return, bacteria supply respired carbon in the form of CO_2 necessary for microalgal photosynthesis (Oswald *et al*., 1953b). Thus, the mixed liquor comprises suspended microbial cells collectively known as mixed liquor suspended solids (MLSS) and their excretory products (EPS) generated in the process of biological interaction and wastewater treatment. MLSS is a term used for the description of the concentration of suspended solids in an aeration tank during an activated sludge process. HRAOPs can be considered as the aeration tanks of an IAPS, where oxygen is introduced by algal photosynthesis to ensure consumption of organic pollutants (Laubscher and Cowan, 2020). In this Chapter, the biological interaction between microalgae and bacteria in MLSS during wastewater treatment is introduced. The influence of this interaction on the performance of IAPS as a peri-urban wastewater treatment process is discussed, and the environmental and biotechnological significance of the resulting EPS is also elaborated.

1.2 Integrated Algae Pond Systems (IAPS)

In South Africa, the operation of wastewater treatment works (WWTW) and discharge standards are regulated by Government. As set by the National Water Act (1998) and recommendations by the Department of Water and Sanitation (previously Department of Water

Affairs; DWA, 2013), there is a general standard discharge limit for any wastewater treatment technology (Table 1.1). Regrettably, over 80% of the municipality owned WWTW in South Africa are dysfunctional, leading to the discharge of partially or untreated wastewater to the environment (Mambo *et al*., 2014a; Cowan *et al*., 2016). Consequently, the discharge of untreated wastewater either leads to eutrophication of water bodies or disease outbreak.

Table 1.1: General Authorisation limits for discharge to the environment as specified by the Department of Water and Sanitation (DWA, 2013).

Variables and substances	General limit	Special limit
Faecal coliforms (CFU 100 mL^{-1})	1000	0
COD (mg L^{-1})	75	30
pH	5.5-9-5	5.5-7.5
Ammonia (ionized and unionized) as Nitrogen (mg L^{-1})	6	2
Nitrate/ Nitrite as Nitrogen (mg L^{-1})	15	1.5
Chlorine as free chlorine (mg L^{-1})	0.25	0
Suspended solids (mg L^{-1})	25	10
Electrical conductivity (mS m^{-1})	70 mS/m above intake to a maximum of 150 mS/m	50 mS/m above background receiving water, to a maximum of 100 mS/m
Ortho-phosphate (mg L^{-1})	10	1(median) and 2.5 (maximum)
Fluoride (mg L^{-1})	1	1
Soap, oil or grease (mg L^{-1})	2.5	0
Dissolved arsenic (mg L^{-1})	0.02	0.01
Dissolved cadmium (mg L^{-1})	0.005	0.001
Dissolved chromium (VI) (mg L^{-1})	0.05	0.02
Dissolved copper (mg L^{-1})	0.01	0.002
Dissolved cyanide (mg L^{-1})	0.02	0.01
Dissolved iron (mg L^{-1})	0.3	0.3
Dissolved lead (mg L^{-1})	0.01	0.006
Dissolved manganese (mg L^{-1})	0.1	0.1
Mercury and its compounds (mg L^{-1})	0.005	0.001
Dissolved selenium (mg L^{-1})	0.02	0.02

Dissolved zinc (mg L^{-1})	0.1	0.04
Boron (mg L^{-1})	1	0.5

Preferred technologies for remediation of municipal wastewater over the years have been biological systems (Mambo *et al*., 2014a). These include mechanical systems such as activated sludge plants and passive systems such as waste stabilization ponds (WSP), constructed wetlands, and others. Although mechanical systems are the most widely used around the world due to their reliability and smaller footprint, they are still the most expensive in terms of management, capital, and operating costs (Young *et al*., 2017). Furthermore, such systems consume a lot of energy, release enormous volumes of greenhouse gases, and the process involves complete nutrient removal from wastewater (nitrification /denitrification), which results in nutrient loss (Corominas *et al*., 2013; Craggs *et al*., 2014; Acién *et al*., 2016). For example, in activated sludge plants, mechanical aeration alone accounts for 45-75% of the total energy consumption and emits 5 kg and 1.5 kg CO_2 per kg of N and COD removed respectively (Henze *et al*., 2008; Van Den Hende *et al*., 2016a; Jia and Yuan, 2016). Passive systems on the other hand are equally reliable, but in addition are simple to construct, manage, and maintain, which makes them the most suitable wastewater treatment systems from an economic point of view (Mambo *et al*., 2014a; Garfi *et al*., 2017). Altogether, these systems have the advantages of simplicity and reliability, but they offer many disadvantages such as inconsistent effluent quality, large capital investment, large footprint, sludge handling, and a tendency to eutrophy (Mambo *et al*., 2014a; Craggs *et al*., 2014; Young *et al*., 2017).

An attempt to mitigate the disadvantages of pond systems led to the innovation of AIWPS® by W. J. Oswald, with first of its kind developed at the University of California, Berkeley, USA. Since then, the technology has been transferred worldwide for wastewater remediation and biomass production at costs within the economic reach of most developing countries, especially in the rural communities (Oswald, 1995; Chen *et al*., 2003; Craggs *et al*., 2003b; Garcia *et al*., 2006). IAPS was transferred to South Africa to evaluate the performance of the system for deployment as a wastewater treatment technology in rural and peri-urban areas of South Africa, and to address other crucial issues such as sewage treatment and management, climate change, and sustainable development (Rose *et al*., 2002). Evaluation of the 500 person equivalent (PE) pilot-scale IAPS at Belmont Valley WWTW in Makhanda following commission revealed that performance of the system did not achieve the 75 mg/L discharge standard for COD, and that nutrient concentration sometimes also exceeded the limits presented in Table 1.1 (Rose *et al*.,

2007). However, it appeared at that time, that operation and performance of the system were based on secondary treated water and no tertiary treatment unit was included for final polishing. Moreover, more emphasis was placed on performance of individual units of IAPS than the system as a whole. Thus, a re-evaluation study of the complete system was conducted, taking into consideration the inclusion of one or a combination of tertiary treatment units for final polishing of IAPS effluent (Mambo *et al*., 2014a; Cowan *et al*., 2016). Indeed, the outcome of the study showed that IAPS-treated water complies with the general limit for either irrigation or discharge into a water source following tertiary treatment by either a maturation pond (MP) in series, slow sand filtration (SSF), or controlled rock filtration (CRF) without the need for faecal sludge handling (Mambo *et al*., 2014a; Cowan *et al*., 2016).

1.2.1 The design and function of IAPS components

A well-designed IAPS system such as the Belmont Valley IAPS was constructed in the middle of a beautiful horticultural softscape (grasses and trees). This green effect helps in purifying the air and thus, neutralizing the greenhouse gasses generated from the system to a reasonable extent. Furthermore, all IAPS components (Figure 1.1) exploit the natural functionality of anaerobic, facultative, and aerobic microorganisms within the system. The system consists of a minimum of four ponds arranged in series both vertically and horizontally with well-arranged structures to prevent overlapping of the distinct unit processes in each pond, avoid short-circuiting of influent to effluent, and maintain the essential biological and physical processes that occur in these ponds (Oswald, 1991). For example, the primary facultative pond (PFP) has at its base, approximately 6 m below surface water level, a separate hydraulically isolated compartment that acts as an in-pond digester (IPD) or fermentation pit. This vertical arrangement of ponds is referred to as an advanced facultative pond (AFP).

Placement over an IPD of a PFP is an advancement over the conventional facultative pond in WSP, where oxygenated water from the aerobic zone is usually carried by wind to the anaerobic zone, thus interrupting the anaerobic digestion process (Oswald, 1991). In an AFP, screened raw sewage enters the IPD for the anaerobic breakdown of organic matter. An upflow velocity of 1.0-1.5 m/d ensures that most of the settleable solids including helminths and the eggs remain within the digester. Thus, gas bubbles that form in and around the solid particles rise and break away creating a sludge blanket through which wastewater flows. The IPD is designed for a complete sludge fermentation such that sludge removal is in the order of decades, thereby eliminating day by day sludge handling. The IPD is also a place for the removal of endocrine-

disrupting compounds and precipitation of metal salts. The aerobic zone of the AFP is an environment for the proliferation of microalgae and bacteria that sequestrate CO_2, and oxidize residual methane, nitrogen, and hydrogen sulphide produced during fermentation in the anaerobic zone (Mambo *et al*., 2014b; Laubscher and Cowan, 2020). A well-designed AFP removes about 80% organic load and virtually all suspended solids from the raw influent prior to secondary treatment in HRAOPs (Oswald, 1991).

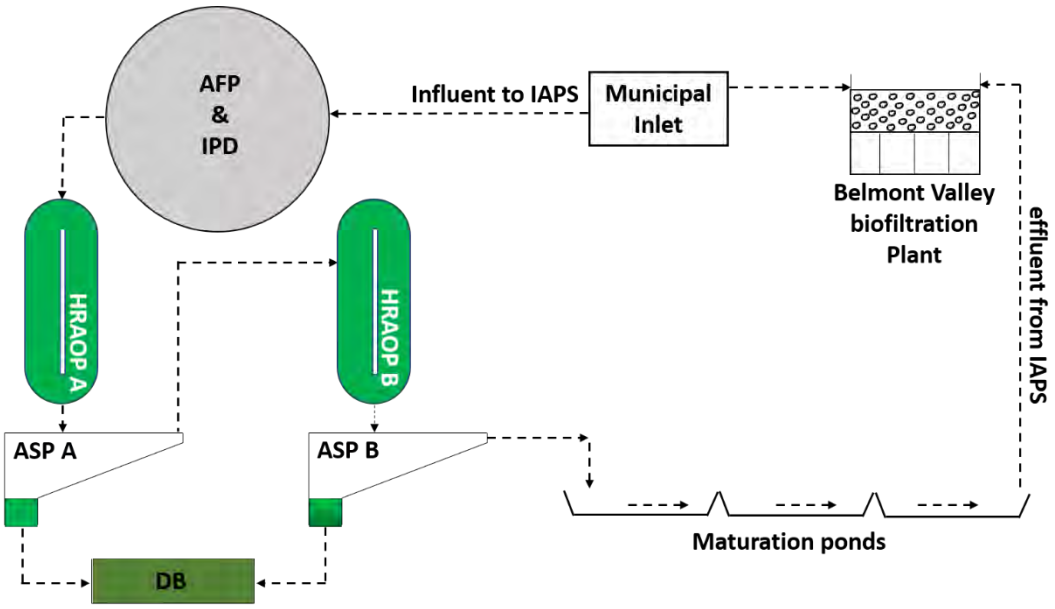

Figure 1.1: A schematic illustration of the process flow through a 500 PE IAPS for municipal wastewater treatment located at the institute for environmental biotechnology Rhodes University, Makhanda (33º 19′ 07″ south, 26º 33′ 25″ east), South Africa. The system is adjacent to the Belmont Valley biofiltration plant and features an advanced facultative pond (AFP) that incorporates an in-pond digester (IPD) that is ~6 m below the surface, where raw sewage is introduced to the system and anaerobic digestion of biosolids takes place. Primary treatment takes place in the AFP and effluent flows to a series of two high rate algal oxidation ponds (HRAOP) for secondary treatment and generation of MaB-floc containing biomass in the mixed liquor. The HRAOPs are connected by algal settling ponds (ASP), where biomass is recovered by gravity sedimentation and collected for beneficiation in drying beds (DB). Treated water from ASP B is transferred to maturation ponds (MP) in series for final polishing and disinfection. Effluent from IAPS is discharged to the biofiltration system.

The HRAOP was developed as one of the four ponds in series that make up an IAPS system specifically for optimal photosynthetic oxygenation and nutrient assimilation into biomass to effect secondary treatment of wastewater (Oswald, 1991; Green *et al*., 1995). These shallow ponds (typically 0.2-0.3 m deep) are usually connected in series and operated at a short retention time for efficient dissolved oxygen (DO) production. To allow microalgal cells to

remain in suspension for optimum photosynthetic oxygenation, gentle mixing of the pond water is provided by an electrical paddlewheel at a velocity between 0.15 and 0.3 m/s. The continuous mixing of HRAOP by paddlewheel facilitates aeration and microalgal growth, which results in a high rate of photosynthesis and supersaturation of DO (up to 3 times saturation) in the ponds. The DO is readily available for the heterotrophic bacteria for further reduction of organic matter, and in turn, CO_2 generated from bacterial metabolism is available as a source of carbon for microalgal photosynthetic activity (Figure 1.2). Thus, HRAOPs serve as continuously stirred reactors for the proliferation of microalgal and bacterial biomass and liquor can therefore be regarded as a MLSS that ensures consumption of organic pollutants (Laubscher and Cowan, 2020). Paddlewheel mixing in HRAOPs also fosters bioflocculation of MLSS constructed of EPS released by the microorganisms to form MaB-flocs (Jimoh and Cowan, 2017).

Because oxygenation in HRAOP is continuous and occurs at a high rate, the oxygenation capacity of MLSS is high and efficiency is 15 kg O_2/kWh (Oswald, 1991; Mambo *et al*., 2014b; Laubscher and Cowan, 2020). This appears to be 15 times more than the oxygenation efficiency in mechanical aeration, indicating HRAOP is more energy-efficient than aeration tanks in activated sludge processes. The photosynthetic activity in HRAOP also raises the pH of pond water during daytime allowing for ammonia stripping by volatilization, and complete disinfection of *E. coli* and other pathogenic bacteria is also common at this elevated pH. Even so, the characteristic short retention time, continuous inflow of water, and mixing may conceal the high disinfection rate in HRAOPs (Oswald, 1991). Therefore, a configuration of two or more ponds in series was found to be more effective for wastewater treatment (Cowan and Render, 2012). Most nutrients such as phosphate, ammonium, and nitrate are assimilated into the MLSS biomass, but other mechanisms such as ammonia volatilization and phosphate precipitation due to elevated pH may also contribute to nutrient abstraction. In addition, denitrification during the anoxic conditions may also account for 15-25% loss of the total influent nitrogen (Mambo *et al*., 2014b).

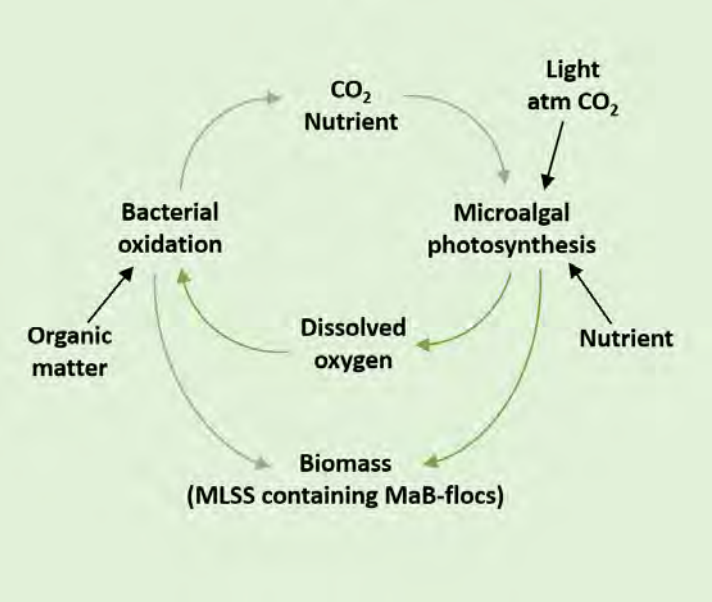

Figure 1.2: Schematic illustration of symbiotic microalgal-bacterial interaction in high rate algal oxidation ponds.

MLSS generated in HRAOP is usually removed in algal settling ponds (ASPs) by sedimentation of the MaB-floc containing biomass. A 70-80% biomass removal is feasible in ASP, but other mechanical methods of harvesting such as dissolved air floatation (DAF) have been used when a higher degree of harvesting is required (Oswald, 1991; Green *et al*., 1995). For final polishing and to improve the quality of IAPS-treated water prior to reuse, MPs are a common tertiary treatment unit included in the configuration of an IAPS system. They are usually constructed as deep ponds with depth of about 1 m and operated in series to achieve an extended retention time (between 10 and 20 d) required for overall removal of residual pathogens (Oswald, 1991; Mambo *et al*., 2014b). In addition, MPs have a high algae diversity and are therefore fully oxygenated as a result of photosynthesis, which provides an ideal condition for adequate removal of pathogenic organisms. Also, residual nitrogen is removed by assimilation into biomass or ammonia volatilization because of a typical high pH in the MPs (Mambo *et al*., 2014a & 2014b).

Clearly, the processes involved in IAPS wastewater treatment such as fermentation, oxygenation, nutrient removal, sedimentation, and disinfection are typical of any WWTW. However, the way these ponds are integrated is unique to the innovation of this technology and its derivatives thereof.

1.2.2 The benefits and challenges of IAPS

IAPS is a passive water treatment technology that combines the activities of natural processes such as gravity, solar energy, and biological activities to treat wastewater (Craggs *et al*., 2014). Therefore, it is cost-effective, requires low to no maintenance, and operational and capital costs are cheaper than that of activated sludge (Mambo *et al*., 2014a; Sutherland and Ralph, 2020). Thus, and in the context of locality, it appears more robust than conventional mechanical systems and may provide a more sustainable solution to imperative issues such as poor sanitation, waterborne diseases, infections, and contamination of the already limited water resource (Laubscher and Cowan, 2020). It has been established that if properly designed, IAPS eliminates sludge handling, minimizes power use, and is more economical and reliable than mechanical systems of equal capacity (Oswald, 1990). Moreover, recent studies have pointed out that the technology may represent a CO_2 sink with an environmental footprint estimated at two times less than conventional systems (i.e. activated sludge plants), as well as an added benefit of biomass recovery for beneficial use (Craggs *et al*., 2014; Jia and Yuan, 2016; Garfi *et al*., 2017; Arashiro *et al*., 2018).

During photosynthetic carbon fixation by unicellular microalgae through the Calvin-Benson cycle, a CO_2 concentration mechanism (CCM) plays a vital role in increasing the level of CO_2 at the active site of ribulose bisphosphate carboxylase oxygenase (Rubisco) by transporting CO_2 to the cell (Zhao and Su, 2014). During the process of dissolved inorganic carbon conversion and assimilation into biomass, carbonate ions (i.e. HCO_3^- and CO_3^{2-}) are formed, and their interaction with cations results in the deposition of metal carbonates that provide an additional driving force (Mambo *et al*., 2014b). This process results in a net photosynthetic rate at optimum light and temperature. Therefore, IAPS might help reduce some of the environmental impacts associated with wastewater treatment as the system has a net consumption of CO_2. Furthermore, since carbon availability for optimal biomass productivity is typically limited (3-7 C:N) in domestic sewage, other methods such as CO_2 addition have been studied with wastewater treatment HRAOPs (Park and Craggs, 2011; Sutherland *et al*., 2015b). These authors reported that the addition of CO_2 enhanced biomass productivity, increased nitrogen assimilation into biomass, reduced ammonia volatilization, improved light utilization, and photosynthetic efficiency. Even so, this method was found to be cost-prohibitive at full-scale.

There is however limited information on the contribution of IAPS to the emission of other greenhouse gases such as ammonia and methane. This indicates the need to conduct a life cycle assessment (LCA) of the system in order to evaluate the environmental impact and footprints of the technology. Nevertheless, Arashiro *et al*. (2018) indicated the possibility of NH_3 emissions due to NH_4^+ volatilization in HRAOP systems, which could result in human and terrestrial toxicity.

Despite the appraisal of this technology and the outstanding benefits IAPS tends to offer in sewage and wastewater treatment (Oswald, 1995; Mambo *et al*., 2014a & 2014b; Sutherland and Ralph, 2020), the technology is yet to be implemented in South Africa at full commercial scale. The reason for this is still not clear, but perhaps is partly due to the shortcomings and limitations faced by the technology. The large footprint coupled with a perception that the technology produces inconsistent COD and TSS that does not comply with South African discharge standards was initially a major concern. Other aspects contributing to hindering the uptake or implementation of this technology for wastewater treatment have been highlighted by Sutherland and Ralph (2020) and Laubscher and Cowan (2020). Some of the factors emphasized by these authors include lack of awareness or inadequate interrogation on microalgal-based wastewater treatment by the public and stakeholders, a disparity of purpose among decision-makers, and absence of well-defined technological framework.

IAPS is constrained by its design and a major challenge is the extensive land area required for its construction (Acién *et al*., 2016; Delanka-Pedige *et al*., 2020). Because of the high oxygenation capacity of the HRAOP component of an IAPS, these ponds are designed to be shallow to provide necessary oxygen that drives the bacterial/microalgal interaction for efficient pollutant decomposition, nutrient uptake, biomass production, and disinfection. Therefore, a large surface area typically between 0.5 and 1.0 ha is required for effective wastewater treatment in a commercial scale system (Cowan *et al*., 2016). For instance, a pilot-scale IAPS treating 75 m^3/d domestic sewage would require between 0.6 ha (in summer) to ~1.0 ha (in winter) HRAOP for effective treatment and biomass productivity (Cowan *et al*., 2016). As such, scaling this system to commercial level means even more land requirements, thereby escalating the costs of implementation. Thus, footprint remains a major challenge hindering the transfer of this technology to a commercial scale, particularly in urban settings. In rural and in the peri-urban space however, the size of the system may be overlooked as land use is majorly for agriculture in these areas. Implementation of an IAPS system would therefore

be most appropriate in a peri-urban setting, where a single installation could cater for water use (for irrigation and ablution purposes), generation of electricity on-site from methane-rich biogas, and biomass for plant and animal feed. Indeed, these products are usually needed to support agricultural and horticultural industries and would therefore position wastewater treatment IAPS at the water-energy-food nexus (Laubscher and Cowan, 2020). In the process, quality of life in such communities would be enhanced, and exploitation of the limited water reserve could be prevented.

It is also pertinent to note that IAPS is subject to influence from prevailing environmental factors. These environmental factors may predispose the system to changes in species composition and cause fluctuations in the efficiency of the bioprocess of the system. These fluctuations may either affect the water treatment efficiency or biomass productivity in HRAOP. Inasmuch as enormous benefits can be derived from the biomass generated in IAPS, there exist some limitations to its valorisation. One such limitation is the harvesting or separation of the biomass from treated water (Van Den Hende *et al*., 2016a; Jia and Yuan, 2016; Phasey *et al*., 2017; Sutherland and Ralph, 2020). Biomass employed in IAPS wastewater treatment (i.e. bacteria and microalgae) are relatively small (1-30 μm), have similar density with their culture medium, and are negatively charged, which results in poor settleability (Park *et al*., 2011a; Hu *et al*., 2017; Quijano *et al*., 2017). As such, harvesting could be a complex and costly technical exercise and has been the major constraint thus far. Moreover, the average biomass concentration (measured as MLSS) in an HRAOP of an IAPS treating domestic wastewater treatment under South African weather conditions is 0.15 g/L indicating highly diluted biomass, which requires separation from the treated water prior to discharge to meet specific standards (Laubscher and Cowan, 2020). Harvesting of algal biomass for biofuel production or any other added-value product was estimated to cost between 20-50% (Wan *et al*., 2015; Hu *et al*., 2017; Quijano *et al*., 2017). In view of this, most microalgal-based research nowadays (including algal-based wastewater treatment like IAPS) focuses on ways to achieve low-cost harvesting or dewatering. By default, the biomass generated in IAPS is produced as relatively stable MaB-flocs, which aids biomass settleability and recovery from treated water (Jimoh and Cowan, 2017). MaB-flocs are formed as a result of the biological interaction involving photosynthetic oxygenation that generates a high level of oxygen, and oxidation of organic pollutants by heterotrophic bacteria. The exchange of O_2 and CO_2 in the continuously mixed MLSS, together with the excreted metabolic products (EPS) results in this bioflocculation process.

1.3 Microalgal-bacterial flocculation

When microorganisms come into contact with surfaces (either biological or not), they produce EPS to enable colonization, followed by a period of bulbous growth that develops into a 3-dimensional biofilm structure (Flemming and Wingender, 2010). Thus, the formation of biofilm or slime follows a biological process of attachment, colonization, and secretion of substances to form a matrix for protection. This is a common tactic used by microorganisms to adapt to the environment, and once formed can endure mechanical, biological, and chemical means of eradication (Whitfield *et al*., 2015). In wastewater treatment, biofilms occur as floating or suspended flocs that accumulate in the mixed liquor suspension. An example is the activated sludge flocs (or granules) that form the basis for efficient pollutant removal in activated sludge plants. In such plants, microorganisms (majorly bacteria) and other suspended particle in the mixed liquor (i.e. MLSS) are aerated by a mechanical process, and the continuous recycling of the bacterial sludge, together with other biological, physical, and chemical mechanisms eventually results in bioflocculation known as activated sludge flocs that provide a clear effluent with low COD and TSS concentrations (Sobeck and Higgins, 2002). Similarly, floc formation has been observed in wastewater treatment HRAOPs (Medina and Neis, 2007; Gutzeit *et al*., 2005; Van Den Hende *et al*., 2011; Jimoh and Cowan, 2017), but since the MLSS is a consortium of microalgal and bacterial biomass, various names have been given in the literature including MaB-flocs (Van Den Hende *et al*., 2011) and microalgal-bacterial aggregates (MABAs; Quijano *et al*., 2017).

Flocculation is the aggregation of single cells to form large aggregates, which can be separated by gravity sedimentation (Vandamme *et al*., 2013). This method is used to separate the low concentration of algal biomass from the large volume of liquid growth medium. Flocculation can be induced by either physical, chemical, or biological (including auto-flocculation) means. Physical flocculation involves the use of processes like ultrasound, electro-flocculation, and magnetic nanoparticle separation (Vandamme *et al*., 2013). However, these processes have proven to be effective but energy-intensive and difficult to scale up for commercial purposes (Wan *et al*., 2015). Chemical flocculation is based on the use of chemicals such as metal ions that can induce the aggregation of microbial cells (De Godos *et al*., 2011). The conventional method of flocculation is the addition of chemical flocculants and polymers such as aluminium and ferric salts, chitosan, polyelectrolytes, polyacrylamides, cationic starch, etc. to aggregate biomass and consequently enhance harvesting and improves effluent quality. However, the use

of chemical flocculants results in contamination, which interferes with the downstream application of the biomass thus generated (Vandamme *et al*., 2013; Wan *et al*., 2015).

Considering sustainability and quality, an inexpensive approach to algal harvest, bioflocculation underpinned the development of IAPS and involves sedimentation under gravity in settling ponds, which involves the use of gravitational forces. This method allows for concentrating the biomass to 40-50 g/L with biomass recovery of about 95% (Acién *et al*., 2016). However, settling by gravity differs greatly between algal species as some species settle more readily (i.e. colonial) than others (i.e. single cell). Particularly, the use of gravity sedimentation favours large-sized microalgae such as *Pediastrum* sp. and *Micractinium* sp., cyanobacteria like *Arthrospira* sp., and diatoms like *Cyclotella* sp. Therefore, to facilitate settling of small-sized microalgae such as *Chlorella* sp. and *Scenedesmus* sp., physical and/or chemical flocculation methods are usually required (Jia and Yuan, 2016). Laboratory studies have demonstrated that growing bacteria with microalgae facilitates floc formation and harvesting of biomass (Wan *et al*., 2013; Li *et al*., 2016). Also, bioflocculation of microalgae and bacteria has been reported in wastewater treatment systems (Gutzeit *et al*., 2005; Van Den Hende *et al*., 2011; Jimoh and Cowan, 2017). Thus, a cost-effective separation of biomass from treated water can be achieved biologically.

1.3.1 Biological interactions and floc formation in HRAOP

With the symbiotic association between microalgae and bacteria, HRAOP show excellent performance in the removal of nutrient from wastewater (Banat *et al*., 1990; Craggs *et al*., 2003b; Park *et al*., 2011b; Sutherland *et al*., 2013). However, nutrient removal efficiency is dependent on algal photosynthesis, which is affected by temperature and light intensity among other factors. Nevertheless, HRAOPs remove on average 59% organic matter, 61% total nitrogen, 77% ammonium, 43% total phosphorus, and 21% orthophosphate (Young *et al*., 2017). Unlike the conventional wastewater treatment systems in which nutrients are not easily recovered, nutrient removed from water in HRAOP is assimilated into harvestable biomass. Theoretically, 40-70 t/ha/y (ash-free dry weight) biomass is achievable in HRAOP treating wastewater (Mehrabadi *et al*., 2015). However, actual values reported so far are yet to reach this due to various factors such as grazing, CO_2 limitation, temperature, solar radiation, pH, and increased DO concentration (Park *et al*., 2011a; Craggs *et al*., 2014; Sutherland *et al*., 2015a).

Biomass production in HRAOP exploits the mutualistic interaction between microalgae and bacteria. In this interaction, bacteria are responsible for the oxidation of organic matter into smaller compounds and inorganics such as CO_2, NH_4^+, and PO_4^{-3}, which are assimilated by microalgae. In turn, microalgae produce O_2 as a product of photosynthesis which is consumed by heterotrophic bacteria during biological oxidation. Hence, they are microbial partners that synergistically affect each other's metabolism and physiology (Jia and Yuan, 2016; Ramanan *et al*., 2016). This interaction is facilitated by paddlewheel mixing and together with the production and secretion of EPS, results in microalgal-bacterial aggregation (Jimoh and Cowan 2017). The result is immobilized microalgae and bacteria embedded in an EPS-containing gel matrix. A suggested interrelationship of EPS with the microorganisms within the MaB-flocs is schematically illustrated in Figure 1.3.

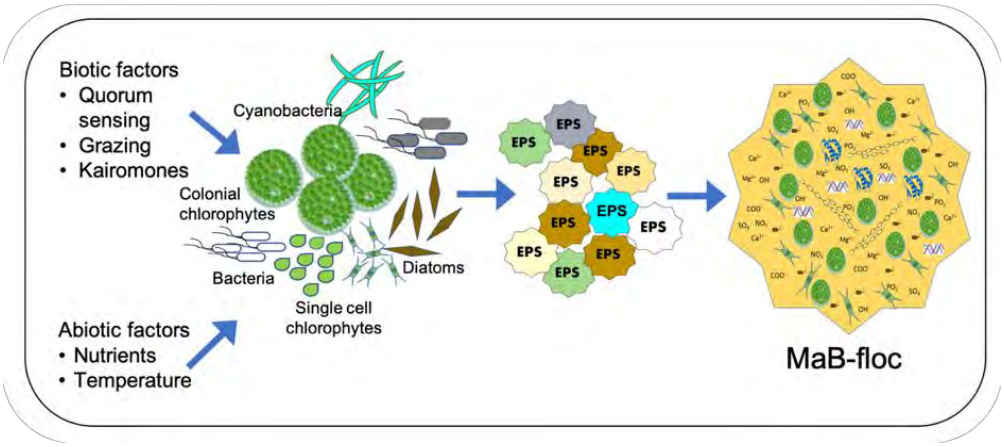

Figure 1.3: Schematic illustration of the formation of Mab-flocs in HRAOPs. Prevailing abiotic and biotic factors including quorum sensing trigger production of EPS by competent cells. Extruded polysaccharides and proteins are adsorbed to the cell surfaces as a scaffold that traps soluble organic carbon, nutrients, and divalent ions such as Ca^{2+} and Mg^{2+} to form an EPS comprising closely associated microalgae, cyanobacteria, bacteria, and other entities as MaB-flocs.

Although the triggers for initiation of MaB-floc formation remain unidentified, it is likely that both biotic and abiotic factors play a major role. For example, many species of phytoplankton respond to herbivore grazer chemical cues (i.e. kairomones) by forming colonies and colony size, which seems to be a consequence of either temperature, light, or nutrient status (O'Donnell *et al*., 2013). Also, quorum sensing (QS) bacteria produce and release signalling molecules in increasing amounts as a function of cell density. QS influences the development of bacterial biofilm and the production of an extracellular matrix that may contain 'bio-phase' and be resistant to dispersion under stress conditions (Tseng *et al*., 2016; Huang *et al*., 2019).

Thus, it is proposed that QS coupled with prevailing conditions triggers EPS production to facilitate microbial aggregation and MaB-floc formation.

Although MaB-flocs are typically composed of microalgae and bacteria, other components such as protozoa, rotifers, ciliates, precipitates, dead cells, and chelated ions are also involved in the floc structure (De Schryver *et al*., 2008; Van Den Hende *et al*., 2011; Sfez *et al*., 2015; Quijano *et al*., 2017). MaB-flocs range in size from 100-5000 μm depending on the operational conditions and the microbial community that make up the floc (De Schryver *et al*., 2008; Van Den Hende *et al*., 2011). Typically, MaB-flocs are irregular in shape, fine, highly porous, easily compressible, and have a broad distribution of particle sizes (De Schryver *et al*., 2008). They also present a high settling characteristic that allows for harvesting by simple and cost-effective gravity sedimentation without the addition of chemical flocculants (Quijano *et al*., 2017).

1.3.2 Importance of microalgal-bacterial interaction and flocculation

Assumptions from the outset of mass microalgal culture were that bacteria were merely unwanted contaminants (Fuentes *et al*., 2016). This has however changed in recent years with the realization of the eco-physiological importance of the interaction that exists between the two and its significance in algal biotechnology (Wang *et al*., 2014; Kouzuma and Watanabe, 2015). It was precisely this mutualism that was targeted in elaborating the design of AIWPS® (Oswald *et al*., 1957; Oswald, 1990; Oswald, 1991; Oswald, 1995) and which was retained and enhanced in the design of IAPS (Mambo *et al*., 2014a; Jimoh and Cowan, 2017). Indeed, the formation of MaB-flocs would be anticipated and, once formed, strengthen the interaction between the component organisms to improve mass transfer within the floc and serves as protection against pathogens and grazers (De Schryver *et al*., 2008; Hom *et al*., 2015). In addition, and from wastewater treatment and a biotechnology perspective, nutrient abstraction, biomass harvesting, and resource recovery are enhanced (Mambo *et al*., 2014b; Ramanan *et al*., 2016).

Naturally, microbial cells, especially bacteria are small, which interferes with nutrient uptake, mass transfer, and diffusion as the organisms move through the water column. In such cases, microorganisms overcome diffusion problems by aggregating into flocs. The permeability of MaB-flocs allows for rapid and efficient diffusion of CO_2, O_2, organic matter, and nutrients, where the scaffold (i.e. EPS) holding the floc structure aids the transport of molecules within the aggregate (De Schryver *et al*., 2008; Quijano *et al*., 2017). As a result, microorganisms

have access to a constant supply of nutrients within the micro-community. In addition to mass transfer between cells, each organism may stimulate the growth of others by providing necessary conditions and compounds to do so. For instance, the mutualistic exchange of CO_2/O_2 by microalgae and bacteria results in effective nutrient uptake/biodegradation. Associated bacteria in a MaB-floc can also promote better algal growth by supplying necessary vitamins, ion chelators, and phytohormones that cannot be synthesized by microalgae (Wang *et al*., 2014). Algal photosynthesis results in O_2 supersaturation, which can inhibit algal growth by reducing carbon fixation. Therefore, O_2 consumption by bacterial components offset the DO concentration in the culture medium, which enhances microalgal growth while serving as an electron acceptor for their organic matter degradation (Subashchandrabose *et al*., 2011; Natrah *et al*., 2013).

Co-existence of microalgae and bacteria in flocs may also confer on them resistance to unfavourable conditions and invasion by unwanted species in their microenvironment (De Schryver *et al*., 2008). For instance, grazing is one of the major factors that limits biomass productivity in HRAOPs but with the aggregation of cells into MaB-flocs, they tend to become resistant to predation by protozoa. Furthermore, the association of microalgae with bacteria in the forms of MaB-flocs has been shown to enhance and reduce the cost of harvesting (Barros *et al*., 2015; Jimoh and Cowan, 2017). Several techniques such as centrifugation, flotation, and filtration employed in the harvesting of microalgal biomass are either energy-intensive, results in contamination, or difficult to maintain. In contrast, bioflocculation (i.e. MaB-flocs) occurs spontaneously, settles rapidly at a velocity of 8.3 m/h, and concentrates the microalgal suspension 20-100 times. Thus, the formation of MaB-flocs would appear to contribute directly to reducing cost and enhancing the sustainability of IAPS as a wastewater treatment system while facilitating resource recovery (Barros *et al*., 2015; Arcila and Buitrón, 2016).

1.3.3 Potential commercial applications for MaB-flocs

When compared to many other wastewater treatment processes, resource recovery can make IAPS economic and sustainable and perhaps, a choice platform technology (Quijano *et al*., 2017). As shown in Table 1.2, MaB-flocs contain a wide range of metabolites such as lipids, proteins, carbohydrates, and bioactive compounds that can be refined and valorised saleable products (Jia and Yuan, 2016; Mehrabadi *et al*., 2016). Potential products include biofuels, fertilizers, animal feeds, nutraceuticals, and pigments (Young *et al*., 2017; Quijano *et al*., 2017). In recent years, one of the targeted options has been the use of algal biomass either for

biofuel production or non-food products. Although an average energy of 800-1400 GJ/ha/y can be generated from MaB-flocs through various conversion processes such as anaerobic digestion, fermentation, transesterification, hydrothermal liquefaction, gasification, and pyrolysis (Milledge and Heaven, 2014), the choice on algae-to-energy process must be exercised carefully to ensure that at the very least, a net positive energy balance is achieved (Mehrabadi *et al*., 2015; Passos *et al*., 2017).

Table 1.2: Microbial and biochemical composition of MaB-flocs from wastewater treatment (Mehrabadi *et al*., 2016).

	Microalgae	Bacteria
Composition (%)	60- 80	20-30
Carbohydrate (%)	10- 30	20-40
Protein (%)	30- 60	25-50
Lipids (%)	15- 30	< 10

Currently, one of the most attractive options for the generation of fuel from MaB-floc biomass is conversion to biogas. More so, microalgae production in mixed culture in raceway ponds (i.e. HRAOP) has been proven as an ideal approach for methane production (Zamalloa *et al*., 2011; Mehrabadi *et al*., 2015). Anaerobic digestion generally requires minimal processing and drying of the feedstock, therefore the cost of production is not considered intensive (Lakaniemi *et al*., 2013; Prajapati *et al*., 2013; Laubscher and Cowan, 2020). Anaerobic digestion has the lowest net energy ratio (35% energy recovery) among other energy conversion processes available (Mehrabadi *et al*., 2015; Acién *et al*., 2016). Even so, a methane yield of 226 mL CH_4 g/VS was measured using MaB-flocs generated in wastewater-fed HRAOP (Van Den Hende *et al*., 2015), and a relationship between biomass and methane potential of MaB-flocs was recently demonstrated (Arcila and Buitrón, 2016). Furthermore, increased methane output was also measured for cyanobacterial biomass over the unicellular chlorophyte *Chlorella* (Mendez et al., 2015). These observations are comparable to the yields of 52-55% and 68% reported by Prajapati *et al*. (2013) and Passos *et al*. (2013) respectively. The data also confirm very early studies showing that microalgae grown on domestic sewage are readily digested to yield a biogas stream containing by volume ~62% methane (Golueke *et al*., 1957). Thus, AIWPS- and IAPS-derived methane can be regularly generated from MaB-floc biomass and used to generate electricity directly (Craggs *et al*., 2014; Passos *et al*., 2017). Indeed, a 500 PE IAPS that produces ~9 kg/d MaB-floc biomass was estimated to generate 0.48 L CH_4 g/VS at a 73% conversion efficiency and a net energy yield of ~150 MJ per day (Laubscher and Cowan, 2020).

Another feasible potential for MaB-floc biomass generated during wastewater treatment by IAPS is as a substrate for the production of fertilizer. Indeed, MaB-flocs are rich in macronutrients such as nitrogen, phosphorus, and potassium and have been shown to promote plant growth (Coppens *et al*., 2016; Garcia-Gonzalez and Sommerfeld, 2016). Cyanobacteria such as *Nostoc* spp. and *Anabaena* spp. are also good nitrogen-fixing photosynthetic protists that improve soil fertility and plant growth (Singh *et al*., 2016; Grzesik *et al*., 2017). Therefore, MaB-flocs containing these organisms might be expected to present as ideal candidates for use as biofertilizers, biostimulants, and soil conditioners or amendments for crop production. Similarly, the presence of nitrogen-fixing and mineral-solubilizing bacteria and plant growth-promoting rhizobacteria renders any biofertilizer produced from MaB-flocs valuable (Leaungvutiviroj *et al*., 2010). It is therefore not surprising that MaB-flocs possess some plant-growth-promoting compounds, vitamins, phytohormones, and amino acids which stimulate and improve the quality of plants (Coppens *et al*., 2016). In addition to agronomic use, MaB-flocs have also found application in aquaculture as animal feed and/or supplements to improve nutrition (Spolaore *et al*., 2006; Van Den Hende *et al*., 2014b). Due to the nutritional content of microalgal biomass particularly protein, it can be used either directly or indirectly as feed for fish and shrimp. Thus, the implementation of IAPS will facilitate the transition towards sustainable agricultural and aquacultural practices.

The choice of product to be produced from MaB-flocs and algal biomass has been a subject of interest in recent times from an economic and sustainability point of view. For instance, Arashiro *et al*. (2018) conducted a life cycle assessment and showed that biogas production is more environmentally friendly than biofertilizer production in terms of climate change, ozone layer depletion, and fossil depletion. Even so, biofertilizer production was more economically feasible, especially in warmer climate regions. Thus, choosing a product from the numerous available biorefinery pathways requires informed thinking. The establishment of biorefineries in which MaB-flocs can be fractionated into many product streams seems preferable (Vanthoor-Koopmans *et al*., 2013; Trivedi *et al*., 2015). Through series of recycling, 99% of the energy stored in the biomass can be recovered in the form of one biofuel or another. For example, an algal biorefinery where biodiesel is the primary product can utilize the residual biomass for biogas production, ethanol production, or be used as fertilizer (Mehrabadi *et al*., 2015; Gupta *et al*., 2017). By either mitigating or preventing resource loss, the associated environmental impact of product valorisation is thus minimized or avoided (Zhu, 2015).

1.4 Extracellular polymeric substances in IAPS

Several mechanisms support and explain the aggregation and flocculation of particles suspended in water. Some of these include the DLVO theory (named after Derjaguin, Landau, Verwey, and Overbeek), the alginate theory, and divalent cation bridging (Sobeck and Higgins, 2002; De Schryver *et al*., 2008). For the aggregation of aqueous dispersions, microorganisms secrete EPS into their microenvironment which binds cells and particulates by ion bridging. According to the divalent cation bridging theory, these polymers bridge with divalent cations such as Mg^{2+} and Ca^{2+} causing aggregation of cells into flocs. Thus, EPS is involved in the intermolecular interaction that results in flocculation and is therefore regarded as the sub-structure of biofilms and MaB-flocs (Sheng *et al*., 2010).

1.4.1 Origin and role of EPS in matrix formation

Progress towards the elucidation of the source of EPS began in earnest following evidence of its adsorption property and after observations that bacteria stick together on solid surfaces by secreting a cementing substance (reviewed by Costerton *et al*., 1978). After removal from the surfaces, a footprint or film-like material remained that appeared to resemble the shape of the bacterial cells and was confirmed as the matrix by which cells stick together and attach to surfaces (Zobell, 1943; Neu and Marshall, 1991). This matrix was initially regarded as extracellular polysaccharide, but more recent research has revealed a diversity of chemical compounds within the structure of this material. Therefore, the term polymeric replaced polysaccharide in describing EPS.

All microbes including bacteria, fungi, yeasts, and algae are genetically predisposed to produce EPS given certain conditions (Singha, 2012; Rühmann *et al*., 2015; Flemming, 2016). Thus, naturally occurring EPS might be expected to be structurally diverse with application-specific properties determined largely by the biological origin and prevailing environmental condition. Because there are more studies on bacterial EPS, it is assumed that bacteria play a major role in mediating the aggregation of microbial cells in wastewater treatment systems. However, there are several reports on algal EPS as well (Parikh and Madamwar, 2006; Mishra and Jha, 2009; Ahmed *et al*., 2014). Even so, it is the combined contribution of all organisms within the floc that results in superior EPS matrix formation and this, in turn, facilitates the formation of a more stable microbial interaction (Figure 1.3).

An EPS matrix is activated by extracellular enzymes (exoenzymes) secreted by the microbial population (Flemming, 2011). These exoenzymes bind with the functional groups of the secreted EPS (i.e. carboxyl, hydroxyl, and amide groups) to form a confined and immobilized environment for microbial interaction. Subsequently, other components such as products from cell lysis are deposited and either assimilated or utilized synergistically by the growing microbial population. Detachment can also occur through biodegradation of the matrix component which results from EPS degrading enzymes. Also, abiotic factors (e.g. light, turbulence) might be expected to impact floc integrity to cause detachment particularly in processes such as wastewater treatment. However, during wastewater treatment in HRAOPs of IAPS, the matrix or scaffold substructure of MaB-flocs appears to exist in a state of dynamic equilibrium such that dark-induced losses are accounted for by light-induced gains to ensure the maintenance of the floc (Jimoh and Cowan, 2017).

1.4.2 Structure and function of EPS

The EPS scaffold or matrix typically ranges in thickness from 0.2 to 1.0 μm but can be much thinner for some bacteria (Czaczyk and Myszka, 2007) and contains about 98% water (Sutherland, 2001). Within the matrix are important EPS components that mediate the aggregation and flocculation properties of constituent cells (De Schryver *et al*., 2008; Irie and Parsek, 2008; Trabelsi *et al*., 2015). Although the structure and molecular composition of EPS vary depending on the microbial community, culture medium, prevailing environmental condition, and extraction method, the presence of proteins and uronic acids is apparently important for the structural integrity of MaB-flocs (Sheng *et al*., 2010; Tourney and Ngwenya, 2014; Quijano *et al*., 2017).

Microbial origin and chemical composition are largely responsible for determining function, and a summary of identified and accepted roles of EPS in microbiological systems is presented in Table 1.3. Approximately 400 different EPS variants have been reported in the literature (Rühmann *et al*., 2015). There are also many accounts of microbes that produce EPS, but the structure of these extracellular polymerics has yet to be elucidated. As stated by Wingender *et al*. (1999), ‘there is no biofilm without an EPS matrix’. Thus, EPS keeps cells in proximity, and by doing so, flocs are able to capture resources, develop cell-cell recognition, and confer tolerance to antimicrobial agents and stress (Wingender *et al*., 1999; Flemming, 2016).

Table 1.3: Identified and accepted roles of the EPS matrix in microbiological systems.

Function	EPS component	Role in floc formation	References
Protection	All	Protects constituent organisms from biotic and abiotic stress including grazing	De Schryver *et al*., 2008; Decho and Gutierrez, 2017
Aggregation	Proteins and polysaccharides	Facilitates floc formation and increases settleability	Sheng *et al*., 2010
	Enzymes	Binds functional groups to form immobilized matrix	Flemming, 2011
Adsorption	Polysaccharides, proteins, humic substances	High affinity for metals and organic matter binding	Sheng *et al*., 2010; More *et al*., 2014
Homeostasis	Enzymes	Biosynthesis and degradation of matrix components	Flemming, 2011; More *et al*., 2014
Gene transfer	Nucleic acid	Typical horizontal gene transfer i.e. where nucleic acid from lysed cells is taken up by cells within the matrix	Wingender *et al*., 1999; Czaczyk and Myszka, 2007
Energy sink	Polysaccharides, humics, chelators	Nutrient repository where cells within the matrix can access nutrients in case of depletion or starvation	Sheng *et al*., 2010; Ding *et al*., 2015; Xiao and Zheng, 2016
Mass transfer	All	Efficient diffusion of CO_2, O_2 and nutrients to facilitate transport of molecules within the matrix	De Schryver *et al*., 2008; Quijano *et al*., 2017
Water retention	All	Maintenance of a hydrated microenvironment	Wingender *et al*., 1999; Flemming, 2016

Extracellular carbohydrates (i.e. exopolysaccharides) contain hexoses, pentoses, deoxyhexoses, and sugar acids with other substituents such as formate, phosphate, pyruvate, acetate esters, and succinate (Czaczyk and Myszka, 2007; Poli *et al*., 2011; More *et al*., 2014). These exopolysaccharides contribute to the adhesive property of EPS and consist of either homopolysaccharides or heteropolysaccharides (Figure 1.4). The homopolysaccharides are neutral and made up of only one monosaccharide type, either D-glucose or L-fructose, and are divided into three groups: α-D-glucans, β-D-glucans, and fructans. Some microbial homopolysaccharides include dextran (glucose that contains consecutive α-(1, 6)-linkages), curdlan (glucose with β-(1,3)-linkage), and cellulose (a repetitive unit of D-glucose with β-(1,4)-linkage). Repeated units of monosaccharide, typically ~5–8 units with exceptions in some cyanobacteria that reach ~15 units as building blocks, form heteropolysaccharides with complex structures such as alginates, xanthan, gellan, and hyaluronic acid (Kehr and Dittmann,

2015). Extracellular proteins determine the adsorption and attachment of flocs to surfaces and contain 40–60% hydrophobic amino acids (Czaczyk and Myszka, 2007). A considerable number of proteins are enzymes that degrade EPS components during starvation by acting on the EPS of the same organism or other species present in the substrate (More *et al*., 2014). EPS also contain non-enzymatic proteins (structural proteins) and some examples include lectins and polyamides (More *et al*., 2014). Lectins are found in the EPS matrix of activated sludge, which helps in bacterial aggregation (Higgins and Novak, 1997).

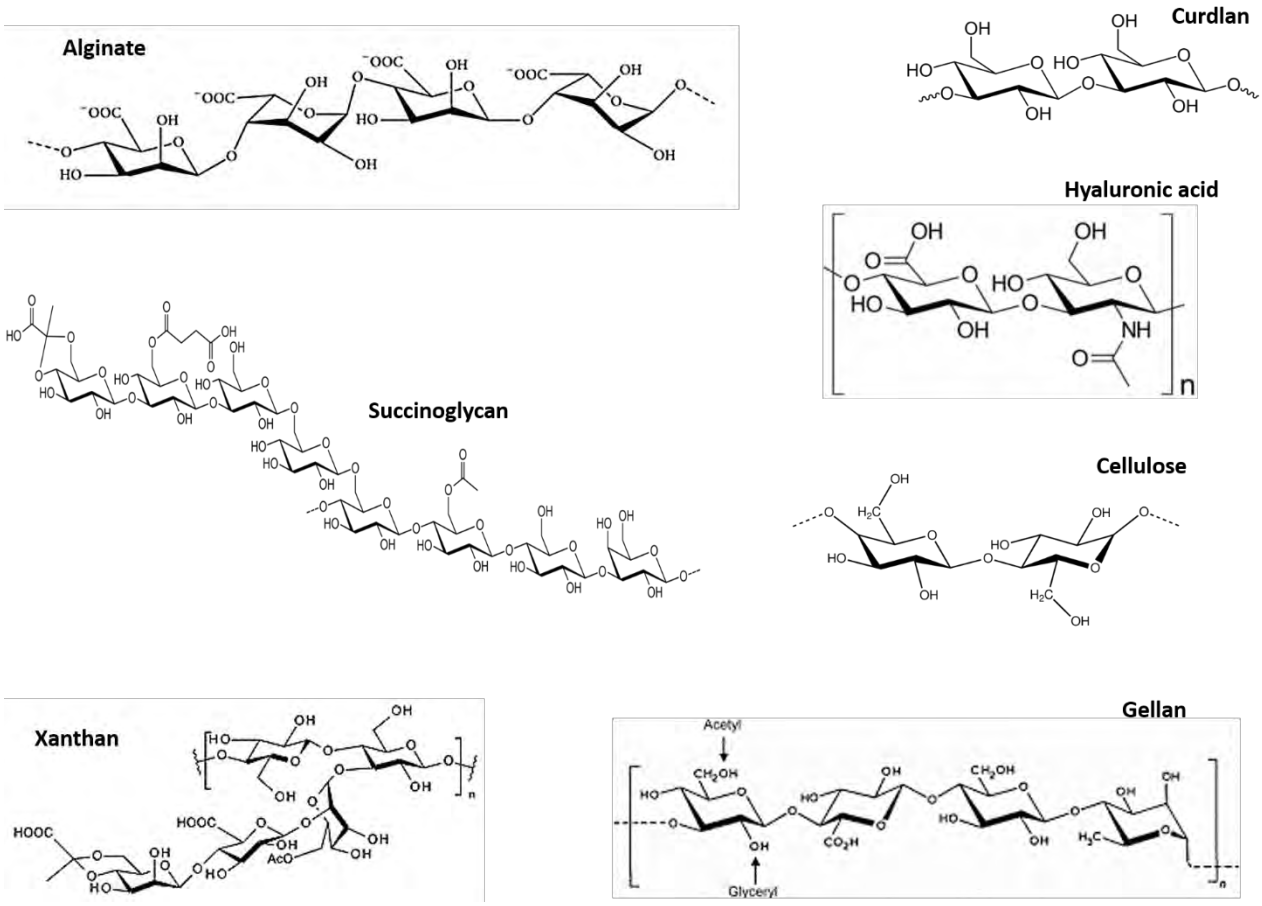

Figure 1.4: Chemical structure of some EPS molecules of bacterial and algal origin. Structures were obtained from Internet references 1-7.

Extracellular DNA is present in EPS particularly those from microbes involved in wastewater treatment. Although dependent on the type of organism, secretion of extracellular DNA is attributed to competent signalling peptides which support horizontal gene transfer between microbial cells and within the matrix (Czaczyk and Myszka, 2007; Flemming, 2011). EPS also contains lipids mainly as phospholipids and lipid derivatives such as lipopolysaccharides (More *et al*., 2014). There are also biosurfactants like surfactin and viscosin in EPS components which help in the dispersal of hydrophobic substances in the medium (More *et al*., 2014).

Humic substances are an essential part of EPS especially in biological wastewater treatment systems but are not typically secreted by microorganisms. Rather, these are adsorbed and incorporated into the matrix or scaffold where they influence the adsorption and biodegradability properties of EPS (More *et al*., 2014).

It has been argued that the formation of EPS is an important factor in determining the performance of microalgal–bacterial-based wastewater treatment systems (García *et al*., 2000; Arcila and Buitrón, 2017; Jimoh and Cowan, 2017). As such, these polymers appear to be among the main drivers of MaB-floc formation in IAPS and consequently increase the settling property of biomass (Barros *et al*., 2015; Arcila and Buitrón, 2017) which in turn, should enhance water treatment efficiency. While the polymers encapsulate microbial cells to bind floc components, activity depends on the source, structure, molecular mass, and composition (Trabelsi *et al*., 2015).

1.4.3 Sub-fractions of EPS and methods of extraction

Identification of EPS components greatly depends on the method of extraction (Wingender *et al*., 1999). Extracting pure EPS is a bit challenging even though various methods have been reported. For example, extracting the true EPS from HRAOP wastewater might be a little tricky due to the presence of other compounds and ions that can influence the composition and structure of the EPS. Therefore, methods must be carefully adapted for efficient EPS isolation and extraction.

EPS is distributed both inside (bound) and outside (soluble) microbial aggregates (Sheng *et al*., 2010). Soluble EPS is dissolved in the medium while bound EPS can be either loosely or tightly bound to the cell (Sheng *et al*., 2010; Ahmed *et al*., 2014). Soluble EPS are dispersed in the culture medium and therefore can be extracted by centrifugation or filtration, followed by organic solvent precipitation (i.e. methanol, ethanol, or 2-propanol). However, bound EPS are highly structured, tightly attached to the cells and they represent up to 50% of the total EPS (Delattre *et al*., 2016). Thus, either a physical or a chemical treatment must precede centrifugation and/or filtration. The physical treatments are carried out by sonication, heating, ultrasound, or the use of a microwave. Chemical treatments include the use of complexing agents such as sodium hydroxide, glutaraldehyde, formaldehyde, ethylene diamine tetraacetic acid (EDTA), and cation exchange resins (Wingender *et al*., 1999; Delattre *et al*., 2016). Organic solvent precipitation allows for selective concentration of EPS and has been used

successfully to extract many different EPS. The solvent can even be recovered by distillation if so desired, and the method is cheaper for industrial scale-up relative to other methods such as ultrafiltration (Delattre *et al*., 2016). While physical treatments always give low EPS yield, most of the chemical extraction methods either result in cell lysis, co-extraction of intracellular polymeric substances, or contamination of the EPS by the extraction chemicals (Delattre *et al*., 2016; Xiao and Zheng, 2016). Consequently, the properties and components of the extracted EPS can be altered in the process. As such, the use of cation exchange resins is widely regarded as the most efficient and reliable method of extraction because it does not result in cell lysis or alter the composition of the extracted EPS (Sheng *et al*., 2010).

1.4.4 Application of EPS

With the increased demand for the replacement of commercially available synthetic polymers with natural ones, there has been greater interest in the extraction of EPS from natural sources. These natural polymers, some of which include xanthan, gellan, dextran, alginates, and glucans, have found application in water treatment, food processing industries, and medicine (Table 1.4).

In water treatment, EPS can be used as a bioflocculant, and in the dewatering and settling of sludge (Czaczyk and Myszka, 2007; More *et al*., 2014). As opposed to chemical flocculants, biopolymer flocculants are biodegradable and nontoxic to most microorganisms (Jia and Yuan, 2016). In addition, they are easily produced and highly effective in the formation of stable flocs leading to a cost-effective removal of MaB-flocs from treated water. Thus, EPS can be a perfect alternative to the commercially available synthetics. Due to their adsorption properties, EPS can be used as biosorbent to remove heavy metals. Rose *et al*. (1998) and Van Hille *et al*. (1999) reported that *Arthrospira platensis* cultivated in wastewater HRAOP on a medium of acid mine produced EPS, which chelated about 94% of copper ions in the contaminated water.

Many reports have shown that EPS has considerably high emulsifying activity (Bramhachari and Dubey, 2006; Mishra and Jha, 2009). This makes them useful in industries as food additives, thickeners, emulsifiers, and biosurfactants to increase the viscosity and hydration of some food products (Xiao and Zheng, 2016). Some EPS are also used as edible coatings to prevent spoilage (Singha, 2012). The emulsification activity of EPS extracted from *Dunaliella salina* EPS under salt stress was 86%, which showed the ability of EPS to retain emulsion at a relatively higher rate than some commercial surfactants such as Tween 20 and Triton X-100

(Mishra and Jha, 2009). Due to the numerous bioactivities of EPS, they are used in medicine as a drug delivery agent, antiviral, antitumor, antioxidant, anti-inflammatories, and anticoagulants (Xiao and Zheng, 2016). Recently, a specific EPS from *Lactobacillus* was demonstrated to have potentials as antibacterial, antioxidant properties, and as a wound-healing agent (Trabelsi *et al*., 2017). Similarly, EPS from microalgae and diatoms such as *Chroococcus disperses*, *Chlamydomonas reinhardtii*, *Chlorella vulgaris*, and *Phaeodactylum tricornutum* possess some of these properties (Guzman *et al*., 2003; Ghasemi *et al*., 2007), which supports their application in medical and biomedical fields.

Table 1.4: Some microbial extracellular polymeric substances and their applications.

EPS	Producer	Application	Reference
Alginate	*Pseudomonas aeruginosa*, *Azotobacter vinelandii*	Food viscosifier, emulsifier, and gelling agent. Pesticide formulation and seed coating.	Galindo *et al*., 2007; Hay *et al*., 2013; Urtuvia *et al*., 2017
Xanthan	*Xanthomonas campestris*	Food thickener and stabilizer. Pharmaceutical formulations and drug administration	Garcia-Ochoa *et al*., 2000; Palaniraj and Jayaraman, 2011; Wang *et al*., 2017
Cellulose	*Acetobacter* sp.	Food, cosmetics and wound healing	Esa *et al*., 2014; Picheth *et al*., 2017
Curdlan	*Agrobacterium* sp., *Alcaligenes faecalis*	Food gelling agent	Shih *et al*., 2009; Yu *et al*., 2011; West and Peterson, 2014
Gellan	*Pseudomonas elodea*	Food stabilizer and gelling agent	Bajaj *et al*., 2007; Fialho *et al*., 2008
Pullulan	*Aureobasidium pullulans*	Edible film coating, drug delivery, flocculant and food additive	Cheng *et al*., 2011a; Sugumaran and Ponnusami, 2017; An *et al*., 2017
Scleroglucan	*Sclerotium* sp.	Cosmetics for skin and hair product formulation. For pesticide formulation	Fariña *et al*., 1998; Survase *et al*., 2007; Castillo *et al*., 2015
Succinoglycan	*Sinorhizobium meliloti*	Oil recovery, Food gelling agent and biocide formulations	Jones, 2012; Jofré *et al*., 2018
Xylinan	*Acetobacter xylinum*	Food viscosifier and gelling agent	Morris and Harding, 2009
Dextran	*Leuconostoc mesenteroides*	Gel filtration medium, cosmetics and anticoagulant therapy	Sarwat *et al*., 2008; Moosavi-Nasab *et al*., 2010; Devi *et al*., 2014
Hyaluronic acid	*Staphylococcus* sp. *Streptococcus* sp.	Drug delivery, wound healing and viscosurgery. Cosmetics moisturizing agent	Chong *et al*., 2005; Vázquez *et al*., 2015; Sze *et al*., 2016

1.5 Extracellular polymeric substances: Essential to MaB-floc formation and IAPS Efficiency

Although there are obvious benefits to be derived from EPS formation during wastewater treatment by IAPS, overproduction of these polymers might also be detrimental if not managed (Shi *et al*., 2017). As outlined above, EPS formation plays a crucial role in cell aggregation, adhesion, adsorption, and flocculation (More *et al*., 2014). Furthermore, polymers within the EPS matrix are amphoteric and possess both hydrophilic and hydrophobic characteristics that contribute to adsorption of organic pollutants, abstraction of nitrates, phosphates and ammonium, and hence water repair (Sheng *et al*., 2010). Thus, aggregation of microalgae, bacteria, and other microbes into MaB-flocs in HRAOPs of IAPS is critical to wastewater treatment and production of an effluent suitable for discharge and/or recycle/reuse. It is therefore important to better understand the structure and function of the EPS matrix of MaB-flocs in order to mitigate potential negative impacts and, to enhance the performance of wastewater treatment plants.

One of the most widespread methods of determining the efficiency of a wastewater treatment process is to measure its ability to reduce organic pollutant load, either as biological oxygen demand (BOD) or COD. This test typically reports the amount of oxygen required to either biologically or chemically oxidize susceptible organic pollutants in a known volume of water. Insofar as IAPS is concerned, effluent COD is mostly due to the soluble microbial product of which about 20% is EPS (Kunacheva and Stuckey, 2014). Indeed, Mambo *et al*. (2014a) reported that effluent COD from a pilot-scale IAPS treating municipal sewage was predominantly soluble organic carbon and, a follow-up study described the generation and characterization of soluble EPS produced in HRAOPs by the accumulating MaB-flocs (Jimoh and Cowan, 2017). Production of EPS can adversely affect performance data collected during routine monitoring by regulatory authorities and as a result, water quality from these systems might be considered below standard. Thus, it appears that the presence of EPS in the effluent following sedimentation of MaB-flocs can significantly contribute elevated COD to IAPS effluent.

Although EPS are biodegradable and aggregated cells do use these polysaccharides harboured within the matrix when carbon is in short supply, not all EPS can be degraded. In some instances, biodegradability depends on molecular weight distribution. For example, Aquino *et al*. (2009) reported that high molecular weight EPS is more difficult to degrade and is only

partially degraded even after extended incubation periods. Thus, biodegradability and degradation of EPS may be detrimental to IAPS in at least two ways. First, the more difficult to degrade EPS may contribute COD to the treated water to reduce overall water quality (Wang and Zhang, 2010; Kunacheva and Stuckey, 2014). Second, the production of more readily biodegradable EPS could result in de-flocculation of the aggregated MaB-flocs. Aside from the loss of floc settleability and reduced ability to harvest biomass, de-flocculation will increase the likelihood of washout and lead to elevated TSS concentration. Since TSS is also used to gauge the quality of treated wastewater, an increase in its value might be taken to indicate poor process efficiency. Biodegradability of EPS formed by MaB-flocs seems therefore to be critical to the efficient performance of IAPS as a wastewater treatment technology. One possible way to guarantee success is to ensure that the appropriate EPS forming microbes (i.e. indicator species) are present and active and in the correct ratio. Indeed, maintaining correct levels of EPS in wastewater treatment plants plays a major role in facilitating floc formation and settling.

In the context of EPS management, it is important to promote the growth of indicator species that are good EPS producers in HRAOPs. Cyanobacteria are a good example of such key species. Many studies have pointed to cyanobacteria in securing and supporting microbial interactions due to a role in primary colonization of immobilized environments (Rossi and De Philippis, 2015). Secondly, in the domain of algal EPS production, they are the most studied (Parikh and Madamwar 2006; Mishra and Jha, 2009; Ahmed *et al*., 2014; Barros *et al*., 2018). Lastly, cyanobacterial EPS have some distinguishing properties such as the presence of sulphate groups and uronic acids which confer stickiness to these EPS (Rossi and De Philippis, 2015). Taken together, the abovementioned reasons suggest that cyanobacteria may be ideal candidates to ensure constant and stable floc formation in HRAOP.

High levels of EPS can also cause foaming and other effluent violations but are essential for good floc formation (Glymph, 2005). Bacteria of the genus *Zoogloea* are known to excrete high levels of EPS and, *Zoogloea ramigera* has long been considered an ideal candidate species for floc formation in activated sludge (Rosselló-Mora *et al*., 1995). Also, an EPS-producing strain of *Cloacibacterium normamense* was isolated from municipal sludge and shown to possess high flocculation activity and good settleability (Nouha *et al*., 2015). Furthermore, in recent studies, Nguyen *et al*. (2017) isolated several EPS-producing bacteria from the treatment of beer and winery wastewater and, mycelial pellets of *Streptomyces* sp. hsn06 caused rapid flocculation of *Chlorella vulgaris* (Li *et al*., 2017a and 2018).

Interestingly, nutrient deficiency due to reduced nutrient supply in the activated sludge process results in bulking, which occurs when sludge does not settle easily due to excessive volume. This is usually associated with the presence of a variety of filamentous bacteria like *Streptomyces* and certain cyanobacteria, that grow as long strands, produce an EPS composed mainly of glucose and mannose, have much greater volume and surface area than conventional flocs, and therefore are very slow to settle (Li *et al*., 2017a; Elnahas *et al*., 2017). Thus, an inability to separate microbial biomass from the treated effluent will decrease the efficiency of wastewater treatment (García *et al*., 2000). Among the causative factors is phosphorous deficiency (Turtin *et al*., 2006). Indeed, nitrogen and/or phosphorous deficiency can influence the formation of both EPS and microalgal coenobia (Peng *et al*., 2003; Glymph, 2005; O'Donnell *et al*., 2013) while the amount of protein and carbohydrate in the EPS appears to influence settling (Sheng *et al*., 2010). Thus, a major function of bacterial EPS seems to be both concentration of nutrients when nutrient-deficient conditions prevail and floc formation. So, both the level and the composition of EPS in HRAOP water of an IAPS might similarly either assist or hinder settling of MaB-flocs.

Performance of WSP could be enhanced by the addition of activated sludge bacteria without the need for either aeration or sedimentation due to the incorporation of algae into flocs (Gutzeit *et al*., 2005). This simple and successful removal of algae indicated that floc formation was key to this innovation. Similarly, early studies on microalgal-bacterial mutualism revealed that hydraulic retention time (HRT) and organic loading were among the main parameters required for symbiotic algal-bacterial (i.e. MaB-floc) growth in pond systems and, that algal growth itself was favoured at short HRT with high loading (Oswald *et al*., 1953a). Confirmation of the principle of the effect of food to microorganism ratio (F/M) and HRT on pond performance followed from studies showing that either the F/M ratio should be low or cell retention sufficient to allow the formation of stable flocs (Medina and Neis, 2007). More recently, recovery efficiencies of more than 99% could be achieved for microalgae, albeit by fast sedimentation of granules, after the formation of activated algae granules by addition of the filamentous cyanobacterium *Phormidium* sp. (Tiron *et al*., 2017).

Taken together, this accumulated information suggests that both environmental and operational conditions impact EPS production, accumulation, and chemical composition which in turn determines MaB-floc formation and stability, settleability and sedimentation, and quality of the final treated water.

1.6 Summary and research needs

This chapter provided an overview of wastewater treatment using IAPS bioprocess technology, and several of its inherent advantages over more energy-expensive mechanical processes and appropriateness for the deployment of the technology in the per-urban space were discussed. Also, some of the co-product streams that can be tapped in addition to the derivation of water for recycle/reuse were highlighted. In addition, the role of microbial interaction and bioflocculation in wastewater treatment was emphasized in relation to the importance of each in IAPS performance and treatment efficiency for domestic sewage. In view of this, the following conclusions were drawn:

- Through a symbiotic microbial interaction in HRAOPs of the IAPS, MaB-flocs are formed and essentially contribute to decreased cost and enhanced sustainability of this wastewater treatment process.
- Given the role of these components in biological systems, EPS appears as the major biocatalyst responsible for MaB-floc formation, and thus, facilitates biomass flocculation and harvesting in the bespoke system. Thus, it is crucial to understand factors that contribute to EPS production to achieve stable floc formation and maintain system efficacy.
- It is also apparent that EPS may contribute a significant proportion of COD as dissolved organic carbon which can be detrimental in terms of the regulations for the quality of the final treated water. It is therefore important to appreciate that poor environmental conditions and operational management can impact floc formation, nutrient abstraction, and water quality.
- For efficient management of EPS in IAPS, it is important to promote the growth of indicator species that are good EPS producers in HRAOPs.
- To date, EPS and MaB-floc formation in HRAOPs have been studied largely at a laboratory scale, and, as such, little information is available on the effect of environmental parameters. The latter is expected to exert a considerable effect on the operation of IAPS in a commercial setting. Thus, the response to changes in various operational and environmental conditions in terms of EPS production and MaB-floc formation in HRAOPs of IAPS must be investigated.

1.7 Aim and objectives

Despite the potential benefits that can be achieved from adoption, uptake and utilization of IAPS as a wastewater treatment system by local government bodies and industries in South Africa and other parts of the world, this is yet to be realized (Cowan *et al*., 2016; Sutherland and Ralph, 2020). Thus, the current study was motivated by the need to investigate MaB-flocs and EPS as essential drivers of fully operational solar-driven IAPS systems for use in peri-urban areas without any adverse impact. The aim of the study was to therefore investigate and address the importance and function of EPS production and MaB-floc formation in wastewater treatment, towards the development of a successful IAPS system that can fit in a circular economy. The specific objectives were to:

- Study the dynamic and structure of MaB-floc and EPS production in the MLSS generated in HRAOP of an IAPS with respect to bioflocculation and biomass recovery from the system.
- Carry out a metagenomics study on MLSS to investigate the influence of microbial diversity on flocculation and settleability of biomass, and identify the major species contributing to this phenomenon.
- Select EPS-producing microorganisms from MLSS and investigate their roles and contribution to the formation of MaB-flocs.
- Extract and study the characteristics of EPS and other valuable product(s) accumulated in MLSS in order to determine their biotechnological and commercial importance.

Chapter 2: Materials and Methods

2.1 IAPS configuration and operation

The IAPS used in this study is located at the Institute for Environmental Biotechnology Rhodes University (EBRU), Belmont Valley WWTW, Makhanda, South Africa (33° 19′ 07″ South, 26° 33′ 25″ East, Figure 2.1). The design and optimization, process flow, and operation of the system have been well described (Rose *et al*., 2002; 2007; Mambo *et al*., 2014a & b). The system (Figure 1.1) is supplied continuously with a maximum of 75 m^3/d domestic sewage and comprises an AFP, two HRAOPs, and two ASPs connected in series. The 840 m^2 AFP has a total volume of 1500 m^3, HRT of 20 d and incorporates a 225 m^3 IPD, where anaerobic biodegradation of suspended and dissolved solids takes place. Each HRAOP has a surface area of 500 m^2, a total volume of 150 m^3, a depth of 0.3 m, and HRT of 2 and 4 d respectively. Mixing and turbulent flow essential for nutrient uptake and biomass productivity are achieved by an eight-bladed paddlewheel powered by an electric motor (0.25 kW). Effluent from AFP decants under gravity to the first HRAOP from where it flows via a 12.5 m^2 ASP A and half of the effluent (37.5 m^3) pumped to the second HRAOP after settling for 0.5 d. The water is further treated in this second HRAOP before effluent flows by gravity to ASP B for another 0.5 d. Biomass slurry from both ASPs is pumped into drying beds (DB) and treated water pumped back to the WWTW.

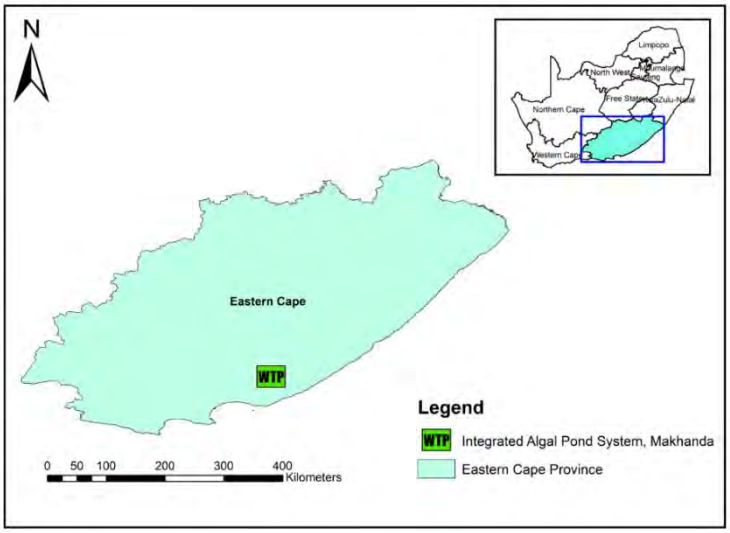

Figure 2.1: A map showing the geographical location of the pilot-scale IAPS used in the current study. The coordinates were taken using Garmin Etrex 20.0GPS devices. The map was plotted in Arc GIS 9.3 software.

2.2 Sampling procedure and analysis of MLSS/water

2.2.1 Sampling

Grab samples of MLSS were collected from the HRAOP for all investigations in the current study. The second HRAOP was selected because it is the pond with the highest nutrient abstraction due to its longer HRT. Samples were taken for investigations of biological components of MLSS, EPS production, biomass concentration as well as isolation and screening of microorganisms (including bacteria, cyanobacteria, and microalgae) associated with MaB-flocs. At all times, sampling was carried out between 16:00 h and 17:00 h since the highest diurnal biomass production in this HRAOP was reported to occur during this period (Jimoh and Cowan, 2017). Approximately 1 L grab samples of MLSS were collected from directly in front of the paddlewheel and transferred to the laboratory for various analyses or refrigerated at 4^{o}C if to be analysed the next morning. For evaluation of biomass and EPS production, sampling was carried out fortnightly while a seasonal sampling interval was adopted for a metagenomic study to achieve a reasonable account of the microbial population in HRAOP. Where necessary, samples were also collected from HRAOP in the absence of paddlewheel mixing to determine its effect on EPS production and formation of MaB-flocs. When necessary, primary-treated water samples were also collected from the effluent of AFP for various experiments.

2.2.2 Physicochemical analysis

Physicochemical parameters including temperature, pH, and electrical conductivity of the MLSS were measured *in situ* during the period of investigation. Temperature and electrical conductivity of water samples were measured using an EC Testr11 Dual range 68X 546 501 detector (Eutech Instruments, Singapore) while pH was measured using a microcomputer pH meter (Eutech Instruments). The daily temperature and direct normal irradiance (DNI) data for the period of sampling were obtained from the Southern African Universities Radiometric Network (SAURAN, Brooks *et al*., 2015) and the most complete data from University of Fort Hare was used (32° 47′ 13.4″ South, 26° 50′ 56.7″ East, Elevation: 540 m).

2.2.3 Chemical analysis

COD and nutrient (ammonium, NH_4^+-N; nitrate, NO_3^-N; and phosphate, PO_4^{3-}-P) analysis were carried out using commercially available test kits (Merck Chem. Co., Darmstadt,

Germany) according to the manufacturer's instructions. Details of standard curve preparation and equations for interpolation of COD and nutrient analysis is given in Appendix A, Table A1.

2.2.4 Estimation of MaB-floc concentration

Biomass production in HRAOP was estimated as the concentration of suspended solids (i.e. MaB-flocs) present in MLSS samples. A known volume of well-stirred water sample from HRAOP was filtered using pre-dried and weighed (placed in a desiccator prior to use) Whatman glass microfiber filter discs of pore size 0.45 µm (grade GF/C; Merck Chemicals, South Africa). The filters containing the suspended solids were oven-dried at 105ºC until a constant weight was achieved (at least 1 h) and cooled in a desiccator for at least 30 min before determining the weight. The weight of the dried filters was recorded, and the concentration calculated using the following expression.

$$\text{MLSS (mg/L)} = [(A - B) \times 1000] \div [\text{Volume of sample (mL)}] \times 1000 \qquad \textbf{Equation 2.1}$$

Where: A = sample + filter weight, and B = weight of the filter paper.

2.2.5 Biomass settleability

The Settleability of MaB-flocs in MLSS, and of microalgal cultures was determined according to standard methods (APHA, 1998; 2540 F). An Imhoff cone was filled with 1 L of well-mixed MLSS sample from HRAOP and allowed to settle for 1 h. A known volume of sample was gently siphoned from the centre of the cone at a point halfway between the surface of the settled biomass and the liquid surface, to determine the concentration of non-settleable solids. Settleability was calculated using the following expression.

$$\text{Settleability (\%)} = [\text{MLSS (mg/L)} - \text{non-settleable (mg/L)} \div \text{MLSS (mg/L)}] \times 100 \qquad \textbf{Equation 2.2}$$

2.2.6 Biomass productivity

The areal productivity of HRAOP in $g/m^2/d$ was calculated from the MLSS concentrations using the following expression adopted from (Al-Shayji *et al*., 1994).

$$P = 10 \times d/t \times n \times \text{MLSS} \qquad \textbf{Equation 2.3}$$

Where: P is pond productivity ($g/m^2/d$),

d = pond depth (m),

t = hydraulic retention time of the pond (d),

MLSS = total mixed liquor suspended solids (g), and

n = algae ratio in the MLSS (0.9-1.0) as estimated by Al-Shayji *et al.* (1994).

2.3 Metagenomic analysis of MLSS

To investigate the microbial composition and diversity of MLSS in HRAOP, samples were taken at seasonal intervals (between March and December 2019) for next-generation sequencing (NGS). MLSS samples (1 L) were collected directly in front of the paddlewheel of HRAOP to obtain a homogeneous sampling and metagenomics study was carried out.

2.3.1 Total Genomic DNA extraction, amplification, and purification

The suspended solids of 500 mL MLSS samples were collected by successive filtration through 0.45 µm membrane filters to retain the MaB-flocs and other suspended microalgae followed by 0.22 µm membrane filters to retain the smaller bacteria. Biomass on both filter sizes were pooled and total genomic DNA was extracted using a DNA isolation kit (Zymo Research), according to the manufacturer's instructions. The resulting genomic DNA extracts were amplified using 16S universal primer pair 515f (5'-GTGYCAGCMGCCGCGGTAA-3') and 926r (5'-CCGYCAATTYMTTTRAGTTT-3') at a region of 450 bp for identification of archaeal and bacterial population. The microalgal and other higher organisms such as rotifers, ciliates, protozoans, and fungi were identified by amplification of 18S target site using universal primer pair 1391f (5'-GTACACACCGCCCGTC-3') and EukBr (5′-TGATCCTTCTGCAGGTTCACCTAC-3′) at a region of approximately 260 bp.

The PCR mix contained 5 µL of extracted genomic DNA, 12.5 µL master mix, 0.5 µL of each respective primer pairs, and 6.5 µL molecular grade water to make up 25 µL reaction volume. The 16S rRNA gene was subjected to initial denaturation of 94ºC for 3 min, followed by 35 cycles of 94ºC for 45 s, 50ºC for 60 s, and 72ºC for 90 s of denaturation, annealing, and extension respectively, and a final extension of 72ºC for 10 min in an Applied Biosystems SimpliAmp™ Thermal Cycler (Thermo Fisher Scientific, Singapore). The 18S rRNA target was amplified by initial denaturation of 90ºC for 15 min, 94ºC for 60 s of denaturation, 60ºC for 60 s of annealing, 72ºC for 60 s of extension, and a final extension at 72ºC for 7 min. For purification of the amplified products, gel electrophoresis was carried out (Figure 2.2) and DNA bands were cut and purified using FavorPrep™ gel purification mini kit (Favorgen),

according to the manufacturer's instructions. The purified products were sequenced using GS Junior Titanium Sequencing Platform (454 Life Sciences, Roche).

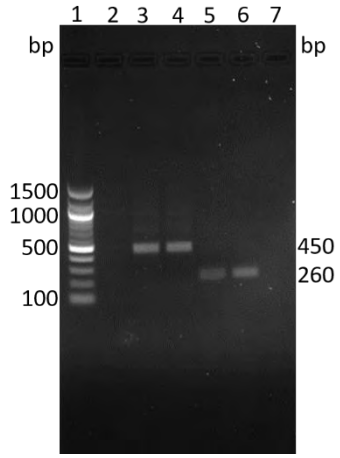

Figure 2.2: Gel electrophoresis of the purified 16S rRNA (Lane 3 and 4) and 18S rRNA (Lane 5 and 6) targets of MLSS from HRAOPs of an IAPS treating domestic sewage. The sizes of the purified fragments were estimated by comparison to a 100 bp DNA marker (BioLabs®, Lane 1).

2.3.2 Pyrosequencing data analysis

Datasets were curated using version 1.41.3 of Mothur software package (Schloss *et al*., 2009), where low-quality reads and ambiguous nucleotides were removed from the sequences. After taxonomic identification, chimeric sequences were also identified and removed using UChime algorithm. Classification and alignment of sequences were done using SILVA (version 132) as a reference database. Following these, a distant matrix of 0.03 was created on the curated datasets to cluster sequences into operational taxonomic units (OTU) at a similarity level of 97%. Following the removal of singletons (OTUs that were assigned only a single read), the OTUs were classified to genus level against the SILVA database to assign taxonomic identity at a confidence threshold of 80%. Dominant OTUs were further compared to the standard nucleotide using the NCBI-BLAST database. The phylogenetic relatedness of the dominant prokaryotic and eukaryotic population in HRAOP (Appendix B; Figure B3 and B4) was carried out using the Neighbour-Joining method in Mega 6.0 software package (Tamura *et al*., 2013).

The microbial phylotype richness and evenness were estimated using abundance-based coverage estimator (ACE), Chao, Shannon, and Inverse Simpson (Invsimpson) index incorporated in Mothur software. Rarefaction analysis was employed to observe and compare differences and diversity between samples. The rarefaction calculations were carried out within

Mothur package and curves were generated for a distance value of 0.03. An account of the community structure and diversity was given in bar plots, and heatmaps constructed using an online platform (Babicki *et al*., 2016).

2.4 Isolation and purification of microorganisms

2.4.1 Isolation of bacterial strains

Bacteria were isolated from MLSS in HRAOPs by serial dilution of aliquots of MaB-floc suspension in phosphate buffered saline (PBS). Diluted samples (0.1 mL) were spread on prepared nutrient agar plates (containing in 1 L of deionized water, 1.0 g meat extract, 5.0 g peptone, 2.0 g yeast extract, 8.0 g sodium chloride and 15.0 g agar, Merck Pty. Ltd., South Africa) and incubated at 37^{o}C for 24 h. Repetitive sub-culturing was by streaking on nutrient agar and incubation at 37^{o}C for 24 h until pure colonies were achieved.

2.4.2 Isolation of cyanobacterial strains

MaB-flocs containing cyanobacterial species were inoculated on sterilized BG-11 enriched agar medium and incubated under continuous cool, white fluorescent light (15 W; 70-90 µmol m^{-2} s^{-1}) in a growth room at 25^{o}C until enough growth was achieved. The BG-11 consisted of (mg/L deionized water) 1500.00 $NaNO_3$, 30.00 K_2HPO_4, 75.00 $MgSO_4.7H_2O$, 36.00 $CaCl_2.2H_2O$, 6.00 citric acid, 6.00 ferric ammonium citrate, 1.00 EDTA, 20.00 Na_2CO_3 and 1 mL/L trace element solution (prepared by adding 2.86 g H_3BO_4, 1.81 g $MnCl_2.4H_2O$, 0.22 g $ZnSO_4.7H_2O$, 0.39 g $NaMoO_4.2H_2O$, 0.08 g $CuSO_4.5H_2O$ and 0.05 g $Co(NO_3)_2.6H_2O$ to 1 L deionized water). Cyanobacterial filaments from the agar plate were transferred to freshly prepared agar plates and incubated for 30 d, and this process was repeated until a pure strain was achieved.

2.4.3 Isolation of microalgal strains

Microalgal species used for investigations were isolated from MLSS in HRAOP of the IAPS used in this study. From a 1 L MLSS sample containing MaB-flocs, 200 µL aliquots were inoculated onto sterilized agar medium using the spread-plate technique. When necessary, samples were first diluted to an appropriate concentration using the serial dilution technique. The medium used was Bold basal (BBM) containing (mg/L deionized water) 62.50 $NaNO_3$, 6.30 $CaCl_2.2H_2O$, 43.75 KH_2PO_4, 18.75 K_2HPO_4, 18.75 $MgSO_4.7H_2O$, 6.30 NaCl, 10.00 Na_2EDTA, 4.98 $FeSO_4.7H_2O$, 2.01 H_3BO_3 and 1 mL/L trace element solution. The trace

element solution contained (g/L deionized water) 1.81 $MnCl_2.4H_2O$, 0.22 $ZnSO_4.7H_2O$, 0.39 $NaMoO_4.5H_2O$, 2.86 H_3BO_3, 0.08 $CuSO_4.5H_2O$ and 0.05 $Co(NO_3)_2.6H_2O$. Agar plates were incubated under continuous cool, white fluorescent light (15 W; 70-90 µmol m^{-2} s^{-1}) in a growth room at 25°C until sufficient cell growth had taken place. Upon the emergence of colonies, single colonies were picked and inoculated into 100 mL freshly sterilized BBM medium and cultured for 14 d.

2.4.4 Cell culture and growth conditions

Pure bacterial isolates were either maintained in Luria Broth (LB) in an incubator at 37°C or stored in 30% glycerol at -40°C and sub-cultured every six months. Growth pattern, colony, and cellular morphology of isolates in LB and on nutrient agar were carried out within 24 and 48 h of incubation at 37°C. The growth of all bacterial isolates was determined by measuring the optical density of cultures at 600 nm in a spectrophotometer (Shimadzu UV-1280, Japan) with LB as background. Colony appearances and pigmentation were observed on nutrient agar, while Gram staining was performed using the standard method. Catalase activity was detected by observing bubble production of freshly cultured bacterial isolate in 3% (v/v) hydrogen peroxide on a glass slide (Hao and Komagata, 1985).

Isolated cyanobacterial strain was maintained in BG-11 medium in a growth room under conditions stated in Section 2.4.2 throughout the study and sub-cultured every 30 d to maintain an axenic culture for other experiments. Selected microalgal strains were cultured and maintained in BBM in a growth room under conditions described in Section 2.4.3. cells were sub-cultured every 30 d to maintain an axenic culture.

2.5 Microscopy

2.5.1 Stereo microscopy

For determination of size distribution and shape of granules formed by cyanobacterial isolates, samples were placed in a dish containing PBS and viewed using an OLYMPUS SVX2-ILLT stereo microscope (Tokyo, Japan). The size and structure of aggregates and flocs were examined, and images were captured with attached camera (Olympus SZX16).

2.5.2 Light microscopy

The composition and structure of the MaB-flocs in MLSS samples and identification of selected microalgal strains were examined using a Zeiss Axiostar plus optical microscope (Carl Zeiss, Jena, Germany). A drop of well mixed MLSS was placed on a glass slide, covered with a glass slip before examination, and images were captured using a Canon PowerShot G12 (Canon Inc., Japan) digital camera. The most abundant and dominating microalgal species in the images were identified by reference to published identification keys and previous studies on the IAPS (Belcher and Swale, 1978; Cassie, 1983; Huynh and Serediak, 2006; Johnson, 2010).

2.5.3 Scanning electron microscopy

Cellular morphology and dimensions of bacteria and cyanobacteria were determined by scanning electron microscopy (SEM). Bacterial culture grown for 24 h in LB was centrifuged 10,000 × *g* for 10 min. The pellet containing bacterial cells was washed thoroughly with PBS to remove residual nutrients from the cells. Bacterial and cyanobacterial cells were fixed in 0.5 mL 2.5% glutaraldehyde in 0.1 M potassium phosphate buffer for 24 h at 4^{o}C. After removal of glutaraldehyde solution by centrifugation, cells were dehydrated using a graded series of ethanol solution with concentrations; 30, 50, 70, 90, and 100% for 10 min. Dehydrated samples were immersed in 1 mL hexamethyldisilazane for 10 min and left to air-dry at room temperature (RT) in a fume cupboard overnight. After drying, samples were mounted on specimen stubs with double-sided conductive tape, gold-coated, and then viewed using a Vega 3 LMU TESCAN analytical scanning electron microscope.

2.6 Molecular identification of microorganisms

2.6.1 Identification of bacterial strains

Total genomic DNA was extracted from bacterial strains of interest using a DNA isolation kit (Zymo Research), according to the manufacturer's instructions. DNA extracts were sent to Inqaba biotec™, South Africa for sequencing and identification. Universal primer pair 27F (5'-AGAGTTTGATCMTGGCTCAG-3') and 1492R (5'-CGGTTACCTTGTTACGACTT-3') were used in amplification followed by gel electrophoresis for extraction of amplicons with Zymoclean™ Gel DNA Recovery Kit (Zymo Research). Extracted fragments were sequenced in the forward and reverse direction using Nimagen, BrilliantDye™ Terminator Cycle Sequencing Kit and purified using ZR-96 DNA Sequencing Clean-up Kit™ (Zymo Research).

Purified fragments were analysed on an ABI 3500XL Genetic Analyzer (Applied Biosystems, ThermoFisher Scientific). Generated ab1 files were trimmed, edited, and aligned using BioEdit (version 7.0.5.3) and Chromas (version 2.6.6), followed by a BLAST search (Internet reference 8) to determine the nearest match in the complete nucleotide database. Phylogenetic trees were constructed with neighbour joining algorithms using 1000 bootstraps consensus available in Mega 6.0 software package (Tamura *et al*., 2013).

2.6.2 Identification of cyanobacterial strains

Total genomic DNA was extracted from cyanobacterial strain using a DNA isolation kit (Zymo Research), according to the manufacturer's instructions. DNA extracts were amplified using 16S universal primer pair and conditions described in Section 2.3.1. Amplified products were cleaned using the EXOSAP protocol by Werle *et al*., (1994), followed by cycle sequencing using Big Dye Sequencing Kit (Applied Biosystems, USA). For cycle sequencing in both forward and reverse direction, reaction volume was 10 µL and contained 1µL of Big Dye sequencing reagent, 1.5 µL of Big Dye Sequencing buffer, 3.2 µM primer and 3-10 ng of cleaned amplicons. The mixture was amplified in a Veriti 96 Well thermocycler (Applied Biosystems, Carlsbad, USA) and conditions were initial denaturation for 1 min at 96°C followed by 25 cycles of denaturation and annealing for 10 s each at 96°C and 50°C respectively, with a final extension step of 4 min at 60°C. The samples were purified using the specific ethanol-EDTA precipitation method for the Cycle Sequencing Kit, and then air-dried. Dried fragments were analysed on a Genetic Analyser (Applied Biosystems 3500, USA) of the Genetic Laboratory of the South African Institute for Aquatic Biodiversity (SAIAB). Generated files were edited, and nearest match determined as described in Section 2.6.1.

2.7 Effect of exogenous chemicals on microorganisms

2.7.1 Effect of antibiotics on bacterial strains

Antimicrobial susceptibility of the isolates was tested using different classes of antibiotics such as kanamycin, tetracycline, chloramphenicol, norfloxacin, and ertapenem. These antibiotics (MastDiscs® AST, Merseyside, UK), infused in 5 mm discs at fixed concentrations (10-30 µg/disc) were placed on nutrient agar plates spread with a fresh culture of each isolate. Agar plates were checked for zones of inhibition around the discs to confirm susceptibility or resistance against the antibiotics after 24 h of incubation at 37^{o}C.

2.7.2 Effect of antibiotics on cyanobacterial flocs

Batch experiments were conducted to investigate the effect of various antibiotics on the growth and floc formation by filamentous cyanobacteria. A stock solution containing either tetracycline, chloramphenicol, ampicillin, streptomycin, kanamycin, actinomycin, or rifampicin was dissolved in either water or ethanol according to their solubility and stored at -20°C. Test solutions were prepared by adding the various antibiotics at a concentration of 50 µg/mL to 50 mL BG-11 medium in 100 mL Erlenmeyer flasks. A control test containing no antibiotic was also prepared for comparison. In this study, a high and constant concentration (higher than the minimum inhibitory concentrations (MIC) was used for all antibiotics in order to make a better comparison, if any, in their effect on the isolate since antibiotic sensitivity is dependent on cyanobacterial strain (González-Pleiter *et al*., 2019). Moreover, MIC varies across all classes of antibiotics, where some are toxic only at high concentrations (Dias *et al*., 2015; González-Pleiter *et al*., 2019). All flasks were adjusted to pH 7.0 and incubated under conditions described in Section 2.4.2 but using a 12/12 h light/dark cycle for 21 d.

2.8 Extraction of pigments and extracellular polymeric substances

2.8.1 Extraction of pigments

Extraction was done according to the method of Mohammadi *et al*. (2012) with some modifications. To determine the most suitable solvent for extraction and enhanced pigment recovery, eight different solvents (acetone, n-hexane, diethyl ether, ethyl acetate, methanol, ethanol, benzene, and chloroform) with a range of different polarity were employed. Pigmented strains were grown in LB at 37°C for at least 48 h with shaking at 120 rpm. Pigmented cells were harvested by centrifuging 2 mL of culture at 10,000 rpm for 10 min. Pellets were resuspended in 500 µL ice-cold methanol and extracted in darkness at RT for 20 min with occasional mixing. Cell debris was removed by centrifugation, and the extraction procedure repeated until complete extraction of pigments was achieved. The supernatants were pooled, and concentrated under vacuum in a centrifugal concentrator (Labconco CentriVap®, Kansas) at 35°C followed by saponification or used directly for various analyses.

When required, extracted pigments were saponified according to a method described by Delgado-Pelayo and Hornero-M ndez (2012) with some modifications. An equal volume of 10% (w/v) methanolic KOH and 2 volumes of dichloromethane was mixed with the crude methanolic extract. The mixture was allowed to react in the dark at RT for 1 h without stirring.

The organic phase containing the carotenoid was washed several times with Milli-Q water to remove KOH, and finally with an equal volume of 2% (w/v) Na_2SO_4 solution to remove traces of water in the organic fraction. The organic fraction was evaporated to dryness under vacuum in a centrifugal concentrator.

Extracted pigments were scanned in a UV-Vis spectrophotometer (Shimadzu UV-1280, Japan) in the range 350-700 nm. Aliquots of the methanolic extract were chromatographed on thin layers of silica gel 60 GF_{254} (Merck, Darmstadt, Germany) under nitrogen gas and developed once to 8 cm in chloroform/methanol/dichloromethane (40:10:50, v/v/v). The Retention factor (R_f) value (calculated by dividing the solvent font by the pigment font) of each pigmented zone after development was determined, and eluted from the silica gel and analysed spectrophotometrically to derive the respective λ_{max}. The relative composition of individual pigment (P_c) to the total crude extract was calculated using the following expression.

$$P_c\,(\%) = {}^*A_{466\ nm} / A_{466\ nm} \times 100 \qquad \textbf{Equation 2.4}$$

Where; P_c is the composition of the individual pigments, $A_{466\ nm}$ is the absorbance of total crude extract and, $^*A_{466\ nm}$ is the absorbance of the individual pigments.

Purified and/or separated pigments were quantified and further analysed by either Fourier transformed infrared (FTIR) and/or Nuclear magnetic resonance (NMR) spectroscopy.

2.8.2 Extraction of extracellular polymeric substances

2.8.2.1 EPS from MLSS

Two forms of EPS were extracted from MLSS in HRAOP of the IAPS. Soluble EPS (S-EPS) and bound EPS (B-EPS; that found in close association with MaB-flocs) were extracted from MLSS samples following methods described by (Lin *et al*., 2010 & 2013; Ahmed *et al*., 2014) from samples collected at 14 d intervals for a period of one year.

Approximately 1 L MLSS samples were centrifuged using an Avanti® J-E centrifuge; Beckman Coulter Inc, USA) at 10,000 × *g* for 15 min to separate mixed liquor (containing S-EPS)) from the MaB-flocs (containing B-EPS). A 100 mL of the supernatant containing the S-EPS was filtered through 0.22 µm filter and two volumes of absolute cold ethanol was added and kept at 4°C overnight to precipitate the EPS. The pellet of MaB-flocs containing the B-EPS was suspended in 20 mL 0.2 M Na_2CO_3 at 60°C in a water bath for 1 h, with occasional mixing.

The suspension was centrifuged at 10,000 × *g* for 15 min and the pellet discarded. The supernatant pH was adjusted to 2 using 0.1 M HCl, followed by precipitation of the EPS using two volumes of absolute cold ethanol. The precipitate of S-EPS and B-EPS were collected from ethanol solution by centrifugation at 16,000 × *g* for 20 min at 4ºC and the EPS pellet suspended in Milli-Q water. The solution was flash-frozen with liquid nitrogen prior to freeze-drying (VirTis Benchtop SLC freeze dryer), and samples weighed and stored in a desiccator for further analysis.

2.8.2.2 EPS from bacterial strains

Screening for EPS producers was carried out as described by Rühmann *et al*. (2015). Those strains showing a ropy, slimy, mucoid, or other distinctive characteristics such as pigmentation on either solid (nutrient agar) or liquid (LB) medium were selected for further investigations.

EPS from selected strains was obtained by production in LB medium containing (g/L deionized water) 10.0 tryptone, 5.0 yeast extract, and 10.0 NaCl over time. Bacterial cells in the exponential growth phase were inoculated into 100 mL medium in 250 mL Erlenmeyer flasks and incubated at 37ºC in a microprocessor-controlled platform shaking incubator (Labcon, South Africa) at 100 rpm for 96 h. For extraction of EPS, samples of bacterial culture were centrifuged at 10,000 × *g* for 10 min, and the supernatant filtered through 0.22 µm membrane filters to remove suspended cells. Two volumes of ice-cold ethanol were added, and the EPS precipitated at 4ºC overnight. Precipitated EPS was recovered by centrifugation, the pellet resuspended in distilled water and lyophilized. Mass of the recovered EPS was determined and stored in a desiccator for further analysis.

2.9 Spectrophotometric analyses

2.9.1 Quantification of pigments

Total pigment yield was determined by estimation of the β-carotene equivalent as described by Quijano-Ortega *et al*. (2020). The absorbance of pigment extracts in methanol was measured in a spectrophotometer at 466 nm. The concentration of pigment in sample extracts was determined by interpolation with a standard curve prepared for β-carotene (Sigma Aldrich, South Africa) using the following expression.

$$P_t\,(\mu g/g) = [(A_{466\ nm} - b) \div m] \times (V \div W) \times DF \qquad \textbf{Equation 2.5}$$

where; P_t is the β-carotene equivalent of the total pigment, $A_{466\ nm}$ is the measured absorbance at 466 nm, *b* and *m* are the intercept and slope of the calibration curve respectively, *V* is the extract volume (mL), *W* is the weight of the freeze-dried sample (g), and DF is the corresponding dilution factor.

2.9.2 Carbohydrate determination

Carbohydrate content of the extracted EPS was quantified spectrophotometrically using the phenol-sulphuric acid assay (Dubois *et al*., 1956). Briefly, 50 µL aliquot of a known concentration of EPS was transferred into a standard well plate to which was added 150 µL sulphuric acid, followed by 30 µL of 5% phenol. The mixture was incubated in a water bath at 90^{o}C for 5 min and cooled in another water bath at RT. Absorbance at 490 nm was read in a SpectraMax® M3 Microplate Reader (China), and concentration was determined by interpolation with a standard curve prepared for D-glucose (Appendix A, Figure A1).

2.9.3 Uronic acid concentration

For quantification of uronic acid, the method described by Mojica *et al*. (2007) was used. In brief, 1.2 mL of 0.0125 M sodium tetraborate solution in concentrated sulfuric acid was added to 200 µL EPS samples in test tubes. The solutions were mixed thoroughly and heated in a water bath at 100^{o}C for 5 min. Samples were cooled on ice for 3 min before the addition of 20 µL 3-Phenylphenol (*m*-hydroxydiphenyl) solution (0.15% w/v in 0.5% NaOH). The solution was mixed gently, and absorbance was read at 520 nm in a spectrophotometer (Shimadzu UV-1280, Japan) after 4 min. The concentration of uronic acid was determined by comparison against a calibration curve (Appendix A, Figure A2) prepared using D-glucuronic acid (Sigma Aldrich, South Africa).

2.9.4 Estimation of protein content

The protein content of EPS was analysed using the dye-binding method of Bradford (1976) by adding 40 µL of reagent (prepared by dissolving 100 mg of Coomassie Brilliant blue in 50 mL 95% ethanol and after addition of 100 mL 85% phosphoric acid, the solution was diluted to 1 L and filtered) to 160 µL of known EPS concentration. The mixture was incubated at RT for 5 min and absorbance was determined at 595 nm in a microplate reader. Concentration was determined by interpolation with a standard curve (Appendix A, Figure A3) for bovine serum albumin (BSA).

2.9.5 Determination of α-amino nitrogen

To quantify α-amino nitrogen content of extracted EPS, the ninhydrin assay described by Lie (1973) was used. To 1 mL of ninhydrin reagent (prepared by dissolving 100 g $Na_2HPO_4.12H_2O$, 60 g anhydrous KH_2PO_4, 5 g ninhydrin, and 3 g fructose in 1 L distilled water, pH 6.7) was added to 2 mL of known EPS concentration in test tubes. The mixture was placed in a boiling water bath for 16 min and transferred immediately to another water bath at 20°C to cool for 20 min. Thereafter, 5 mL of dilution reagent (prepared by dissolving 2 g KIO_3 in 600 mL distilled water, which was then made to 1 L with 96% ethanol) was added to the tubes and mixed thoroughly. Absorbance was measured at 570 nm within 30 min in a microplate reader. Concentration was determined by interpolation from a standard curve prepared with a known concentration of glycine (Appendix A, Figure A4).

2.9.6 Lipid determination

Lipid content quantification was by a method modified from the sulfo-phospho-vanillin (SPV) (Cheng *et al*., 2011b, Mishra *et al*., 2014) protocol using hexane to prepare the calibration instead of chloroform. To 100 µL of known concentrations of EPS in microplate wells, 100 µL of concentrated sulfuric acid was added and the mixture incubated at 90°C for 20 min in a water bath and cooled on ice bath for 5 min. 50 µL phospho-vanillin reagent (prepared by dissolving 0.2 mg of vanillin in 1 mL 17% phosphoric acid) was added to the mixture and incubated at RT for 10 min. The absorbance of the colour developed was taken at 540 nm in a microplate reader and concentration interpolated from a standard curve prepared with a known concentration of canola oil (Appendix A, Figure A5). The standard lipid stock was prepared using 2 mg commercial canola oil in 1 mL hexane. A 100 µL of series of lipid concentration was aliquot in microplate wells and the well-plate was kept at 60°C for about 10 min to evaporate the solvent followed by the SPV reaction as described above.

2.9.7 Rhamnolipids quantification

Rhamnolipids quantification was carried out by adapting the methylene blue complexation method described by Pinzon and Ju (2009) and Rasamiravaka *et al*. (2016), which involves three steps of rhamnolipids extraction, quantification followed by the final measurement step. Rhamnolipids was extracted from a 24 h grown culture of all bacterial isolates. After centrifugation at 5,000 × *g* for 5 min and filtration using 0.22 µm membrane filters to remove bacterial cells, the pH of the supernatant was adjusted to 2.3 ± 0.2 using 1 M HCl. The acidified

sample was extracted with a fivefold volume of chloroform. For quantification, 4 mL of the chloroform containing rhamnolipids was put in contact with 400 µL of methylene blue solution (freshly prepared by mixing 200 µL of 1g/L methylene blue solution in 10 mM borax buffer to 4.8 mL of deionized water and pH adjusted to 8.6 ± 0.2 using 50 mM borax buffer) in test tubes. Tubes were mixed vigorously for 5 min in a vortex and the immiscible solution was left to stand for 15 min at RT. For measurement, 1 mL of the chloroform phase was transferred into a 2 mL centrifuge tube and 500 µL 0.2 N HCl was added and mixed vigorously. Phase separation was achieved by centrifugation in a centrifuge at 500 × g for 1 min. Finally, 200 µL of the acidic phase was transferred in a 96-well microplate, and absorbance was measured at 638 nm against 0.2 N HCl as blank. Concentration was interpolated with rhamnolipids standard curve (Appendix A, Figure A6) prepared by carrying out the same analysis (excluding the extraction step) for a series of concentrations of rhamnolipids (90% pure; Sigma Aldrich, South Africa).

2.9.8 Estimation of Phenolics

For estimation of phenolic compounds in EPS, a modified Lowry assay described by Redmile-Gordon *et al*. (2013 & 2014) was used. To 100 µL samples in two separate wells (well A and well B), 100 µL of reagent A (prepared by combining solutions of 3.5% copper sulphate, 7% sodium potassium tartrate, and 7% anhydrous sodium carbonate in 0.35N NaOH in proportions of 1:1:100 respectively) was added to well A. An equal volume of reagent B (prepared as A except for the substitution of copper sulphate with Milli-Q water) was also added to well B and both wells were mixed thoroughly and incubated at RT for 10 min. A 10-fold dilution of 2N Folin-Ciocalteu's phenol reagent (Sigma Aldrich, South Africa) was prepared and 100 µL added to both wells before further incubation for 30 min in the dark at RT. The absorbance of both wells was measured at 750 nm in a microplate reader and the actual absorbance for estimation of humic acid was derived using mathematical expressions. The concentration of phenolic compounds was determined by interpolation from a standard curve (Appendix A, Figure A7) prepared using commercially available humic acid (Sigma Aldrich, South Africa). The protein interference was eliminated using the following expressions.

$$A_{Protein} = 1.25\ (A_a - A_b) \qquad \textbf{Equation 2.6}$$

$$A_{Humic} = A_b - 0.2\ (A_{Protein}) \qquad \textbf{Equation 2.7}$$

Where, $A_{Protein}$ and A_{Humic} are the new absorbances derived for estimation of protein and humic acid content of EPS respectively from absorbances measured at 750 nm for well A (A_a) and well B (A_b).

2.10 Spectroscopic analyses

2.10.1 Fourier Transformed Infrared (FTIR)

FTIR analysis of sub-samples of the extracted EPS (~1 mg) and pigments (~1 mg) was carried out using a PerkinElmer Spectrum 100 instrument (PerkinElmer, Waltham, MA, USA) with attenuated total reflectance (ATR) accessory eliminating the need for mixing of samples with potassium bromide (KBr). The ATR accessory, fitted with a diamond top-plate, has a spectral range of 25,000–100 cm^{-1}, refractive index of 2.4, and 2.01 µ depth of penetration. FTIR spectra of EPS samples were recorded in the range of 4,000–650 cm^{-1} and vibrational modes interpreted using an online IR Wizard 2019^{beta} interpretation platform (St. Thomas, 2019), and reference to the literature (Bramhachari and Dubey, 2006; Mishra and Jha, 2009; Wang *et al*., 2012; Zhu *et al*., 2012).

For the bacterial pigments and subsequent to bulk extraction from ≥2 g of dried pigmented cells, crude saponified extracts were dissolved in 1 mL methanol and the individual pigments separated on 20×20 cm preparatory silica gel glass plates (Analtech Uniplate™, Newark) and eluted using the previously described solvent combination (Section 2.8.1). FTIR absorption spectra of purified carotenoids of bacterial strains and a standard β-carotene (93% purity; Sigma Aldrich, South Africa) were obtained in the region 4000 and 600 cm^{-1} using the same instrument described above and interpretation of spectra and assignment of functional groups made using an online tool (St. Thomas, 2019) and reference to reported carotenoid FTIR spectra (Berezin and Nechaev, 2005; Sujak *et al*., 2007; Quijano-Ortega *et al*., 2020).

2.10.2 Nuclear Magnetic Resonance (NMR)

The ^{1}H and ^{13}C NMR analysis of carotenoids from bacterial strains were carried out in a Bruker Avance II 400 MHz (Germany) spectrophotometer equipped with cryoprobe. After bulk extraction and saponification of pigmented cells in methanol, pigments were separated by thin layer chromatography (TLC) on a silica gel, followed by the elution of the main pigment in methanol. Approximately 2 mg of the main carotenoids was dissolved in 0.6 mL deuterated chloroform ($CDCl_3$; Sigma Aldrich, South Africa). NMR spectra of carotenoid samples in $CDCl_3$ were acqiured by means of standard pulse sequences and run by Topspin package. The

chemical shifts (δ) were recorded in ppm and compared to a standard of β-carotene. Generated spectra were processed and analysed using the software program MestReNova 10.0.0 (Mestrelab Research). The chemical shifts were interpreted by reference to an online tool (St. Thomas, 2019) and reference to reported study on NMR analysis of carotenoids (Englert, 1985; Britton and Young, 1993).

2.11 Application studies

2.11.1 Flocculation efficiency of EPS

Experiments were carried out to determine the flocculating property of EPS using a strain of *Chlorella* sp. culture that had been previously isolated from MLSS in HRAOP and maintained in BBM at 25°C. Flocculation efficiency was determined using the methods described by Salim *et al*. (2011) and Papazi *et al*. (2010). A 14 d *Chlorella* culture was diluted to an optical density ≤ 1.0 at 750 nm, the pH adjusted to 7.0 using 1M HCl, and increasing mass amounts of extracted EPS was added. Microalgal suspensions were transferred to cuvettes and allowed to settle in the dark for 180 min at RT. During the period of settling, the optical density of each cuvette was carefully measured at 750 nm every 15 min using a spectrophotometer (Shimadzu UV-1280 spectrophotometer, Japan). Different chemical flocculants including a monovalent (KCl), divalent ($CaCl_2$), and trivalent ($FeCl_3$) chloride salts were used as a positive control for the determination of flocculation efficiency while *Chlorella* cells in Milli-Q water was used as a negative control, and biomass recovery (R) calculated as:

$$R\ (\%) = [OD\ 750(t_0) - OD\ 750\ (t) \div OD\ 750(t_0)] \times 100 \qquad \textbf{Equation 2.8}$$

Where, OD 750(t_0) is the initial optical density of the culture and, OD 750 (t) is the optical density of the culture at time t.

2.11.2 Emulsification activity of EPS

To determine if EPS from MLSS are suitable as emulsifiers, the emulsifying activity was carried out according to the method described by Burgos-Díaz *et al*. (2011) and Chowdhury *et al*. (2011). Various amounts of extracted EPS were resuspended in 1 mL of Milli-Q water and an equal amount of a hydrocarbon substrate was added and mixed vigorously for 5 min. The ability of microbial EPS to form and retain emulsion was determined after 24 h. The emulsifying activity of EPS was also tested on different hydrocarbon substrates and Emulsification activity was calculated as:

$$E\ (\%) = (H_e \div H_t) \times 100 \qquad \textbf{Equation 2.9}$$

Where E is the 24 h emulsification index, H_e is the height of the emulsion layer (cm) and H_t is the total height of the mixture (cm).

2.11.3 Effect of cyanobacterial granules on flocculation

MLSS containing mainly MaB-flocs were harvested from HRAOP of the IAPS and added to a culture of cyanobacterial granules to investigate its role in biomass flocculation. Freshly collected 1 L of MLSS samples was left to settle in Imhoff cones for 1 h and settled biomass containing MaB-flocs was washed in 0.9% NaCl prior to inoculation in sterilized primary treated wastewater collected from the effluent of AFP as the culture medium. The wastewater used as the culture medium was pre-treated by filtration through 0.22 μm filters and autoclaved at 121°C for 15 min. New MLSS was therefore prepared in Erlenmeyer flasks containing 500 mL of culture medium and inoculated with 10% w/v MaB-flocs, with or without the addition of equal concentration of cyanobacterial granules. Inoculated flasks were incubated under continuous cool, white fluorescent light (15 W: 70-90 μmol m^{-2} s^{-1}) in a growth room at 25°C using a 12/12 h light/dark cycle for 21 d. The development of flocs/granules was monitored over 21 d and samples were taken every 7 d for measurement of biomass, settleability, and nutrient analysis.

2.12 Data and statistical analysis

All sampling, experiments and analyses were carried out in triplicate and data computed in Microsoft Excel 2016 for the determination of mean ± standard error (S.E.). Graphs were plotted using SigmaPlot Version 13.0 (Systat Software Inc., Chicago, IL, USA) and Microsoft Excel 2016. Statistical analyses performed using IBM SPSS (Version 20.0). Where applicable, one-way analysis of variance (ANOVA) was used to test for significant difference between datasets at 95% confidence level by Post HOC analysis using Duncan Multiple Range Test (IBM SPSS, Version 20.0). Where stated, a *t* test analysis was used to test for a significant difference between two means.

Chapter 3: The microbial composition and extracellular polymeric substances of mixed liquor suspended solids

3.1 Introduction

WWTWs have a high microbial diversity including bacteria, fungi, algae, viruses, protozoans, and even higher organisms, all of which play a crucial role in the stability and performance of such systems (Xu *et al*., 2018). Systems such as activated sludge are typically dominated by bacteria (95%) of which Proteobacteria account for 21-65% of this microbial population (Cydzik-Kwiatkowska and Zielinska, 2016; Xu *et al*., 2018). Algae-based wastewater treatment systems such as IAPS on the other hand are dominated by 60-80% microalgae and 20-30% heterotrophic bacteria (Mehrabadi *et al*., 2016), as well as the seasonal occurrence of protozoans, and zooplanktons, which together make up the MLSS and contribute to the formation of MaB-flocs when conditions are ideal (Benemann *et al*., 1977; Garciá *et al*., 2000; Larsdotter, 2006; Park *et al*., 2011b).

MLSS is the concentration of suspended solids in wastewater mixed liquor that ensures decomposition of organic pollutant in an aeration basin. HRAOPs are considered the aeration basin of an IAPS, where oxygen is introduced into the system at a high rate through algal photosynthesis and paddlewheel mixing (Laubscher and Cowan, 2020). The aerobic condition in HRAOP selects for the proliferation of heterotrophic bacteria that consume and degrade organic pollutants in the mixed liquor. In the process of bacterial metabolism, CO_2 and other metabolic products are released and used by microalgae during photosynthesis as a source of carbon. Therefore, MLSS is a medium composed of biomass (majorly microalgae and bacteria) and their metabolic products, EPS that results from wastewater treatment. The EPS produced may then form part of the mixed liquor as soluble microbial products (Kunacheva and Stuckey, 2014) or attached to the microbial cells and provide a structure for the aggregation of biomass to form MaB-flocs (Flemming and Wingender, 2001a, 2001b, 2010).

Microbial flocculation in IAPS is critical in the performance of IAPS such as enhancing the quality of the final treated water to meet regulatory standards and facilitate cost-effective beneficiation of the harvested biomass (Van Den Hende *et al*., 2014a; Ramanan *et al*., 2016; Kouzuma and watanabe, 2015). Many factors including F/M, HRT, and recycling of biomass in HRAOP have been identified to influence the symbiotic association between microalgae and bacteria to achieve the formation of readily settleable MaB-flocs (Gutzeit *et al*., 2005; Medina

and Neis, 2007; Park *et al*. 2011b). At high HRT and low F/M ratio, microalgal cells reach a steady growth phase that allows for aggregation and incorporation of individual cells into MaB-flocs reducing the concentration of young and planktonic cells (Gutzeit *et al*., 2005; Medina and Neis, 2007). In addition, Park *et al*. (2013a) reported that recycling gravity-harvested biomass promoted the formation of >500 µm MaB-flocs in HRAOP. Microalgae such as *Pediastrum* sp. naturally form large colonies or flocs that settle rapidly due to their lower surface area to volume ratio thus enhancing the productivity and energy yield from the harvested biomass (Park *et al*., 2011b; Park *et al*., 2013a).

The formation of MaB-flocs has also been attributed to EPS (Jimoh and Cowan, 2017; Park *et al*., 2013b). Since EPS are secreted by microorganisms into the surroundings to provide resistance to unfavourable conditions, structural and biochemical support, protective barriers, adhesion to surfaces, and most importantly contribute to aggregation and the formation of flocs/biofilm (Sheng *et al*., 2010; More *et al*., 2014). However, they can also be involved in de-flocculation of MaB-flocs when degraded where they contribute immensely to COD concentrations thereby affecting the efficiency of wastewater treatment plants (Kunacheva and Stuckey, 2014). Therefore, it is important to study the dynamics of EPS production in IAPS and particularly how it affects MaB-floc formation in HRAOP.

Given its important role in the mediation of wastewater treatment and bioflocculation in IAPS, it may be crucial to study the structure and diversity of microbial population in MLSS for a better understanding of its biological components. Therefore, a molecular toolbox would be an ideal approach since all microbial domains of interest can be identified and accounted for. Microbial diversity in WWTWs has been traditionally and commonly studied by microscopic observation and cultivation-dependent techniques. Similarly, microbial composition in wastewater treatment HRAOP has also been studied using these methods (Van Den Hende *et al*., 2011: Park *et al*., 2011b). However, while some MaB-floc components such as microalgae, rotifers, and ciliates are visible and identifiable under a light microscope, the bacterial components can only be reasonably identified with the aid of molecular techniques. Thus, cultivation-dependent techniques have been considered inadequate for a proper description of a microbial community structure (Wagner and Loy, 2002). High-throughput sequencing was introduced and has been employed in the evaluation of phytoplankton and bacterial communities in wastewaters and other aquatic systems (Matcher *et al*., 2011; Xu *et al*., 2016; Xu *et al*., 2018; Pujari *et al*., 2019). This approach facilitates evaluation and understanding of

microbial diversity and interaction within a micro-community (Xu *et al*., 2018). It also helps in the identification of uncultured, but biotechnologically important organisms (Wagner and Loy, 2002).

In this chapter, a high-throughput sequencing of MLSS generated during wastewater treatment in HRAOP was carried out using NGS of 16S and 18S gene targets in order to: 1) determine the structure and diversity of the microbial components of MLSS; 2) investigate and compare the diversity, similarity and dissimilarity in MLSS accumulated at seasonal intervals (i.e. summer, winter and spring) within the same year. This was followed by studying the dynamic of MaB-floc formation in MLSS in an effort to establish the relationship between microbial composition, EPS production, biomass aggregation, and harvestability in HRAOP of an IAPS treating domestic sewage.

For a detailed metagenomic study, generated sequences were computed and analysed using various software programs for the classification and identification of dominant microbes. Biomass production was measured as the concentration of MLSS in the mixed liquor, the dynamic of floc formation was determined from the settling ability of the suspended solids and correlated with EPS production.

3.2 Results

3.2.1 Microscopic analysis of MLSS

A microscopic examination of MLSS samples from HRAOP collected at intervals during the experimental period showed they consist predominantly of microalgae and bacteria that in most cases were present as MaB-flocs (Figure 3.1). These flocs occurred as aggregates comprising different materials and microorganisms including bacteria, microalgae, and occasionally some rotifers and ciliates. Changes in microalgal dominance were observed sporadically and consequently resulted in changes in MaB-floc structure and size. On few occasions however, MaB-flocs were either loose, scarce, or absent in MLSS samples, causing microalgae to occur mostly in planktonic states. The dominant microalgae were the chlorophytes such as *Pediastrum* sp., *Desmodesmus* sp., *Scenedesmus* sp., *Micractinium* sp. and *Chlorella* sp. Other species that were present occasionally include *Dictyosphaerium* sp., *Coelastrum* sp., *Pyrobotrys* sp., *Closterium* sp., *Actinastrum* sp., Diatoms, and filamentous cyanobacteria. These changes were accompanied by variation in the monthly solar irradiance, temperature,

and pH which varied between 149-327 W/m^2, 14-23^{o}C, and, 8-11 respectively during the period of investigation (Appendix B, Figure B1).

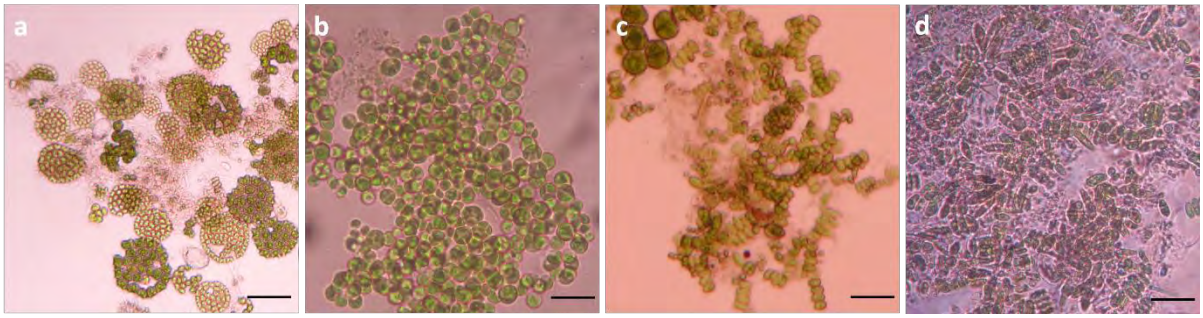

Figure 3.1: Composition of MLSS in HRAOPs. Light microscopic images of *Pediastrum*-dominated (a), *Micractinium*-dominated (b), *Desmodesmus*-dominated (c), and *Nitschia*-dominated (d) flocs in the mixed liquor. Scale bar = 54 µm.

3.2.2 Microbial richness and diversity in MLSS

For a detailed elucidation and identification of the microbial components of MLSS, an NGS analysis was carried out on samples collected from HRAOP within a period of 10 months. A total of six samples were taken at intervals in the experimental period including S1 and S2 collected in summer (March), S3 and S4 in winter (June-July), and S5 and S6 in spring (November-December). Following the removal of ambiguities and chimeras, a total of 131,599 and 243,883 sequence reads were generated for 16S rRNA and 18S rRNA respectively (Table 3.1). The 16S rRNA sequences belonged to the Bacteria domain (including cyanobacteria) while the 18S rRNA sequences consisted of eukaryotes such as microalgae, fungi, ciliates, and rotifers. It was however observed that the number of bacterial reads in S5 and S6 were relatively low (Table 3.1) indicating that the PCR library used for the sequencing reaction was not of the best quality. Therefore, the sequences of rare bacterial species that make up the bacterial population may be missing in these samples. Nevertheless, all samples showed a good coverage (Table 3.2) especially the eukaryotes indicating that the depth of sequences used for analysis was an adequate representation of the microbial community structure in HRAOP at the time of sampling.

Table 3.1: Sequences generated for MLSS samples from a high rate algal oxidation pond of an integrated algal pond system treating domestic sewage.

Season	Sampling date	Sample ID	No of reads	
			Bacteria*	Eukaryotes
Summer	04 March	S1	55277	37874
	29 March	S2	46161	42628
Winter	11 June	S3	20473	20243
	30 July	S4	20984	23122
Spring	05 November	S5	2568	70582
	10 December	S6	6609	49434

* Bacterial sequences also include the cyanobacterial components of the MLSS.

To determine the microbial richness, evenness, and diversity in HRAOP, a diversity index comprising ACE, Chao, Shannon, and Invsimpson was estimated on Mothur, and the results presented in Table 3.2. The microbial diversity revealed and perhaps as expected that ACE and Chao (microbial community richness) were highest in warmer months for bacteria and eukaryotes (S1 and S2), while the lowest values were recorded in winter (S3 and S4). Even though the number of bacterial sequences in spring (S5 and S6) was relatively low, samples collected during this period appeared to be more evenly distributed than in winter. Thus, the evenness of community structure measured as Shannon and Invsimpson was higher in warmer months for bacteria and eukaryotes sequence reads while the lowest values were observed in winter (Table 3.2). Considering these results, the order of microbial diversity of bacteria and eukaryotes appeared to be S1>S2>S6>S5>S3>S4. Indeed, the rarefaction curves (Appendix B, Figure B2) indicated much lower biodiversity in winter, while summer had the highest diversity probably due to a significantly higher richness and evenness in the population size. Irrespective of these differences, rarefaction curves reached a plateau in all samples indicating an equal and accurate sampling to saturation across all samples, except in spring (S5 and S6), where the bacteria population was found to be significantly low as a result of the missing rare bacterial species.

Table 3.2: Summary of the alpha diversity indices and generated OTU of the microbial population in HRAOP of an IAPS treating domestic sewage.

Sample ID	OTU	ACE	Chao	Shannon	Invsimpson	Coverage (%)
Bacteria						
S1	138	80.13	79.20	3.30	18.00	95.22
S2	138	90.59	81.72	3.29	18.00	94.69
S3	28	28.75	15.29	0.77	1.47	99.05
S4	22	14.99	11.65	0.76	1.49	99.35
S5	33	77.60	44.38	2.16	5.15	96.54
S6	63	65.30	55.94	2.59	8.91	96.20
Eukaryotes						
S1	96	98.89	98.64	1.55	2.73	99.91
S2	92	93.67	93.41	1.57	3.19	99.91
S3	41	72.86	52.14	1.32	2.42	99.93
S4	45	53.15	51.80	1.37	2.62	99.95
S5	72	72.16	69.91	1.34	2.44	99.92
S6	88	87.42	87.49	2.07	5.12	99.93

3.2.3 Microbial community structure and composition of MLSS in HRAOP

3.2.3.1 Analysis of microbial diversity

The phylogenetic classification using the SILVA database revealed that the bacterial population within the period of sampling consists of a total of 29 phyla, and the dominant bacteria phyla are presented in Figure 3.2 a. Proteobacteria was the most abundant phylum and accounted for 27-79% of the classified sequences. Within the Proteobacteria phylum, Gammaproteobacteria was the most abundant (51-98%) especially at S3 and S4 samples where they accounted for almost all sequences (>98%). Other members of Proteobacteria (Alphaproteobacteria and Deltaproteobacteria) were therefore relatively low in S3 and S4 (≤2%) but significantly higher at other sampling intervals. Cyanobacteria were the most abundant phylum in S5 (49%) and were also significantly represented in S3, S4, and S6 accounting for 18-21% of the sequences. Furthermore, the phyla Bacteroidetes and Planctomycetes were also abundant in all samples, except those collected in winter (S3 and S4), and accounted for 12-34% and 3-18% respectively. Also present but relatively low (≤4%) were bacteria belonging to the Gemmatimonadetes, Verrucomicrobia, Firmicutes, Actinobacteria, and some unclassified bacteria (Figure 3.2 a).

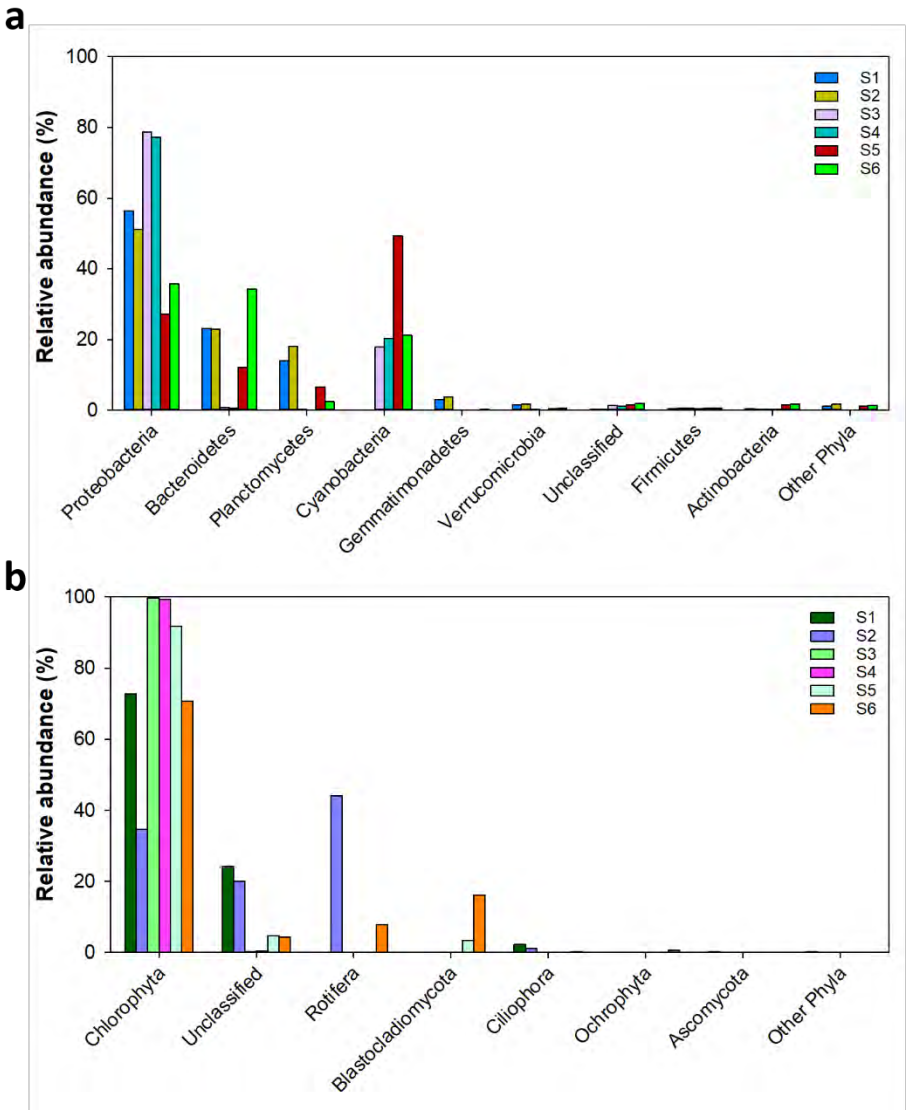

Figure 3.2: Microbial diversity and community structure of MLSS in HRAOP. The dominant phyla of bacteria (a) and eukaryotes (b) are expressed as the relative percentage of the total sequences in each sample.

Within the eukaryotes, a total of 24 phyla were present for all samples. Aside from sample S2, the phylum Chlorophyta was the most abundant (71-99%) through the period of analysis and comprised of the family Chlorophyceae, which accounted for 62-86% of the total number of sequences (Figure 3.2 b). The sample S2 was dominated by the phylum Rotifera (44%) and only contained 35% of chlorophytes in the Chlorophyceae family. Other dominant chlorophytes include those found in the Tribouxiophyceae family (>23%) and some unclassified chlorophytes (>15%) most of which are sequences in S3 and S4. Furthermore, a significant proportion (16%) of fungi belonging to the phylum Blastocladiomycota was observed in S6 only while a significant proportion of unclassified eukaryotes (>20%) was also found in S1 and S2 (Figure 3.2 b). These sequences were either not included in the database of

the SILVA version used for analysis or are entirely new and novel phylotypes. Overall, it was evident that S1 and S2 showed relatively higher diversity and variation in the distribution of prokaryotic (comprising an average of 26 phyla) and eukaryotic (comprising an average of 16 phyla) phylotypes.

3.2.3.2 Identification of operational taxonomic units (OTU)

All sequences were grouped into OTUs at 97% confidence level using the Mothur platform and a total of 166 OTUs were clustered successfully for bacterial sequences while 174 were clustered for the eukaryotes. The dominant OTUs (Appendix B, Table B1) in each sample were pooled and combined in a heatmap analysis as illustrated in Figure 3.3. A total of 33 bacterial genera classified within the Proteobacteria, Bacteroidetes, Planctomycetes, and Cyanobacteria phyla constitute the dominant microbial population and represented 86% of the total bacteria sequence reads. From the results obtained, the bacterial population appeared to be seasonal such that samples collected within the same season had similar bacterial populations as illustrated in Fig 3.3a. Thus, S1 and S2 (collected in March; summer) appeared to share similar OTU distribution, while S3 and S4 (July-August; winter), and S5 and S6 (November-December; spring) also present a similar bacterial population that is absent in other samples. Likewise, the population dynamic of eukaryotes was also observed to be seasonal such that samples collected around the same period shared similar OTUs with a total of 21 genera dominating the ponds over the period of sampling (Figure 3.3 b). So, seasonality has a major impact on the population dynamic of the HRAOP and this must have in turn influenced floc formation and the accumulation of MaB-flocs.

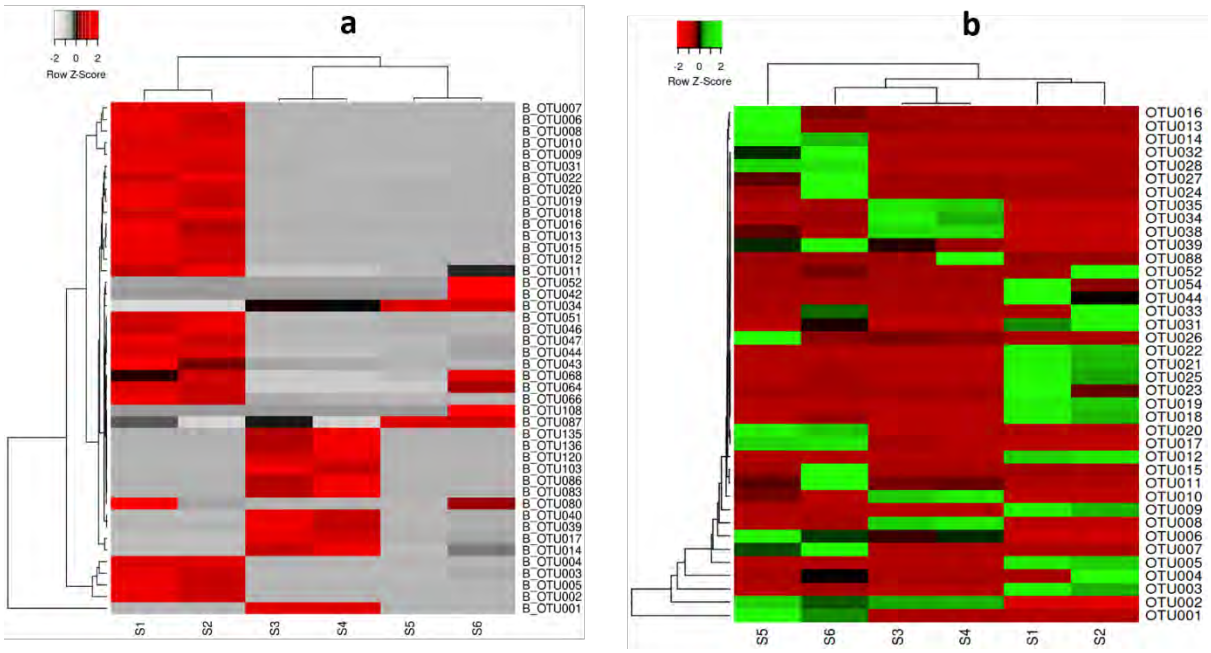

Figure 3.3: Heatmap analysis showing the dominant OTUs of bacteria (a) and eukaryotic (b) components of MLSS in HRAOP in a period of 10 months. The taxonomic classification of each OTU is listed in Appendix B, Table B1.

Using the SILVA database, the OTUs generated were taxonomically identified and the dominant species in each sample were pooled for a bar plot analysis represented in Figure 3.4. *Thiothrix* was the most abundant genus (17%) in the total bacterial population (Figure 3.4 a) and clustered into three OTUs (B_OTU001, B_OTU083, and B_OTU086). However, this filamentous bacterium was more dominant in S3 and S4 (i.e. winter) and accounted for almost all the sequence reads present (>80%). A more diverse bacterial population was observed during the warmer seasons when *Porphyrobacter* (B_OTU005 and B_OTU006), *Silanimonas* (B_OTU002), *Mariniradius* (B_OTU003), *SM1A02* (B_OTU004 and B_OTU009), *Algoriphagus* (B_OTU007 and B_OTU136), *Flavobacterium* (B_OTU042 and B_OTU046), Cyanobacteria (B_OTU014, B_OTU017, B_OTU034, B_OTU103, and B_OTU120), *Dokdonella* (B_OTU011) and others accounted for a significant proportion of sequences. Also present but in lesser proportion include bacterial species such as *Zoogloea*, *Thauera*, *Malikia*, *Candidatus Halomonas phosphatis*, *Truepera*, *Roseomonas*, *Ideonella,* and others.

The OTUs generated for eukaryotes were dominated by chlorophytes including *Desmodesmus*, *Scenedesmus*, *Pseudopediastrum*, *Chlorella*, *Micractinium,* and *Hariotina*. (Figure 3.4 b). *Pseudopediastrum* (OTU003 and OTU031) was the most abundant in S1 and accounted for 58% of the reads in the sample, but declined in S2 to 27% possibly due to the emergence of the rotifer, *Brachionus* (OTU004, OTU033, and OTU052), which accounted for 49% of the

population. On the other hand, *Desmodesmus* (OTU001, OTU002, OTU009, OTU014, OTU017, OTU020, OTU028, and OTU039) was found to be distributed in all samples but more abundant in S5 (i.e. spring) where it accounted for 85% of the sequences. Other chlorophytes that were in abundance include *Chlorella*, *Micractinium,* and *Scenedemus* spp. *Nitzschia* (OTU024) was the only diatom species detected and was present at S6, which coincides with the transition from spring to summer. In addition, fungi, ciliates, rotifers, and arthropods such as *Sanchytrium*, *Paraphysoderma*, *Amphileptus*, *Telotrochidium*, *Cephalodella*, *Moina,* and *Stenocypris* were also present (Figure 3.4 b).

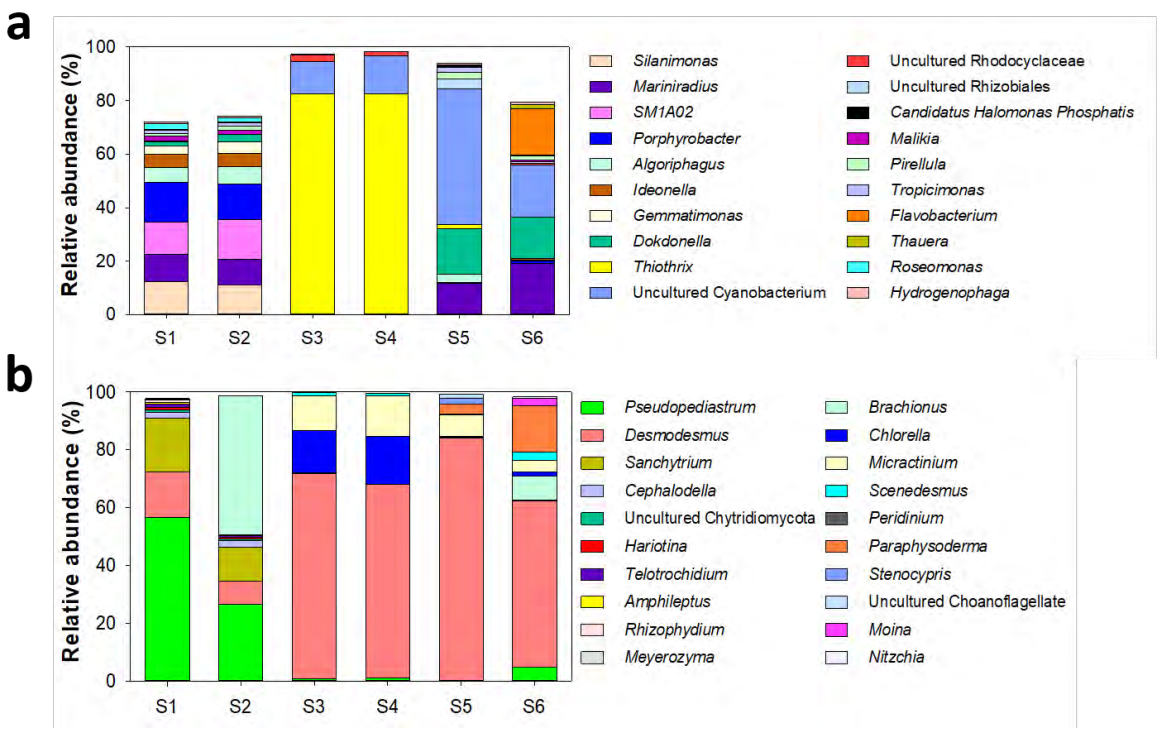

Figure 3.4: Relative abundance of the dominant bacterial (a) and eukaryotic (b) species present in MLSS of HRAOP. Sequences were clustered into OTUs and phylogenetic classification was carried out with SILVA as the reference database using the Mothur platform.

3.2.3.3 Determination of distinct and similar microbial communities

In an effort to identify shared and unique microbial species at seasonal interval in HRAOP, generated OTUs were analysed using Venn diagram as illustrated in Figure 3.5. In the bacterial sequences (Figure 3.5 a), only 3 OTUs (*Mariniradius*, *Hydrogenophaga*, and uncultured Rhizobiales) were shared by all samples suggesting that 9% of the bacterial species were present in all seasons. Samples S1 and S2 (summer samples) had the highest number of OTUs (138) and consequently shared the highest number of species indicating both samples contain

similar and more diverse bacterial species. The winter samples shared the least number of species (12) as might be expected since the lowest number of OTUs and least diversity were recorded for S3 and S4 (28 and 22 respectively). All samples had unique OTUs except for S4 and S5 where less bacterial population and diversity were observed. On the other hand, 12 species, accounting for 69% of the eukaryotic population were found in all samples including *Pseudopediastrum*, *Desmodesmus*, *Scenedesmus*, *Chlorella,* and uncultured Chytridiomycota spp. among others (Figure 3.5 b). Like the bacterial population, the summer-time samples (S1 and S2) shared 43 and had the highest number of OTUs (96 and 92 respectively) while those from winter, S3 and S4 had the lowest. Sample S3 was however the only sample with no unique eukaryotic OTU.

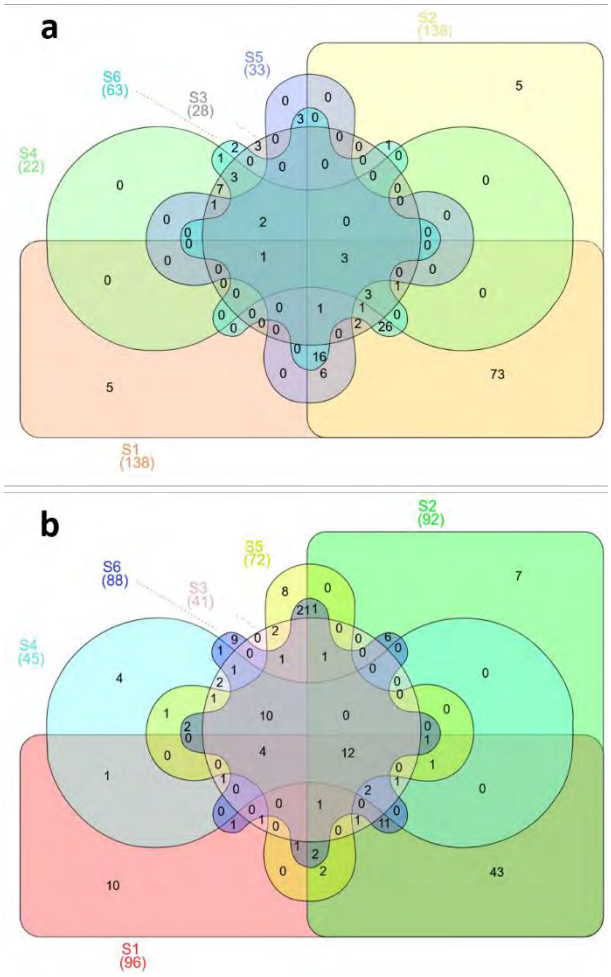

Figure 3.5: Venn diagram showing the shared and unique bacteria (a) and eukaryotic (b) OTUs in HRAOP of an IAPS treating domestic sewage.

3.2.4 Biomass production and formation of MaB-flocs in HRAOP

Biomass production and formation of flocs were measured concomitantly as MLSS concentration and biomass settleability respectively in HRAOP and results presented in Figure 3.6. MLSS concentrations varied between 70 and 190 mg/L during the experimental period (Figure 3.6 a). A gradual decline in biomass concentration from 190 to 80 mg/L was observed between February and May but was followed by a consistent increase to 170 mg/L in December. Such variation in biomass concentration could be attributed to the changes in environmental conditions such as variation in pH, temperature, and solar irradiance that are known to affect biomass production in HRAOPs (Park *et al*., 2011a; Sutherland and Ralph, 2020).

Irrespective of the MLSS concentration however, settleability of biomass appeared to be dependent on the formation of good and stable flocs. The settling efficiency of MLSS after 1 h settleability in Imhoff cones ranged between 36 and 95% (Figure 3.6 b). Between February and May, considerably large flocs were observed in HRAOPs and as such, an average of 78% settleability was achieved. In the same vein, good biomass settleability was also achieved in November and December where settling efficiency reached 95%. However, relatively little to no flocs were observed in June and July, which resulted in significantly low settleability with an average of 41%. Flocculation also appeared to impact biomass productivity, which was found to be higher (10 ± 0.8 g/m^2/d) when floc formation was good and stable (Table 3.3). This period of poor flocculation also coincided with the detection of a high concentration of *Thiothrix* in MLSS that accounted for over 80% of the bacterial population (Figure 3.4 a), indicating this species may be responsible for the poor settleability of suspended biomass in the MLSS. Indeed, the proportion of non-settleable biomass was higher in the same period, which was in most cases >50% of the total biomass concentration (Appendix B, Table B2). Results therefore suggest that lack of flocculation in HRAOP could lead to low biomass recovery by gravity sedimentation and that the non-settleable biomass could form part of residual COD and TSS in ASP and thus affect the quality of effluent from the system.

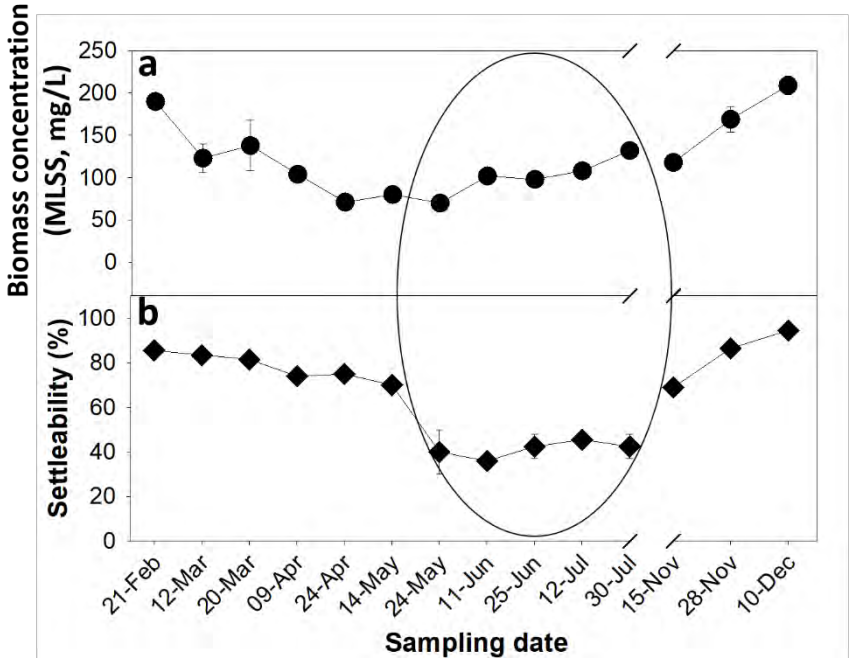

Figure 3.6: Biomass concentrations (a) and settleability of MaB-flocs (b) generated in MLSS of HRAOP over a period of one year. Area within the circle is the period of poor flocculation during the experimental period. Error bars represent S.E. of replicated samples.

Table 3.3: Biomass productivity for all sampling intervals presented in Figure 3.6. Values are mean ± S.E.

Condition	Productivity ($g/m^2/d$)
Good flocculation*	10.0 ± 0.8
Poor flocculation**	7.7 ± 0.2
Total***	8.5 ± 0.7

*n=9, **n=5, ***n=14.

3.2.5 EPS production in HRAOP

To investigate the influence of EPS production on the formation and stability of MaB-flocs in MLSS, the dynamic of EPS generated in the 'mixed liquor' (S-EPS) and that associated with MaB-flocs (B-EPS) in HRAOP were extracted and quantified. Similar to the pattern observed for biomass production (Figure 3.6 a), a gradual decrease in S-EPS concentration from 100 to 42 mg/L was observed between February and April, while production increased to 91 mg/L in December of the experimental period (Figure 3.7). S-EPS production was however constant and significantly lower between May and July with an average of 34 mg/L. The low EPS production during this period is perhaps indicative of reduced photosynthesis and lower productivity, which may also explain the poor flocculation and biomass settleability recorded.

On the other hand, B-EPS extracted from the suspended solids (i.e. MaB-flocs) appeared to be constant during the experimental period with an average of 36 mg/L, except for the period between June and July during where a sudden increase was observed (Figure 3.7). Thus, B-EPS concentration attained the highest of 55 mg/L. Except on few occasions (i.e. between June and July), S-EPS concentration was mostly 2 times higher than the B-EPS at all time intervals suggesting continued production and release of EPS into the mixed liquor in HRAOP.

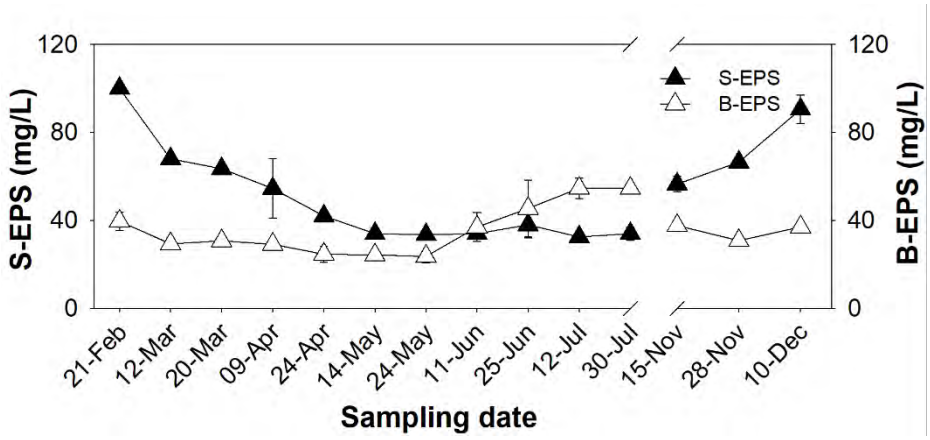

Figure 3.7: The concentration of soluble (S-EPS) and bound (B-EPS) EPS extracted from MLSS generated in HRAOP over a period of one year. Results are mean ± S.E. of three replicates of samples taken directly in front of the paddlewheel. Error bars represent S.E. of replicated samples.

3.2.6 Relationship between EPS production and formation of MaB-flocs in MLSS

Results presented so far indicate a clear variation in the behaviour of IAPS with respect to biomass production, EPS production, and floc formation within a period of one year. Between November and May, which coincides with the summer season in South Africa, a higher biomass and EPS production resulted in better flocculation and biomass recovery by settleability (Figure 3.6 b). On the other hand, floc formation was observed to be reduced between June and July (winter season), which consequently resulted in poor settleability and biomass recovery. The relationship between MLSS, EPS production, and biomass settleability was further investigated in a regression analysis and results are shown in Figure 3.8. A positive correlation (R^2=0.571) was found between MLSS and biomass settleability (Figure 3.8 a), indicating biomass recovery from the mixed liquor is dependent on its concentration and floc formation. S-EPS obtained from the mixed liquor was also strongly correlated with MLSS concentration (R^2=0.797) and its settleability (R^2=0.795) as indicated in Figures 3.8 b and c. The B-EPS was however found to have a poor or no correlation with these parameters (Figure 3.8 d and e), more likely due to the constant amount extracted over the period of sampling.

Results therefore suggest that the presence of EPS in the mixed liquor could be one of the drivers that control floc formation and biomass recovery in HRAOP of an IAPS.

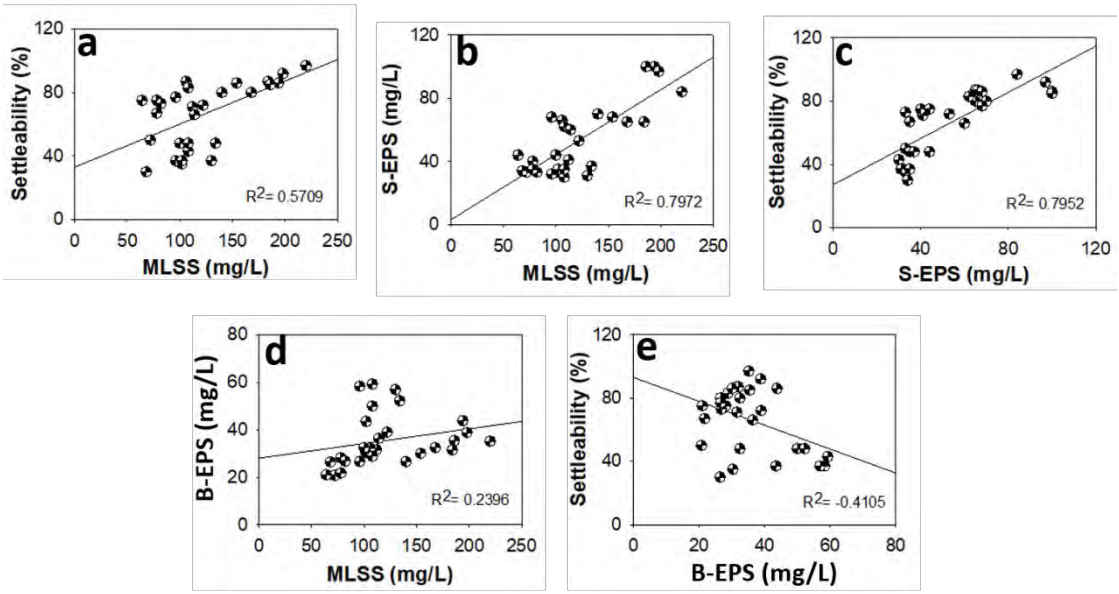

Figure 3.8: A regression analysis showing the relationship between biomass concentration, settleability, and EPS extracted from MLSS in HRAOP.

3.3 Summary

The execution and results of a metagenomic study for the elaboration of the biological component of MLSS mediating wastewater treatment in HRAOP and a study of biomass and EPS production dynamic in the system showed that:

- The biological components of MLSS are composed of bacteria (including cyanobacteria) and eukaryotes including microalgae, fungi, ciliates, rotifers, and arthropods in suspended aggregates of MaB-flocs. In the bacteria domain, proteobacteria were the most abundant followed by bacteroidetes and cyanobacteria, while Eukaryota was dominated by chlorophytes that were mainly colonial microalgae distributed across all samples. Only 3 bacterial and 12 eukaryotic OTUs were shared by all MLSS samples inferring a diverse microbial population in MLSS especially in warmer months.

- MLSS also contained EPS produced by the microbial population in loose (S-EPS) and bound (B-EPS) forms. The majority of the EPS occurred in the soluble form (42-100 mg/L) and only a small proportion is attached to the MaB-flocs as B-EPS (24-55 mg/L). S-EPS therefore had a positive correlation with biomass concentration and settleability, and thus

appeared to be more involved in the formation and accumulation of MaB-flocs compared to the B-EPS.

- Ideal conditions of higher biomass and EPS production facilitated flocculation in MLSS, and Imhoff cone settleability of the MaB-flocs demonstrated that up to 95% biomass recovery is achievable. However, on occasions when MaB-flocs were either loose, scarce, or absent in MLSS samples, biomass recovery was found to be <40%.

- The period of poor floc formation also coincided with the appearance of *Thiothrix* with >80% dominance in the MLSS. The dominance of this filamentous bacterium could have resulted in sludge bulking effect and loss of floc in the pond. Metagenomics is therefore a useful method of monitoring the processes of flocculation and/or deflocculation in HRAOPs.

Results demonstrated that microbial population dynamic, composition and EPS production together with seasonality have a major impact on floc formation in MLSS, which in turn would influence water quality and biomass recovery.

Chapter 4: Investigating the role of microbial components in the formation of MaB-flocs.

4.1 Introduction

The metagenomic study of MLSS reported in Chapter 3 showed that the mixed liquor is largely composed of microalgae, cyanobacteria, and bacteria. Most notably was the presence of the colonial chlorophytes, *Pseudopediastrum,* and *Desmodesmus* spp. that accounted for more than half of the eukaryotic population indicating dominance in MLSS. Likewise, several bacterial and cyanobacterial species were also found in association with microalgae suggesting that all these microbes may possess unique physiological characteristics or mechanisms contributing to the process of floc formation.

In many wastewater treatment systems, bacteria are usually flagged as the EPS producers, probably because of their higher growth rate, tendency to genetic manipulations, and versatility in their genetic make-up, such that strains within the same species can produce EPS with unique and extraordinary properties (Li *et al*., 2017b). This has resulted in them being the most studied for EPS production. Even so, it may also occur that some species are either low or non-EPS producers probably because they do not possess the genes responsible for EPS production, which has brought about genetic modifications to improve EPS yield (Pi *et al*., 2020). This is not to say that microalgae do not produce EPS and in fact, many studies have reported the isolation and characterization of EPS from microalgae (Staats *et al*., 1999; Mishra and Jha, 2009; Nguyen *et al*., 2020) indicating that microalgal EPS production cannot be overlooked. However, despite their potential benefits, microalgae have been poorly investigated for EPS production and most microalgal EPS reported are of cyanobacterial origin rather than eukaryotic microalgae (Pierre *et al*., 2019). Therefore, the slime (i.e. EPS) of biofilm and flocs have been attributed more to bacteria and cyanobacteria (Roeselers *et al*., 2008; Flemming, 2011; Rossi and De Philippis, 2015). Indeed, the slimy and sticky characteristics of EPS, which are important in the structural stability of biofilms and flocs have been observed majorly in pure cultures of bacteria and cyanobacteria (Ortega-Morales *et al*., 2007; Ahmed *et al*., 2014; Abid *et al*., 2018; Sun *et al*., 2020), which has led to the perception that they are more important in these microenvironments. Even so, the presence of large and colonial microalgae such as *Pediastrum*, *Desmodesmus*, *Scenedesmus,* and *Micractinium* commonly present in HRAOP

also influence the formation of microbial aggregates, settleability, and harvestability of biomass in such systems (Park *et al*., 2011b).

In wastewater treatment systems, the presence of cyanobacteria has also been shown to enhance bioflocculation and have been considered to play a major part in the secretion of EPS that provides a scaffold for attachment and aggregation of other heterotrophs and autotrophs to form an immobilized microenvironment or flocs (Olguin, 2003; Roeselers *et al*., 2008; Taton *et al*., 2012). These photosynthetic prokaryotes can assimilate phosphorus and nitrogenous compounds such as ammonium, nitrate, and amino acids from wastewater and are therefore as important a component of biomass as eukaryotic microalgae in algal pond systems. In fact, some cyanobacterial species are self-flocculating, where they form dense interwoven and entangled granules due to their filamentous structure and are therefore viable in the recovery of unicellular and poorly settleable microalgal species (Tiron *et al*., 2017; Stauch-White *et al*., 2017).

Similarly, several bacteria such as *Zoogloea* spp. have been identified as candidate species for floc formation (Rosselló-Mora *et al*., 1995; An *et al*., 2016; Gao *et al*., 2018). Also, EPS-producing bacteria are associated with brewery and winery wastewater (Nguyen *et al*., 2017) and, EPS-producing *Cloacibacterium normamense* and *Agrobacterium tumefaciens* with high flocculation activity and good settleability have been isolated and identified from municipal wastewater (Nouha *et al*., 2015; Wu *et al*., 2015; Pi *et al*., 2020). The occurrence of filamentous bacteria in WWTWs is considered important for proper floc formation and good sludge settleability (Wagner and Loy, 2002; Wagner *et al*., 2002). However, their presence in high concentrations (such as *Thiothrix* sp. observed in MLSS composition reported in Chapter 3) may equally be detrimental and cause sludge bulking that counteracts floc settleability. Thus, the identification of floc-forming and EPS-producing organisms is important in developing control strategies to improve biological wastewater treatment processes such as IAPS.

Antibiotic treatment has been used since time immemorial in maintaining pure cultures of microalgae. Specifically, the purification and identification of cyanobacterial strains from a mixed population of microorganisms can be a difficult process and the methods employed to achieve this purpose include micromanipulation by physical observation (Garcia-Pichel *et al*., 1996), molecular cloning (Nelissen *et al*., 1996), the use of oligonucleotide primers for specific amplification of 16S rRNA gene segments from cyanobacteria (Nubel *et al*., 1997), and more commonly antibiotic treatment (Dias *et al*., 2015). However, many cyanobacterial strains are

only cultivable in the company of other microbial counterparts, especially heterotrophic bacteria that are tightly attached, hence an axenic cyanobacterial culture may not be achievable (Nubel *et al*., 1997; Dias *et al*., 2015). Moreover, antibiotics are regarded as emerging pollutants and their persistence in water bodies results in increasing development of antibiotic resistance within the microbial community, which consequently reduces their therapeutic effects. In environmental biofilms, (of which MaB-flocs might be considered an example), exposure to antibiotics may suppress the growth of the cyanobacterial strain of interest since they are also susceptible to a wide range of antibiotics groups (González-Pleiter *et al*., 2019; Wang *et al*., 2020). This could have a great effect on cyanobacterial diversity in the ecosystem and impede their activity and role in an immobilized environment (Wang *et al*., 2020).

In an effort to further understand the process of bioflocculation and MaB-floc formation which appears critical in the treatment of wastewater, some of the major microbial components of the MLSS (reported in Chapter 3) including microalgae, cyanobacteria, and bacteria were selected as model organisms and their involvement and role in microbial aggregation were investigated. In addition, the effect of antibiotic treatment on the behaviour and stability of floc structure was examined in a series of experiments.

4.2 Results

4.2.1 Influence of microalgal components in MLSS on the formation of MaB-flocs

To study the contribution of microalgal components of MLSS in the formation of MaB-flocs, some microalgal species were isolated and identified by microscopic examination. *Pediastrum* sp., *Desmodesmus* sp. and *Chlorella* sp. that appeared to be predominant in MLSS across all seasons as observed in the metagenomics study reported in Chapter 3 were therefore selected (Figure 4.1). *Pediastrum* sp. (Figure 4.1 a) occurred as circular colonial species comprising 8-64 celled coenobia arranged in a concentric pattern. Similarly, the *Desmodesmus* sp. was also colonial and found in either 4 or 8-celled coenobia (Figure 4.1 b) arranged in an alternating pattern with two spines on the cells at each end. *Chlorella* sp. on the other hand is single-celled and appeared as planktonic cells with a cup-shaped nucleus (Figure 4.1 c).

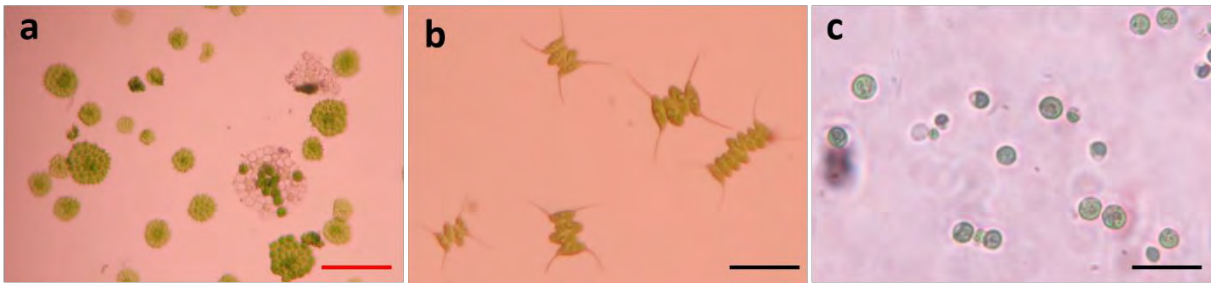

Figure 4.1: Light microscopic images of *Pediastrum* sp. (a), *Desmodesmus* sp. (b), and *Chlorella* sp. (c) isolated from MLSS in HRAOP. Red scale bar is 218 µm and black scale bar is 54 µm.

In an effort to further understand the involvement and role of these colonial and unicellular microalgal isolates in the physical properties of larger and heterogenous MaB-flocs, a settleability test was carried out and the outcome presented in Figure 4.2. Results showed that the larger *Pediastrum* sp. had a remarkable settling ability of 82% within 15 min. with a gradual increase to a maximum of 92% after 180 min. without the addition of any flocculant. *Desmodesmus* sp. culture also showed a gradual increase in settling ability and up to 75% was achieved. The unicellular alga, *Chlorella* sp. showed the lowest and poor settling ability of <20% after 180 min. The results therefore indicate that the presence of colonial microalgae in the MLSS could be important in HRAOP and their dominance in the MaB-floc structure would facilitate settleability and separation of IAPS-treated water from the biomass.

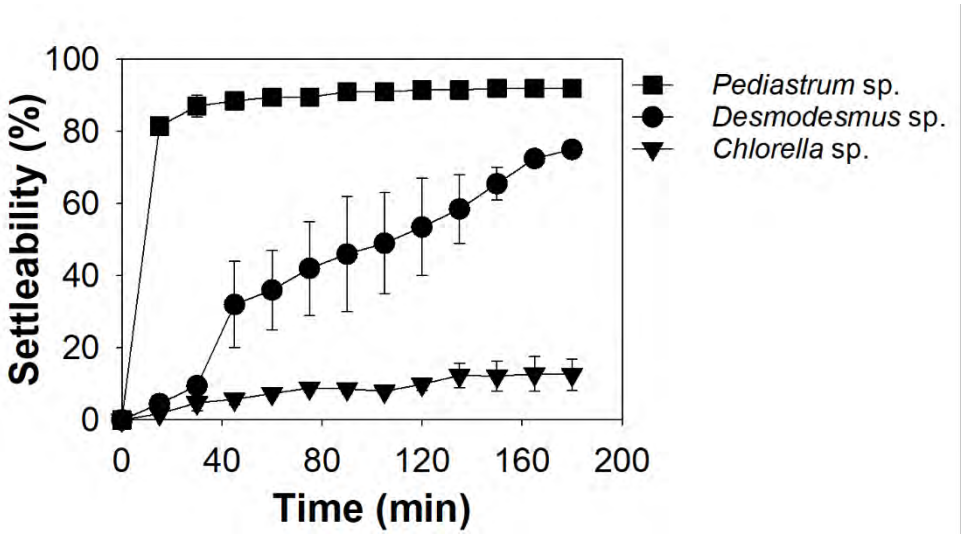

Figure 4.2: The settling efficiency of colonial and unicellular microalgal strains isolated from MLSS. Error bars represent S.E. of replicated samples.

4.2.2 Influence of cyanobacterial components in the MLSS on formation of MaB-flocs

4.2.2.1 Identification of a prominent cyanobacterial isolate

Cyanobacteria were also found to be an integral component of MLSS. In order to study their role in the aggregation process, a strain was isolated from MLSS and subjected to intense study. On this filamentous strain designated ECCN 20BG, DNA was extracted, and Sanger sequencing carried out for its taxonomic identification. Subsequent to amplification and sequencing of the 16S rRNA target site, ECCN 20BG showed 94% similarity to *Leptolyngbya geysericola* and other uncultured cyanobacteria. A phylogenetic tree constructed using the neighbour-joining algorithm of 1000 bootstraps showed strain ECCN 20BG clustered and formed a clade with many *Leptolyngbya* spp. that originated from aquatic and terrestrial environments (Figure 4.3). Based on these findings, the isolate was identified as *Leptolyngbya* sp. strain ECCN 20BG and deposited in GenBank with accession No MT723895.

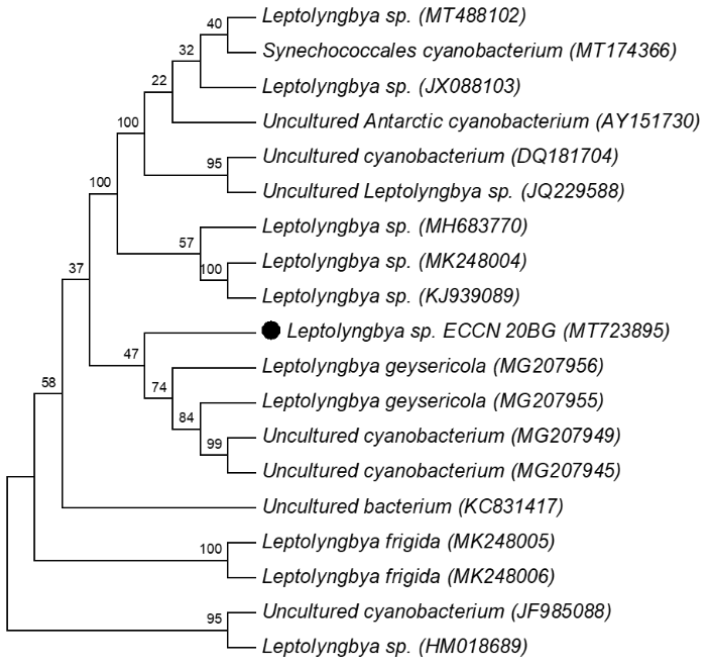

Figure 4.3: Phylogenetic tree constructed for ECCN 20BG and other closely related sequences obtained from GenBank. The evolutionary history was inferred using the Neighbour-Joining method and bootstrap values are indicated at the nodes. Evolutionary analysis was conducted in MEGA6.

4.2.2.2 Growth characteristics and structure of Leptolyngbya strain ECCN 20BG

The growth of *Leptolyngbya* sp. was studied in BG-11 medium under a 12/12 h light/dark illumination for 30 d. A transition from tiny flocs (Figure 4.4 a) to granule-sized biomass

(Figure 4.4 b) was observed as a typical growth characteristic of ECCN 20BG indicating the strain to be self-flocculating. The isolate appeared to form tightly aggregated biomass resembling a granular structure when agitated, but without agitation forms a thin cyanobacterial mat at the bottom of the culture medium. The sizes (as measured using a stereomicroscope) of 30 d grown granules with continuous agitation ranged from <100 µm to >2000 µm with an average size of 780 ± 22 µm (Figure 4.4 c). The size distribution of the granules obtained from three independent experiments as illustrated in Figure 4.4 d showed that the highest proportion (50.9 ± 3.0%) were between 600 and 900 µm, while granules of <600 and >900 µm accounted for 21.3 ± 0.2% and 16.1 ± 0.5% respectively. Only a small fraction (5.3 ± 1.6%) of the granules were < 300 µm and others were larger granules >1200 µm that accounted for 5.6 ± 1.0%.

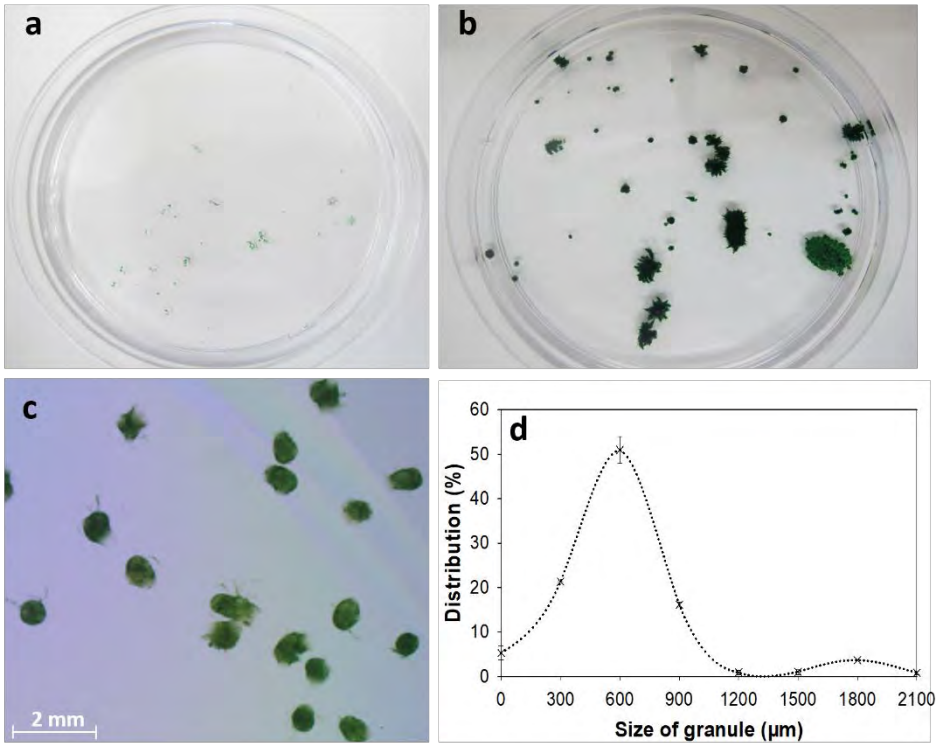

Figure 4.4: The development of filamentous *Leptolyngbya* strain ECCN 20BG into aggregates and the size distribution in a 30 d culture. Photograph of the flocs in 90 mm plates before (a) and after (b) development into granules. Microscopic image (scale bar = 2 mm) of fully grown granules (c) and their size distribution (d). Error bars represent the S.E. of three independent experiments.

Bio-granules of strain ECCN 20BG ranged from irregular to round-shaped and the dry weight of an average-sized granule was estimated to be about 27 µg. SEM analysis revealed the granules as dense, compact structures (Figure 4.5 a). On closer scrutiny, an entangled network of filaments including what appears to be the presence of an EPS-like matrix was revealed

(Figure 4.5 b). Results therefore suggested that this self-flocculating cyanobacterium may play an important role in the structural stability and settleability of MaB-flocs in MLSS of HRAOP.

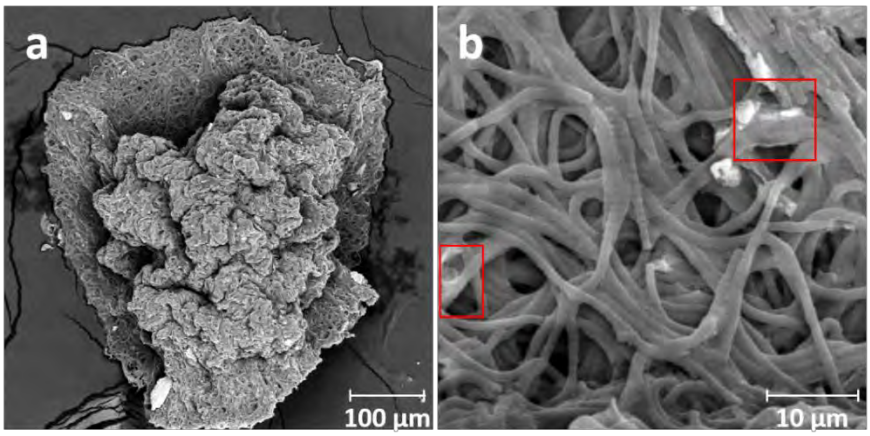

Figure 4.5: SEM micrograph of the structure of a fully developed granule of *Leptolyngbya* ECCN 20BG (a) and the entangled network of filaments within the granule (b). Areas within the red boxes indicate an EPS-like matrix observed within the structure.

4.2.2.3 Effect of antibiotics on the granulation of Leptolyngbya sp.

In an effort to maintain a pure culture of *Leptolyngbya* sp. and prevent bacterial contamination, the antibiotic, chloramphenicol was added. Surprisingly, cell growth of this cyanobacterium was altered by this antimicrobial agent and the details are shown in Figure 4.6. No granules were produced indicating a possible link between antibiotic treatment and floc formation (cf, Figure 4.6a and 4.6b). This prompted an investigation into the effect of antibiotics on biological aggregation and other components of flocs. The microalgal isolates previously described in Section 4.2.1 (i.e. *Pediastrum* sp., *Desmodesmus* sp. and *Chlorella* sp.) were co-cultured with the self-flocculating *Leptolyngbya* sp. with and without the addition of chloramphenicol as an antimicrobial agent, and the growth and granule formation monitored over a period of 30 d.

As presented in Figure 4.6, formation of granules by *Leptolyngbya* in the absence of an antimicrobial agent proceeded normally and consequently, resulted in a 99% settleability of biomass by gravity sedimentation within 5 min at a rate of 12 m/h (Figure 4.6 a). In addition, the bio-granules also served as a refuge for the growth of the chlorophytes (Figure 4.6 a1 and a2). Following treatment with chloramphenicol that exerts its action by blocking peptidyl transferase required for 50S ribosomal protein synthesis, the growth of floc forming *Leptolyngbya* was altered causing liberation of chlorophytes from the flocs and significantly poor settleability (Figure 4.6 b). Thus, green cultures with planktonic cells were obtained after

1 h of settleability (Figure 4.6 b1 and b2). And, a closer look at the antibiotic-affected granules by microscopic examination clearly revealed loss of the blue-green colour of the prokaryotic cyanobacterium, but the interwoven structure had been retained and harboured some unicellular chlorophytes such as *Chlorella* sp. and *Pediastrum* sp. (Figure 4.6 b3 and b4).

Altogether, the results of the experiment suggest that the antibiotic molecule was taken up by the cyanobacterial cells from the culture medium through diffusion into the cell membrane that inhibited protein synthesis thus stopping cell growth and reproduction. The dead filaments that served as a refuge for the proliferation of other chlorophytes however indicate the interwoven network serves as a support for trapping and settling poor or non-flocculating microorganisms.

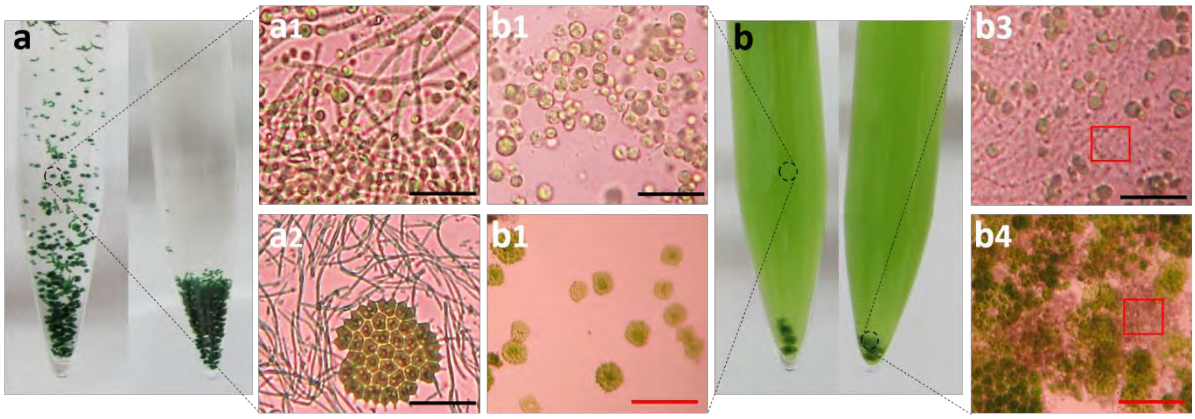

Figure 4.6: Microbial flocculation and settleability efficiency of *Leptolyngbya* strain ECCN 20BG before and after treatment with chloramphenicol for 30 d in a controlled growth room. The bio-granules formed by *Leptolyngbya* and other microalgal strains and the settleability after 5 min in cone-shaped test tubes before treatment with antibiotics (a), microscopic image of a granule showing the entangled filaments of *Leptolyngbya* with entrapped *Chlorella* cells (a1) and *Pediastrum* cells (a2). Liberation of microalgal cells from granules after treatment with antibiotic and the settleability after 5 min (b), microscopic image of liberated *Chlorella* (b1) and *Pediastrum* (b2) cells, and their respective antibiotic-affected granules (b3 and b4). Areas in the red boxes indicate the dead cyanobacterial cells after antibiotic treatment. The black scale bar is 54 µm and the red scale bar is 218 µm.

In a further experiment to elucidate the effect of antibiotics on granulation of *Leptolyngbya* sp., the activity of various antimicrobial agents including streptomycin, rifampicin, tetracycline, actinomycin D, ampicillin, kanamycin, and chloramphenicol on growth and floc formation was studied. To achieve a better resolution especially of floc formation and settling ability among the various antibiotic treatments, a *Chlorella* sp. with poor settleability that appeared not to be

affected by chloramphenicol was selected and co-cultured with the self-flocculating *Leptolyngbya* sp. and results presented in Figure 4.7.

Exposure to various classes of antibiotic appeared to affect the growth and reproduction of *Leptolyngbya* cells resulting in filaments that appeared dead due to the observed brownish colour (Figure 4.6 b3 and b4) while *Chlorella* was less affected. This resulted in the liberation of the chlorophyte from the granules and variation in biomass concentration (Figure 4.7 a). The greatest impact was observed with rifampicin-, streptomycin- and ampicillin-treated cells that yielded only 22.3 ± 3.5, 28.0 ± 4.0, and 33.3 ± 2.9 mg/L biomass respectively within the period of incubation. Since *Chlorella* within the *Leptolyngbya* granules was less affected by actinomycin-D, chloramphenicol, and tetracycline treatment, biomass concentrations were higher. Even so, at 52.0 ± 9.2, 55.3 ± 5.2 and 55.3 ± 1.8 mg/L, these data were not statistically different (ANOVA at $P < 0.05$) from results obtained with the control at 69.3 ± 9.8 mg/L (Appendix E, Table E1). Thus, and as a result of exposure to antibiotics, *Leptolyngbya* sp. was not capable of forming granules. Thus, a distinct and remarkable settleability of 99% was achieved without antibiotic treatment relative to the low settleability of 8.4-16.8% with antibiotic treatment (Figure 4.7 b). Results of this experiment therefore further suggest that the slow growth rate and inability to generate characteristic settleable flocs/granules was due to a requirement for either transcription or translation and indeed be a consequence of loss of protein and cell wall synthesis.

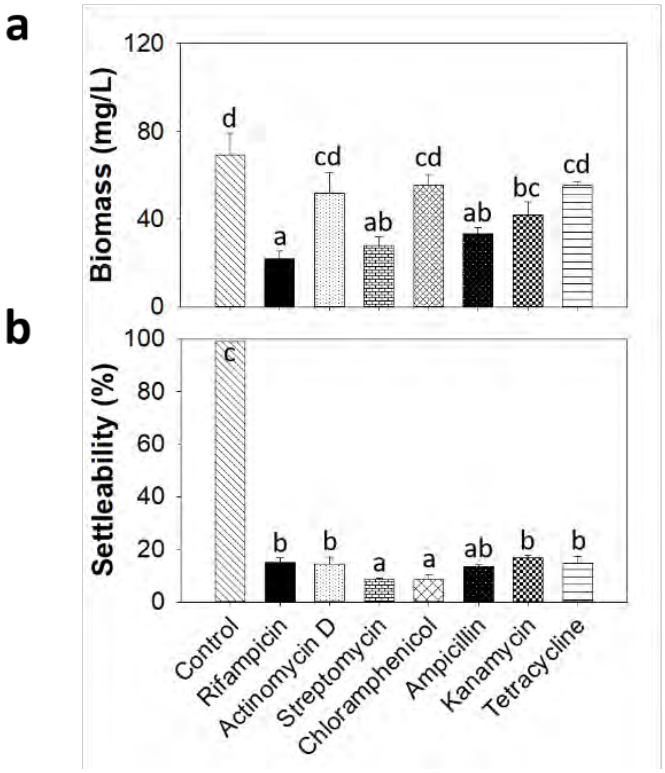

Figure 4.7: The effect of various antibiotics on the growth and formation of flocs in *Leptolyngbya* ECCN 20BG co-cultured with *Chlorella* sp. for 30 d in a controlled growth room. Cell growth measured as biomass concentration (a), formation and stability of flocs measured by 1 h settleability in cone-shaped test tubes (b). Error bars represent S.E. of replicated samples. Values with different letters are significantly different at $P < 0.05$ for each parameter.

4.2.2.4 The role of self-flocculating Leptolyngbya sp. on MaB-flocs

In an effort to confirm the role of *Leptolyngbya* granules in HRAOP floc formation**,** the strain was inoculated into MLSS samples collected from the HRAOP and incubated for a period of 21 d. Results show that the addition of the filamentous cyanobacterium *Leptolyngbya* strain ECCN 20BG appeared to rapidly initiate the conversion of MLSS into suspended MaB-flocs (Figure 4.8 a and b). The initial settleability of MLSS before the commencement of the experiment was found to be 55%. Incubation of the MLSS without the addition of *Leptolyngbya* aggregates showed no significant improvement in floc-sizes (measured as settleability) with more cells in the planktonic state (Figure 4.8 a). In the presence of this self-aggregating isolate however, cells were found to be incorporated into suspended aggregates and larger MaB-flocs were formed (Figure 4.8 b). The formation of larger flocs therefore facilitated settleability to a maximum of 75% (Figure 4.8 c), indicating a 20% improvement in the rate of MLSS

settleability. These differences were also found to be statistically significant indicating an important role for *Leptolyngbya* sp. in MaB-floc formation in HRAOPs.

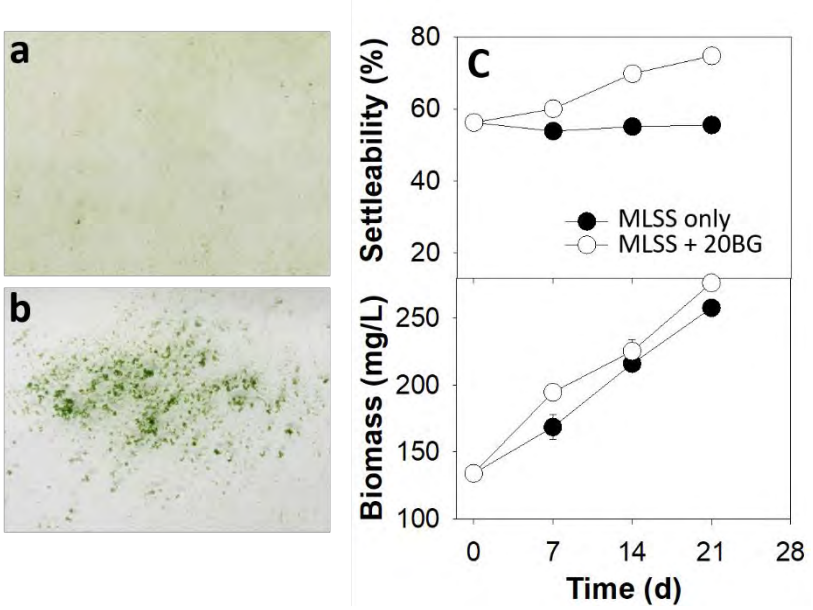

Figure 4.8: Biomass production and settling characteristic of MaB-flocs generated with MLSS in the presence and absence of *Leptolyngbya* strain ECCN 20BG cultured for 21 d in a controlled environment. Images of the suspended solids of MLSS in 90 mm Petri dishes before (a) and after (b) MaB-floc formation with *Leptolyngbya* sp. A time course of the biomass concentration and settleability of the generated MaB-flocs. Error bars represent S.E. of replicated samples.

In addition to the improved flocculation and settleability, the presence of floc forming *Leptolyngbya* strain also enhanced biomass production (Figure 4.8 c). Although no significant difference was observed either in the presence or absence of *Leptolyngbya* strain ECCN 20BG, a 60% increase in biomass concentration from 134.0 ± 2.0 to 276.3 ± 5.5 mg/L was achieved after the experiment (Figure 4.8 c) indicating that this cyanobacterium does not negatively impact microbe proliferation.

The addition of *Leptolyngbya* strain ECCN 20BG indeed brought about a reduction in COD concentration of the MLSS from 162.7 ± 10.0 to 45.3 ± 4.7 mg/L indicating a 72% removal efficiency in 21 d (Figure 4.9 a). In the same vein, ammonium and phosphate concentrations were reduced considerably from 6.6 ± 0.9 and 13.3 ± 0.6 mg/L to 0.2 ± 0.02 and 3.1 ± 0.1 mg/L (Figure 4.9 b and d) respectively, indicating nutrient enhanced nutrient removal by the MaB-flocs. However, nitrate concentration increased from 0.3 ± 0.02 to either 4.0 ± 0.9 mg/L or 7.5 ± 0.1 mg/L in the presence and absence of ECCN 20BG respectively. These increments were found to be statistically significant (*t* test at $P < 0.05$) and therefore suggest that nitrification

by the microbial population, and possibly an effect of the addition of ECCN 20BG (Figure 4.9 d). In general though, there was no significant difference in removal of COD and nutrient with and without the addition of ECCN 20BG to MLSS except for the nitrate concentration, which could also be a result of the insignificant differences in the biomass concentration. Results therefore suggest that the addition of the *Leptolyngbya* sp. was more important in enhancing floc formation and recovery of biomass by gravity sedimentation.

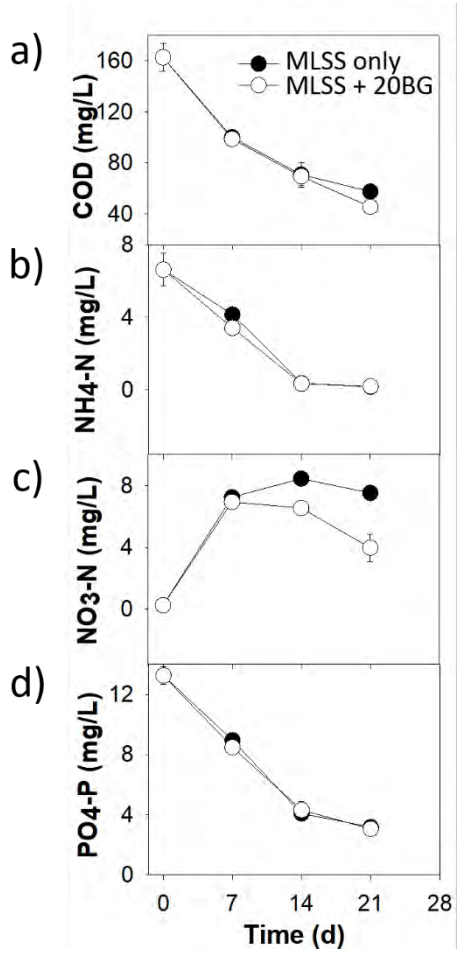

Figure 4.9: COD and nutrient removal of MLSS either in the presence or absence of self-flocculating *Leptolyngbya* strain ECCN 20BG cultured for 21 d in a controlled environment. Error bars represent S.E. of replicated analysis.

4.2.3 Influence of bacterial components in MLSS on the formation of MaB-flocs

4.2.3.1 Isolation and screening of bacteria

Since EPS production is one of the indicators of floc formation by microorganisms, some EPS-producing bacteria were screened for EPS production by real time observation of the colonies. Isolation and purification of strains were carried out by streaking on plates until pure colonies were obtained. Using the method of physical colony observation described by Rühmann *et al*.

(2015), two isolates showed EPS production potential by having sticky, ropy, and/or mucoid colonies when picked with an inoculating loop on either solid (nutrient agar) or liquid (LB) medium. These isolates appeared as large, rough-edged colonies of 3-4 mm with irregular shapes, and were referred to as strain ECCN 40b and strain ECCN 41b prior to molecular characterization (Table 4.1). In addition to EPS production potential, two isolates from MLSS samples that showed distinctive characteristics such as pigmentation were also selected for further investigation. The pigmented isolates appeared as small, smooth-edged, circular, with raised colonies of 1-2 mm and were assigned ECCN 45b and ECCN 46b (Table 4.1).

Table 4.1: Physiological and morphological characteristics of bacterial strains isolated from MLSS in HRAOP.

Characteristics	ECCN 40b	ECCN 41b	ECCN 45b	ECCN 46b
Colony shape	Irregular	Irregular	Circular	Circular
Colour	Cream	Cream	Orange	Orange
Cell shape	Long rod	Long rod	Cocci	Short rods
Gram reaction	+	+	+	+
Growth pH range	7-9	7-9	7-10	7-11
Catalase test	+	+	+	+
Identification	*Bacillus* strain	*Bacillus* strain	*Planococcus* strain	*Exiguobacterium* strain
Accession No	MT705987	MT706002	MT706005	MT706012

4.2.3.2 Taxonomic identification and phylogenetic analysis of isolates

For molecular characterization and taxonomic identification of the four isolates, total ribosomal DNA was extracted, sequenced, and analysed (Appendix C, Figure C1). Using the NCBI database, ECCN 40b and ECCN 41b were determined to be close relatives of the genus *Bacillus* while closest relatives to strains ECCN 45b and 46b were from the genus *Planococcus* and *Exiguobacterium* respectively. ECCN 40b was 99.9% identical to *B. cereus*, *B. thuringiensis,* and *B. proteolyticus* while ECCN 41b was only 99.3% identical to *B. amyloliquefaciens*, *B. velezensis,* and *B. subtilis*. The closest relatives to ECCN 45b appeared to be *Planococcus* sp. (99.5%) and *Planomicrobium* sp. (99.1%) while ECCN 46b was 99.5% matched *E. profundum* and *E. arabatum*.

To establish the phylogenetic positions of these isolates, the 16S rRNA sequences were compared with related species retrieved from the NCBI database that had been isolated from either water or wastewater. As shown in Figure 4.10, all isolates differed from one another, each forming a compact clade with members within the same genus. The topology of the tree also clearly showed that within their respective clades, the closest phylogenetic neighbours of ECCN 40b, ECCN 41b, ECCN 45b, and ECCN 46b are *Bacillus* spp., *Planococcus* sp. and *E. arabatum* respectively. On this basis, isolates were identified as new typed strains and deposited in the NCBI database as *Bacillus* sp. strain ECCN 40b with accession No MT705987, *Bacillus* sp. strain ECCN 41b with accession No MT706002, *Planococcus* sp. strain ECCN 45b with accession No MT705002 and *Exiguobacterium* sp. strain ECCN 46b with accession No MT706012.

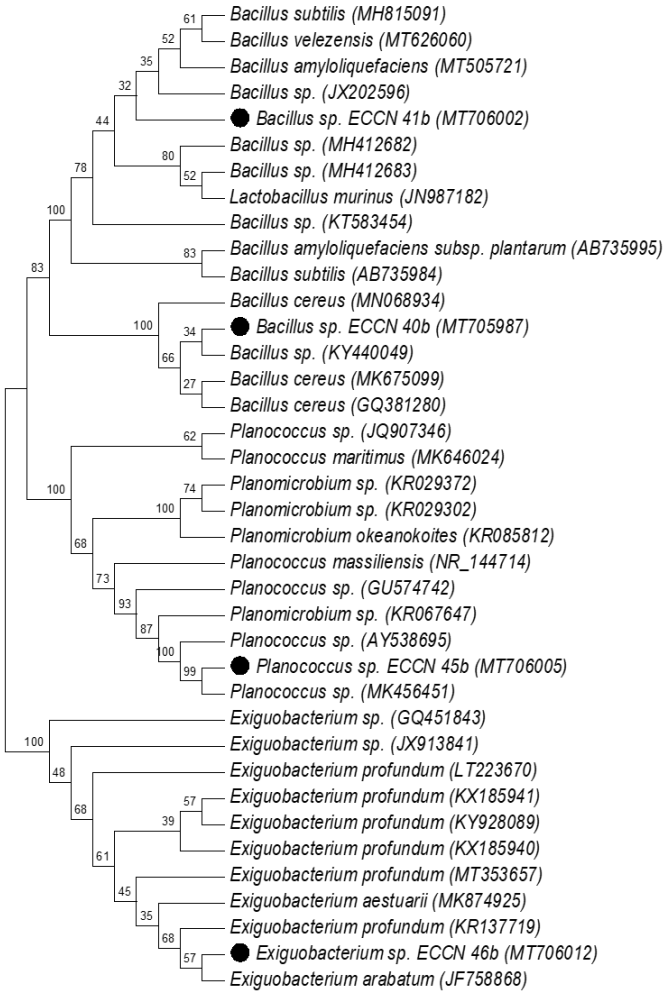

Figure 4.10: Neighbour-joining tree constructed based on the 16S rRNA gene sequencing of *Bacillus* sp. ECCN 40b, *Bacillus* sp. ECCN 41b, *Planococcus* sp. ECCN 45b and *Exiguobacterium* ECCN 46b. Tree was constructed using closely related sequences obtained from GenBank. The phylogenetic analysis was carried out on MEGA6 using 1000 bootstrap.

4.2.3.3 Morphology and biochemical characteristics of bacterial strains

All bacterial strains were Gram positive (Appendix C, Figure C2) and displayed catalase activity (Table 4.1). To determine antimicrobial sensitivity of these strains, bacteria were exposed to commercially available kanamycin, tetracycline, chloramphenicol, norfloxacin, and ertapenem all of fixed concentration. Perhaps not surprisingly, all strains were susceptible to these antimicrobial agents, and zones of growth inhibition were clearly present around each antibiotic test disc.

Cellular structure and morphology of the strains was determined by SEM and *Bacillus* strain ECCN 40b appeared as long rod-shaped cells (Figure 4.11 a) while cells of *Bacillus* strain ECCN 41b appeared as clumped short rods (Figure 4.11 b). Although *Planococcus* strain ECCN 45b and *Exiguobacterium* strain ECCN 46b appeared morphologically alike due to presence of the characteristic pigmentation of both strains, SEM analysis revealed ECCN 45b to be coccoid (Figure 4.11 c) while ECCN 46b appeared as short rod-shaped cells (Figure 4.11 d). These micrographs seemed also to show what appeared to be an EPS-matrix that conferred stickiness to the bacterial cells indicating their EPS production potential.

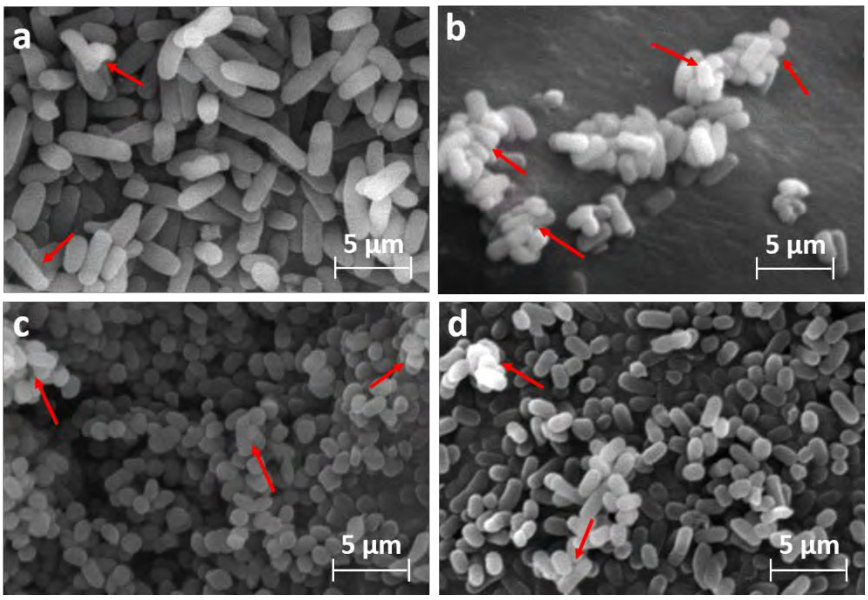

Figure 4.11: SEM micrographs of *Bacillus* strain ECCN 40b (a), *Bacillus* strain ECCN 41b (b), *Planococcus* strain ECCN 45b (c), and *Exiguobacterium* strain ECCN 46b (d) isolated from MLSS in HRAOP of an IAPS. The red arrows show clumped cells as a result of an EPS-like matrix.

4.2.3.4 Growth characteristics of bacterial strains

The growth of each bacterial strain was determined by measuring the turbidity at 600 nm using a spectrophotometer. Typical sigmoid growth patterns were derived for each strain and these are presented in Figure 4.12. *Bacillus* strain ECCN 40b showed rapid growth within 6 h of inoculation in LB (Figure 4.12 a). Similarly, *Bacillus* strain ECCN 41b also showed a rapid growth rate but for this isolate, stationary phase was reached after 8 h (Figure 4.12 b). Pigmented *Planococcus* strain ECCN 45b presented a completely different and relatively slow growth rate with a prolonged lag phase of 5 h and as such, stationary phase was achieved only after 18 h (Figure 4.12 c). The growth of the other pigmented strain, *Exiguobacterium* ECCN 46b however reached stationary phase after 10 h of incubation (Figure 4.12 d). Overall, results show that all strains have different growth which might be expected to impact either EPS or pigment production, or both.

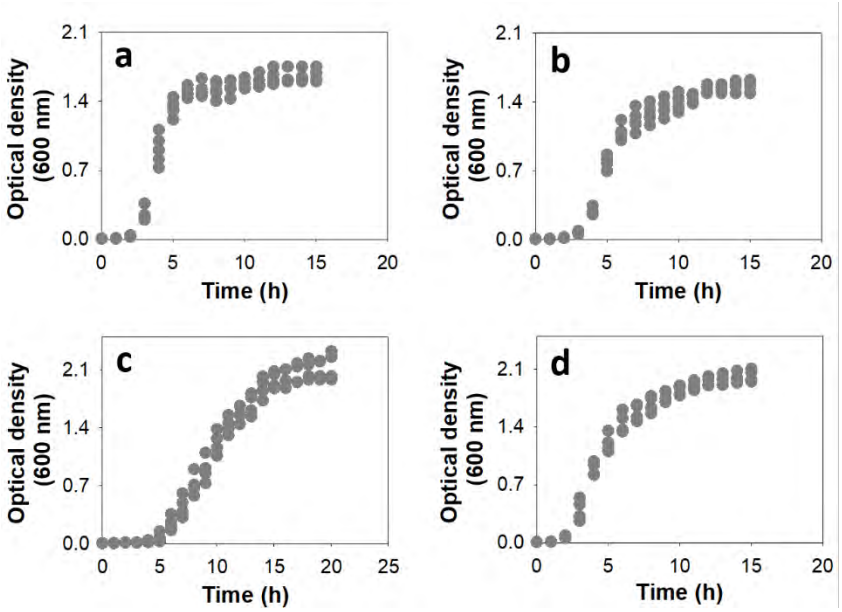

Figure 4.12: Typical growth pattern of *Bacillus* strain ECCN 40b (a), *Bacillus* strain ECCN 41b (b), *Planococcus* strain ECCN 45b (c), and *Exiguobacterium* strain ECCN 46b (d) cultured in Luria Broth over time.

4.2.3.5 Bacterial EPS production

In an effort to investigate further the sticky material that appeared as EPS on bacterial cells (Figure 4.11), the four isolates were grown in LB medium and EPS production monitored over time. EPS production appeared to be growth associated and all strains showed different patterns of production. EPS production was highest for *Bacillus* strain ECCN 41b where a maximum of 585 ± 50 mg/L was achieved within 24 h (Figure 4.13 b). By comparison, other strains

produced significantly ($P < 0.05$) lower EPS concentrations with a maximum of 108 mg/L, 100 mg/L, and 95 mg/L for *Bacillus* strain ECCN 40b, *Planococcus* strain ECCN 45b, and *Exiguobacterium* strain ECCN 46b respectively over a period of 96 h (Figure 4.13 a, c, d). Nevertheless, in strains ECCN 40b (Figure 4.13a) and ECCN 46b (Figure 4.13d), EPS accumulation was up to 48 or 72 h, which coincided with the period of stationary phase. On the other hand, EPS production in ECCN 45b (Figure 4.13c) follows growth pattern such that as growth increases so thus EPS production, while in ECCN 41b (Figure 4.13b), there was a sharp decline in EPS production with the onset of stationary phase. Taken together, these results therefore suggest that both accumulation and decline in EPS occurred predominantly after stationary phase is reached. The prominent decline in EPS concentration in all strains was not observed for *Planococcus* ECCN 45b (Figure 4.13 c) presumably due to its relatively slow growth.

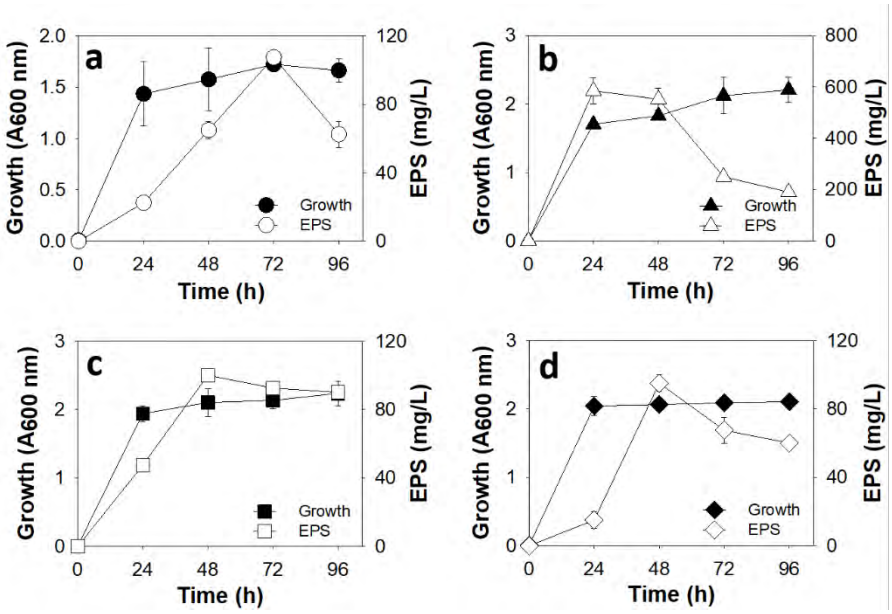

Figure 4.13: Growth and accumulation of EPS in *Bacillus* sp. ECCN 40b (a), *Bacillus* sp. ECCN 41b (b), *Planococcus* sp. ECCN 45b (c) and *Exiguobacterium* ECCN 46b (d) cultured in LB medium over a period of 96 h. Results are presented as the mean of two independent experiments and error bars represent S.E.

4.3 Summary

Work in this chapter described a series of experiments conducted to investigate the contribution of various microbial components of MLSS to MaB-floc formation. Findings are summarized below:

- Pure cultures of *Pediastrum* sp. and *Desmodesmus* sp., which were found to be the most dominant microalgal species in MLSS showed remarkable settleability of 92 and 75%

respectively after 3 h and formed large settleable colonies. The settleability of *Chlorella* sp. was < 20% indicating poor settleability of the single-cell microalga.

- A filamentous cyanobacterium identified as *Leptolyngbya* strain ECCN 20BG (Accession No. MT723895) isolated from HRAOP MLSS formed tightly aggregated structures resembling a granule with an average size of 780 ± 22 µm and 99% settleability within 5 min at a rate of 12 m/h. SEM revealed that these flocs were a compact structure and included what appeared to be an EPS that afforded stability to the entangled cyanobacterial filaments.
- Co-cultivation of ECCN 20BG with other microalgal strains demonstrated that the compact structure of the granules served as a refuge for the growth and proliferation of these chlorophytes. Therefore, planktonic microalgal cells were well incorporated into the bio-granules. The addition of this self-flocculating strain to MLSS also initiated and enhanced the formation of MaB-flocs and biomass settleability was consequently improved by 20%.

- Chemical dissection of *Leptolyngbya* strain ECCN 20BG cell growth, granule formation and maintenance using sub-lethal concentrations of a wide variety of antimicrobial agents revealed that DNA-directed RNA polymerase, and to a lesser extent 30S ribosomal protein synthesis and prokaryotic cell wall synthesis are essential processes. This effect was more pronounced in co-cultures with *Chlorella* sp., and caused liberation of this poor flocculating microalga, which resulted in low biomass production and settleability < 20%.

- Some bacterial isolates from HRAOP MLSS were identified as *Bacillus* strain ECCN 40b (Accession No: MT705987), *Bacillus* strain ECCN 41b (Accession No: MT706002), *Planococcus* strain ECCN 45b (Accession No: MT705002), and *Exiguobacterium* strain ECCN 46b (Accession No: MT706012), and appeared to contribute to floc formation by releasing sticky EPS to form aggregated cells as observed by SEM analysis.

- EPS production by the isolated bacteria was growth associated and production occurred predominantly during the exponential phase. Highest EPS production was observed for *Bacillus* strain ECCN 41b that generated a maximum of 585 ± 50 mg/L. EPS production was relatively low in other strains at between 95 and 108 mg/L.

Taken together, the above results demonstrated that several factors and/or mechanisms are impacted by microbes in the MLSS and that these contribute to formation and settleability of MaB-flocs. Included are: (1) the presence of large and colonial microalgae within MaB-flocs may prevent floc disintegration and enhance recovery of biomass by gravity sedimentation, (2) the presence of filamentous cyanobacterial species that self-flocculate to form an interwoven network of filaments may play an important role in the structural stability and settleability of MaB-flocs, and (3) production or formation of EPS matrix whereon all microbial components can aggregate and develop a microenvironment.

Chapter 5: Isolation and partial identification of novel carotenoid pigments

5.1 Introduction

Apart from EPS-producing and floc-forming organisms, MaB-flocs also contain other organisms with potential biotechnological application including plant-growth-promoting rhizobacteria (Kumari *et al*., 2011; Coppens *et al*., 2015; Krug *et al*., 2020) and other bioactive substances such as vitamins, pigments, and antibiotics (Spolaore *et al*., 2006). Pigments such as chlorophylls, carotenoids, and phycobiliproteins are important metabolites especially in algal-based wastewater treatment systems, where they are required in the process of photosynthesis for the conversion of light energy by microalgae, cyanobacteria, and other phototropic bacteria for growth and reproduction. In addition, these pigments have attracted attention and gained commercial interest in place of the synthetic counterparts due to their health and industrial benefits (Saini *et al*., 2019). Phycobiliproteins, the light-harvesting pigments in cyanobacteria and red algae have been employed in the biomedical field as a fluorescent agent, in food industries as colorants, and in pharmaceutical industries due to their antioxidant, anticancer, and anti-inflammatory properties (Sekar and Chandramohan, 2008; Galetovic *et al*., 2020). Similarly, carotenoids which are the most commercialized pigments have also been reported to possess these properties, and in addition, are used in medicine as a precursor of vitamin A in humans (Asker *et al*., 2018).

Carotenoids are a widely distributed natural pigment responsible for the red, yellow, or orange colour in some fruits and vegetables such as carrots, corns, pumpkins, and tomatoes. About 1100 naturally occurring carotenoids have been identified from various sources including the most common ones containing C_{40} hydrocarbon backbone (polyene chain), the glycosylated carotenoids, and carotenoid esters. Carotenoids with a further extension of the polyene chain containing C_{45} or C_{50} have also been identified in different microorganisms (Vila *et al*., 2018). In living organisms, they serve the main purpose of light-harvesting in photosynthetic organisms and for protection against photooxidation in cells (Asker *et al*., 2007; Harvey and Ben-Amotz, 2020). They are also responsible for most of the various shades of bright colours observed in bacteria and fungi, hence are considered as a biomarker in the morphological characterization of these organisms in natural environments (Sahin, 2011). The bright colour of these isoprenoid compounds is important biologically by facilitating the attraction of pollinators and dispersal of seeds in flowers and fruits (Mercadante *et al*., 2016). Similarly, the

compounds are added to foods as colourants to enhance their appeal to consumers and subsequently increase their commercial usage and market value.

More importantly, carotenoids (mostly β-carotene α-carotene, γ-carotene, and β-cryptoxanthin) are provitamin A active because they possess unmodified β-ionone ring(s). By the action of carotene dioxygenase, Provitamin A is converted to retinol, which is then oxidized to retinal and retinoic acid, the active forms of vitamin A to support biological functions such as vision and immune system (Saini *et al*., 2015). Thus, since higher animals are not capable of synthesizing carotenoids, they are ingested through diets as precursors of vitamin A biosynthesis. In addition, carotenoids also possess antioxidant activity as they can react and quench oxygen reactive species and deactivate free radicals. These bioactive compounds therefore have therapeutic benefits as precursors for vitamin A, antioxidants, anticancer and anti-inflammation, which has increased their demand as natural colourants in food, feed, cosmetics, and pharmaceutical industries (Asker *et al*., 2018). Carotenoids are commercially produced by chemical synthesis, but only their natural counterparts are generally recognized as safe for food additives and dietary supplements, indicating the need for industrial production of naturally derived carotenoids (Ram *et al*., 2020). Carotenoids currently have a high market share greater than 150 million USD and projected to grow to 2.0 billion USD by 2026 (Harvey and Ben-Amotz, 2020). Indeed, the biotechnological and industrial importance of carotenoids cannot be over-emphasized.

Plants and other photosynthetic organisms have a long history in the commercial production of carotenoids due to their ability to synthesize these bioactive molecules. Bacteria are only recently explored as alternative sources due to their nontoxicity, easy cultivation, and extraction processes (Ram *et al*., 2020). Even so, only a few bacterial species such as *Paracoccus* sp. have been employed in the commercial production of carotenoids indicating more species are required for sustainable carotenoid production from bacteria. In Chapter 3, many pigment-producing microorganisms including *Flavobacterium*, *Planococcus*, *Exiguobacterium*, *Porphyrobacter*, *Truepera*, and *Roseomonas* among others were identified in a metagenomic study conducted to elaborate the biological components of MLSS generated in the HRAOPs of the IAPS used for municipal sewage treatment. Some of these bacteria (i.e. *Planococcus* strain ECCN 45b and *Exiguobacterium* strain ECCN 46b) were investigated further and identified as EPS-producers in Chapter 4, and confirmed as pigmented due to their appearance when grown in either liquid culture or on nutrient plates. This indicates the diversity

of carotenoid-producing microorganisms in the MaB-flocs generated in IAPS. Indeed, MaB-flocs have been explored as a potential source of these bioactive compounds for use as aquaculture and poultry feed supplements (Van Den Hende *et al*., 2014a; Ram *et al*., 2020). The animals accumulate pigments from the diet which enhances the quality of the animal products as seen in egg yolks, birds' feathers, fishes, and other kinds of seafood. Additionally, MaB-flocs was reported to contain 60% protein and are therefore regarded as an excellent alternative source of protein in animal diets (Mehrabadi *et al*., 2016; Jung *et al*., 2020).

Since these bioactive compounds are of immense commercial interest and value due to their various pharmaceutical and nutraceutical applications, it would be beneficial to consider them as a product stream in addition to water, biomass, biogas and biofertilizer that can be valorised from MaB-floc. Thus, recovery of high-value products like carotenoids with provitamin A or antioxidant activity may facilitate implementation and establishment of a biorefinery with IAPS-based wastewater treatment. Work in this chapter therefore describes in more detail the isolation and tentative identification of the pigments from *Planococcus* strain ECCN 45b and *Exiguobacterium* strain ECCN 46b isolated from MaB-flocs generated in an IAPS treating domestic sewage.

5.2 Results

5.2.1 Pigment accumulation by *Planococcus* strain ECCN 45b and *Exiguobacterium* strain ECCN 46b

Pigment accumulation by strains ECCN 45b and ECCN 46b was studied by harvesting cells from LB medium during the exponential, early and late stationary phases of growth and the results are shown in Figure 5.1. An increase in colour intensification of *Planococcus* cells during transition from exponential (i.e. after 13 h) to late stationary phase (up to 7 d) was indicative of pigment accumulation over the growth period (Figure 5.1 a). Preliminary analysis using UV-Vis spectrophotometry revealed a characteristic spectrum with carotenoid features with maximum absorption (i.e. λ_{max}) at 465 nm and less defined shoulder peaks at 437 and 490 nm (Figure 5.1 c). In addition, the UV-Vis spectrum of pigment extracts from *Planococcus* cells also revealed what appeared to be a *cis* peak at 400 nm during the exponential phase (Figure 5.1 c). This peak was more intense at early stationary phase (i.e. after 18 h) where little to no pigmented cells were observed, but gradually disappeared and by the late stationary

growth phase (i.e. after 48 h of incubation), the peak had reduced significantly allowing for the appearance and increased intensity of the characteristic carotenoid peaks.

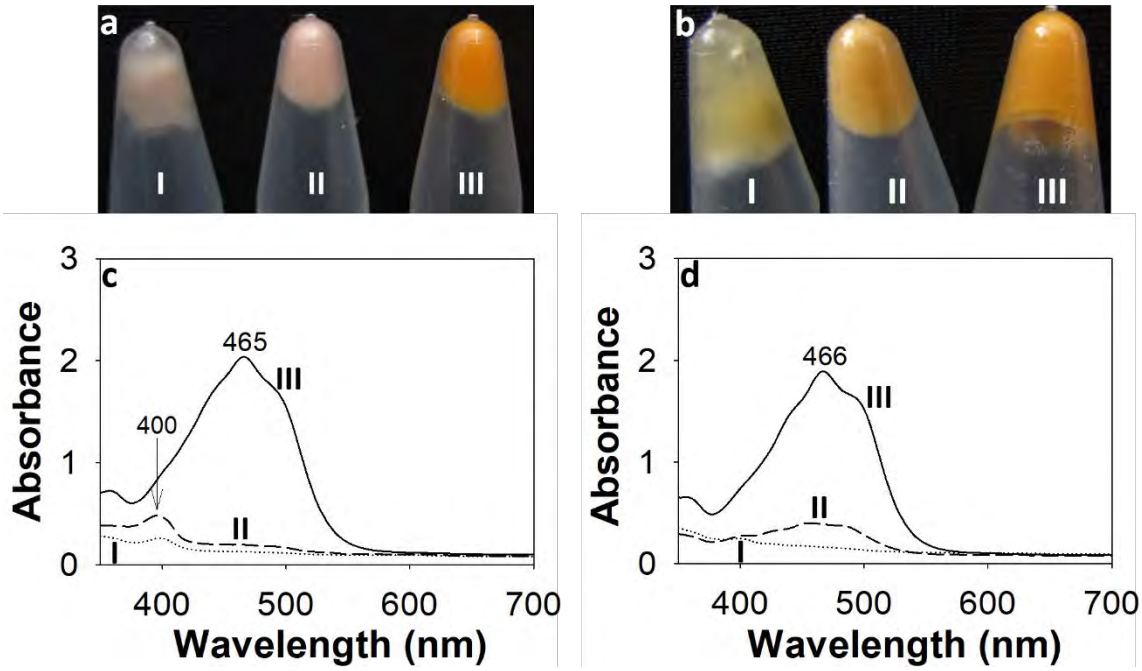

Figure 5.1: Pigment accumulation and colour intensification of cultured cells at different growth stages of *Planococcus* strain ECCN 45b (a) and *Exiguobacterium* strain ECCN 46b (b) in Luria Broth at 37°C. UV/Vis spectra of *Planococcus* and *Exiguobacterium* extracts in methanol at different growth stages are represented in Figure c and d respectively. Cells were harvested during exponential (I), early stationary (II), and late stationary phase (III) for pigment extraction.

Exiguobacterium strain ECCN 46b also displayed pigment accumulation during the stationary growth phase and a gradual increase in colour intensity of harvested cells from yellow to orange was observed over the growth period (Figure 5.1 b). While little to no pigment production was observed during the exponential phase (i.e. after 6 h), pigment accumulation started at the early stationary phase (i.e. after 10 h) with significant pigment production at the late stationary phase (i.e. after 24 h). Similar to *Planococcus* extracts, the UV/Vis spectrum of *Exiguobacterium* pigment extracts was typical of a carotenoid with an absorption maximum at 466 nm and two less defined shoulder peaks at 439 and 492 nm (Figure 5.1 d). No *cis* peak at 400 nm was present in pigments extracted from *Exiguobacterium* ECCN 46b suggesting a difference in the structural conformation of pigments accumulated by these organisms.

5.2.2 Determination of total carotenoid content

Extraction in a range of different solvents in order of increasing polarity, *n*-hexane < diethyl ether < chloroform < ethyl acetate < acetone < ethanol < methanol indicated that methanol was the most efficient at rendering pigmented extracts. The total carotenoid content extracted from both strains at exponential and stationary phases is presented in Figure 5.2. As might be expected, the highest carotenoid content was achieved at the late stationary phase for both strains where a maximum of 452.1 ± 4.7 and 574.4 ± 35.0 µg/g carotenoid was estimated for *Planococcus* strain ECCN 45b and *Exiguobacterium* strain ECCN 46b respectively. These results therefore suggest pigment accumulation could occur as a response to stressful conditions such as nutrient starvation usually experienced by cells in the stationary phase. Nevertheless, carotenoid production was usually higher in *Exiguobacterium* irrespective of the growth stage most likely due to its higher growth rate. A statistical analysis (*t* test at $P< 0.05$) also revealed that carotenoid production measured as β-carotene equivalent is higher in *Exiguobacterium* strain ECCN 46b than *Planococcus* strain ECCN 45b.

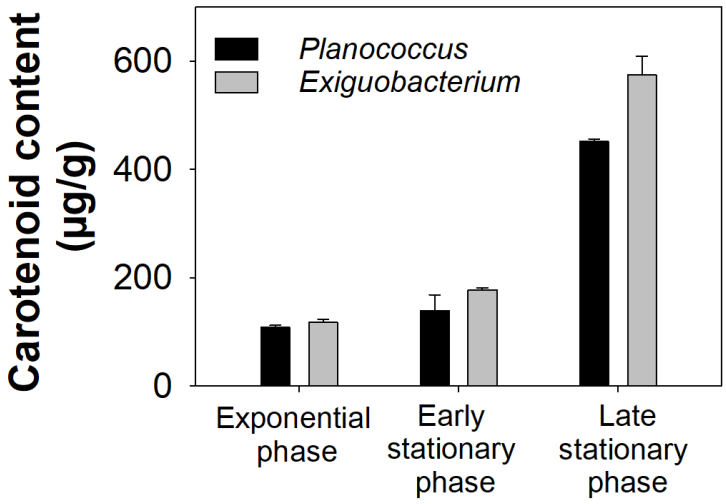

Figure 5.2: Estimation of total carotenoid accumulated by *Planococcus* strain ECCN45b and *Exiguobacterium* strain ECCN 46b at exponential and stationary growth phase. The total carotenoid content is expressed per gram of dry cell weight. Error bars represent S.E. of replicated samples.

5.2.3 Identification and tentative characterization of carotenoid pigments

5.2.3.1 Thin-layer Chromatography

Crude methanolic extracts containing carotenoid from *Planococcus* and *Exiguobacterium* strains were separated on thin layers of silica gel using chloroform/methanol/dichloromethane (40:10:50, v/v/v), which resolved extracts into three pigments for each strain (Figure 5.3 a). The more polar orange-coloured pigment (Zone 1) with an R_f value of 0.50 appeared as the major carotenoid in the two strains. The other two Zones (Zone 2 and 3) appeared as yellow and red with R_f values indicative of non-polar pigments at 0.84, 0.94 respectively.

The composition of each pigment relative to total carotenoid from each strain after saponification was estimated and results presented in Figure 5.3 b. Results show that pigments in Zone 1 were predominant and constitute 56 and 50% for *Planococcus* ECCN 45b (Lane 1) and *Exiguobacterium* ECCN 46b (Lane 2) respectively, suggesting these carotenoids might be responsible for the characteristic orange colour in both strains. Pigments in Zone 2 constitute 18 and 20%, while those in Zone 3 contained 26 and 29% for *Planococcus* and *Exiguobacterium* strains respectively (Figure 5.3 b).

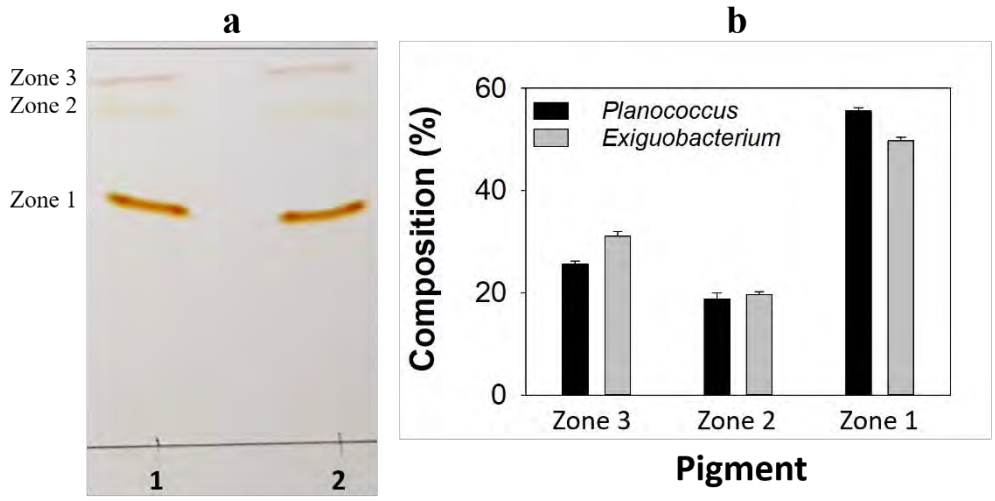

Figure 5.3: Thin layer chromatography of carotenoid-containing methanolic extracts of *Planococcus* strain ECCN 45b (Lane 1) and *Exiguobacterium* strain ECCN 46b (Lane 2) on silica gel (a), and the relative composition of each component to the saponified total extracts (b). Chromatography was carried out using a solvent combination of chloroform/methanol/dichloromethane in a ratio of 40:10:50 (v/v/v). The carotenoid composition was obtained by measuring the absorbance at a wavelength of λ_{max} after separation by TLC and elution in either methanol or dichloromethane. Error bars represent S.E. of replicated samples.

To gain further insight into the identity of these carotenoids and characteristics of the chromophore, the main pigment of each strain (Zone 1; Figure 5.3 a and b) was eluted from silica gel and analysed spectrophotometrically in different solvents and results are presented in Table 5.1. Some differences were observed in the spectra of these carotenoids especially the λ_{max}. Changes in λ_{max} absorption was across a gradient of solvent polarity, such that the most polar solvent, 85% methanol had the lowest wavelength at 458 and 462 nm while less polar chloroform had the highest at 474 and 477 nm for *Planococcus* and *Exiguobacterium* extract respectively. Thus, the change in the wavelength of λ_{max} was in the order of 85% methanol < methanol < acetone < dichloromethane < chloroform.

Table 5.1: Absorption characteristic of the main carotenoids extracted from *Planococcus* strain ECCN 45b and *Exiguobacterium* strain ECCN 46b in various solvents after separation and purification by thin-layer chromatography. Values in parentheses are polarity index of respective solvents.

Solvent	UV/Vis spectrum (λ_{max} nm)	
	***Planococcus* extract**	***Exiguobacterium* extract**
Chloroform (4.1)	444, 474, 507	445, 477, 508
Dichloromethane (3.1)	442, 470, 506	442, 472, 506
Acetone (5.1)	441, 462, 494	442, 468, 495
Methanol (5.1)	436, 460, 492	441, 466, 493
85% Methanol (>8)	437, 458, 491	441, 462, 493

5.2.3.2 FTIR analysis

Purified carotenoids (i.e. Zone 1; Figure 5.3) of *Planococcus* and *Exiguobacterium* strains were analysed by FTIR for partial characterization by the detection and identification of functional groups associated with these compounds. Generally, both carotenoids presented pronounced and intense peaks at 2846 and 2915 cm^{-1} corresponding to symmetrical and asymmetrical C-H stretching vibrations of CH_2 groups, while the peak at 2950 cm^{-1} corresponds to an asymmetrical C-H stretching of CH_3 groups (Lorand *et al*., 2002; Quijano-Ortega *et al*., 2020).

Strong peaks at approximately 1740 cm^{-1} and the weak ones in the region 1650 cm^{-1} also appeared on both spectra corresponding to the non-conjugated and conjugated C=O groups respectively (Sujak *et al*., 2007). Similarly, weak bands in the region 1460-1300 cm^{-1} of both carotenoid extracts correspond to bending and scissoring vibrations and what is called umbrella

deformation vibrations of CH_2 and CH_3 functional groups found on the polyene chain and β-ionone rings typical of most carotenoids (Berezin and Nechaev, 2005; Sujak *et al*., 2007). A series of peaks in the region 1200-1150 cm^{-1} are assigned to stretching vibrations of C-C of CH_3 on the polyene chain, while weak bands between 1100 and 1000 cm^{-1} are C-H deformation vibration on the polyene chain. A medium to strong peak observed at 963 cm^{-1} in the standard β-carotene (Figure 5.4; shown in purple) corresponds to the in-plane rocking vibration of CH_3 on the polyene chain and β-end groups.

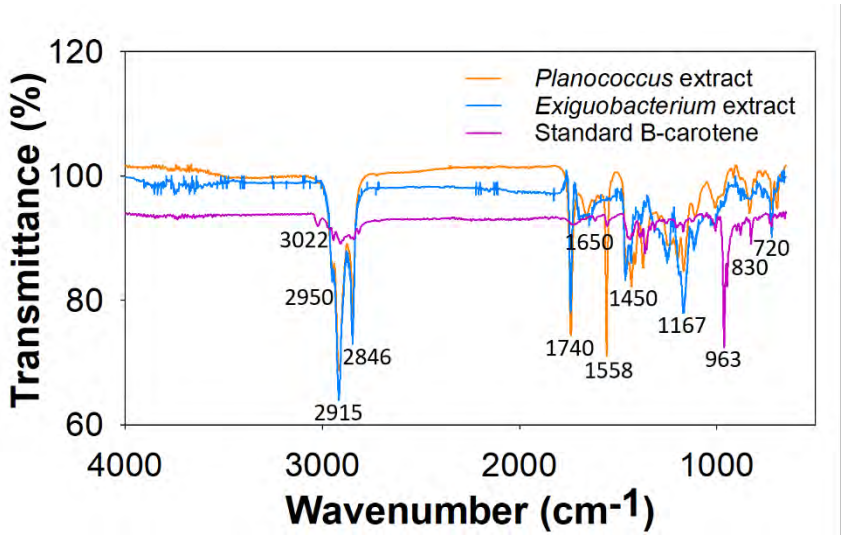

Figure 5.4: Vibrational FTIR absorption spectra of saponified pigments extracted from *Planococcus* strain ECCN 45b, *Exiguobacterium* strain ECCN 46b, and standard β-carotene. Solvent was removed from purified samples by evaporation in a CentriVap® and ~1 mg dried samples were used for analysis.

An important and notable difference in the spectra of both carotenoids appeared to be the presence of an intense peak at 1558 cm^{-1} in *Planococcus* extract but absent in *Exiguobacterium* extract (Figure 5.4; shown in blue). This peak corresponds to C=C of conjugated bonds typically present in carotenoids. The C=C peaks of carotenoids tend to be absent or weaker in less-conjugated molecules when a reduction of C=C to C-C occurs in the structural conformation (Lorand *et al*., 2002). Taken together, these results suggest the main carotenoid(s) extracted from cells of *Planoccocus* and *Exiguobacterium* are oxygenated and most probably ketocarotenoids due to the presence of characteristic intense carbonyl functional groups (i.e. keto groups). Moreover, both spectra have distinct features from the spectrum of a standard β-carotene, which contains only carbon and hydrogen in their chemical structure.

5.2.3.3 NMR analysis

NMR analysis was employed in an effort to further elucidate the structural components of the carotenoids accumulated by ECCN 45b and 46b strains and spectral data were interpreted using an online interpretation tool (St. Thomas, 2019), and reference to those described by Englert (1985) and Britton and Young (1993). A conclusive result could not be obtained for ^{13}C analysis due to the low concentration of the analysed sample and therefore interpretation was restricted to signals generated from ^{1}H analysis. Figure 5.5 shows the ^{1}H NMR spectra of an authentic β-carotene standard and the TLC-purified carotenoids extracted from *Planococcus* strain ECCN 45b and *Exiguobacterium* ECCN 45b. The respective proton chemical shifts, their characteristics and signal assignments are presented in Table 5.2.

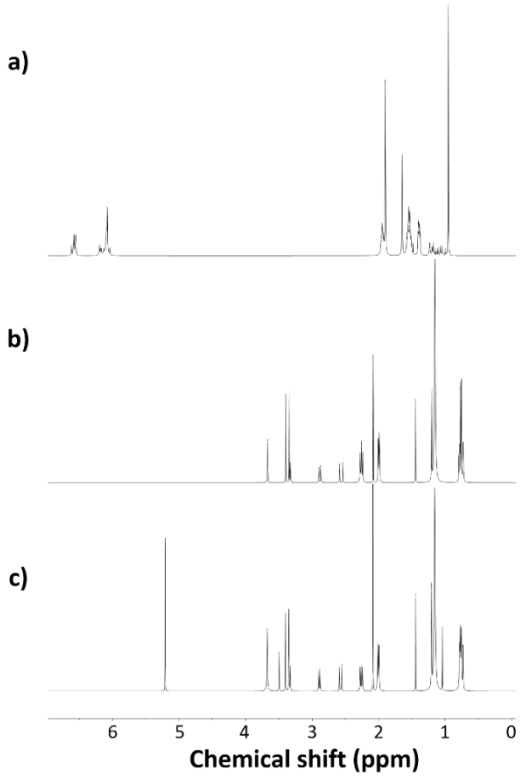

Figure 5.5: ^{1}H NMR spectra of β-carotene (a), and pigments from *Planococcus* strain ECCN 45b (b) and *Exiguobacterium* strain ECCN 46b (c). TLC-purified carotenoid samples (~2 mg) were dissolved in 0.6 mL $CDCl_3$ in 5 mm NMR tubes and ^{1}H NMR analysis carried out in a 400 MHz NMR spectrometer.

Proton signals bonded to methyl groups on the polyene chain and the β-end groups were detected around 0.76 and 2.00 ppm in all samples (Figure 5.5 a-c). In addition, most peaks of the novel carotenoid-like compounds were found in the region 2.0-4.0 ppm (Figure 5.5 b and c) corresponding to protons that are bonded to functional groups such as carbonyl, epoxide,

esters, and hydroxyl groups (Englert, 1985; Britton and Young, 1993) and therefore appears to support the FTIR data (Figure 5.4), where similar functional groups were detected. Results thus suggest that the main carotenoids produced by these strains are oxygenated and thus closely related to xanthophylls. The olefinic proton signals associated with conjugated bonds of carotenoids were observed in the region 6.0-7.0 ppm of the standard β-carotene (Figure 5.5 a). An olefinic signal in the spectrum of extract from *Exiguobacterium* strain was detected around 5.21 ppm but more intense in this region possibly due to the presence of oxygen functions in the chemical structure (Figure 5.5 c). Even so, this peak appeared to be absent in the spectrum of extract from the *Planococcus* strain.

Table 5.2: The ^{1}H NMR chemical shifts (δ in ppm) of the main carotenoids obtained from *Planococcus* strain ECCN 45b and *Exiguobacterium* strain ECCN 46b in $CDCl_3$. Letters in parentheses indicate signal multiplicity; singlet (s), doublet (d), triplet (t), and multiplet (m).

***Planococcus* extract**	***Exiguobacterium* extract**	**Standard β-carotene**
0.76 (m)	0.76 (m)	0.96 (s)
1.18 (d)	1.04 (s)	1.14 (m)
1.45 (s)	1.18 (d)	1.40 (m)
2.00 (m)	1.44 (s)	1.54 (m)
2.08 (s)	2.00 (m)	1.65 (s)
2.26 (m)	2.09 (s)	1.90 (s)
2.57 (d)	2.26 (m)	1.95 (t)
2.89 (d)	2.57 (d)	6.12 (m)
3.34 (d)	2.89 (d)	6.29 (d)
3.40 (s)	3.34 (d)	6.57 (m)
3.68 (s)	3.40 (s)	
	3.50 (s)	
	3.68 (s)	
	5.21 (s)	

5.3 Summary

Attempts to identify and partially characterize the pigments isolated from *Planococcus* strain ECCN 45b and *Exiguobacterium* ECCN 46b by UV/Vis spectrophotometry, thin-layer chromatography, FTIR, and NMR analyses revealed that:

- Pigment accumulation occurred mostly during the stationary phase in both strains. UV/Vis spectrum generated for both strains indicated that the pigment produced is carotenoid with

characteristic λ_{max} and shoulder peaks. carotenoid production was greater in the *Exiguobacterium* strain, which accumulated 574.4 ± 35.0 µg/g, while pigment concentration was significantly lower (452.1 ± 4.7 µg/g) in the *Planococcus* strain.

- Spectrophotometric analysis of accumulated pigment by UV/Vis revealed an identical characteristic carotenoid chromophore with absorption maxima at 466 nm and shoulder peaks at 437 and 490 nm in extracts from both strains. Separation on TLC revealed an orange-coloured predominant polar carotenoid of 0.5 R_f value constituting >50% of the total crude extracts, with different absorption wavelengths in various solvents and solvent combinations.

- Further analysis by NMR and FTIR spectroscopy revealed the presence of important functional groups such as methyl, methylene, and carbonyl groups, and protons associated with the characteristic conjugated polyene chain and terminal end-groups of carotenoids. Therefore, tentative identification of the major carotenoids from both strains was suggested to be closely related to xanthophylls (oxygenated carotenoids) and most likely ketocarotenoids due to the presence of intense peaks of carbonyl group in the FTIR spectra.

Findings indicate that in addition to the photosynthetically derived carotenoids from microalgae, bacterial components are also a potential source of these bioactive compounds, making IAPS and MaB-flocs a promising source of important carotenoids of biotechnological importance.

Chapter 6: Characterization of extracellular polymeric substances in mixed liquor suspended solids and bacterial isolates

6.1 Introduction

EPS are an important matrix regarded as requisite for microbial aggregates such as biofilms and flocs (Flemming and Wingender, 2001 and 2001b). In Chapters 3 and 4, it was shown that the production of EPS is indeed essential in the aggregation and formation of MaB-flocs in a mixed microbial population (i.e. MLSS) and attachment of bacterial cells in pure cultures. Based on association with microbial cells, EPS forms are categorized as either capsular that is directly attached to cells, or slimy that is excreted into the surrounding medium (Higgins and Novak, 1997). The extraction efficiency of the two fractions of EPS may however vary depending on the method used, as well as the origin, composition, and constituent microorganisms in the microbial aggregates (Jachlewski *et al*., 2015). It is therefore not surprising that both forms exist in HRAOP as reported in Chapter 3. These biopolymers typically contain polysaccharides and proteins, and other compounds such as uronic acid, amino acids, humic substances, and lipids may also be present depending on the environment and may have a significant effect on the bioflocculation process (Sheng *et al*., 2010; More *et al*., 2014).

In the process of floc formation, the positive and negatively charged functional groups of EPS components act as adsorption site to bind microbial cells through different mechanisms such as van der Waals forces, hydrophobic interactions, electrostatic interactions, ionic interactions, and hydrogen bonding (Sobeck and Higgins, 2002; Ding *et al*., 2015). The polysaccharides are considered as the principal components of the EPS matrix responsible for various functions (Table 1.3) such as aggregation, protection, adsorption, mass transfer, and as energy sink in various biological systems (Flemming and Wingender, 2010; Flemming, 2011). Even so, protein-rich EPS such as those extracted from activated sludge systems also play a role in the bioflocculation process by binding sugar residues in a cross-linkage protein-polysaccharide interaction, which is enhanced by divalent cation bridging with negatively charged sites of EPS to stabilize the matrix (Higgins and Novak, 1997). Anionic and surface-active EPS could act as a binding site for metals and are therefore used in the remediation of metal-contaminated water and in oil spillage and oil production sites to remove residual oil from surfaces

(Flemming and Wingender, 2001b). EPS are therefore capable of adsorbing various pollutants and nutrients present in wastewater, thus contributing to treatment efficiency.

Furthermore, microbial EPS also have other biotechnological importance that can be exploited. Different applications of EPS are compiled in Table 1.4., in addition to a bioflocculating characteristic that is frequently reported (Pi *et al*., 2020; Taghavijeloudar *et al*., 2020), EPS has found application in medicine, pharmaceutical, and food industries as wound healing and drug delivery agents, for cosmetics, as food thickener, emulsifier, oil recovery and chelators of metals (Trabelsi *et al*., 2015; Gupta and Diwan, 2017; Ajao *et al*., 2020). This has led to EPS extraction from various biological systems and microorganisms as a potential replacement of the more common chemical polymers.

In an effort to determine the environmental and biotechnological importance and further elucidate the function of biopolymers produced in the IAPS treatment process, this chapter describes the partial characterization of EPS generated from both 'mixed liquor' (S-EPS) and 'suspended solids' (B-EPS) in HRAOP treating domestic wastewater. Characterization was based on their biological, biochemical, and chemical properties, determined by carrying out flocculating efficiency, biochemical and FTIR analyses, and their emulsification ability using EPS materials generated at intervals described in Chapter 3. Research was also extended to elucidating the properties of EPS generated by the identified EPS-producing bacterial strains in Chapter 4.

6.2 Results

6.2.1 Bio-flocculating properties of EPS

In an effort to investigate the contribution of EPS to bioflocculation and aggregation of microorganisms, EPS fractions extracted from MLSS sourced from HRAOPs were added to cultures of unicellular microalga, *Chlorella* sp. Results show that the addition of S-EPS and B-EPS brought about coagulation of cells into flocs resembling those found in HRAOP (Figure 6.1). Even so, S-EPS appeared to be more effective at coagulation of the microalgal cells after 180 min of incubation at RT. In addition, microscopic examination before and after the addition of each form of EPS and aggregation showed *Chlorella* cells were still intact, indicating the addition of EPS as flocculant may not have resulted in any physiological changes.

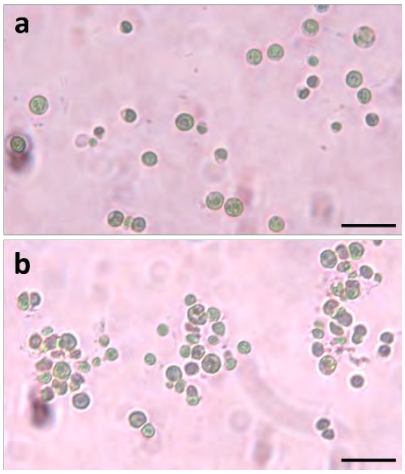

Figure 6.1: Microscopic images of *Chlorella* cells before (a) and after (b) flocculation with the addition of either S-EPS or B-EPS extracted from MLSS sourced from HRAOP. Scale bar = 54 µm.

To gain more insight into the coagulation and formation of flocs by EPS, biomass recovery efficiency after flocculation with different concentrations of EPS was further investigated. As presented in Figure 6.2 a, flocculation and recovery of *Chlorella* cells were evident upon increasing the concentration of S-EPS in the culture. An effect of 2 mg/mL S-EPS to flocculate cells was observed after 90 min, and by 180 min, 16% biomass recovery was achieved. Increasing the S-EPS concentration to 5 mg/mL resulted in an increased rate of flocculation to 30% after 180 min. A further increase of up to 60% biomass recovery with 10 mg/mL confirmed that the formation of stable cell aggregates is dependent on EPS concentration. In contrast, B-EPS resulted in 36% biomass recovery at a lower concentration of 2mg/mL and a further increment did not necessarily cause any significant changes in the flocculation process (Figure 6.2 b). These results indicate that the rate of flocculation is faster with B-EPS and that a higher concentration of S-EPS concentration is required for efficient biomass flocculation and recovery.

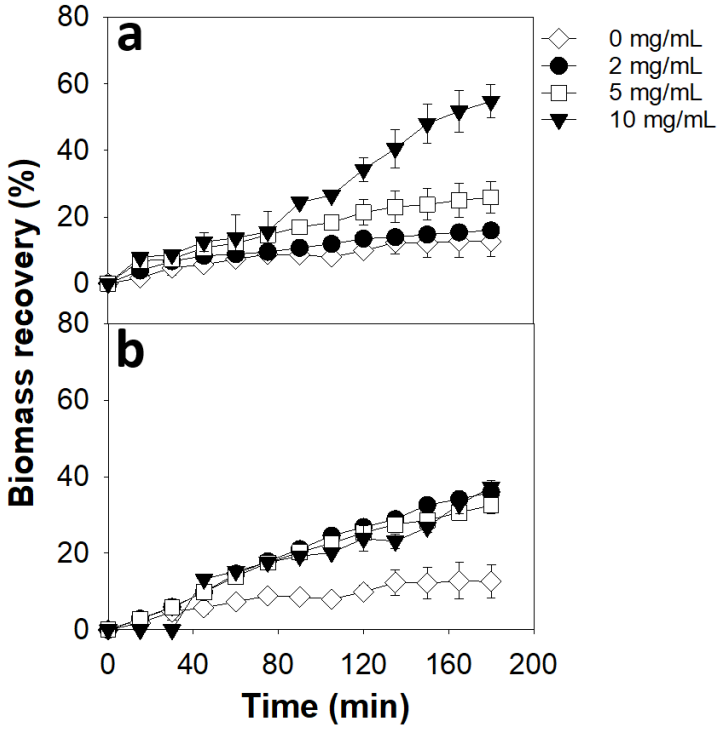

Figure 6.2: Recovery efficiency of *Chlorella* biomass in suspension after flocculation with different concentrations of S-EPS (a) and B-EPS (b). Results are mean ± S.E. of replicated experiments.

In an effort to determine the effectiveness of EPS as bioflocculant, biomass recovery after flocculation with S-EPS and B-EPS was compared to that of known chemical flocculants and the results are presented in Figure 6.3. Using ANOVA, some significant differences were observed between the flocculation efficiency of chemical flocculants and that of EPS fractions (Appendix E, Table E2). At a concentration of 2 mg/mL, biomass recovery of 60% achieved with a trivalent flocculant, $FeCl_3$ was significantly higher ($P<0.05$) than 17 and 36% recovery of S-EPS and B-EPS respectively. However, results showed that 26% and 24% recovery achieved with $CaCl_2$ and KCl respectively at the same concentration was significantly less effective than B-EPS but more than S-EPS. At 5 mg/mL flocculant concentration, $FeCl_3$ and $CaCl_2$ appeared to be more effective than both EPS fractions while KCl was less effective. At a higher concentration of 10 mg/mL, only $CaCl_2$ appeared to be more effective than both EPS fractions while other flocculants ($FeCl_3$ and KCl) showed much lower flocculating activity than S-EPS. The B-EPS as flocculant however appeared to be less effective than S-EPS and other bioflocculants except for KCl at higher concentration. Overall, these results suggest that EPS recovered from MLSS has a bioflocculating property that appeared to be more efficient or comparable to some chemical flocculants.

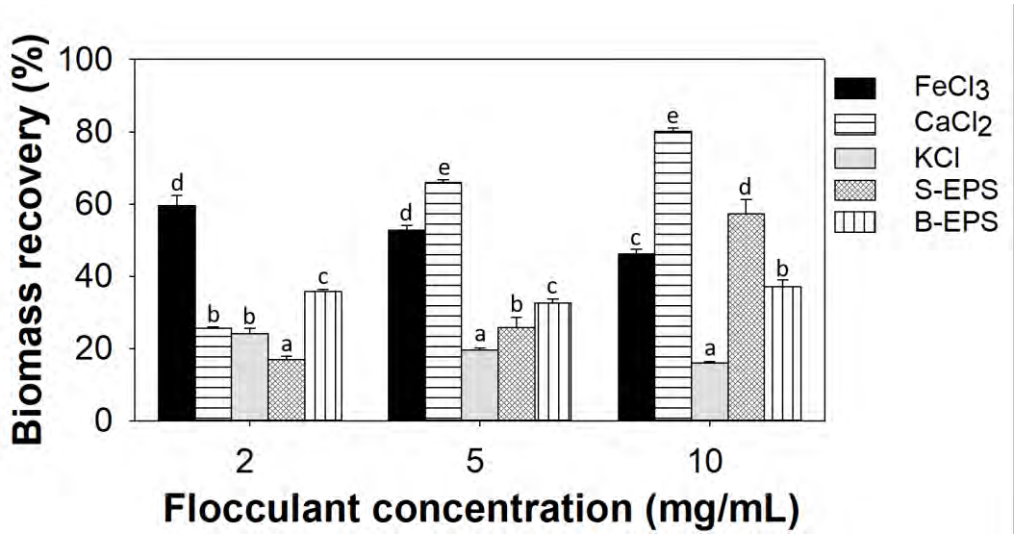

Figure 6.3: Comparison of the biomass recovery of *Chlorella* sp. mediated by different concentrations of MLSS EPS and metal ions as flocculants after 3 h. Values are the mean of replicated experiments and error bars represent S.E. The letters show the level of significance within each group at $P < 0.05$.

EPS sourced from bacterial strains also showed an ability to flocculate *Chlorella* cells at different concentrations (Figure 6.4). Similar to the trend observed with EPS generated from MLSS, flocculation of cells was dependent on the concentration of bacterial EPS added to the culture and as expected therefore, a 10 mg/mL EPS gave the highest biomass recovery. EPS produced by *Planococcus* strain ECCN 45b had the highest flocculating ability with a 37% biomass recovery after 3 h, while EPS of *Exiguobacterium* strain ECCN 46b and *Bacillus* strain ECCN 40b presented 31% and 22% biomass recovery respectively (Figure 6.4). When dissolved in water, EPS of *Bacillus* strain ECCN 41b forms a soluble and highly viscous solution, which prevented flocculation and settleability of biomass to occur, as such no biomass was recovered using this EPS. A statistical analysis (ANOVA at $P < 0.05$) therefore showed significant differences in the ability of the various bacterial EPS to flocculate *Chlorella* cells especially at higher concentrations (Appendix E, Table E2).

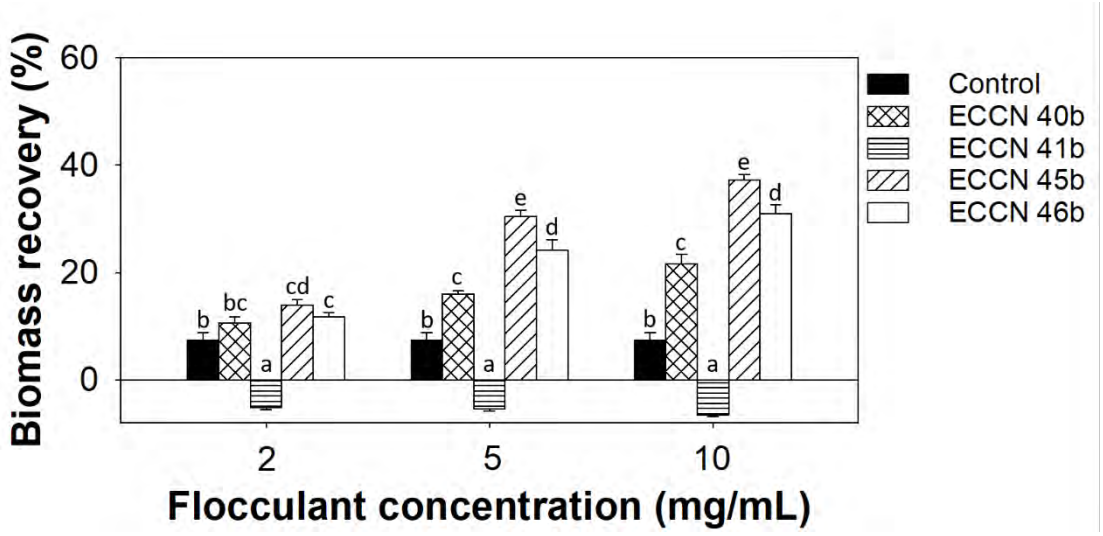

Figure 6.4: Percentage biomass recovered after flocculation of *Chlorella* sp. using bacterial EPS from different strains as flocculants. Results are presented as the mean of replicated experiments and error bars indicate S.E. The letters represent the level of significance within each group at $P < 0.05$.

6.2.2 Biochemical properties of EPS fractions

To determine the biochemical composition of EPS, the material was extracted from MLSS in HRAOP and prepared as described in Chapter 2. Aliquots of EPS materials were dissolved in Milli-Q water and analysed for the presence of carbohydrate, uronic acid, lipid, phenolic compounds, protein, and α-amino nitrogen. The data in Tables 6.1-6.3 show the biochemical composition of S-EPS and B-EPS extracted within a period of one year.

The carbohydrate content of S-EPS ranged between 84 and 367 mg/g with an average of 232.4 ± 25.2 mg/g (Table 6.1). The concentration of uronic acid appeared to be much lower at a range of 12-39 mg/g of S-EPS and an average of 24.0 ± 2.3 mg/g. The lipid concentration of S-EPS was found to be higher than the uronic acid content and ranged between 78 and 191 mg/g with an average of 155.2 ± 15.0 mg/g. Some amounts of phenolic compounds were also detected in a range of 49-126 mg/g of S-EPS to give an average of 97.1 ± 7.9 mg/g during the experimental period. Protein content was however found to be relatively low within the range of 29 and 45 mg/g and an average of 37.2 ± 1.3 mg/g, while the lowest biochemical content analysed was α-amino nitrogen with an average of 14.3 ± 0.9 mg/g of S-EPS. Statistical analysis (ANOVA at alpha level 0.05) showed a significant difference in some of these biochemical components, indicating a variation in the S-EPS fraction of MLSS extracted over an extended period (Appendix E, Table E3).

Biochemical analysis of B-EPS showed that carbohydrate content was relatively higher than S-EPS in the range of 115-744 mg/g and an average of 352.5 ± 62.7 mg/g (Table 6.2). Similarly, uronic acid was also relatively higher in B-EPS, which was within the range of 29 and 117 mg/g and an average of 53.9 ± 6.2 mg/g. However, the lipid content of B-EPS was much lower than that of S-EPS at a range of 38 and 224 mg/g with an average of 87.5 ± 12.9 mg/g. Phenolic compounds also appeared to be slightly higher in B-EPS and within the range of 78 and 200 mg/g with an average of 139.1 ± 13.1 mg/g. In addition, the protein and α-amino nitrogen content with an average of 65.2 ± 2.8 and 19.0 ± 1.9 mg/g were also significantly higher in B-EPS than S-EPS of MLSS. ANOVA at $P < 0.05$ (Appendix E, Table E4) also indicated a clear variation in all biochemical components analysed, except for α-amino nitrogen where no significant difference was observed in almost all values at interval.

A summary of the biochemical composition of EPS extracted from MLSS in HRAOP is presented in Table 6.3. The result shows that carbohydrate is the highest biochemical component in both EPS fractions and accounted for 26% and 41% of the total S-EPS and B-EPS respectively. Other components in high proportion were lipids and phenolic compounds that accounted for 18 and 10%, and 10 and 15% of the total S-EPS and B-EPS respectively. However, other components such as protein, α-amino nitrogen, and uronic acid were significantly low with each accounting for < 10% in both EPS fractions. These results provide a strong indication that a substantial amount of the EPS composition is bound to the microbial cells (i.e. the suspended solids of MLSS), which is important in the formation of a matrix in which the microbes are attached and embedded.

The biochemical properties of bacterial EPS are presented in Table 6.4. The highest carbohydrate content of 179.4 mg/g was found in EPS extracted from *Planococcus* sp., while EPS from *Exiguobacterium* sp. had the lowest carbohydrate concentration at 124.1 mg/g. There was however no significant difference in the carbohydrate concentrations of EPS from both *Bacillus* strains, which were in the range of 145.7-158.3 mg/g. The concentration of uronic acid appeared to be higher in EPS from *Bacillus* strains with an average of 35 mg/g, while concentration was lower in *Planococcus* sp. and *Exiguobacterium* sp. at 29.5 and 22.9 mg/g respectively.

The lipid content of all bacterial EPS was similar with an average of 52 mg/g and no significant difference ($P < 0.05$) was observed in all concentrations. Meanwhile, Rhamnolipids analysis showed that the biosurfactant is abundant in EPS of *Bacillus* sp. ECCN 41b, which accounted

for an average of 32% of the total EPS extracted from the isolate. The biosurfactant was however found to be either absent or in low concentration in other isolates. A significant concentration of phenolic compounds was also present in EPS synthesized by all isolates and concentrations ranged from 86 to 131.3 mg/g. Similar to the trend seen in EPS materials from MLSS, the concentration of protein and α-amino nitrogen was the lowest and accounted for less than 5% of the total EPS in most cases. Given these results, it was rationalized that differences may exist in the structural composition of EPS from various strains. Analysis of variance (ANOVA at $P < 0.05$) revealed a significant difference in all components except the lipid content (Appendix E, Table E5). In addition, the high rhamnolipid content of the highly viscous EPS of *Bacillus* strain ECCN 41b suggests it produces an anionic EPS, which may be one reason for its low bioflocculating ability reported in Section 6.2.1, Figure 6.4.

Table 6.1: Biochemical characteristics of soluble EPS (S-EPS) extracted from the mixed liquor of MLSS in HRAOP within a period of one year (February-December 2019). Data are mean ± S.E. of three analyses. The different letters represent a significant difference within each biochemical component at $P < 0.05$.

Sampling date	Carbohydrate (mg/g)	Uronic acid (mg/g)	Lipid (mg/g)	Phenolics (mg/g)	Protein (mg/g)	α-amino N (mg/g)
21-Feb	198.9 ± 2.7^{b}	17.4 ± 0.2^{b}	130.0 ± 5.3^{bcd}	49.0 ± 1.6^{a}	29.0 ± 1.0^{a}	16.4 ± 0.8^{f}
12-Mar	212.9 ± 15.0^{b}	15.1 ± 0.0^{ab}	148.8 ± 24.6^{bcde}	54.0 ± 6.6^{ab}	38.6 ± 1.0^{efg}	16.4 ± 1.3^{f}
20-Mar	275.8 ± 14.1^{c}	26.4 ± 2.5^{d}	314.5 ± 14.4^{f}	66.2 ± 13.0^{b}	42.3 ± 0.7^{gh}	23.9 ± 0.7^{g}
09-Apr	126.1 ± 7.5^{a}	15.4 ± 3.2^{ab}	147.7 ± 10.2^{bcde}	96.0 ± 7.4^{cd}	30.2 ± 1.1^{ab}	12.2 ± 0.5^{abc}
24-Apr	84.3 ± 5.7^{a}	34.7 ± 1.3^{f}	100.1 ± 11.4^{ab}	142.9 ± 5.0^{g}	33.7 ± 1.1^{bcd}	11.6 ± 0.3^{ab}
14-May	109.1 ± 16.6^{a}	11.9 ± 0.6^{a}	129.5 ± 13.9^{bcd}	65.8 ± 7.4^{b}	34.5 ± 2.1^{cde}	10.6 ± 0.3^{a}
24-May	116.0 ± 5.6^{a}	14.8 ± 0.7^{ab}	78.4 ± 15.5^{a}	114.0 ± 20.8^{ef}	31.8 ± 0.6^{abc}	12.8 ± 1.0^{bcd}
11-Jun	296.9 ± 36.7^{cd}	23.1 ± 1.8^{cd}	152.5 ± 20.5^{cde}	84.7 ± 1.6^{c}	35.4 ± 1.6^{cde}	11.7 ± 0.4^{ab}
25-Jun	214.1 ± 20.9^{b}	21.2 ± 3.5^{c}	110.4 ± 11.7^{abc}	97.4 ± 2.6^{cd}	42.2 ± 1.1^{gh}	14.1 ± 0.2^{cde}
12-Jul	344.6 ± 17.9^{de}	26.0 ± 3.4^{d}	141.9 ± 13.3^{bcde}	113.1 ± 11.6^{ef}	40.1 ± 0.6^{fg}	14.1 ± 0.7^{cde}
30-Jul	306.0 ± 5.0^{cd}	38.5 ± 3.3^{f}	186.8 ± 27.3^{e}	126.7 ± 6.3^{f}	36.9 ± 1.6^{def}	12.5 ± 0.1^{abcd}
15-Nov	366.7 ± 8.7^{e}	36.8 ± 2.2^{e}	191.2 ± 14.9^{e}	122.9 ± 4.5^{f}	40.4 ± 1.0^{fgh}	12.9 ± 0.5^{bcd}
28-Nov	296.1 ± 13.6^{cd}	30.0 ± 1.6^{f}	177.5 ± 8.6^{de}	126.0 ± 3.1^{f}	40.9 ± 2.7^{fgh}	14.5 ± 0.9^{def}
10-Dec	305.7 ± 10.6^{cd}	24.1 ± 1.3^{cd}	163.8 ± 8.2^{de}	100.7 ± 4.8^{de}	44.7 ± 1.1^{h}	15.9 ± 0.2^{ef}

Table 6.2: Biochemical characteristics of bound EPS (B-EPS) extracted from the suspended solids containing MaB-flocs of MLSS in HRAOP within a period of one year (February-December 2019). Data are mean ± S.E. of three analyses. The different letters represent a significant difference within each biochemical component at $P < 0.05$.

Sampling date	Carbohydrate (mg/g)	Uronic acid (mg/g)	Lipid (mg/g)	Phenolics (mg/g)	Protein (mg/g)	α-amino N (mg/g)
21-Feb	153.0 ± 10.1^{a}	39.5 ± 0.6^{ab}	37.8 ± 1.1^{a}	77.9 ± 1.1^{a}	49.6 ± 0.5^{ab}	12.8 ± 1.3^{a}
12-Mar	397.7 ± 44.1^{c}	47.0 ± 7.9^{bc}	224.3 ± 10.3^{f}	89.1 ± 6.9^{ab}	88.2 ± 4.5^{g}	35.6 ± 7.1^{b}
20-Mar	394.2 ± 49.7^{c}	33.3 ± 4.1^{ab}	73.8 ± 3.6^{bc}	78.8 ± 8.7^{a}	75.8 ± 3.6^{f}	35.2 ± 3.1^{b}
09-Apr	118.5 ± 6.9^{a}	46.4 ± 3.7^{bc}	42.2 ± 2.0^{a}	90.2 ± 0.8^{ab}	46.9 ± 2.5^{a}	16.5 ± 1.2^{a}
24-Apr	115.4 ± 5.0^{a}	28.5 ± 4.4^{a}	58.2 ± 2.2^{ab}	142.9 ± 3.6^{d}	61.5 ± 2.0^{cde}	15.8 ± 0.9^{a}
14-May	125.1 ± 9.8^{a}	47.2 ± 2.8^{bc}	50.4 ± 6.8^{a}	106.2 ± 9.5^{bc}	56.7 ± 4.1^{bc}	16.2 ± 0.9^{a}
24-May	171.6 ± 6.0^{a}	54.6 ± 3.2^{cd}	47.8 ± 1.5^{a}	122.2 ± 7.6^{c}	67.7 ± 1.2^{def}	14.3 ± 0.6^{a}
11-Jun	517.8 ± 73.6^{d}	29.3 ± 6.8^{a}	82.7 ± 4.0^{cd}	154.7 ± 10.0^{d}	58.8 ± 2.7^{bcd}	17.2 ± 0.9^{a}
25-Jun	742.3 ± 30.5^{e}	71.7 ± 0.5^{ef}	79.8 ± 6.5^{bcd}	175.8 ± 25.3^{e}	63.6 ± 4.2^{cde}	14.2 ± 0.1^{a}
12-Jul	687.6 ± 47.7^{e}	46.2 ± 7.0^{bc}	78.2 ± 2.2^{bc}	109.2 ± 3.4^{bc}	65.3 ± 0.4^{cde}	17.1 ± 0.9^{a}
30-Jul	743.8 ± 48.8^{e}	116.5 ± 22.3^{g}	109.8 ± 14.7^{e}	200.0 ± 23.2^{fg}	69.7 ± 4.4^{ef}	16.7 ± 0.6^{a}
15-Nov	304.0 ± 22.4^{bc}	76.4 ± 9.0^{f}	119.4 ± 3.8^{e}	203.5 ± 11.3^{fg}	70.8 ± 2.8^{ef}	17.9 ± 0.4^{a}
28-Nov	232.0 ± 19.9^{ab}	61.8 ± 7.7^{de}	119.7 ± 13.2^{e}	211.1 ± 9.4^{g}	68.5 ± 2.6^{def}	18.1 ± 0.5^{a}
10-Dec	231.7 ± 23.4^{ab}	55.8 ± 2.9^{cd}	100.8 ± 5.0^{de}	186.0 ± 10.3^{ef}	69.1 ± 3.3^{ef}	17.7 ± 0.7^{a}

Table 6.3: Percentage composition of EPS fractions of MLSS generated in HRAOP.

EPS fraction	Carbohydrates (%)	Protein (%)	Lipid (%)	α-amino N (%)	Phenolics (%)	Uronic acid (%)
S-EPS	26	4	18	2	10	3
B-EPS	41	7	10	2	15	6

Table 6.4: Biochemical characteristics of EPS produced by different bacterial strains in LB medium for 96 h. Results are mean of three independent analysis ± S.E. The different letters represent significant difference within each biochemical component at $P < 0.05$.

Strain	Carbohydrate (mg/g)	Uronic acid (mg/g)	Lipids (mg/g)	Rhamnolipids (mg/g)	Phenolics (mg/g)	Protein (mg/g)	α-amino N (mg/g)
Bacillus sp. ECCN 40b	158.3 ± 11.5^{bc}	35.8 ± 0.6^{c}	54.8 ± 2.4^{a}	23.3 ± 7.3^{a}	110.0 ± 0.6^{b}	59.0 ± 5.5^{b}	13.7 ± 0.0^{b}
Bacillus sp. ECCN 41b	145.7 ± 5.1^{ab}	34.8 ± 0.6^{c}	48.7 ± 2.1^{a}	315.0 ± 3.9^{b}	112.6 ± 3.3^{b}	43.1 ± 2.9^{a}	15.8 ± 0.2^{c}
Planococcus sp. ECCN 45b	179.4 ± 2.5^{c}	29.5 ± 0.3^{b}	51.7 ± 0.8^{a}	-	86.1 ± 5.3a	42.6 ± 0.1^{a}	11.4 ± 0.2^{a}
Exiguobacterium sp. ECCN 46b	124.1 ± 5.6^{a}	22.9 ± 0.4^{a}	52.4 ± 2.4^{a}	-	131.3 ± 12.0^{b}	43.9 ± 1.0^{a}	12.1 ± 0.3^{a}

6.2.3 FTIR analysis of EPS fractions

For a better understanding of the molecular composition and chemical structure of all EPS materials, FTIR spectroscopy was carried out and the spectra obtained are shown in Figure 6.5 and 6.6. Interpretation of absorption frequencies was carried out using an online tool (St. Thomas, 2019), and reference to the literature (Bramhachari and Dubey, 2006; Mishra and Jha, 2009; Wang *et al*., 2012; Zhu *et al*., 2012).

For S-EPS, the spectrum (Figure 6.5 a) shows a broad and intense peak in the range of 3000 and 3700 cm^{-1} (i.e. 3288 cm^{-1}), which signifies O-H stretching of either carboxylic acids or alcohols. A weak absorption at 2922 cm^{-1} corresponds to CH_3 symmetrical stretching vibration of aldehydes and ketones, while similar weak doublet peaks between 2159 and 2017 cm^{-1} represent a stretching vibration of C≡N of nitrile groups of cyanate compounds. A peak observed at 1631 cm^{-1} was found in the region of stretching vibrations of C=O of amides and C=C of alkenes or aromatics. A very strong peak at 1401 cm^{-1} corresponds to asymmetrical stretching of N-O of nitrate salts, while a medium peak at 1069 cm^{-1} is usually attributed to stretching vibration of C-O of alkoxy group in esters, ethers, alcohols, and carbohydrates.

The spectrum generated for B-EPS (Figure 6.5 b) showed the presence of functional groups such as the broad band of O-H observed at 3272 cm^{-1}. Similarly, a stronger CH_3 peak of aldehydes and ketones was present at 2921 cm^{-1}, while peaks at 2164 and 2020 corresponding to C≡C of alkynes and C-H of aromatics, respectively, appeared to be weaker in B-EPS compared to S-EPS. A peak at 1632 cm^{-1} of either a C=O of amides or C=C of alkenes and aromatics was observed to be significantly stronger in B-EPS. However, the N-O group (at 1407 cm^{-1}) indicating the presence of nitro compounds, which is very strong in S-EPS appeared to be very weak to absent in B-EPS. On the other hand, a striking difference observed between the two forms of EPS was the presence of a medium peak at 1529 cm^{-1} that corresponds to deformation vibrations of N-H of amines and amides in the spectrum of B-EPS. In addition, a peak, also found to be present in B-EPS but absent in S-EPS, was present at 1223 cm^{-1} and attributed to C-O stretching vibrations of acyl or phenol in carboxylic acids, acid anhydrides, esters, and phenolic compounds. The peak at 1038 cm^{-1} of C-O of alkoxy groups was also present and very strong in the B-EPS spectrum.

Overall, the functional groups observed in both forms of EPS showed the presence of nitrogen-, carbonyl-, hydroxyl- amino-, and phenol-containing compounds, indicating the

heterogeneous nature of these polymeric substances. Moreover, the functional groups are characteristics of sugars, proteins, amino acids, lipids, and possibly some aromatic compounds. This is specifically more so for the spectrum from B-EPS which showed an increased intensity of these functional groups suggesting a possible reason for a significantly higher concentration of some biochemical components (Table 6.3).

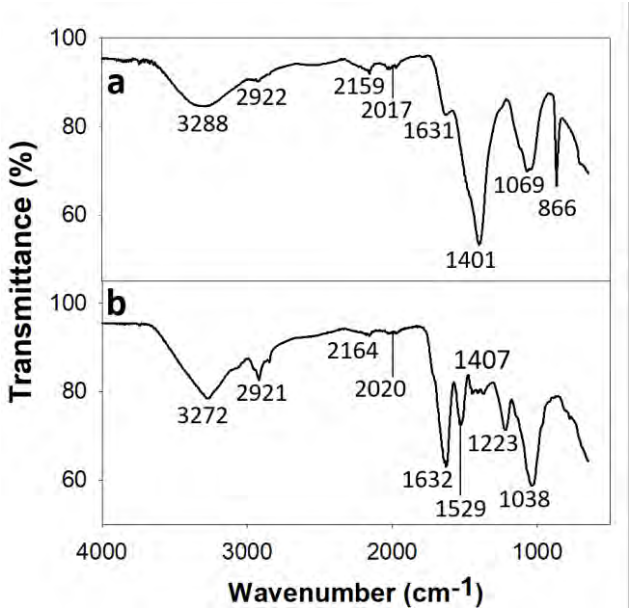

Figure 6.5: Typical FTIR spectra revealing the characteristic functional groups of S-EPS (a) and B-EPS (b) extracted from MLSS in HRAOP.

The FTIR spectra generated for EPS from all bacterial isolates were found to be similar but with some differences (Figure 6.6). The notable and intense peaks observed in all spectra included the characteristic broad band in the region 3271 cm^{-1} corresponding to O-H stretching of carboxylic acids, which overlaps a C-H stretching at 2926 cm^{-1} that corresponds to methyl functional groups. Peaks in the region 1636 cm^{-1} are assigned to C=C stretching vibrations of alkenes and aromatics. A distinct and broad peak at 1580 cm^{-1} (in the spectrum represented with cyan colour) was observed in *Bacillus* ECCN 41b but absent in other spectra. The peak corresponds to stretching vibration of C=O but appeared to be absent in other spectra suggesting a possible dissimilarity in the EPS exuded by this strain.

The medium peaks at 1540 cm^{-1} correspond to the bending vibrations of N-H groups in imines or amines, while the very weak peaks at 1447 cm^{-1} correspond to deformation vibration of C-H in esters, ethers, acetates, and ketones. Medium to weak peaks that appeared to be more prominent in ECCN 41b spectrum are assigned to deformation vibration in C-H bonds that are bounded to aldehydes, alcohols, amines, and amides. Strong peaks observed in the region of

1045 cm^{-1} are assigned to C-O stretching vibration of acyl, alkoxy, and ester groups, which are known to be characteristics of sugar derivatives such as carbohydrates, ethers, alcohols, esters, and aromatic compounds. Generally, the FTIR spectra of bacterial EPS closely resembled those generated for S-EPS and B-EPS suggesting that these too can contribute to the aggregation of MaB-flocs in MLSS.

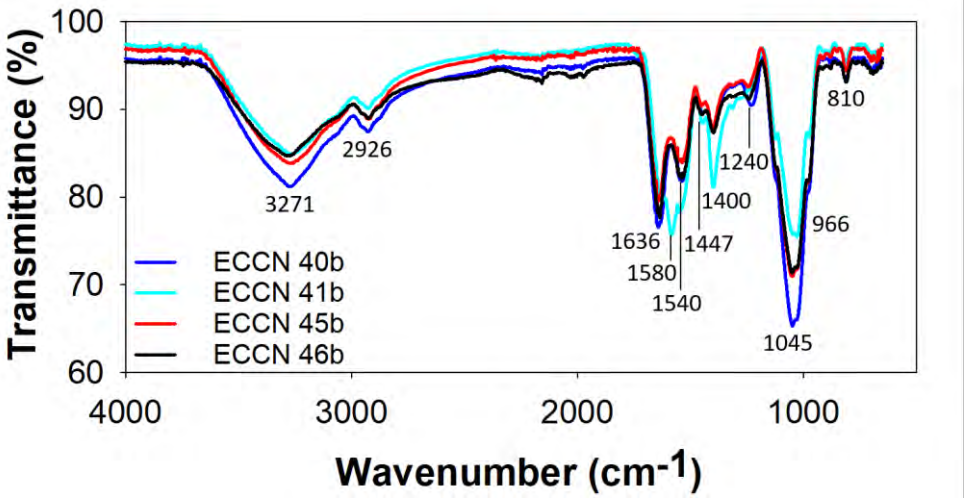

Figure 6.6: FTIR spectra of EPS generated by bacterial strains isolated from MLSS in HRAOP of an IAPS.

6.2.4 Emulsification activity of EPS

The ability of various EPS materials to form an emulsion and retain this surface-active property was investigated by determination of emulsification activity in different hydrocarbon and hydrophobic substrates and results are presented in Table 6.5. All forms of EPS generated in this study were shown to possess the ability to form and retain emulsions, and sunflower oil appeared to be the most efficient substrate for the formation of an emulsion irrespective of the EPS used. At a concentration of 10 mg/mL, S-EPS formed an emulsion that was stable for up to 48 h. While S-EPS showed no emulsification property against *n*-decane, the highest EA of 52% was achieved with sunflower oil and the lowest (48%) was against *n*-dodecane. Similarly, emulsion formed by B-EPS against different substrates was also stable for a long period of time and showed the highest emulsification ability against sunflower oil at 64%, while the lowest was achieved with paraffin at 52%.

EPS obtained from *Bacillus* strains ECCN 40b and ECCN 41b also showed biosurfactant properties by forming an emulsion with the tested substrates except for *n*-decane (Table 6.5). A 53% emulsification activity that was stable for a period up to 48 h was achieved with ECCN

40b EPS using sunflower oil as the substrate, while emulsification was found to be relatively low (37%) in paraffin. Similarly, the highest emulsification in ECCN 41b EPS was also with sunflower oil and a 62% EA was achieved after 24 h. However, EPS of *Planococcus* strain ECCN 45b and *Exiguobacterium* strain ECCN 46b showed no emulsification ability against all tested substrates. On the other hand, a commercial surfactant Triton X-100 appeared to be more efficient at forming and retaining emulsions than all EPS forms using the same concentration and substrates. Even so, a statistical analysis (t test at $P < 0.05$) showed no significant difference in the emulsification ability of Triton X-100, B-EPS, and ECCN 41b EPS when sunflower oil is used as the substrate. Results thus suggest that EPS generated from MLSS and some of its bacterial components possess some surface-active properties with the ability to emulsify hydrophobic compounds, indicating their potential application in the bioremediation and recovery of oil from contaminated soil and water.

Table 6.5: The emulsification activity of EPS fractions obtained from MLSS and bacterial strains against different hydrocarbon and hydrophobic substrates. Values are mean ± S.E. of replicated analyses.

Substrate	Emulsification index (%) *						
	MLSS EPS		Bacterial EPS				Chemical surfactant
	S-EPS	B-EPS	ECCN 40b	ECCN 41b	ECCN 45b	ECCN 46b	Triton X-100
n-Dodecane	48.0 ± 3.5	58.8 ± 3.4	48.5 ± 5.5	49.0 ± 1.9	-	-	63.4 ± 4.6
Paraffin	51.0 ± 1.9	51.0 ± 1.9	37.3 ± 5.2	52.9 ± 3.4	-	-	54.9 ± 2.0
n-Decane	-	-	-	-	-	-	56.8 ± 2.0
Sunflower oil	51.9 ± 1.0	63.8 ± 2.7	52.9 ± 3.4	62.0 ± 2.0	-	-	66.7 ± 5.2

***** Emulsification activity was conducted with 10 mg/mL of each sample and incubated at RT for 24 h

6.3 Summary

The study in this chapter investigated the structural features, properties and characteristics of EPS generated from MLSS (in Chapter 3) and bacterial strains identified (in Chapter 4). The findings confirmed that:

- EPS from MLSS coagulated *Chlorella* sp. cells to form flocs resembling those found in HRAOP. Thus, biomass recovery of up to 60 and 37% was achieved for S-EPS and B-EPS respectively and, at a concentration of 10 mg/mL and incubated for 3 h. EPS obtained from bacterial strains also showed bioflocculating properties that ranged from 22 to 37%, except for the highly viscous EPS produced by *Bacillus* strain ECCN 41b, where no flocculation or biomass recovery was achieved. While S-EPS from MLSS and other bacterial EPS was more effective at a higher concentration, there was no significant difference in the efficiency of B-EPS at lower or higher concentrations. When compared to chemical flocculants at a concentration of 10 mg/mL, biomass recovery was higher for S-EPS than KCl and $FeCl_3$, while B-EPS was only more effective than KCl.

- The biochemical components of both forms of EPS from MLSS varied over an extended period but comprised predominantly carbohydrates, lipids, and phenolics while other components such as protein, uronic acid, and α-amino N were detected in low concentrations. Due to a close association with microbial cells, B-EPS generally had a higher biochemical content of carbohydrates (41%), proteins (7%), lipids (10%), and humic-like substances (15%) compared to 26%, 4%, 18% and 10% of S-EPS respectively. All bacterial strains showed carbohydrate enrichment of between 12 and 18% while other components were relatively low. In addition, rhamnolipids were detected only in EPS obtained from *Bacillus* spp. especially ECCN 41b, where it accounted for 32% of the total EPS.

- The detection of nitro, carbonyl, hydroxyl, amino, alkoxy, and methyl functional groups by FTIR in EPSs obtained from MLSS and bacterial strains indicated the heterogeneous nature of these polymeric substances. Increased intensity of some of these functional groups in B-EPS indicated a possible reason for a significantly higher concentration of some biochemical components and their importance and function in the aggregation

and attachment of microbial cells. The nitro functional group was however observed to be more intense in S-EPS, possibly because it was extracted from an environment containing nitrate and nitrite salts. The viscous EPS exuded by *Bacillus* strain ECCN 41b also had a distinct peak of C=O, which indicated a different characteristic or chemical structure from other bacterial EPS.

- S-EPS and B-EPS were able to form emulsions with EA up to 52 and 64 % respectively against substrates such as *n*-dodecane, paraffin, and sunflower oil. Thus, B-EPS appeared to possess more surface-active property especially against sunflower oil that was comparable to a commercial biosurfactant, Triton X-100. Similarly, EPS generated by *Bacillus* strain ECCN 41b also had a significant EA of 62% and was therefore also comparable to Triton X-100, while no EA was achieved with *Planococcus* and *Exiguobacterium* strains. Results thus suggest that EPS generated from MLSS and ECCN 41b possess some surface-active properties with the ability to emulsify hydrophobic compounds, indicating their potential application in the bioremediation and recovery of oil from contaminated soil and water.

Chapter 7: General discussion and conclusion

7.1 General discussion

In an era when scarcity of freshwater is rampant, proper treatment of wastewater is of paramount importance and new, less costly technologies are emerging to achieve this outcome. Furthermore, it is particularly important for authorities to begin to utilize processes that add value to wastewater treatment and enable resource recovery. The IAPS is a good example of a technology that exploits the ecological dynamic to achieve sustainable wastewater treatment and resource recovery. Ecological dynamic refers to how organisms form processes of action to achieve perception and cognition within the environment. In so doing, organisms are able to link seemingly unrelated components within a system to facilitate perception and response i.e. signal-response coupling. Processes like IAPS, one of the many derivatives of AIWPS®, use an amalgamation of anaerobic and aerobic biological and microalgal-bacterial mutualism to achieve primary, secondary and tertiary biological wastewater treatment. Anaerobic digestion and breakdown of organic pollutants in the IPD of an IAPS can generate biogas with methane content >80%, and assimilation of nutrients to biomass in HRAOP components by photosynthetic oxygenation and bacterial oxidation apparently generates ~9 kg/d MaB-floc biomass or MLSS (Laubscher and Cowan, 2020). Consequently, IAPS and its relatives have been considered a platform technology for a fully operational solar-driven microalgae biorefinery for use not only in wastewater remediation but to produce biomass and energy.

Advanced pond systems (i.e. IAPS) were developed to provide solutions to sanitary management, support agriculture and food production in order to improve quality of life, especially in developing countries and rural communities with limited water supply (Oswald, 1995; Laubscher and Cowan, 2020). As envisaged by one of the pioneers of the technology, uses for wastewater would be more common in the 21st Century, and indeed, many products have been established for biomass generated from algal-based wastewater treatment systems as discussed extensively in Chapter 1 (Section 1.3.3). Even so, this can only be realized following the implementation of full-scale systems, which is currently hindered by land footprint. However, the generation of biomass was considered as a valuable commodity that makes IAPS stand out as a wastewater treatment system and if shown to be sustainable, could be key in transforming the technology. It is well-known and has been reiterated in many reports that harvesting is the main techno-economic challenge facing algal-based bioprocess systems (Sutherland and Ralph, 2020; Laubscher and Cowan, 2020). Thus, enhancing harvestability is

fundamental to guarantee a successful and sustainable microalgal biorefinery. Removal of algae and other biologicals from treated wastewater is also a regulatory prerequisite for effluent discharge to the environment. To this end, microbial interaction to form larger aggregates (i.e. flocs) has been found as a potential solution to the harvesting problem facing the industry and it appears that co-cultivation of microalgae with bacteria is one way forward. Formation of flocs in such systems would ensure discharged water meets municipal discharge standards as set by regulatory authorities. Moreover, this may also eliminate the need for a tertiary treatment unit since disinfection and complete removal of pathogens is achievable in HRAOP through elevated pH, oxygen, and exposure to UV radiation, even in winter (Young *et al*., 2016; Fallowfield *et al*., 2017; Laubscher and Cowan, 2020).

Since MaB-flocs (biomass formed as a result of microbial interaction between microalgae and bacteria) have been established to naturally form in MLSS of HRAOPs treating domestic sewage (Jimoh and Cowan, 2017), it seemed pertinent to study how this impacts the operation and maintenance of IAPS. The work presented in this thesis was carried out to investigate and address the importance and function of EPS production and MaB-floc formation in wastewater treatment, towards the development of a successful IAPS system that can fit in a circular economy. All investigations made use of a fully operational 500 PE pilot-scale IAPS that is supplied 75 m^3/d of domestic sewage. Emphasis was on elucidation of the importance and contribution of EPS and MaB-flocs in further developing the biorefinery concept for implementation of a system that can generate water for recycle and/or reuse and co-product beneficiation.

7.2 The impact of the microbial community on the dynamic of bioflocculation in HRAOP

The natural phenomenon of bioflocculation occurs in HRAOP, where microbial populations form aggregates through biological interaction. Even so, it appears that flocs are periodically lost in the system which results in poor settleability of biomass and poor water quality. This was a major concern for the performance of IAPS particularly in terms of TSS and COD of effluent quality (Mambo *et al*., 2014a). An investigation of the microbial component of MLSS in HRAOP over the course of one year was conducted through a metagenomic study in order to determine how the microbial composition or dominance may affect bioflocculation in the system. MLSS comprised eukaryotes dominated by the colonial microalgae *Pseudopediastrum* sp. and *Desmodesmus* sp., and bacteria (including cyanobacteria).

While the microbial community has been reported not to affect nutrient removal efficiency and biomass production in HRAOP (Sutherland and Ralph, 2020), the current study observed its impact on the bioflocculation of microbial constituents. Initially (February-May 2019), good flocs of settleable characteristic were formed in HRAOP. During this period, the colonial microalgae, *Pseudopediastrum* was observed as the dominant species indicating that the presence of this microalga facilitated the formation of flocs. Because of its large size, the dominance of *Pediastrum* efficiently enhances gravity-based harvesting by forming larger MaB-flocs than other colonial microalgae (Park *et al*., 2013a). In addition, selecting for the dominance of this species also increases biomass yield and resilience to grazing (Sutherland and Ralph, 2020). The change in microalgal dominance to *Desmodesmus* between June and July 2019 in the current study occurred with a simultaneous loss of flocculation in HRAOP. While this observation corroborates reports by Garcia *et al*. (2000) that the presence of *Scenedesmus*/*Desmodesmus* affects floc formation in HRAOP, the dominance of *Desmodesmus* persisted when floc formation was later restored (November-December 2019) in the pond. Results thus suggested that *Desmodesmus* was less likely responsible for the disappearance of flocs, and that other microbial components may play a role in the deflocculation process. Moreover, this study also reported a 75% settleability of the colonial strain, which corroborates other findings that have reported the involvement of *Scenedesmus* in the flocculation of biomass (Su *et al*., 2012; Guo *et al*., 2013).

Dominance by a filamentous bacterium, *Thiothrix*, coincided with a period of poor flocculation and settleability (< 40%) indicating that microbial composition of MLSS most likely determines the extent of MaB-floc formation. Generally, an overgrowth of filamentous microorganisms (including cyanobacteria) causes bulking in wastewater treatment processes by lowering floc density significantly, thus causing poor settleability. Important microorganisms necessary for COD and nutrient removal may also be lost from the microbial population (Henriet *et al*., 2017). *Thiothrix* has been particularly associated with biomass washout and loss of performance in wastewater treatment systems (Henriet *et al*., 2017; Stauch-White *et al*., 2017) and can therefore be attributed to the poor biomass production and flocculation that occurred during the period of its dominance. Although other filamentous cyanobacteria were detected, they occurred in lesser concentration, and were also detected during the period of good flocculation and therefore could not be attributed to the loss of flocs. Moreover, flocs with good settling characteristics are also made up of a moderate number of

filamentous bacteria that provide a structural backbone onto which other floc components can attach (Parker *et al*., 1972; Tiron *et al*., 2017).

This observation is also supported by studies where *Thiothrix* was reported as the dominant species in filamentous bulking sludge and negatively impacted the settling ability of flocs (Wu *et al*., 2019). In their report, Wu and co-workers further stated that the sulphur-oxidizing bacterium also interfered with oxygen transfer within the aerobic system due to their long filaments and other rheological properties. In an aerobic system like HRAOP where a symbiotic transfer of CO_2 and O_2 takes place between microalgae and bacteria, the dominance of *Thiothrix* that hinders oxygen transfer might have tampered with the performance and operation of the system, hence the low biomass production and poor MaB-floc formation experienced during this period. Indeed, the complete disappearance of *Thiothrix* from the microbial population, even when the cyanobacterial population had increased (but not in excess) restored the natural floc formation in the system irrespective of the dominating microalgae. Also, dominance of sulphur-oxidising bacteria such as *Thiothrix* and *Thiocapsa* that were detected in the bacterial population may be an indication of sulphur oxidation, which could increase the concentration of sulphur and sulphur compounds in the system. Although not measured in the current study, studies in the past have reported that AFP-treated water contains as high as 30.7 mg/L SO_4^{2-} (Tebitendwa, 2017), indicating a possible source of such compounds and the proliferation of microbial population responsible for their oxidation in HRAOP.

The presence of a rotifer, *Brachionus* in significant numbers also appeared to affect microalgal dominance in the current study. While the bacterial population was not affected, the presence of this rotifer appeared to reduce the microalgal and fungal population by almost half. On the contrary, Montemezzani *et al*. (2016) reported that grazers, especially rotifers in HRAOP usually target unicellular microalgae and those colonial organisms like *Pseudopediastrum* and *Desmodesmus* are able to survive grazing by producing spines as a defensive mechanism. It is therefore most likely that the absence of single-celled microalgae could have resulted in grazing on the dominant colonial species. Even so, flocculation was not affected and settleability was still significantly high during this period indicating that grazing pressure does not affect flocculation in HRAOP. Another possibility might be that the rotifer also secretes some infochemicals that aid the aggregation and settleability of biomass. Generally, a low zooplankton diversity was observed in HRAOP during the period of sampling most likely due

to the mixing, turbulent flow, and short HRT that facilitate washout of the system (Montemezzani *et al*., 2016).

The high throughput sequencing also detected quite a few fungal species that were found in significant quantity. Fungi have also been well associated with flocculation, but much research has not been directed towards the possibility. Self-palletisation occurs in many fungal strains either by spore coagulation or intertwining of hyphae that eventually result in aggregates or flocs (Nazari *et al*., 2020; Muradov *et al*., 2015). Moreover, a natural symbiotic relationship exists between fungi and microalgae and/or cyanobacteria, where fungi benefit from carbohydrates produced by microalgae during photosynthesis, and in return, fungi offer protection by retaining water and serving as a reservoir for minerals and nutrients (Zhou *et al*., 2013). Although not dominant, the fungal strains detected in the HRAOP microbial community were observed during the period of good flocculation indicating participation in the formation of microbial aggregates. Research reported by Zhou *et al*. (2013) developed a bioflocculation method involving the use of fungal pellets to harvest *Chlorella* cells from culture medium. The method proved to be efficient as almost 100% of microalgae was harvested. Using the same microalga as a model species, Muradov *et al*. (2015) and Li *et al*. (2020) also described fungal-assisted flocculation and harvesting of *Chlorella* sp. and the potential to use these microbes in a sustainable commercial microalgal production. This observation therefore suggests the feasibility of fungal-microalgal interaction in HRAOPs of IAPS. Also present and of significant importance, albeit not dominant in the microbial population are methane oxidizing bacteria. The presence of these methanotrophs in MaB-flocs could therefore play an important role in reducing the methane concentration in HRAOP, since the system is likely to receive methane-saturated water from AFP.

Apart from microbial factors, it was also observed that good and settleable flocs were formed mostly in warmer months when temperature and irradiance were higher, indicating a significant impact of these environmental factors on floc formation. This corroborates earlier findings that reported the presence of settleable flocs in summer, but no flocs were observed in winter (Dube, 2020).

7.3 A role for cyanobacteria in formation of HRAOP MaB-flocs

Cyanobacteria have been associated with various environmental problems such as algal blooms and production of toxic secondary metabolites that pose serious health risks to humans, animals

and damage to aquatic ecosystems (Wall *et al*., 2014; Zhu *et al*., 2015). However, they have also been shown to play an important role in microbial interaction for wastewater remediation and biomass recovery (Tiron *et al*., 2017; Stauch-White *et al*., 2017). Cyanobacteria secrete EPS, which have been described as either mucilaginous (Xu *et al*., 2013) or gelatinous (Tiron *et al*., 2017), essential in their attachment to surfaces and to provide a backbone structure for colonization and formation of microbial mats and biofilm. In addition, filamentous cyanobacteria have also been reported to provide a network structure for the formation of flocs in a heterogeneous environment for protection from unfavourable conditions (Tiron *et al*., 2017). While filamentous heterotrophic bacteria in conventional activated sludge systems play a similar role in the aggregation of biomass to form activated flocs (Liu *et al*., 2019), their excessive growth may cause bulking and an increase in sludge volume index that results in poor settleability of biomass as the case of *Thiothrix* described earlier. On the contrary, there are no reports of similar behaviour with filamentous cyanobacteria indicating their presence may serve as a refuge for other autotrophs and heterotrophs to promote stable floc formation.

The metagenomic study identified many cyanobacterial species such as *Phormidium*, *Nostoc*, *Leptolyngbya*, *Pseudoanabaena,* and *Synechococcus*, and these were more abundant during the period of floc formation. Using *Leptolyngbya* as a model species, this study reported a role of filamentous cyanobacteria in the structural formation of tightly aggregated flocs. Although not as dominant as other green microalgae in HRAOP, *Leptolyngbya* strain ECCN 20BG was chosen as a representative of cyanobacteria because it was culturable in selected media and most importantly, found in association with other microbial population present in the ponds. Moreover, *Leptolyngbya* spp. have been previously reported for their robust growth and tolerance to high temperature, pH, and solar irradiance in out-door growth conditions (Taton *et al*., 2012). Due to the self-flocculating characteristic of *Leptolyngbya* strain ECCN 20BG, a high settling velocity resulted in a 99% settleability and complete recovery of biomass and was comparable to that reported for *Phormidium* sp. (Pouliot *et al*., 1989; Tiron *et al*., 2015).

Certainly, incorporation of ECCN 20BG to MLSS generated in HRAOP promoted the development and maintenance of unicellular microalgae and bacteria cells in the entangled structure of the cyanobacterium. As a result, biomass settleability was improved by 20%. These findings are comparable to that reported by (Tiron *et al*., 2017), where the same principle was applied in the flocculation and recovery of *Chlorella* cells using filamentous cyanobacteria. The co-existence of ECCN 20BG with other microalgae and bacteria in a microenvironment

resulted in the significant removal of organic pollutants and nutrients supposedly through cell assimilation and nitrification processes. The observed porous and compact structure of cyanobacteria could promote efficient diffusion of organic matter, nutrients, oxygen, and light for other microbes within an immobilized environment. Indeed, previous studies have shown that a symbiotic association within a microenvironment of cyanobacteria, microalgae, and bacteria usually results in organic matter and nutrient assimilation into the development of flocs (Tiron *et al*., 2017). Moreover, the EPS matrix of cyanobacteria is known to be responsible for the storage and distribution of this organic matter and nutrients, by functioning as a reservoir for C and N uptake for heterotrophic bacteria in a microenvironment (Xu *et al*., 2013; Stuart *et al*., 2016). The findings in this study therefore indicate that secreted EPS and characteristic filaments of cyanobacteria are two important aspects that could be associated with the formation and development of large-sized flocs in HRAOP. Even so, downstream valorisation of MaB-floc biomass would therefore require screening for toxins as some cyanobacteria may produce certain toxic substances that could render the biomass not suitable for some purposes such as feed/fertilizer applications.

Loss of flocs in HRAOP of an IAPS may be in response to various conditions, including an allelopathic effect of one microorganism over another (Qiu *et al*., 2019). On the other hand, the presence of toxic compounds as part of organic pollutants could also affect floc formation (Wang *et al*., 2020). Antibiotics are emerging pollutants present in wastewaters and have been reported to have toxic effects on cyanobacteria by decreasing their abundance, diversity, and activity in a natural environment (González-Pleiter *et al*., 2019). Chemical dissection of floc formation and maintenance by *Leptolyngbya* strain ECCN 20BG, using sub-lethal concentration of a wide variety of antimicrobial agents revealed that DNA-directed RNA polymerase, and to a lesser extent 30S ribosomal protein synthesis and prokaryotic cell wall synthesis are essential processes. This concentration may however be different from the concentration in the real system since the system is continuous and passive, which may cause constant variation in the type or concentration of antibiotics in the influent and effluent. Nevertheless, the experiment gave an indication of a contributory effect of antibiotic on floc formation, which can be further studied in the real system for validation.

Loss of flocs upon exposure to antibiotics resulted in the liberation of unicellular microalgae since the scaffold onto which they attached had been destroyed. These findings agree with previous reports by Wang *et al*. (2020), who observed that tetracycline treatment of MaB-flocs

resulted in a gradual disappearance of the cyanobacterial population in floc composition. Furthermore, a previous study by Taton *et al*. (2012) has reported the sensitivity of a *Leptolyngbya* sp. to both chloramphenicol and streptomycin. These findings elucidate a scenario that may occur in a heterogeneous microbial community such as a HRAOP. In such an environment, the presence of different classes of antibiotics may inhibit the growth of certain cyanobacteria species necessary for biomass flocculation, while some may inherit antibiotic-resistant genes to develop resistance against these emerging pollutants, hence the possible loss of flocs observed in HRAOP. Studies have reported photodegradation and absorption as the major processes of antibiotic removal in HRAOPs (Home-Diaz *et al*., 2017; Villar-Navarro *et al*., 2018; Sutherland and Ralph, 2019). Adsorption of these pharmaceutical agents onto biomass may however facilitate their resistance and transfer within a floc microenvironment, which could propagate the distribution of antimicrobial resistance gene flow in IAPS.

The toxic effect of antibiotics on bacteria and cyanobacteria observed in this study indicates their presence in wastewater stream may also have an inhibitory effect on the formation of MaB-flocs in MLSS. A safe approach to alleviating the development of antibiotic resistance and ensure the removal of antibiotics to reduce their availability in wastewater would therefore be the formation of EPS-antibiotic complex. Studies have shown that EPS interacts with antibiotics by adsorption and thereby contributes to the removal of organic pollutants from wastewater (Chen *et al*., 2015). Moreover, the over-production of EPS by microorganisms has been suggested as a strategic response to the toxic effect of antibiotics (Wang *et al*., 2020). In addition, Xu *et al*. (2020) reported that these EPS-antibiotic complex could be efficiently removed by the addition of chemical coagulants to serve as flocculating agents. Given the adverse effect of chemical flocculants on the quality of treated effluent, the use of bioflocculant (i.e. EPS) could serve as an alternative.

7.4 Carotenoids as potential products of value in IAPS-produced MaB-flocs

Carotenoids are the most diverse pigments found in nature and are classified as either carotenes, containing hydrogen and carbon in their structures such as lycopene and β-carotene or the oxygenated derivatives known as xanthophylls. Depending on the functional group attached to the terminal end-group, xanthophylls could be epoxy-, hydroxy-, methoxy-, or keto-carotenoids. Interestingly, and from a commercial standpoint, the bacterial isolates characterized as *Planococcus* strain ECCN 45b and *Exiguobacterium* strain ECCN 46b accumulated pigments that were tentatively identified and partially characterized as carotenoid

using a combination of FTIR and NMR. The presence of broad peaks and loss of fine structure (mere shoulder peaks) in the UV/Vis spectra suggested the presence of cyclic β-end groups and certain functional groups such as hydroxy, methoxy, epoxy, keto and aldehyde, which are typical of carotenoids (Rodriguez-Amaya and Kimura, 2004; Takaichi, 2014). Detection of carbonyl groups in these carotenoids confirmed the close relatedness to xanthophylls, and most likely ketocarotenoids containing the typical C_{40} carbon in their structure. However, *Planococcus* sp. have been reported to synthesize glycosylated carotenoids with a unique structure of C_{50} carbons and the presence of sugar moieties in their terminal end-group (Vila *et al*., 2018). On the other hand, Shindo *et al*. (2008) and Kim *et al*. (2015) reported the production of C_{30} carotenoids from other strains of *Planococcus.* Similarly, White *et al*. (2018) reported that the C_{30} carotenoid biosynthetic pathway is responsible for pigmentation in most *Exiguobacterium* spp. This results therefore indicate the possibility of diversity in carotenoids that could be synthesized within the same genus.

Astaxanthin, and other common ketocarotenoids are produced commercially due to their extraordinary antioxidant activity and are therefore highly sort after as health care products, feed additives, and as food colorants. Although these carotenoids are chemically synthesized for use as feed supplements, natural pigments have an advantage over the chemically synthesized ones owing to the presence of a vast array of unique and important derivatives such as the C_{45} and C_{50} carotenoids (Fang *et al*., 2010; Venil *et al*., 2013; Yang *et al*., 2015). Moreover, chemically synthesized carotenoids are difficult and costly due to their structural complexity and are not generally recognized as safe for consumption or advised as dietary supplements (Heider *et al*., 2012; Ram *et al*., 2020). Even so, the production of natural carotenoids may not be sustainable due to the low pigment content in wild strains for commercial purposes. This resulted in a quest for the discovery of novel pigment-producing microorganisms and strategies to enhance pigment productivity.

Research has suggested the involvement of quorum sensing (QS) in the production of pigments in microorganisms (Venil *et al*., 2013). In response to certain conditions in their immediate environment, microorganisms are able to communicate and transfer genes amongst one another through pheromones or autoinducers, a basis in the formation of biofilm or MaB-flocs. Through this process, carotenoid biosynthesis has been reported in aphids by means of lateral gene transfer from fungi (Moran and Jarvik, 2010). Regulation of pigment production has also been associated with QS, where the accumulation of carotenoids during stationary phase was

dependent on the production of 3-oxo-C_6- AHL signal, a cell density-responsive transcriptional regulator protein (Mohammadi *et al*., 2012). This observation is also in accordance with findings in the current study where pigment production in *Planococcus* and *Exiguobacterium* strains seemed to have occurred in a cell-density dependent manner. This indicates that pigment production within a microenvironment such as MaB-flocs may be involved in cell to cell communication in order for colonization or aggregation to occur. This may therefore be promising for the commercial production of natural carotenoids from IAPS.

Furthermore, carotenoid production has also been reported to be stress-mediated by up-regulating the carotenoid biosynthetic pathway as a response to evading degradation or eradication (Patel *et al*., 2018; Ram *et al*., 2019). This phenomenon is therefore employed as a strategy in the production of considerable concentrations of carotenoids in microorganisms (Fang *et al*., 2010). The observed accumulation of carotenoid during the late stationary growth phase in the current study may also be attributed to response to nutrient starvation suggesting a fundamental role in cell adaptability to stress. Considering these findings, carotenoid accumulation in MaB-flocs may occur in response to a number of triggers including reaction to various environmental factors such as temperature, solar irradiance, and pH that are known to affect biomass production in HRAOPs as a means of surviving these harsh conditions. In addition to *Exiguobacterium* and *Planococcus* strains, a few other pigment-producing bacterial strains including *Flavobacterium*, *Porphyrobacter*, *Truepera*, *Sphingobacteria,* and *Roseomonas* were detected across all samples collected for metagenomic study suggesting bacterial pigments are an integral part of MaB-flocs.

Carotenoids are traditionally sourced from plants, fruits vegetables due to the biological role they play in photosynthesis. The detection of carotenoid-producing organisms in MaB-flocs presents it as a promising source of important bioactive compounds for biotechnological and industrial application. Indeed, many reports have highlighted their significance as fertilizer and feed supplement in agriculture and aquaculture. Because animals are not able to synthesize carotenoids, they are incorporated into their diet to enhance their quality and appearance, and in turn, increase the market value of these animal products. Van Den Hende *et al*. (2014b) reported that the carotenoid component of MaB-flocs incorporated into the diet of shrimp resulted in increased pigmentation. Similarly, studies have also shown that the use of MaB-flocs as organic fertilizer significantly increased carotenoid content in the tomato fruits and its effect was more profound than pure strain of *Nannochloropsis* sp. (Coppens *et al*., 2015).

Although comparisons were not made with extracts from flocs, the above findings suggest that pigments directly from MaB-flocs would likely contain increased concentration of carotenoids due to the presence of various pigmented species as opposed to a single strain. Thus, carotenoids are important and desirable property of MaB-flocs that could project IAPS as an attractive technology for wastewater treatment and generation of carotenoid-rich biomass in agriculture and aquaculture industries.

7.5 EPS: The structural backbone of MaB-flocs in HRAOP

EPS plays a crucial role in biological wastewater treatment systems by influencing microbial aggregate functions (Flemming and Wingender, 2001a and 2001b; Sheng *et al*., 2010; More *et al*., 2014). Also, in the current study, EPS appeared to be some sort of "chemical signal" responsible for the symbiotic relationship between microalgae and heterotrophic bacteria in an HRAOP. MLSS was found to contain EPS in loose form (S-EPS) and in association with suspended aggregates (B-EPS). Accumulation of these polymeric substances (especially S-EPS) was positively correlated with biomass concentration and settleability. Thus, formation of MaB-flocs was confirmed to be dependent on EPS production and under conditions of good floc formation, up to 95% biomass was recovered. Some bacterial isolates such as *Bacillus* spp., *Planococcus* sp., and *Exiguobacterium* sp. also produced EPS that caused aggregation of cells. *Bacillus* strain ECCN 41b produced relatively high amounts of EPS (>500 mg/L), which is comparable to or significantly higher than previously reported EPS-producing bacteria (More *et al*., 2012b; Drakou *et al*., 2018).

Paddlewheel mixing is an integral part of an HRAOP set-up. The eight-bladed mechanical stirrer ensures vertical and horizontal mixing of biomass for exposure to light and mass transfer between microbial cells (Pham *et al*., 2020). Even so, flocculation in a bioreactor (such as HRAOP) may also depend on the turbulent shear rate (mixing speed), the smaller the particle size and the higher its surface charge, the higher the turbulent shear required for the flocculation process (Oyegbile *et al*., 2016). Therefore, shear stresses due to turbulence may induce flocculation, usually at a very low shear rate. Once the shear stress reaches a threshold when turbulent shear force (i.e. frictional forces) becomes stronger than the flocs binding force, this instigates floc breakage (Manning, 2004; Markussen and Andersen, 2014; Oyegbile *et al*., 2016). Indeed, supplementary results obtained when the paddlewheel of HRAOP was under repair showed that although biomass productivity is enhanced with paddlewheel mixing, its absence resulted in the formation of larger flocs with higher settling velocity, and more B-EPS

was recovered from MaB-flocs (see Appendix D, Table D1 for details). This observation thus suggests that apart from the polymer-mediated interactions in HRAOP, other hydrodynamic interactions may also be involved in the bioflocculation process and therefore, requires further investigation.

Larger flocs are especially more fragile and easily broken down through high shear stress while small flocs are more resistant to breakage by turbulent shear (Manning, 2004). Therefore, turbulent flow caused by paddlewheel mixing may weaken the structure of the aggregate such that the loosely bound EPS is released into the medium and consequently, constitute the soluble microbial products that were measured as S-EPS in the current study. Although S-EPS may function in cell interaction and attachment, it also plays an unfavourable and detrimental role in bioflocculation by causing cell erosion or detachment from flocs in a turbulent environment (Li and Yang, 2007). Soluble microbial products (i.e. S-EPS) extracted in the current study were up to a maximum of 100 mg/L and this too might have an implication on the quality of IAPS-treated water. Indeed, Kunacheva and Stuckey (2014) reported that this S-EPS contributes 20% of the COD concentration, and given the consistent fluctuation reported on IAPS is a major concern. From all indications, it is therefore possible that the S-EPS may contribute significantly to the periodic elevation of COD in IAPS-treated water.

While various methods of extracting bound EPS (i.e. B-EPS) exists in the literature, the alkaline and heat treatment was adopted since it was reported to be efficient in EPS extraction by destabilizing EPS matrix and causing the release of common EPS components (Hong *et al*., 2017). Even so, it was observed that this method was not efficient in the case of a more compact cyanobacterial floc/granule and even an additional step of sonication was not effective. This indicates that a more stringent method of extraction might be required to break the compact structure in order to access the EPS matrix on the cell wall. The same method of extraction appeared to be rather too harsh on MaB-floc biomass (especially when floc formation is poor). Indeed, Hong *et al*. (2017) reported that this method of extraction may cause cell membrane lysis and leakage of intracellular substances. Therefore, the choice of an EPS extraction method would depend on the physical characteristic of flocs or aggregates to be analysed.

Bacterial and soluble EPS from the MLSS showed bioflocculating ability and up to 60% of *Chlorella* biomass was recovered when these were used as flocculant. Since all biologicals are negatively charged, a repulsive force exists between neighbouring cells that prevent close contact and poor settleability in suspension. The presence of positive binding sites in the EPS

matrix that surround cells offset the repulsive force through ion bridging or Van der Waals force of attraction to facilitate cell attraction and attachment (Li and Yang, 2007; More *et al*., 2012a). FTIR analysis revealed the characteristic functional groups present in these biopolymers, which together with cations might lead to ion bridging between the negatively charged *Chlorella* cells bringing the cells together to form a floc. On the contrary, the highly viscous EPS obtained from *Bacillus* strain ECCN 41b prevented flocculation and settleability of *Chlorella* cells. Based on these properties and coupled with its high rhamnolipid content (32%) and surface-active properties, the EPS from *Bacillus* sp. ECCN 41b was considered anionic and may have potential application in metal or oil recovery (Ajao *et al*., 2020). The results therefore suggest that the EPS-producing *Bacillus* strain is suitable and could be employed in the treatment of acid-mine drainage, a destructive process left behind after mining activities.

Furthermore, EPS from MLSS also showed some surface-active properties and an ability to emulsify up to 62% hydrophobic compounds such as sunflower oil. Because of their surface-active property, extracellular lipids and biosurfactants can disperse hydrophobic substances and are therefore employed in bioremediation and recovery of oil spills (Flemming and Wingender, 2001a). The results in the current study therefore suggest the potential application of these microbial EPS as an adsorption site of hydrophobic pollutants in wastewater treatment and as an emulsifier in food industries.

All EPS forms were polysaccharide-rich, while other components such as proteins, α-amino nitrogen, and uronic acids were detected in low quantities. On the contrary, most studies usually report a high protein content in EPS from activated sludge probably due to the presence of high amount of exoenzymes (Flemming and Wingender, 2001b; Comte *et al*., 2006; Li and Yang, 2007). The carbohydrate enrichment of MaB-floc EPS may stem from its microbial composition being predominantly microalgae. Indeed, EPS generated from microalgae have been reported to have a higher carbohydrate content consisting of different sugars including glucose, galactose, rhamnose, fructose, and fucose (Mishra and Jha, 2009; Ahmed *et al*., 2014; Nguyen *et al*., 2020). The generally low protein content could also be attributed to the choice of extraction method. Hong *et al*. (2017) suggested that the heat method of extraction could denature or hydrolyze protein components of EPS into amino acids and therefore may lead to underestimation. The detection of α-amino nitrogen in the EPS supports this theory even though only a small proportion exists in both fractions of EPS.

Interestingly, lipids and phenolic compounds were found to be significantly high in both fractions of EPS and therefore indicate the biosurfactant property and presence of aromatics in EPS generated in this study. Lipids are known to participate in the adhesive property of EPS and the presence of lipid derivatives such as biosurfactants also help in microbial colonization (More *et al*., 2014). Since phenolics were measured as humic acid equivalent in the current study, it is also possible that the presence of some humic materials from wastewater also contributed to the high phenolic concentration. Although humic-like substances are not directly secreted by microbes, their presence also influences the adsorption and biodegradation ability of EPS (More *et al*., 2014). Indeed, Tong *et al*. (2020) reported that the presence of humic acids reduced the biotoxicity of tetracycline on the microalgae *Coelastrella* sp. In another report by Xu *et al*. (2020), tetracycline removal in wastewater was found to occur by ion bridging between amino functional groups in EPS and Al^{3+} of polyaluminium chloride. Results in the current study therefore indicate that the presence of humic acid is significant to MaB-floc EPS by acting as a binding site for the remediation of antibiotics and thus improve the quality of IAPS-treated water. Moreover, the presence of these polymeric substances has also been shown to prevent lateral transfer of antibiotic-resistant genes by ion bridging (Hu *et al*., 2019).

Overall, almost all the B-EPS (81%) was accounted for through the biochemical analysis. On the contrary, only 63% of the total S-EPS could be fixed to either carbohydrate, protein, lipids, or phenolics indicating that a significant proportion of the EPS was not accounted for. The remaining proportion is likely to be in the form of inorganic nutrients such as phosphates and nitrates. Indeed, qualitative analysis by FTIR showed the presence of an intense peak of nitro compounds in the S-EPS spectrum generated. This implies that in addition to its effect on COD concentration, EPS may also contribute a significant proportion to nutrient concentration in the final effluent of IAPS-treated water. It is however also possible that the remaining proportion of EPS are nucleic acids and unknown organic acids that were not measured in the current study.

7.6 Evaluation of IAPS for biomass recovery and valorisation

Microalgae are a diverse group of organisms considered as next-generation biomass simply because they are able to meet industrial and agricultural demand. More so, cultivation in wastewater makes the process more sustainable and has therefore been considered for various applications ranging from biofuel to more refined and high commodity products. As reported in the current study, association with bacteria means more biomass and recovery of potentially

beneficial biomass for commercial use. However, production costs remain the main hindrance in the viability of microalgal-based biorefinery. Coupling biomass production with wastewater treatment allows for a circular economy, where natural methods are utilized to recover nutrients and energy for economic reuse (Sutherland *et al*., 2020). Regardless of the dominant microalgal species, biomass production in HRAOP is typically low compared to the theoretical maximum productivity of 50-60 g/m^2/d.

In this study, biomass productivity was very similar to a value of 10 g/m^2/d reported by Sutherland *et al*. (2013) for a wastewater treatment HRAOP. It however appeared that the period of floc formation experienced higher productivity compared to the period of no flocculation. Even though seasonal changes in temperature and solar radiation may be a contributing factor, a positive correlation of EPS production, floc formation dynamic and biomass productivity indicate the involvement of EPS in the performance and productivity of an IAPS. The implication therefore is that during the period of poor MaB-floc formation, the TSS concentration of final effluent may increase and consequently reduces biomass recovery. Taken these observations suggest that EPS production may be a prerequisite in IAPS operation, performance, and biomass recovery for valorisation.

The existing options for the valorisation of MaB-flocs have been discussed extensively in Chapter 1 (Section 1.3.3). Judging by the low productivity (compared to the theoretical value) observed in the current study, conversion to biofuel may not be an attractive option for IAPS. Rather, focus should be more on locations and environments where land would not be a major constraint and where the generated biomass will be fully maximized. Peri-urban spaces are rapidly evolving locations and indeed, the suitability of IAPS in such areas has been reported (Cowan *et al*., 2019; Laubscher and Cowan, 2020). Moreover, agricultural and aquaculture practices are more common in these areas thus positioning IAPS at the water-food nexus. Algae-based wastewater treatment systems have gained interest in agriculture and aquaculture industries due to the dual ability to treat wastewater and generate biomass for fertilizers and animal feed (Han *et al*., 2019). Aquaculture wastewater contains the essential nutrient necessary for microalgal growth and can therefore be assimilated into biomass that is in turn used as feed. Moreover, the production of biofertilizer from MaB-flocs have been shown to be more economically feasible than biofuel (Arashiro *et al*., 2018).

Land availability or footprint remains the major criteria hindering the establishment of a full-scale IAPS. Thus, consideration should be given to reinvigoration of the technology into a more

sustainable one. For example, the use of revolving algal biofilm (RAB) could be adopted. Indeed, it has been observed that biofilm develops on the paddlewheel of HRAOP (personal observation), indicating the feasibility of this process if incorporated into the IAPS configuration. In addition, promoting the growth of filamentous cyanobacteria or fungi may be a potential solution to improve flocculation within HRAOP in order to improve on the established gravity sedimentation as a method of biomass harvesting for IAPS.

7.7 Conclusion

Implementation and uptake of IAPS for commercial purposes is still low despite its benefits. Operation of a full-scale system is therefore required without which beneficiation of the by-products would not be realized. To address improvement on biomass recovery and harvesting, which is a limitation of the system, the current study highlighted and demonstrated the importance and function of *in situ* EPS production and flocculation towards a cost-effective recovery of resources from the bespoke technology. Some MLSS components were demonstrated as indicator species that could facilitate MaB-floc formation. This together with the production of carbohydrate-rich EPS with high flocculating ability could lead to successful exploitation of biomass generated within the system. These two products therefore appeared to be essential in the operation and maintenance of an IAPS. The current study also demonstrated that recovery of high-value products such as carotenoids is achievable with IAPS and thus gives the system an added advantage over other wastewater treatment technologies. However, an LCA analysis may be required to determine the cost implication or economic feasibility of generating such high-value product. For instance, it is pertinent to determine the best and sustainable extraction and purification methods while generating sufficient material for downstream application.

Once a sustainable biomass recovery can be realized through gravity settling of flocs, the establishment of a biorefinery would then be possible to recover a range of products such as methane-rich biogas, fertilizer, animal feed, and other fine chemicals and compounds. In this way, the size of the system may be overlooked or ignored particularly in peri-urban or rural communities where these products are highly sorted to support agriculture and food production while addressing poor sanitation, contamination of water bodies, and preservation of the limited water sources through recycle and/or reuse.

References

Abid, Y., Joulak, I., Amara, C. B., Casillo, A., Attia, H., Gharsallaoui, A. and Azabou, S. (2018). Study of interactions between anionic exopolysaccharides produced by newly isolated probiotic bacteria and sodium caseinate. *Colloids and Surfaces B*, *167*, 516-523.

Acién, F. G., Gómez-Serrano, C., Morales-Amaral, M. M., Fernández-Sevilla, J. M. and Molina-Grima, E. (2016). Wastewater treatment using microalgae: how realistic a contribution might it be to significant urban wastewater treatment? *Applied Microbiology and Biotechnology, 100 (21)*, 9013-9022.

Ahmed, M., Moerdijk-Poortvliet, T. C. W., Wijnholds, A., and Hasnain, S. (2014). Isolation, characterization and localization of extracellular polymeric substances from the cyanobacterium *Arthrospira platensis* strain MMG-9. *European Journal of Phycology, 49 (2),* 143-150.

Ajao, V., Nam, K., Chatzopoulos, P., Spruijt, E., Bruning, H., Rijnaarts, H. and Temmink, H. (2020). Regeneration and reuse of microbial extracellular polymers immobilised on a bed column for heavy metal recovery. *Water Research*, *171*, 115472.

Al-Shayji, Y. A., Puskas, K., Al-Daher, R. and Esen, I. I. (1994). Production and separation of algae in a high-rate ponds system. *Environment International*, *20 (4)*, 541-550.

An, C., Ma, S. J., Chang, F. and Xue, W. J. (2017). Efficient production of pullulan by *Aureobasidium pullulans* grown on mixtures of potato starch hydrolysate and sucrose. *Brazilian Journal of Microbiology, 48,* 180-185.

An, W., Guo, F., Song, Y., Gao, N., Bai, S., Dai, J., Wei, H., Zhang, L., Yu, D., Xia, M., Yu, Y., Qi, M., Tian, C., Chen, C., Wu, Z., Zhang, T. and Qiu, D. (2016). Comparative genomics analyses on EPS biosynthesis genes required for floc formation of *Zoogloea resiniphila* and other activated sludge bacteria. *Water Research*, *102*, 494-504.

Aquino, S. F., Gloria, R. M., Silva, S. Q. and Chernicharo, C. A. L. (2009). Quantification of the inert chemical oxygen demand of raw wastewater and evaluation of soluble microbial product production in Demo-scale upflow anaerobic sludge blanket reactors under different operational conditions. *Water Environment Research*, *81 (6)*, 608-616.

Arashiro, L. T., Montero, N., Ferrer, I., Acien, F. G. and Garfi, M. (2018). Life cycle assessment of high rate algal ponds for wastewater treatment and resource recovery. *Science of the Total Environment*, *622-623*, 1118-1130.

Arashiro, L.T., Ferrer, I., Rousseau, D.P.L., Van Hulle, S.W.H. and Garfí, M. (2019) The effect of primary treatment of wastewater in high rate algal pond systems: Biomass and bioenergy recovery. *Bioresource Technology*, *280*, 27-36.

Arcila, J. S. and Buitrón, G. (2016). Microalgae-bacteria aggregates: effect of the hydraulic retention time on the municipal wastewater treatment, biomass settleability and methane potential. *Journal of Chemical Technology and Biotechnology*, *91*, 2862-2870.

Arcila, J. S. and Buitrón, G. (2017). Influence of solar irradiance levels on the formation of microalgae-bacteria aggregates for municipal wastewater treatment. *Algal Research*, *27*, 190-197.

Asker, D., Awad, T. S., Beppu, T. and Ueda, K. (2018). Screening and profiling of natural ketocarotenoids from environmental aquatic bacterial isolates. *Food Chemistry*, *253*, 247–254.

Asker, D., Beppu, T. and Ueda, K. (2007). Unique diversity of carotenoid-producing bacteria isolated from Misasa, a radioactive site in Japan. *Applied Microbiology and Biotechnology*, *77*, 383–392.

Babicki, S., Arndt, D., Marcu, A., Liang, Y., Grant, J. R., Maciejewski, A., and Wishart, D. S. (2016). Heatmapper: web-enabled heat mapping for all. *Nucleic Acids Research*, *17*.

Bajaj, I. B., Survase, S. A., Saudagar, P. S. and Singhal, R. S. (2007). Gellan Gum: Fermentative Production, Downstream Processing and Applications. *Food Technology and Biotechnology, 45 (4),* 341-354.

Banat, I. M., Puskas, K., Esen, I. I. and Al-Daher, R. (1990). Wastewater treatment and algal productivity in an integrated ponding system. *Biological Wastes*, *32*, 265-275.

Barros, A. C., Gonçalves, A. L. and Simões, M. (2018). Microalgal/cyanobacterial biofilm formation on selected surfaces: the effects of surface physicochemical properties and

culture media composition. *Journal of applied Phycology*, doi.org/10.1007/s10811-018-1582-3.

Barros, A. I., Goncalves, A. L., Simoes, M. and Pires J. C. M. (2015). Harvesting techniques applied to microalgae: A review. *Renewable and Sustainable Energy Reviews*, *41*, 1489-1500.

Belcher, H. and Swale, E. (1978). A beginner's guide to freshwater algae. The Culture Centre of algae and protozoa, Institute of Terrestrial Ecology, Natural Environment Research Council. ISBN 0 11 881393 5.

Benemann, J. R., Weissman, J. C., Koopman, B. L. and Oswald, W. J. (1977) Energy production by microbial photosynthesis. *Nature*, *268 (5615)*, 19-23.

Berezin, K. V. and Nechaev, V. V. (2005). Calculation of the IR spectrum and the molecular structure of β-carotene. *Journal of Applied Spectroscopy*, *72 (2)*, 164-171.

Bradford, M. M. (1976). A rapid and sensitive method for the quantification of microgram quantities of protein utilizing the principle of protein-dye binding. *Analytical Biochemistry*, *72*, 248-254.

Bramhachari, P. V. and Dubey, S. K. (2006). Isolation and characterization of exopolysaccharide produced by *Vibrio harveyi* strain VB23. *Letters in Applied Microbiology*, *43 (5)*, 571-577.

Britton, G. and Young, A. J. (1993). Methods for the isolation and analysis of carotenoids. *In Carotenoids in Photosynthesis* 409-459.

Brooks, M. J., du Clou, S., van Niekerk, J. L., Gauche, P., Leonard, C., Mouzouris, M. J., Meyer, A. J., van der Westhuizen, N., van Dyk, E. E. and Vorster, F. (2015). "SAURAN: A new resource for solar radiometric data in Southern Africa". *Journal of Energy in Southern Africa*, *26*, 2-10.

Brownlee, C. (2002). Role of the extracellular matrix in cell-cell signalling: paracrine paradigms. *Current Opinion in Plant Biology, 5 (5)*, 396-401.

Burgos-Diaz, C., Pons, R., Espuny, M. J., Aranda, F. J., Teruel, J. A., Manresa, A., Ortiz, A. and Marques, A. M. (2011). Isolation and partial characterization of a biosurfactant mixture produced by *Sphingobacterium* sp. isolated from soil. *Journal of Colloid and Interface Science*, *361*, 195-204.

Cassie, V. (1983). A guide to algae in oxidation ponds in the Auckland district. *TANE*, *29*, 119-132.

Castillo, N. A., Valdez, A. L. and Fariña, J. I. (2015). Microbial production of scleroglucan and downstream processing. *Frontiers in Microbiology, 6,* 1106. doi: 10.3389/fmicb.2015.01106.

Chambonniere, P., Bronlund, J. and Guieyesse, B. (2020). Escherichia coli removal during domestic wastewater treatment in outdoor high rate algae ponds: long-term performance and mechanistic implications. *Water Science and Technology*, *82 (6)*, 1166-1175.

Chen, P., Zhou, Q., Paing, J., Le, H. and Picot, B. (2003). Nutrient removal by the integrated use of high rate algal ponds and macrophyte systems in China. *Water Science and Techno*logy, *48 (2)*, 251-257.

Chen, Z., Zhang, Y., Gao, Y., Boyd, S.A., Zhu, D. and Li, H. (2015). Influence of dissolved organic matter on tetracycline bioavailability to an antibiotic-resistant bacterium. *Environmental Science and Technology*, *49 (18)*, 10903–10910.

Cheng, K. C., Demirci, A. and Catchmark, J. M. (2011a). Pullulan: biosynthesis, production, and applications. *Applied Microbiology and Biotechnology, 92,* 29-44.

Cheng, Y-S., Zheng, Y. and VanderGheynst, J. S. (2011b). Rapid quantitative analysis of lipids using a colorimetric method in a microplate format. *Lipids*, *46*, 95-103.

Chong, B. F., Blank, L. M., Mclaughlin, R. and Nielsen, L. K. (2005). Microbial hyaluronic acid production. *Applied Microbiology and Biotechnology, 66,* 341-351.

Chowdhury, S. R., Basak, R. K., Sen, R. and Adhikari, B. (2011). Characterization and emulsifying property of a carbohydrate polymer produced by *Bacillus pumilus* UW-02 isolated from wastewater irrigated agricultural soil. *International Journal of Biological Macromolecules*, *48*, 705-712.

Comte, S., Guibaud, G. and Baudu, M. (2006). Biosorption properties of extracellular polymeric substances (EPS) resulting from activated sludge according to their type: Soluble or bound. *Process Biochemistry*, *41*, 815–823.

Coppens, J., Grunert, O., Van Den Hende, S., Vanhoutte, I., Boon, N., Haesaert, G. and De Gelder, L. (2016). The use of microalgae as a high-value organic slow-release fertilizer results in tomatoes with increased carotenoid and sugar levels. *Journal of Applied Phycology*, *28 (4)*, 2367-2377.

Corominas, L. I., Foley, J., Guest, J. S., Hospido, A., Larsen, H. F., Morera, S. and Shaw, A. (2013). Life cycle assessment applied to wastewater treatment: state of the art. *Water Research*, *47 (15)*, 5480–5492.

Costerton, J. W., Geesey, G. G. and Cheng, K. J. (1978). How bacteria stick. *Scientific American*, *238*, 85-95.

Cowan, A. k., Jimoh, T. A., Laubscher, R. and Askew, D. (2019). Golden ponds peroxonated-for water, energy and food. *Water Sewage & Effluent* (December/January edition). 31-33.

Cowan, A. K., Mambo, P. M., Westensee, D. K. and Render, D. S. (2016). Evaluation of integrated algae pond systems for municipal wastewater treatment: The Belmont Valley WWTW pilot-scale IAPS case study. Report to Water Research Commission. No: TT 649/15.

Cowan, A.K. and Render, D.S. (2012). Integrated algae ponding system, technical description. Unpublished report for the Institute of Environmental Biotechnology. Rhodes University, South Africa.

Craggs, R. J., Davies-Colley, R. J., Tanner, C. C. and Sukias, J. P. S. (2003b). Advanced ponds systems: performance with high rate ponds of different depths and areas. *Water Science and Technology*, *48*, 259-267.

Craggs, R., Park, J., Heubeck, S. and Sutherland, D. (2014). High rate algal pond systems for low-energy wastewater treatment, nutrient recovery and energy production. *New Zealand Journal of Botany*, *52 (1)*, 60-s73.

Craggs, R., Tanner, C., Sukias, J. and Davies-Colley, R. (2003a). Dairy farm wastewater treatment by an advanced pond system. *Water Science and Technology*, *48*, 291-297.

Cydzik-Kwiatkowska, A. and Zielinska, M. (2016). Bacterial communities in full-scale wastewater treatment systems. *World Journal of Microbiology and Biotechnology*, *32 (4)*, 66.

Czaczyk, K. and Myszka, K. (2007). Biosynthesis of extracellular polymeric substances (EPS) and its role in microbial biofilm formation. *Polish Journal of Environmental Study*, *16 (6)*, 799-806.

De Godos, I., Guzman, H. O., Soto, R., García-Encina, P. A., Becares, E., Muñoz, R. and Vargas, V. A. (2011). Coagulation/flocculation-based removal of algal–bacterial biomass from piggery wastewater treatment. *Bioresource Technology*, *102*, 923-927.

De Schryver, P., Crab, R., Defoirdt, T., Boon, N. and Verstraete, W. (2008). The basics of bio-flocs technology: The added value for aquaculture. *Aquaculture*, *277 (3-4)*, 125-137.

Decho, A. W. and Gutierrez, T. (2017). Microbial extracellular polymeric substances (EPSs) in ocean systems. *Frontiers in Microbiology*, *8*, 922. doi:10.3389/fmicb.2017.00922.

Delanka-Pedige, H. M. K., Cheng, X., Munasinghe-Arachchige, S. P., Bandara, G. L. C. L., Zhang, Y., Xu, P., Schaub, T. and Nirmalakhandan, N. (2020). Conventional vs. algal wastewater technologies: Reclamation of microbially safe water for agricultural reuse. *Alga Research*, *51*, 102022.

Delattre, C., Pierre, G., Laroche, C. and Michaud, P. (2016). Production, extraction and characterization of microalgal and cyanobacterial exopolysaccharides. *Biotechnology Advances*, *34*, 1159-1179.

Delgado-Pelayo, R. and Hornero-Mendez, D. (2012). Identification and quantitative analysis of carotenoids and their esters from Sarsaparilla (*Smilax aspera* L.) Berries. *Journal of Agricultural and Food Chemistry*, *60 (33)*, 8225−8232.

Department of Water Affairs (2013). Government Notice No. 665, Revision of General Authorizations in terms of Section 39 of the National Water Act, 1998 (Act No. 36 of 1998). Government Gazette Vol No. 36820, Cape Town.

Devi, C. S., Reddy, S. and Mohanasrinivasan, V. (2014). Fermentative production of dextran using *Leuconostoc* spp. isolated from fermented food products. *Frontiers in Microbiology, 9 (3),* 244-253.

Dias, E., Oliveira, M., Jones-Dias, D., Vasconcelos, V., Ferreira, E., Manageiro, V. and Caniça, M. (2015). Assessing the antibiotic susceptibility of freshwater cyanobacteria spp. *Frontiers in Microbiology*, *6*, 799.

Ding, Z., Bourven, I., Guibaud, G., van Hullebusch, E. D., Panico, A., Pirozzi, F. and Esposito, G. (2015). Role of extracellular polymeric substances (EPS) production in bioaggregation: Application to wastewater treatment. *Applied Microbiology and Biotechnology*, *99*, 9883-9905.

Drakou, E-M., Amorim, C. L., Castro, P. M. L., Panagiotou, F. and Vyrides. I. (2018). Wastewater Valorization by Pure Bacterial Cultures to Extracellular Polymeric Substances (EPS) with High Emulsifying Potential and Flocculation Activities. *Waste Biomass Valorisation*, *9*, 2557–2564.

Dube, A. (2020). Performance of an integrated algal pond for treatment of domestic sewage: a process audit. Thesis Dissertation, Rhodes University, South Africa.

Dubois, M., Gilles, K. A., Hamilton, J. K., Rebers, P. A. and Smith, F. (1956). Colorimetric method for determination of sugars and related substances. *Analytical Chemistry*, *28 (3)*, 350-356.

Elnahas, M. O., Amin, M. A., Hussein, M. M. D., Shanbhag, V. C., Ali, A. E. and Wall, J. D. (2017). Isolation, characterization and bioactivities of an extracellular polysaccharide produced from *Streptomyces* sp. MOE6. *Molecules*, *22 (9)*, 1396. doi: 10.3390/molecules22091396.

Englert, G. (1985). NMR of carotenoids—new experimental techniques. *Pure and Applied Chemistry*, *57 (5)*, 801—821.

Esa, F., Tasirin, S. M. and Abd Rahman, N. (2014). Overview of Bacterial Cellulose Production and Application. *Agriculture and Agricultural Science Procedia, 2,* 113-119.

Fallowfield, H. and Garrett, M. (1985). The photosynthetic treatment of pig slurry in temperate climatic conditions: a pilot-plant study. *Agricultural Wastes*, *12*, 111-136.

Fallowfield, H. J., Young, P., Taylor, M. J., Buchanan, N., Cromar, N., Keegan, A. and Monis, P. (2017). Independent validation and regulatory agency approval for high rate algal ponds to treat wastewater from rural communities. *Environmental Science: Water Research & Technology*. DOI: 10.1039/c7ew00228a.

Fang, C-J., Ku, K-L., Lee, M-H. and Su, N-W. (2010). Influence of nutritive factors on C50 carotenoids production by *Haloferax mediterranei* ATCC 33500 with two-stage cultivation. *Bioresource Technology*, *101*, 6487–6493.

Fariña, J. I., Sinrez, F., Molina, O. E. and Perotti, N. I. (1998). High scleroglucan production by *Sclerotium rolfsii*: Influence of medium composition. *Biotechnology Letters, 20 (9),* 825-831.

Fialho, A. M., Moreira, L. M., Granja, A. T., Popescu, A. O., Hoffmann, K. and Sá-Correia, I. (2008). Occurrence, production, and applications of gellan: current state and perspectives. *Applied Microbiology and Biotechnology*, *79*, 889-900.

Flemming, H.-C. (2016). EPS - Then and Now. *Microorganisms*, *4*, 41. doi:10.3390/microorganisms4040041.

Flemming, H-C. and Wingender, J. (2001a). Relevance of microbial extracellular polymeric substances (EPSs) - Part I: Structural and ecological aspects. *Water science and Technology*, *43 (6)*, 1-8.

Flemming, H-C. and Wingender, J. (2001b). Relevance of microbial extracellular polymeric substances (EPSs) – Part II: Technical aspects. *Water science and Technology*, *43 (6)*, 9-16.

Flemming, H-C. and Wingender, J. (2010). The biofilm matrix. *Nature Reviews Microbiology*, *8*, 623–633.

Flemming, H-C. (2011). The perfect slime. *Colloids and Surfaces B: Biointerfaces*, *86*, 251-259.

Fuentes, J. L., Garbayo, I., Cuaresma, M., Montero, Z., González-del-Valle, M. and Vílchez, C. (2016). Impact of Microalgae-Bacteria Interactions on the Production of Algal Biomass and Associated Compounds. *Marine Drugs*, *14 (5)*, 100-115.

Galetovic, A., Seura, F., Gallardo, V., Graves, R., Cortes, J., Valdivia, C., Nunez, J., Tapia, C., Neira, I., Sanzana, S. and Gomez-Silva, B. (2020). Use of phycobiliproteins from Atacama cyanobacteria as food colorants in a dairy beverage prototype. *Foods*, *9*, 244, doi:10.3390/foods9020244.

Galindo, E., Peña, C., Núñez, C., Segura, D. and Espín, G. (2007). Molecular and bioengineering strategies to improve alginate and polydydroxyalkanoate production by *Azotobacter vinelandii*. *Microbial Cell Factories*, *6*, 7. doi: 10.1186/1475-2859-6-7.

Gao, N., Xia, M., Dai, J., Yu, D., An, W., Li, S., Liu, S., He, P., Zhang, L., Wu, Z., Bi, X., Chen, S., Haft, D. H. and Qiu, D. (2018). Both widespread PEP-CTERM proteins and exopolysaccharides are required for floc formation of *Zoogloea resiniphila* and other activated sludge Bacteria. *Environmental Microbiology*, *20 (5)*, 1677-1692.

García, J., Green, B. F., Lundquist, T., Mujeriego, R., Hernández-Mariné, M. and Oswald, W. J. (2006). Long term diurnal variations in contaminant removal in high rate ponds treating urban wastewater. *Bioresource Technology*, *97 (14)*, 1709-1715.

García, J., Hernández-Mariné, M., and Mujeriego, R. (2000). Influence of phytoplankton composition on biomass removal from high-rate oxidation lagoons by means of sedimentation and spontaneous flocculation. *Water Environment Research*, *72 (2)*, 230-237.

Garcia-Gonzalez, J. and Sommerfeld, M. (2016). Biofertilizer and biostimulant properties of the microalga *Acutodesmus dimorphus*. *Journal of Applied Phycology*, *28*, 1051-1061.

Garcia-Ochoa, F., Santos, V. E., Casa, J. A. and Gomez, E. (2000). Xanthan gum: production, recovery, and properties. *Biotechnology Advances, 18,* 549-579.

Garcia-Pichel, F., Prufert-Bebout, L., and Muyzer, G. (1996). Phenotypic and phylogenetic analyses show *Microcoleus chthonoplastes* to be a cosmopolitan cyanobacterium. *Applied and Environmental Microbiology*, *62 (9)*, 3284–3291.

Garfí, M., Flores, L. and Ferrer, I. (2017). Life cycle assessment of wastewater treatment systems for small communities: activated sludge, constructed wetlands and high rate algal ponds. *Journal of Cleaner Production*, *161*, 211–219.

Ghasemi, Y., Moradian, A., Mohagheghzadeh, A., Shokravi, S. and Morowvat, M. H., (2007). Antifungal and antibacterial activity of the microalgae collected from paddy fields of Iran: characterization of antimicrobial activity of *Chlorococcus dispersus*. *Journal of Biological Sciences*, *7 (6)*, 904-910.

Glymph, T. (2005). Wastewater Microbiology: A Handbook for Operators. American Water Works Association, Denver, CO.

Golueke, C. G., Oswald, W. J. and Gotaas, H. B. (1957). Anaerobic digestion of algae. *Applied and Environmental Biotechnology*, *5 (1)*, 47-55.

González-Pleiter, M., Cirés, S., Hurtado-Gallego, J., Leganés, F., Fernández-Piñas, F. and Velázquez, D. (2019). Ecotoxicological assessment of antibiotics in freshwater using cyanobacteria. *Cyanobacteria*, *Chapter 20*, 399-417.

Green, F. B., Lundquist, T. J. and Oswald, W. J. (1995). Energetics of advanced integrated wastewater pond systems. *Water Science and Technology*, *31 (12)*, 9-20.

Grzesik, M., Romanowska-Duda, M. and Kalaji, H. M. (2017). Effectiveness of cyanobacteria and green algae in enhancing the photosynthetic performance and growth of willow (*Salix viminalis* L.) plants under limited synthetic fertilizers application. *Photosynthetica*, *55 (3)*, 510-521.

Guo, S. L., Zhao, X. Q., Wan, C., Huang, Z. Y., Yang, Y. L., Asraful Alam, M., Ho, S. H., Bai, F. W. and Chang, J. S. (2013). Characterization of flocculating agent from the self-flocculating microalga *Scenedesmus obliquus* AS-6-1 for efficient biomass harvest. *Bioresource Technology*, *145*, 285–289.

Gupta, P. and Diwan, B. (2017). Bacterial Exopolysaccharide mediated heavy metal removal: A Review on biosynthesis, mechanism and remediation strategies. *Biotechnology Reports*, *13*, 58–71.

Gupta, S. S., Shastri, Y. and Bhartiya, S. (2017). Integrated microalgae biorefinery: Impact of product demand profile and prospect of carbon capture. *Biofuels Bioproducts & Biorefining*, *11*, 1065-1076.

Gutzeit, G., Lorch, D., Weber, A., Engels, M., and Neis, U. (2005). Bioflocculent algal–bacterial biomass improves low-cost wastewater treatment. *Water Science and Technology*, *52 (12)*, 9–18.

Guzman, S., Gato, A., Lamela, M., Freire-Garabal, M. and Calleja, J. (2003). Anti-inflammatory and immunomodulatory activities of polysaccharide from *Chlorella stigmatophora* and *Phaeodactylum tricornutum*. *Phytotherapy Research*, *17 (6)*, 665-670.

Han, P., Lu, Q., Fan, L. and Zhou, W. (2019). A Review on the Use of Microalgae for Sustainable Aquaculture. *Applied Sciences*, *9*, 2377.

Hao, M. V. and Komagata, K. (1985). A new species of *Planococcus*, *P. Kocurii* isolated from fish, frozen foods, and fish curing brine. *Journal of General and Applied Microbiology*, *31 (5)*, 441-455.

Harvey, P. J. and Ben-Amotz, A. (2020). Towards a sustainable *Dunaliella salina* microalgal biorefinery for 9-cis β-carotene production. *Algal Research*, *50*.

Hay, I. D., Rehman, Z. U., Moradali, M. F., Wang, Y. and Rehm, B. H. A. (2013). Microbial alginate production, modification and its applications. *Microbiology Biotechnology, 6 (6),* 637-650.

Heider, S. A. E., Peters-Wendisch, P. and Wendisch, V. F. (2012). Carotenoid biosynthesis and overproduction in *Corynebacterium glutamicum*. *BMC Microbiology*, *12*, 198.

Henriet, O., Meunier, C., Henry, P. and Mahillon, J. (2017). Filamentous bulking caused by *Thiothrix* species is efficiently controlled in full-scale wastewater treatment plants by implementing a sludge densification strategy. *Scientific Reports*, *7*, 1430.

Henze, M., van Loosdrecht, M. C. M., Ekama, G. A. and Brdjanovic, D. (2008). Biological Wastewater Treatment: Principles, Modelling and Design. IWA Publishing, UK, London.

Higgins, M. J. and Novak, J. T. (1997). Characterization of exocellular protein and its role in bioflocculation. *Journal of Environmental Engineering*, *123 (5)*, 479-485.

Hom, E. F. Y., Aiyar, P., Schaeme, D., Mittag, M. and Sasso, S. (2015). A chemical perspective on microalgal-microbial interactions. *Trends in Plant Science*, *20 (11)*, 689-693.

Hom-Diaz, A., Norvill, Z. N., Blánquez, P., Vicent, T. and Guieysse, B. (2017). Ciprofloxacin removal during secondary domestic wastewater treatment in high rate algal ponds. *Chemosphere*, *180*, 33–41.

Hong, P-N., Honda, R., Noguchi, M. and Ito, T. (2017). Optimum selection of extraction methods of extracellular polymeric substances in activated sludge for effective extraction of the target components. *Biochemical Engineering Journal*, *127*, 136–146.

Hu, X., Kang, F., Yang, B., Zhang, W., Qin, C. and Gao, Y. (2019). Extracellular Polymeric Substances Acting as a Permeable Barrier Hinder the Lateral Transfer of Antibiotic Resistance Genes. *Frontiers in Microbiology*, *10*, 736.

Hu, Y., Hao, X., van Loosdrecht, M. and Chen, H. (2017). Enrichment of highly settleable microalgal consortia in mixed cultures for effluent polishing and low-cost biomass production. *Water Research*, *125*, 11-22.

Huang, H., Peng, C., Peng, P., Lin, Y., Zhang, X. and Ren, H. (2019). Towards the biofilm characterization and regulation in biological wastewater treatment. *Applied Microbiology and Biotechnology*, *103*, 1115-1129.

Huynh, M. and Serediak, N. (2006). Algae identification field guide. *Agriculture and Agri-Food Canada*. 40 pages.

Internet reference 1. https://www.google.com/search?q=chemical+structure+of+alginate&tbm/ (accessed 11 January 2021).

Internet reference 2. https://www.google.com/search?q=chemical+structure+of+succinoglycan&tbm/ (accessed 11 January 2021).

Internet reference 3. https://www.google.com/search?q=chemical+structure+of+xanthan&tbm/ (accessed 11 January 2021).

Internet reference 4. https://www.google.com/search?q=chemical+structure+of+curdlan&tbm/ (accessed 11 January 2021).

Internet reference 5. https://www.google.com/search?q=structure+of+hyaluronic+acid&sxsrf/ (accessed 11 January 2021).

Internet reference 6. https://www.google.com/search?q=chemical+structure+of+cellulose&tbm/ (accessed 11 January 2021).

Internet reference 7. https://www.google.com/search?q=chemical+structure+of+gellan&tbm/ (accessed 11 January 2021).

Internet reference 8. http://www.blast.ncbi.nlm.nih.gov/Blast.cgi/

Irie, Y. and Parsek, M. R. (2008). Quorum Sensing and Microbial Biofilms. *Current Topics in Microbiology and Immunology*, *322*, 67-84.

Islam, S. T. and Lam, J. S. (2014). Synthesis of bacterial polysaccharide via the Wzx/Wzy-dependent pathway. *Canadian Journal of Microbiology*, *60*, 697-716.

Jachlewski, S., Jachlewski, W. D., Linne, U., Brasen, C., Wingender, J. and Siebers, B. (2015). Isolation of extracellular polymeric substances from biofilms of the thermoacidophilic archaeon *Sulfolobus acidocaldarius*. *Frontiers in Bioengineering and Biotechnology*, *3*, *123*, doi: 10.3389/fbioe.2015.00123.

Jia, H. and Yuan, Q. (2016). Removal of nitrogen from wastewater using microalgae and microalgae–bacteria consortia. *Cogent Environmental Science*, *2*, 1275089.

Jimoh, T. A. and Cowan, A. K. (2017). Extracellular polymeric substance production in high rate algal oxidation ponds. *Water Science and Technology*, *76 (10)*, 2647–2654.

Jofré, E., Liaudat, J. P., Medeot, D. and Becker, A. (2018). Monitoring succinoglycan production in single *Sinorhizobium meliloti* cells by Calcofluor white M2R staining and time-lapse microscopy. *Carbohydrate Polymers, 181,* 918-922.

Johnson, H. E. (2010). Co-utilization of microalgae for wastewater treatment and the production of animal feed supplements. Thesis dissertation, Rhodes University, South Africa.

Jones, K. M. (2012). Increased production of the exopolysaccharide succinoglycan enhances *Sinorhizobium meliloti* 1021 symbiosis with the host plant *Medicago truncatula*. *Journal of Bacteriology, 194 (16),* 4322-4331.

Jung, J-Y., Hur, J. W., Kim, K. and Han, H-S. (2020). Evaluation of floc-harvesting technologies in biofloc technology (BFT) system for aquaculture. *Bioresource Technology*, *314*, 123719.

Kehr, J. C., and Dittmann, E. (2015). Biosynthesis and Function of Extracellular Glycans in cyanobacteria: A review. *Life*, *5*, 164-180.

Kim, J. H., Kang, H. J., Yu, B. J., Kim, S. C., Lee and P. C. (2015). *Planococcus faecalis* sp. nov., a carotenoid-producing species isolated from stools of Antarctic penguins. *International Journal of Systematic and Evolutionary Microbiology*, *65 (10)*, 3373–3378.

Kouzuma, A. and Watanabe, K. (2015). Exploring the potential of algae/bacteria interactions. *Current Opinion in Biotechnology*, *33*, 125-129.

Krug, L., Morauf, C., Donat, C., Muller, H., Cernava, T. and Berg, G. (2020). Plant growth promoting Methylobacteria selectively increase the biomass of biotechnologically relevant microalgae. *Frontiers in Microbiology*, *11*, 427, doi: 10.3389/fmicb.2020.00427.

Kumari, R., Kaur, I. and Bhatnagar, A. K. (2011). Effect of aqueous extract of *Sargassum johnstonii* Setchell & Gardner on growth, yield and quality of *Lycopersicon esculentum* Mill. *Journal of Applied Phycology*, *23*, 623-633.

Kunacheva, C. and Stuckey, D.C. (2014). Analytical methods for soluble microbial products (SMP) and extracellular polymers (ECP) in wastewater treatment systems: A review. *Water Research*, *61*, 1-18.

Lakaniemi, A-M., Tuovinen, O.H. and Puhakka, J. A. (2013). Anaerobic conversion of microalgal biomass to sustainable energy carriers – A review. *Bioresource Technology*, *135*, 222-231.

Larsdotter, K. (2006) Wastewater treatment with microalgae-a literature review. *Vatten*, *62*, 31–38.

Laubscher, R. K. and Cowan, A. K. (2020). Elaboration of an algae-to-energy system and recovery of water and nutrients from municipal sewage. *Engineering in Life Sciences*, *20 (7)*, 305-315.

Leaungvutiviroj, C., Ruangphisarn, P., Hansanimitkul, P., Shinkawa, H. and Sasaki K. (2010). Development of a new biofertilizer with a high capacity for N_2 fixation, phosphate and potassium solubilization and auxin production. *Bioscience Biotechnology and Biochemistry*, *74 (5)*, 1098-1101.

Li, L., Liu, W., Liang, T. and Ma, F. (2020). The adsorption mechanisms of algae-bacteria symbiotic system and its fast formation process. *Bioresource Technology*, *315*, 123854.

Li, X. Y. and Yang, S. F. (2007). Influence of loosely bound extracellular polymeric substances (EPS) on the flocculation, sedimentation and dewaterability of activated sludge. *Water Research*, *41*, 1022– 1030.

Li, Y., Xu, Y., Liu, L., Jiang, X., Zhang, K., Zheng, T. and Wang H. (2016). First evidence of bioflocculant from *Shinella albus* with flocculation activity on harvesting of *Chlorella vulgaris* biomass. *Bioresource Technology*, *218*, 807-815.

Li, Y., Xu, Y., Song, R., Tian, C., Liu, L., Zheng, T. and Wang, H. (2018). Flocculation characteristics of a bioflocculant produced by the actinomycete *Streptomyces* sp. hsn06 on microalgae biomass. *BMC Biotechnology*, *18*, 58. doi.org/10.1186/s12896-018-0471-9.

Li, Y., Xu, Y., Zheng, T. and Wang, H. (2017a). Flocculation mechanism of the actinomycete *Streptomyces* sp. hsn06 on *Chlorella vulgaris*. *Bioresource Technology*, *239*, 137-143.

Li, Y., Zhang, G., Du, C., Mou, H., Cui, J., Guan, H., Hwang, H. and Wang, P. (2017b). Characterization of high yield exopolysaccharide produced by *Phyllobacterium* sp. 921F exhibiting moisture preserving properties. *International Journal of Biological Macromolecules*, *101*, 562–568.

Lin, Y. M., de Kreuk, M., van Loosdrecht, M. C. M. and Adin, A. (2010). Characterization of alginate-like exopolysaccharides isolated from aerobic granular sludge in pilot-plant. *Water Research*, *44*, 3355-3364.

Lin, Y. M., Sharma, P. K. and van Loosdrecht, M. C. M. (2013). The chemical and mechanical differences between alginate-like exopolysaccharides isolated from aerobic flocculent sludge and aerobic granular sludge. *Water Research*, *47*, 57-65.

Liu, J., Li, J., Xie, K. and Sellamuthu, B. (2019). Role of adding dried sludge micropowder in aerobic granular sludge reactor with extended filamentous bacteria. *Bioresource Technology Reports*, *5*, 51–58.

Lorand, T., Deli, J., Molnar, P. and Toth, G. (2002). FT-IR Study of Some Carotenoids. *Helvetica Chimica Acta*, *85*, 1691-1697.

Ludwig, H. F., Oswald, W. J., Gotaas, H. B. and Lynch, V. (1951). Algae symbiosis in oxidation ponds I: Growth characteristics of *Euglena gracilis* cultured in sewage. *Sewage and Industrial Wastes*, *23 (11)*, 1337-1355.

Mambo, P. M., Westensee, D. K., Render, D. S. and Cowan, A. K. (2014a). Operation of an integrated algae pond system for the treatment of municipal sewage: A South African case study. *Water Science and Technology*, *69 (12)*, 2554-2561.

Mambo, P.M., Westensee, D. K., Zuma, B. M. and Cowan, A. K. (2014b). The Belmont Valley integrated algae pond system in retrospect. *Water SA*, *40 (2)*, 385-393.

Manning, A. J. (2004). The Observed effects of turbulence on estuarine flocculation. *Journal of Coastal Research*, *1 (41)*, 90-104.

Markussen, T. N. and Andersen, T. J. (2014). Flocculation and floc break-up related to tidally induced turbulent shear in a low-turbidity, microtidal estuary. *Journal of Sea Research*, *89*, 1-11.

Matcher, G. F., Dorrington, R. A., Henninger, T. O. and Froneman, P. W. (2011). Insights into the bacterial diversity in a freshwater-deprived permanently open Eastern Cape estuary, using 16S rRNA pyrosequencing analysis. *Water SA*, *37 (3)*, 381-390.

Medina, M., and Neis, U. (2007). Symbiotic algal bacterial wastewater treatment: Effect of food to microorganism ratio and hydraulic retention time on the process performance. *Water Science and Technology*, *55 (11)*, 165–171.

Mehrabadi, A., Craggs, R. and Farid, M. M. (2015). Wastewater treatment high rate algal ponds (WWT HRAP) for low-cost biofuel production. *Bioresource Technology*, *184*, 202-214.

Mehrabadi, A., Farid, M. M. and Craggs, R. (2016). Variation of biomass energy yield in wastewater treatment high rate algal ponds. *Algal Research*, *15*, 143-151.

Meiring, P. G. J. and Oellermann, R. A. (1995). Biological removal of algae in an integrated pond system. *Water Science and Technology*, *31 (12)*, 21-31.

Mendez, L., Mahdy, A., Ballesteros, M. and González-Fernández, C. (2015). *Chlorella vulgaris* vs cyanobacterial biomasses: comparison in terms of biomass productivity and biogas yield. *Energy Conversion and Management*, *92*, 137-142.

Mercadante, A. Z., Rodrigues, D. B., Petry, F. C. and Mariutti, L. R. B. (2016). Carotenoid esters in foods - A review and practical directions on analysis and occurrence. *Food Research International*, *99 (2)*, 830-850.

Milledge, J. J. and Heaven, S. (2014). Methods of energy extraction from microalgal biomass: A review. *Reviews in Environmental Science and Biotechnology*, *13*, 301-320.

Mishra, A. and Jha, B. (2009). Isolation and characterization of extracellular polymeric substances from microalgae *Dunaliella salina* under salt stress. *Bioresource Technology*, *100*, 3382-3386.

Mishra, S. K., Suh, W. I., Farooq, W., Moon, M., Shrivastav, S., Park, M. S. and Yang, J-W. (2014). Rapid quantification of microalgal lipids in aqueous medium by a simple colorimetric method. *Bioresource Technology*, *155*, 330-333.

Mohammadi, M., Burbank, L. and Roper, M. C. (2012). Biological role of pigment production for the bacterial phytopathogen *Pantoea stewartii* subsp. Stewartia. *Applied and Environmental Microbiology*, *78 (19)*, 6859 – 6865.

Mojica, K., Elsey, D. and Cooney, M. J. (2007). Quantitative analysis of biofilm EPS uronic acid content. *Journal of Microbiological Methods*, *71*, 61-65.

Montemezzani, V., Duggan, I. C., Hogg, I. D. and Craggs, R. J. (2016). Zooplankton community influence on seasonal performance and microalgal dominance in wastewater treatment High Rate Algal Ponds. *Algal Research*, *17*, 168–184.

Moosavi-Nasab, M., Gavahian, M., Yousefi, A. R., and Askari, H. (2010). Fermentative production of dextran using food industry wastes. *International Journal of Nutrition and Food Engineering, 4 (8),* 1921-1923.

Moran, N. A., and Jarvik, T. (2010). Lateral transfer of genes from fungi underlies carotenoid production in aphids. *Science*, *328 (5978)*, 624–627.

More, T. T., Yadav, J. S. S., Yan, S., Tyagi, R. D. and Surampalli, R. Y. (2014). Extracellular polymeric substances of bacteria and their potential environmental applications. *Journal of Environmental Management*, *144*, 1-25.

More, T. T., Yan, S., Hoang, N. V., Tyagi, R. D. and Surampalli, R. Y. (2012a). Bacterial polymer production using pre-treated sludge as raw material and its flocculation and dewatering potential. *Bioresource Technology*, *121*, 425–431.

More, T. T., Yan, S., John, R. P., Tyagi, R. D. and Surampalli, R. Y. (2012b). Biochemical diversity of the bacterial strains and their biopolymer producing capabilities in wastewater sludge. *Bioresource Technology*, *121*, 304–311.

Morris, G. and Harding, S. E. (2009). Polysaccharides, Microbial. In: Encyclopedia of Microbiology (Third Edition). *Elsevier*, 482-494. ISBN 9780123739445.

Muradov, N., Taha, M., Miranda, A. F., Wrede, D., Kadali, K., Gujar, A., Stevenson, T., Ball, A. S. and Mouradov, A. (2015). Fungal-assisted algal flocculation: application in wastewater treatment and biofuel production. *Biotechnology for Biofuels*, *8*, 24.

Natrah, F. M. I., Bossier, P., Sorgeloos, P., Yusoff, F. M. and Defoirdt, T. (2013). Significance of microalgal–bacterial interactions for aquaculture. *Reviews in Aquaculture*, *5*, 1-14.

Nazari, M. T., Freitag, J. F., Cavanhi, V. A. F. and Colla, L. M. (2020). Microalgae harvesting by fungal-assisted bioflocculation. *Reviews in Environmental Science and Biotechnology*, *19*, 369-388.

Nelissen, B., De Baere, R., Wilmotte, A. and De Wachter. R. (1996). Phylogenetic relationships of nonaxenic filamentous cyanobacterial strains based on 16S rRNA sequence analysis. *Journal of Molecular Evolution*, *42*, 194-200.

Neu, T. R. and Marshall, K. C. (1991). Microbial “footprint”- A new approach to adhesive polymers. *Biofouling*, *3*, 101-112.

Nguyen, T. D. P., TuanVo, C., Nguyen-Sy, T., Tran, T. N. T., Le, T. V. A., Chiu, C-Y., Sankaran, R. and Loke, S. P. (2020). Utilization of Microalgae for Self-regulation of extracellular polymeric substance production. *Biochemical Engineering Journal*, *159*, 107616.

Nguyen, V. H., Nguyen, H. K., Nguyen, T. D., Pham, T., Dang-Thi, C. H., Song, Y. and Tyagi, R. D. (2017). Sources for isolation of extracellular polymeric substances (EPS) producing bacterial strains which are capable using wastewater sludge as solo substrate. *Environmental Technology*, *21*, 1-10. doi: 10.1080/09593330.2017.1351488.

Nouha, K., Hoang, N. V., Song, Y., Tagi, R. D. and Surampalli, R. Y. (2015). Characterization of extracellular polymeric substances (EPS) produced by *Cloacibacterium normanense* isolated from wastewater sludge for sludge settling and dewatering. *Journal of Civil and Environmental Engineering*, *5*, 191. doi:10.4172/2165-784X.1000191.

Nubel, U., Garcia-Pichel, F. and Muyzer, G. (1997). PCR primers to amplify 16s rRNA genes from cyanobacteria. *Applied and Environmental Microbiology*, *63 (8)*, 3327–3332.

O'Donnell, D. R., Fey, S. B. and Cottingham, K. L. (2013). Nutrient availability influences kairomone-induced defenses in *Scenedesmus acutus* (Chlorophyceae). *Journal of Plankton Research*, *35 (1)*, 191-200.

Olguín, E. J. (2003). Phycoremediation: key issues for cost-effective nutrient removal processes. *Biotechnology Advances*, *22*, 81–91.

Ortega-Morales, B. O., Santiago-Garcia, J. L., Chan-Bacab, M. J., Moppert, X., Miranda-Tello, E., Fardeau, M. L., Carrero, J. C., Bartolo-Perez, P., Valadez-Gonzalez, A. and Guezennec, J. (2007). Characterization of extracellular polymers synthesized by tropical intertidal biofilm bacteria. *Journal of Applied Microbiology*, *102*, 254-264.

Oswald, W. J. (1990). Advanced integrated wastewater pond systems. In: Supplying water and saving the environment for six billion people: proceedings of the 1990 ASCE convention, San Francisco, California, November. New York, *American Society of Civil Engineers*, Environmental Engineering Division. Pp. 78–85.

Oswald, W. J. (1991) Introduction to advanced wastewater ponding systems. *Water Science and Technology*, *24 (5)*, 1-7.

Oswald, W. J. (1995) Ponds in the twenty-first century. *Water Science and Technology*, *31 (12)*, 1-8.

Oswald, W. J., Gotaas, H. B., Golueke, C. G., Kellen, W. R., Gloyna, E. F. and Hermann, E. R. (1957) Algae in waste treatment [with Discussion]. *Sewage and Industrial Wastes*, *29 (4)*, 437-457.

Oswald, W. J., Gotaas, H. B., Ludwig, H. F. and Lynch, V. (1953a). Algae symbiosis in oxidation ponds II: Growth characteristics of *Chlorella pyrenoidosa* cultured in sewage. *Sewage and Industrial Wastes*, *25 (1)*, 26-37.

Oswald, W. J., Gotaas, H. B., Ludwig, H. F. and Lynch, V. (1953b). Algae symbiosis in oxidation ponds III: Photosynthetic Oxygenation. *Sewage and Industrial Wastes*, *25 (6)*, 692-705.

Oyegbile, B., Ay, P. and Satyanarayana, N. (2016). Flocculation kinetics and hydrodynamic interactions in natural and engineered flow systems: A review. *Environmental Engineering Research*, http://dx.doi.org/10.4491/eer.2015.086.

Palaniraj, A. and Jayaraman, V. (2011). Production, recovery and applications of xanthan gum by *Xanthomonas campestris*. *Journal of Food Engineering, 106,* 1-12.

Papazi, A., Makridis, P. and Divanach, P. (2010). Harvesting *Chlorella minutissima* using cell coagulants. *Journal of Applied Phycology*, *22*, 349-355.

Parikh, A. and Madamwar, D. (2006). Partial characterization of extracellular polysaccharides from cyanobacteria. *Bioresource Technology*, *97*, 1822-1827.

Park, J. B. K. and Craggs, R. J. (2011). Nutrient removal in wastewater treatment high rate algal ponds with carbon dioxide addition. *Water Science and Technology*, *62 (8)*, 1758-1764.

Park, J. B. K., Craggs, R. J. and Shilton, A. N. (2011a). Wastewater treatment high rate algal ponds for biofuel production. *Bioresource Technology*, *102*, 35-42.

Park, J. B. K., Craggs, R. J. and Shilton, A. N. (2011b) Recycling algae to improve species control and harvest efficiency from a high rate algal pond. *Water Research*, *45 (20)*, 6637-6649.

Park, J. B. K., Craggs, R. J. and Shilton, A.N. (2013a). Enhancing biomass energy yield from pilot-scale high rate algal ponds with recycling. *Water Research*, *47 (13)*, 4422-4432.

Park, J. B. K., Craggs, R. J. and Shilton, A. N. (2013b). Investigating why recycling gravity harvested algae increases harvestability and productivity in high rate algal ponds. *Water Research*, *47*, 4907-4917.

Parker, D. S., Kaufman, W. J. and Jenkins, D. (1972). Floc breakup in turbulent flocculation processes. *Journal of the Sanitary Engineering Division*, *98 (1)*, 79-99.

Passos, F., Gutiérrez, R., Uggetti, E., Garfi, M., García, J. and Ferrer, I. (2017). Towards energy neutral microalgae-based wastewater treatment plants. *Algal Research*, *28*, 235-243.

Passos, F., Sole, M., Garcia, J. and Ferrer, I. (2013). Biogas production from microalgae grown in wastewater: Effect of microwave pretreatment. *Applied Energy*, *108*, 168-175.

Patel, V. K., Srivastava, R., Sharma, A., Srivastava, A. K., Singh, S., Srivastava, A. K., Kashyap, P. L., Chakdar, H., Pandiyan, K., Kalra, A. and Saxena, A. K. (2018). Halotolerant *Exiguobacterium profundum* PHM11 tolerate salinity by accumulating L-proline and fine-tuning gene expression profiles of related metabolic pathways. *Frontiers in Microbiology*, *9*, 423.

Peng, Y., Gao, C., Wang, S., Ozaki, M., and Takigawa, A. (2003). Non-filamentous sludge bulking caused by a deficiency of nitrogen in industrial wastewater treatment. *Water Science and Technology*, *47 (11)*, 289-295.

Pham, L. A., Laurent, J., Bois, P. and Wanko, A. (2020). A coupled RTD and mixed-order kinetic model to predict high rate algal pond wastewater treatment under different operational conditions: Performance assessment and sizing application. *Biochemical Engineering Journal*, *162*, 107709.

Phasey, J., Vandamme, D. and Fallowfield, H. J. (2017). Harvesting of algae in municipal wastewater treatment by calcium phosphate precipitation mediated by photosynthesis, sodium hydroxide and lime. *Algal Research*, *27*, 115-120.

Pi, S., Qiu, J., Li, A., Feng, L., Wu, D., Zhao, H-P. and Ma, F. (2020). Uncovering the biosynthetic pathway of polysaccharide-based microbial flocculant in *Agrobacterium tumefaciens* F2. *Applied Microbiology and Biotechnology*, *104*, 8479–8488.

Picheth, G. F., Pirich, C. L., Sierakowski, M. R., Woehl, M. A., Sakakibara, C. N., de Souza, C. F., Martin, A. A., da Silva, R. and Freitas, R. A. (2017). Bacterial cellulose in biomedical applications: A review. *International Journal of Biological Macromolecules, 104,* 97-106.

Pierre, G., Delattre, C., Dudessay, P., Jubeau, S., Vialleix, C., Cadoret, J-P., Probert, I. and Michaud, P. (2019). What is in store for EPS microalgae in the next decade? *Molecules*, *24*, 4296. doi:10.3390/molecules24234296.

Pinzon, N. M. and Ju, L. K. (2009). Analysis of rhamnolipid biosurfactants by methylene blue complexation. Applied Microbiology Biotechnology. *82 (5)*, 975-981.

Poli, A., Donato, P. D., Abbamondi, G. R. and Nicolaus, B. (2011). Synthesis, production and biotechnological applications of exopolysaccharides and polyhydroxyalkanoates by Archaea. *Archaea*, *2011*, Article ID 693253, 13 pages. doi.org/10.1155/2011/693253.

Pouliot, Y., Buelna, G., Racine, C. and de la Noüe, J. (1989). Culture of cyanobacteria for tertiary wastewater treatment and biomass production. *Biological Wastes*, *29 (2)*, 81–91.

Prajapati, S. K., Kaushik, P., Malik, A. and Vijay, V. K. (2013). Phycoremediation and biogas potential of native algal isolates from soil and wastewater. *Bioresource Technology*, *135*, 232-238.

Pujari, L., Wu, C., Kan, J., Li, N., Wang, X., Zhang, G., Shang, X., Wang, M., Zhou, C. and Sun, J. (2019). Diversity and spatial distribution of chromophytic phytoplankton in the Bay of Bengal revealed by RuBisCO genes (*rbc*L). *Frontiers in Microbiology*, *10 (1501)*, doi:10.3389/fmicb.2019.01501.

Qiu, Y., Wang, Z., Liu, F., Liu, J., Tan, K. and Ji, R. (2019). Inhibition of *Scenedesmus quadricauda* on *Microcystis flos-aquae*. *Applied Microbiology and Biotechnology*, *103*, 5907-5916.

Quijano, G., Arcila, J. S. and Buitrón, G. (2017). Microalgal-bacterial aggregates: Applications and perspectives for wastewater treatment. *Biotechnology Advances*, *35*, 772-781.

Quijano-Ortega, N., Fuenmayor, C. A., Zuluaga-Dominguez, C., Diaz-Moreno, C., Ortiz-Grisales, S., García-Mahecha, M. and Grassi, S. (2020). FTIR-ATR Spectroscopy Combined with Multivariate Regression Modeling as a Preliminary Approach for Carotenoids Determination in *Cucurbita* spp. *Applied Sciences*, *10*, 3722.

Ram, S., Mitra, M., Shah, F., Tirkey, S. R. and Mishra, S. (2020). Bacteria as an alternate biofactory for carotenoid production: A review of its applications, opportunities and challenges. *Journal of Functional Foods*, *67*, 103867.

Ram, S., Paliwal, C. and Mishra, S. (2019). Growth medium and nitrogen stress sparked biochemical and carotenogenic alterations in *Scenedesmus* sp. CCNM 1028. *Bioresource Technology Reports*, *7*, 100194.

Ramanan, R., Kim, B.-H., Cho, D.-H., Oh, H.-M., and Kim, H.-S. (2016). Algae–bacteria interactions: Evolution, ecology and emerging applications. *Biotechnology Advances*, *34*, 14–29.

Rasamiravaka, T., Vandeputte, O. M. and El Jaziri, M. (2016). Procedure for rhamnolipids quantification using methylene blue. *Bio-protocol*, *6 (7)*.

Redmile-Gordon, M. A., Armenise, E., White, R. P., Hirsch, P. R. and Goulding, K. W. T. (2013). A comparison of two colorimetric assays, based upon Lowry and Bradford techniques, to estimate total protein in soil extracts. *Soil Biology and Biochemistry*, *67*, 166-173.

Redmile-Gordon, M. A., Brookes, P. C., Evershed, R. P., Goulding, K. W. T. and Hirsch, P. R. (2014). Measuring the soil-microbial interface: Extraction of extracellular polymeric substances (EPS) from soil biofilms. *Soil Biology and Biochemistry*, *72*, 163-171.

Rodriguez-Amaya, D. B. and Kimura, M. (2004). Harvestplus Handbook for Carotenoid Analysis. HarvestPlus Technical Monograph 2. Washington, DC and Cali: International Food Policy Research Institute (IFPRI) and International Center for Tropical Agriculture (CIAT). Copyright HarvestPlus.

Roeselers, G., van Loosdrecht, M. C. M. and Muyzer, G. (2008). Phototrophic biofilms and their potential applications. *Journal of Applied Phycology*, *20*, 227–235.

Rose, P. D., Hart O. O., Shipin, O. and Ellis, P. J. (2002). Integrated algal ponding systems and the treatment of domestic and industrial wastewaters. Part 1: The AIWPS model. WRC Report No. TT 190/02. Water Research Commission, Pretoria.

Rose, P., Boshoff, G., Van Hille, R., Wallace, L., Dunn, K. and Duncan, J. (1998). An integrated algal sulphate reducing high rate ponding process for the treatment of acid mine drainage wastewaters. *Biodegradation*, *9*, 247-257.

Rose, P., Maart, B., Dunn, K., Rowswell, R. and Britz, P. (1996). High rate algal oxidation ponding for the treatment of tannery effluents. *Water Science and Technology*, *33*, 219–227.

Rose, P.D., Wells, C., Dekker, L., Clarke, S., Neba, A., Shipin, O. and Hart, O. (2007). Integrated Algal Ponding Systems and the Treatment of Domestic and Industrial Wastewaters. Part 4: System Performance and Tertiary Treatment Operations. *Salinity, Sanitation and Sustainability* 3 (WRC Report No: TT 193/07).

Rosselló-Mora, R. A., Wagner, M., Amann, R. and Schleifer, K-H. (1995). The abundance of *Zoogloea ramigera* in sewage treatment plants. *Applied and Environmental Microbiology*, *61 (2)*, 702-707.

Rossi, F. and De Philippis, R. (2015). Role of cyanobacterial exopolysaccharides in phototrophic biofilms and in complex microbial mats. *Life*, *5*, 1218-1238.

Rühmann, B., Schmid, J. and Sieber, V. (2015). Methods to identify the unexplored diversity of microbial exopolysaccharides. *Frontiers in Microbiology*, *6 (565)*. doi: 10.3389/fmicb.2015.00565.

Sahin, N. (2011). Significance of absorption spectra for the chemotaxonomic characterization of pigmented bacteria. *Turkish Journal of Biology*, *35 (2)*, 167-175.

Saini, D. K., Chakdar, H., Pabbi, S. and Shukla, P. (2019). Enhancing production of microalgal biopigments through metabolic and genetic engineering. *Critical Reviews in Food Science and Nutrition*, https://doi.org/10.1080/10408398.2018.1533518.

Saini, R. K., Nile, S. H. and Park, S. W. (2015). Carotenoids from fruits and vegetables: Chemistry, analysis, occurrence, bioavailability and biological activities. *Food Research International*, *76*, 735-750.

Salim, S., Bosma, R., Vermue, M. H. and Wijffels, R. H. (2011). Harvesting of microalgae by bio-flocculation. *Journal of AppliFed Phycology*, *23*, 849-855.

Sarwat, F., Qader, S. A. U., Aman, A. and Ahmed, N. (2008). Production & Characterization of a Unique Dextran from an Indigenous *Leuconostoc mesenteroides* CMG713. *International Journal of Biological Sciences, 4 (6),* 379-386.

Schlafer, S. and Meyer, R. L. (2017). Confocal microscopy imaging of the biofilm matrix. *Journal of Microbiological Methods*, *138*, 50-59.

Schmid, J., Sieber, V. and Rehm, B. (2015). Bacterial exopolysaccharides: biosynthesis pathways and engineering strategies. *Frontier in Microbiology*, *6 (496),* doi: 10.3389/fmicb.2015.00496.

Sekar, S. and Chandramohan, M. (2008). Phycobiliproteins as a commodity: trends in applied research, patents and commercialization. *Journal of Applied Phycology*, *20*, 113-136.

Sfez, S., Van Den Hende, S., Taelman, S. E., De Meester, S. and Dewulf, J. (2015). Environmental sustainability assessment of a microalgae raceway pond treating aquaculture wastewater: From up-scaling to system integration. *Bioresource Technology*, *190*, 321-331.

Sheng, G-P., Yu, H-Q. and Li, X-Y. (2010). Extracellular polymeric substances (EPS) of microbial aggregates in biological wastewater treatment systems: A review. *Biotechnology Advances*, *28*, 882–894.

Shi, Y., Huang, J., Zeng, G., Gu, Y., Chen, Y., Hu, Y., Tang, B., Zhou, J., Yang, Y. and Shi, L. (2017). Exploiting extracellular polymeric substances (EPS) controlling strategies for performance enhancement of biological wastewater treatments: An Overview. *Chemosphere*, *180*, 396-411.

Shih, I. L., Yu, J. Y., Hsieh, C. and Wu, J. Y. (2009). Production and characterization of curdlan by *Agrobacterium* sp. *Biochemical Engineering Journal, 43,* 33-40.

Shindo, K., Endo, M., Miyake, Y., Wakasugi, K., Morritt, D., Bramley, P. M., Fraser, P. D., Kasai, H. and Misawa, N. (2008). Methyl Glucosyl-3,4-dehydro-apo-8′-lycopenoate, a novel antioxidative glyco-C30-carotenoic acid produced by a marine bacterium *Planococcus maritimus*. *The Journal of Antibiotics*, *61 (12)*, 729–735.

Singh, J. S., Kumar, A., Rai, A. N. and Singh, D. P. (2016). Cyanobacteria: A precious bio-resource in agriculture, ecosystem, and environmental sustainability. *Frontiers in Microbiology*, *7*, 529.

Singha, T. K. (2012). Microbial extracellular polymeric substances: production, isolation and applications. *IOSR Journal of Pharmacy*, *2 (2)*, 276-281.

Sobeck, D. C. and Higgins, M. J. (2002). Examination of three theories for mechanisms of cation-induced bioflocculation. *Water Research*, *36*, 527-538.

Spolaore, P., Joannis-Cassan, C., Duran, E. and Isambet, A. (2006). Commercial applications of microalgae. *Journal of Bioscience and Bioengineering*, *101 (2)*, 87-96.

St. Thomas (2019). “Spectroscopic Tools” URL: http://www.science-and-fun.de/tools/

Staats, N., De Winder, B., Stal, L. and Mur, L. (1999). Isolation and characterization of extracellular polysaccharides from the epipelic diatoms *Cylindrotheca closterium* and *Navicula salinarum*. *European Journal of Phycology*, *34 (2)*, 161-169.

Stauch-White, K., Srinivasan, V. N., Kuo-Dahab, W. C., Park, C. and Butler, C. S. (2017). The role of inorganic nitrogen in successful formation of granular biofilms for wastewater treatment that support cyanobacteria and bacteria. *AMB Express*, *7*, 146.

Stuart, R. K., Mayali, X., Boaro, A. A., Zemla, A., Everroad, R. C., Nilson, D., Weber, P. K., Lipton, M., Bebout, B. M., Pett-Ridge, J. and Thelen, M. P. (2016). Light regimes shape utilization of extracellular organic C and N in a cyanobacterial biofilm. *mBio*, *7 (3)*, 00650-16.

Su, Y., Mennerich, A. and Urban, B. (2012) Comparison of nutrient removal capacity and biomass settleability of four high-potential microalgal species. *Bioresource Technology*, *124*, 157–162.

Subashchandrabose, S. R., Ramakrishnan, B., Megharaj, M., Venkateswarlu, K. and Naidu, R. (2011). Consortia of cyanobacteria/microalgae and bacteria: Biotechnological potential. *Biotechnology Advances*, *29*, 896-907.

Sugumaran, K. R. and Ponnusami, V. (2017). Review on production, downstream processing and characterization of microbial pullulan. *Carbohydrate Polymers, 173,* 573-591.

Sujak, A., Gagos, M., Serra, M. D. and Gruszecki, W. I. (2007). Organization of two-component monomolecular layers formed with dipalmitoylphosphatidylcholine and the carotenoid pigment, canthaxanthin. *Molecular Membrane Biology*, *24 (5-6)*, 431-441.

Sun, F., Zhang, H., Qian, A., Yu, H., Xu, C., Pan R. and Shi, Y. (2020). The influence of extracellular polymeric substances on the coagulation process of cyanobacteria. *Science of the Total Environment*, *720*, 137573. https://doi.org/10.1016/j.scitotenv.2020.137573

Survase, S. A., Saudagar, P. S. and Singhal, R. S. (2007). Enhanced production of scleroglucan by *Sclerotium rolfsii* MTCC 2156 by use of metabolic precursors. *Bioresource Technology, 98,* 410-415.

Sutherland, D. L. and Ralph, P. J. (2020). 15 years of research on wastewater treatment high rate algal ponds in New Zealand: discoveries and future directions. *New Zealand Journal of Botany*, doi.org/10.1080/0028825X.2020.1756860.

Sutherland, D. L. and Ralph, P. J. (2019). Microalgal bioremediation of emerging contaminants-opportunities and challenges, *Water Research*, *161 (1)*, 114921.

Sutherland, D. L., Howard-Williams C., Turnbull, M. H., Broady, P. A. and Craggs, R. J. (2015b). The effects of CO2 addition along a pH gradient on wastewater microalgal photo-physiology, biomass production and nutrient removal. *Water Research*, *70*, 9–26.

Sutherland, D. L., Howard-Williams, C., Turnbull, M. H., Broady, P. A. and Craggs, R. J. (2013). Seasonal variation in light utilisation, biomass production and nutrient removal

by wastewater microalgae in a full-scale high rate algal pond. *Journal of Applied Phycology*, *26 (3)*, 1317-1329.

Sutherland, D. L., Howard-Williams, C., Turnbull, M. H., Broady, P. A. and Craggs, R. J. (2015a). Enhancing microalgal photosynthesis and productivity in wastewater treatment high rate algal ponds for biofuel production. *Bioresource Technology*, *184*, 222-229.

Sutherland, D. L., Park, J., Heubeck, S., Ralph, P. J. and Craggs, R. J. (2020). Size matters – Microalgae production and nutrient removal in wastewater treatment high rate algal ponds of three different sizes. *Algal Research*, *45*, 101734.

Sutherland, D. L., Turnbull, M. H. and Craggs, R. J. (2017). Environmental drivers that influence microalgal species in full scale wastewater treatment high rate algal ponds. *Water Research*, *124*, 504–512.

Sutherland, I. W. (2001). The biofilm matrix- an immobilized but dynamic microbial environment. *Trends in Microbiology*, *9 (3)*, 222-227.

Sze, J. H., Brownlie, J. C. and Love, C. A. (2016). Biotechnological production of hyaluronic acid: a mini review. *3 Biotech*, *6 (1)*, 67. doi: 10.1007/s13205-016-0379-9.

Taghavijeloudar, M., Kebria, D. Y. and Yaqoubnejad, P. (2020). Simultaneous harvesting and extracellular polymeric substances extrusion of microalgae using surfactant: Promoting surfactant-assisted flocculation through pH adjustment. *Bioresource Technology*, *319*, *124224*.

Takaichi, S. (2014). General methods for identification of carotenoids. *Biotechnology Letters*, *36*, 1127-1128.

Tamura, K., Stecher, G., Peterson, D., Filipski, A. and Kumar, S. (2013). MEGA6: Molecular evolutionary genetics analysis version 6.0. *Molecular Biology and Evolution*, *30*, 2725-2729.

Taton, A., Lis, E., Adin, D. M., Dong, G., Cookson, S., Kay, S. A., Golden, S. S. and Golden, J. W. (2012). Gene Transfer in *Leptolyngbya* sp. strain BL0902, a cyanobacterium suitable for production of biomass and bioproducts. *PLoS ONE*, *7 (1)*, 30901.

Tebitendwa, S. M. (2017). Performance evaluation and cost analysis of subsurface flow constructed wetlands designed for ammonium-nitrogen removal. Thesis dissertation, Rhodes University, South Africa.

Theocharis, A. D., Skandalis, S. S., Gialeli, C. and Karamanos, N. K. (2016). Extracellular matrix structure. *Advanced Drug Delivery Reviews*, *97*, 4-27.

Tiron, O., Bumbac, C., Manea, E., Stefanescu, M. and Lazar, M. N. (2017). Overcoming microalgae harvesting barrier by activated algae granules. *Scientific Reports*, *7*, 4646.

Tiron, O., Bumbac, C., Patroescu, I. V., Badescu, V. R. and Postolache, C. (2015). Granular activated algae for wastewater treatment. *Water Science & Technology*, *71 (6)*, 832-839.

Tong, M., Li, X., Luo, Q., Yang, C. Lou, W., Liu, H., Du, C., Nie, L. and Zhong, Y. (2020). Effects of humic acids on biotoxicity of tetracycline to microalgae *Coelastrella* sp. *Algal Research*, *50*, 101962.

Tourney, J. and Ngwenya, B. T. (2014). The role of bacterial extracellular polymeric substances in geomicrobiology. *Chemical Geology*, *386*, 115-132.

Trabelsi, I., Ktari, N., Slima, S. B., Triki, M., Bardaa, S., Mnif, H. and Salah, R. B. (2017). Evaluation of dermal wound healing activity and in vitro antibacterial and antioxidant activities of a new exopolysaccharide produced by *Lactobacillus* sp. Ca6. *International Journal of Biological Macromolecules*, *103*, 194-201.

Trabelsi, I., Slima, S. B., Chaabane, H. and Riadh, B. S. (2015). Purification and characterization of a novel exopolysaccharides produced by *Lactobacillus* sp. Ca6. *International Journal of Biological Macromolecules*, *74*, 541–546.

Trivedi, J., Mounika A., Bangwal, D. P., Kaul S. and Garg, M. O. (2015). Algae based biorefinery-How to make sense? *Renewable and Sustainable Energy Reviews*, *47*, 295-307.

Tseng, B. S., Majerczyk, C. D., Passos da Silva, D., Chandler, J. R., Greenberg, E. P. and Parsek, M. R. (2016). Quorum sensing influences *Burkholderia thailandensis* biofilm

development and matrix production. *Journal of Bacteriology*, *198 (19)*, 2643-2650. doi: 10.1128/JB.00047-16.

Turtin, I., Vatansever, A. and Sanin, F. D. (2006). Phosphorus defficiency and sludge bulking. *Environmental Technology*, *27 (6)*, 613-621.

Ummalyma, S. B., Gnansounou, E., Sukumaran, R. K., Sindhu, R., Pandey, A. and Sahoo, D. (2017). Bioflocculation: an alternative strategy for harvesting of microalgae - an overview. *Bioresource Technology*, *242*, 227-235.

Urtuvia, V., Maturana, N., Acevedo, F., Peña, C. and Díaz-Barrera, A. (2017). Bacterial alginate production: an overview of its biosynthesis and potential industrial production. *World Journal of Microbiology and Biotechnology*, *33 (11)*, 198. doi 10.1007/s11274-017-2363-x.

Van Den Hende, S., Beelen, V., Julien, L., Lefoulon, A., Vanhoucke, T., Coolsaet, C., Sonnenholzner, S., Vervaeren, H. and Rousseau, D. P. L. (2016b). Technical potential of microalgal bacterial floc raceway ponds treating food-industry effluents while producing microalgal bacterial biomass: An outdoor pilot-scale study. *Bioresource Technology*, *218*, 969-979.

Van Den Hende, S., Beyls, J., De Buyck, P.-J. and Rousseau, D.P.L. (2016a). Food-industry-effluent-grown microalgal bacterial flocs as a bioresource for high-value phycochemicals and biogas. *Algal Research*, *18*, 25-32.

Van Den Hende, S., Carré, E., Cocaud, E., Beelen, V., Boon, N., and Vervaeren, H. (2014a). Treatment of industrial wastewaters by microalgal bacterial flocs in sequencing batch reactors. *Bioresource Technology*, *161*, 245–254.

Van Den Hende, S., Claessens, L., De Muylder, E., Boon, N. and Vervaeren, H. (2014b). Microalgal bacterial flocs originating from aquaculture wastewater treatment as diet ingredient for *Litopenaeus vannamei* (Boone). *Aquaculture Research*, *47 (4)*, 1075-1089.

Van Den Hende, S., Laurent, C. and Bégué, M. (2015). Anaerobic digestion of microalgal bacterial flocs from a raceway pond treating aquaculture wastewater: need for a biorefinery. *Bioresource Technology*, *196*, 184-193.

Van Den Hende, S., Vervaeren, H., Saveyn, H., Maes, G. and Boon, N. (2011). Microalgal bacterial floc properties are improved by a balanced inorganic/organic carbon ratio. *Biotechnology and Bioengineering*, *108 (3)*, 549-558.

Van Hille, R. P., Boshoff, G. A., Rose, P. D. and Duncan, J. R. (1999). A continuous process for the biological treatment of heavy metal contaminated acid mine water. *Resources Conservation and Recycling*, *27*, 157-167.

Vandamme, D., Foubert, I. and Muylaert, K. (2013). Flocculation as a low-cost method for harvesting microalgae for bulk biomass production. *Trends in Biotechnology*, *31 (4)*, 233-239.

Vanthoor-Koopmans, M., Wijffels, R. H., Barbosa, M. J. and Eppink, M. H. M. (2013). Biorefinery of microalgae for food and fuel. *Bioresource Technology*, *135*, 142-149.

Vázquez, J. A., Pastrana, L., Piñeiro, C., Teixeira, J. A., Pérez-Martín, R. I. and Amado, I. R. (2015). Production of Hyaluronic Acid by *Streptococcus zooepidemicus* on Protein Substrates Obtained from *Scyliorhinus canicula* Discards. *Marine Drugs*, *13*, 6537-6549.

Venil, C. K., Zakaria, Z. A. and Ahmad, W. A. (2013). Bacterial pigments and their applications *Process Biochemistry*, *48*, 1065–1079.

Vila, E., Hornero-Méndez, D., Azziz, G., Lareo, C. and Saravia, V. (2018). Carotenoids from heterotrophic bacteria isolated from Fildes Peninsula, King George Island, Antarctica. *Biotechnology Reports*, *20*, 00306.

Villar-Navarro, E., Baena-Nogueras, R. M., Paniw, M., Perales, J. A. and Lara-Martín, P. A. (2018). Removal of pharmaceuticals in urban wastewater: high rate algae pond (HRAP) based technologies as an alternative to activated sludge based processes. *Water Research*, *139*, 19–29.

Wagner, M. and Loy, A. (2002). Bacterial community composition and function in sewage treatment systems. *Current Opinion in Biotechnology*, *13*, 218-277.

Wagner, M., Loy, A., Nogueira, R., Purkhold, U., Lee, N. and Daims, H. (2002). Microbial community composition and function in wastewater treatment plants. *Antonie van Leeuwenhoek*, *81*, 665–680.

Wall, J. M., Wood, S. A., Orlovich, D. A., Rhodes, L. L. and Summerfield, T. C. (2014). Characterisation of freshwater and marine cyanobacteria in the Hokianga region, Northland, New Zealand. *New Zealand Journal of Marine and Freshwater Research*, *48 (2)*, 177–193.

Wan, C. Zhao, X-Q., Guo, S-L., Alam, M. A. and Bai, F-W. (2013). Bioflocculant production from *Solibacillus silvestris* W01 and its application in cost-effective harvest of marine microalga *Nannochloropsis oceanica* by flocculation. *Bioresource Technology*, *135*, 207-212.

Wan, C., Alam, M. A., Zhao, X-Q., Zhang, X-Y., Guo, S-L., Ho, S-H, Chang, J-S. and Bai, F-W. (2015). Current progress and future prospect of microalgal biomass harvest using various flocculation technologies. *Bioresource Technology*, *184*, 251-257.

Wang, H., Hill, R. T., Zheng, T., Hu, X. and Wang, B. (2014). Effects of bacterial communities on biofuel-producing microalgae: stimulation, inhibition and harvesting. *Critical Reviews in Biotechnology*, *36 (2)*, 341-352.

Wang, L-L., Wang, L-F., Ren, X-M., Ye, X-D., Li, W-W., Yuan, S-J., Sun, M., Sheng, G-P., Yu, H-Q. and Wang, X-K. (2012). pH dependence of structure and surface properties of microbial EPS. *Environmental Science and Technology*, *46*, 737-744.

Wang, S., Ji, B., Zhang, M., Ma, Y., Gu, J. and Liu, Y. (2020). Defensive responses of microalgal-bacterial granules to tetracycline in munic- ipal wastewater treatment. *Bioresource Technology*, *312*, 123605.

Wang, Z., Wu, J., Zhu, L. and Zhan, X. (2017). Characterization of xanthan gum produced from glycerol by a mutant strain *Xanthomonas campestris* CCTCC M2015714. *Carbohydrate Polymers*, *157*, 521-526.

Wang, Z-P. and Zhang, T. (2010). Characterization of soluble microbial products (SMP) under stressful conditions. *Water Research*, *44*, 5499-5509.

Werle, E., Schneider, C., Renner, M., Völker, M. and Fiehn, W. (1994). Convenient single-step, one tube purification of PCR products for direct sequencing. *Nucleic acids research*, *22 (20)*, 4354-4355.

West, T. P. and Peterson, J. L. (2014). Production of the polysaccharide curdlan by an *Agrobacterium* strain grown on a plant biomass hydrolysate. *Canadian Journal of Microbiology*, *60*, 53-56.

White, R. A., Soles, S. A., Gavelis, G., Gosselin, E., Slater, G. F., Lim, D. S. S., Leander, B. and Suttle, C. A. (2018). The complete genome and physiological analysis of the eurythermal firmicute *Exiguobacterium chiriqhucha* strain RW2 isolated from a freshwater microbialite, widely adaptable to broad thermal, pH, and salinity ranges. *Frontiers in Microbiology*, *9*, 3189.

Whitfield, G. B., Marmont, L. S. and Howell, P. L. (2015). Enzymatic modifications of exopolysaccharides enhance bacterial persistence. *Frontiers in Microbiology*, *6* (471) doi: 10.3389/fmicb.2015.00471.

Wieczorek, N., Kucuker, M. A. and Kuchta, K. (2015). Microalgae-bacteria flocs (MaB-Flocs) as a substrate for fermentative biogas production. *Bioresource Technology*, *194*, 130-136.

Wingender, J., Neu, T. R. and Flemming, H-C. (1999). What are bacterial extracellular polymeric substances? In, Microbial Extracellular Polymeric Substances, eds. Wingender, J., Neu, T. & Flemming, H.-C., Springer, Heidelberg. pp 1-19.

Wu, D., Li, A., Yang, J., Ma, F., Chen, H., Pi, S. and Wei, W. (2015). *N*-3-Oxo-octanoyl-homoserine lactone as a promotor to improve the microbial flocculant production by an exopolysaccharide bioflocculant producing bacterium *Agrobacterium tumefaciens* F2. *RSC Advances*, *5 (109)*, 89531-89538.

Wu, X., Huang, J., Lu, Z., Chen, G., Wang, J. and Liu, G. (2019). *Thiothrix eikelboomii* interferes oxygen transfer in activated sludge. *Water Research*, *151*, 134-143.

Xiao, R. and Zheng, Y. (2016). Overview of microalgal extracellular polymeric substances (EPS) and their applications. *Biotechnology Advances*, *34*, 1225-1244.

Xu, H., Yu, G. and Jiang, H. (2013). Investigation on extracellular polymeric substances from mucilaginous cyanobacterial blooms in eutrophic freshwater lakes. *Chemosphere*, *93*, 75–81.

Xu, Q., Han, B., Wang, H., Wang, Q., Zhang, W. and Wang, D. (2020). Effect of extracellular polymer substances on the tetracycline removal during coagulation process. *Bioresource Technology*, *309*, 123316.

Xu, S., Yao, J., Ainiwaer, M., Hong, Y. and Zhang, Y. (2018). Analysis of bacterial community structure of activated sludge from wastewater treatment plants in winter. *Biomed Research International*, https://doi.org/10.1155/2018/8278970.

Xu, Z., Chen, Y., Meng, X., Wang, F. and Zheng, Z. (2016). Phytoplankton community diversity is influenced by environmental factors in the coastal East China Sea. *European Journal of Phycology*, *51(1)*, 107-118.

Yang, Y., Yatsunami, R., Ando, A., Miyoko, N., Fukui, T., Takaichi, S. and Nakamura, S. (2015). Complete biosynthetic pathway of the C50 carotenoid bacterioruberin from lycopene in the extremely halophilic Archaeon *Haloarcula japonica*. *Journal of Bacteriology*, *197 (9)*, 1614-1623.

Young, P., Buchanan, N. and Fallowfield, H. J. (2016). Inactivation of indicator organisms in wastewater treated by a high rate algal pond system. *Journal of Applied Microbiology*, *121*, 577-586.

Young, P., Taylor, M. and Fallowfield, H. J. (2017). Mini-review: high rate algal ponds, flexible systems for sustainable wastewater treatment. *World Journal of Microbiology and Biotechnology*, *33 (6)*, 117-129.

Yu, L., Wu, J., Liu, J., Zhan, X., Zheng, Z. and Lin, C. C. (2011). Enhanced Curdlan Production in *Agrobacterium* sp. ATCC 31749 by Addition of Low-polyphosphates. *Biotechnology and Bioprocess Engineering*, *16*, 34-41.

Zamalloa, C., Vulsteke, E., Albrecht, J., Verstraete, W. (2011). The techno-economic potential of renewable energy through the anaerobic digestion of microalgae. *Bioresource Technology*, *102*, 1149-1158.

Zhao, B. and Su, Y. (2014). Process effect of microalgal-carbon dioxide fixation and biomass production: A review. *Renewable and Sustainable Energy Reviews*, *31*, 121-132.

Zhou, W., Min, M., Hu, B., Ma, X., Liu, Y., Wang, Q., Shi, J., Chen, P. and Ruan, R. (2013). Filamentous fungi assisted bio-flocculation: A novel alternative technique for harvesting heterotrophic and autotrophic microalgal cells. *Separation and Purification Technology*, *107*, 158–165.

Zhu, L. (2015). Biorefinery as a promising approach to promote microalgae industry: An innovative framework. *Renewable and Sustainable Energy Reviews*, *41*, 1376-1384.

Zhu, L., Qi, H-Y., Lv, M-L., Kong, Y., Yu, Y-W. and Xu, X-Y. (2012). Component analysis of extracellular polymeric substances (EPS) during aerobic sludge granulation using FTIR and 3D-EEM technologies. *Bioresource Technology*, *124*, 455-459.

Zhu, M., Yu, G., Song, G., Chang, J., Wan, C. and Li, R. (2015). Molecular specificity and detection for *Pseudoanabaena* (cyanobacteria) species based on *rbcLX* sequences. *Biochemical Systematics and Ecology*, *60*, 110-115.

ZoBell, C. E. (1943). The effect of solid surfaces upon bacterial activity. *Journal of Bacteriology*, *46*, 39-56.

Appendices

Appendix A: Standard calibration curves for chemical and biochemical analysis

Table A1: Kinetics derived from standard calibrations used for interpolation of COD and nutrient concentrations of water samples.

Parameter (mg/L)	Absorbance (nm)	Equation	Correlation coefficient (R^2)
COD	610	y = 0.0005x	0.997
NH_4-N	683	y = 0.5015x	0.999
NO_3-N	510	y = 0.0693x	0.999
PO_4-P	715	y = 0.2540x	0.999

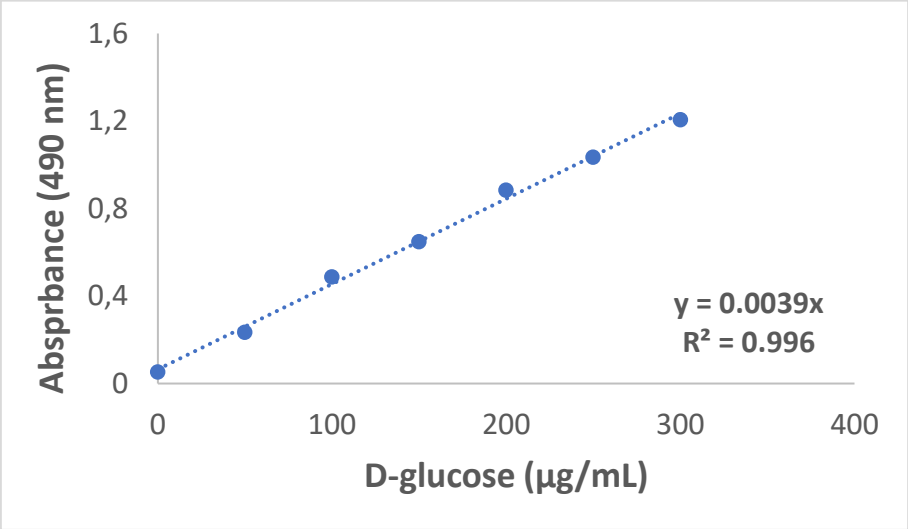

Figure A1: Standard calibration for D-glucose using phenol-sulfuric acid assay for the estimation of carbohydrate concentration in EPS.

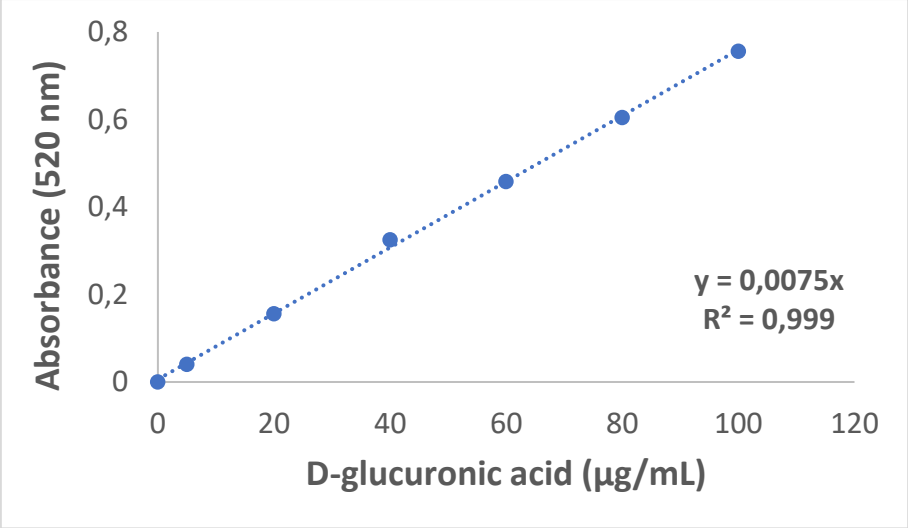

Figure A2: Standard calibration of D-glucuronic acid using sulfuric acid-*m*-hydroxydiphenyl assay for the estimation of uronic acid concentration in EPS.

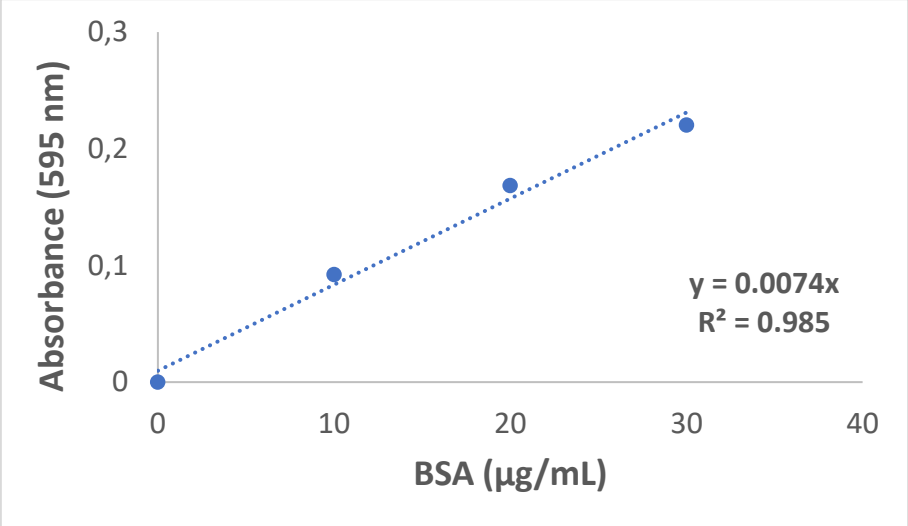

Figure A3: Standard calibration for BSA using Bradford assay for the estimation of protein concentration in EPS.

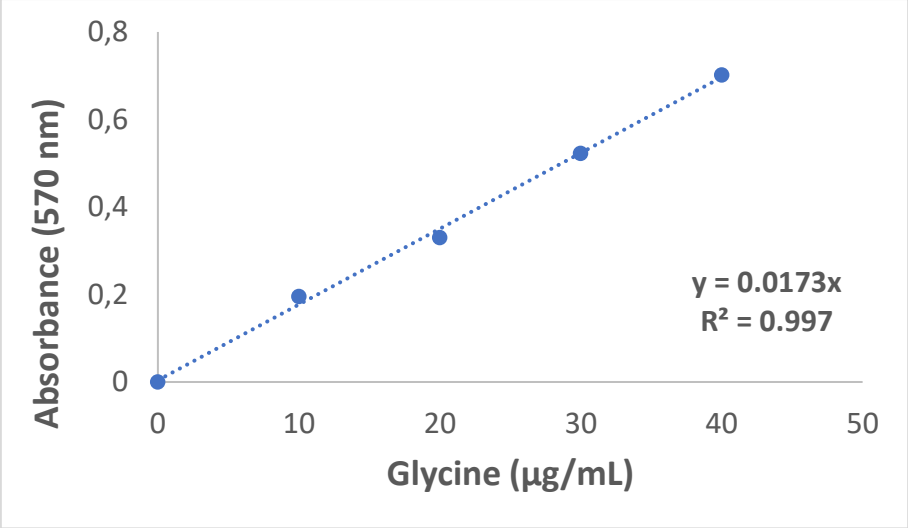

Figure A4: Standard calibration for glycine using ninhydrin assay for the estimation of α-amino nitrogen concentration in EPS.

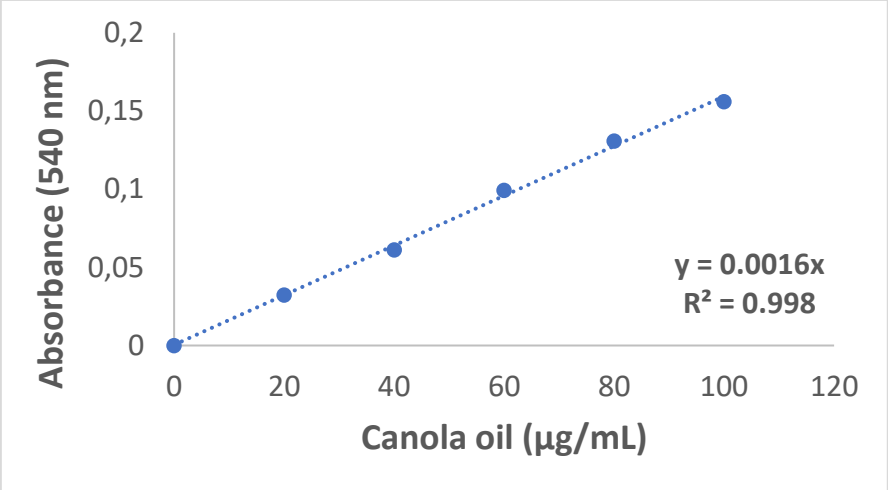

Figure A5: Standard calibration for canola oil using sulfo-phospho-vanillin assay for the estimation of lipid concentration in EPS.

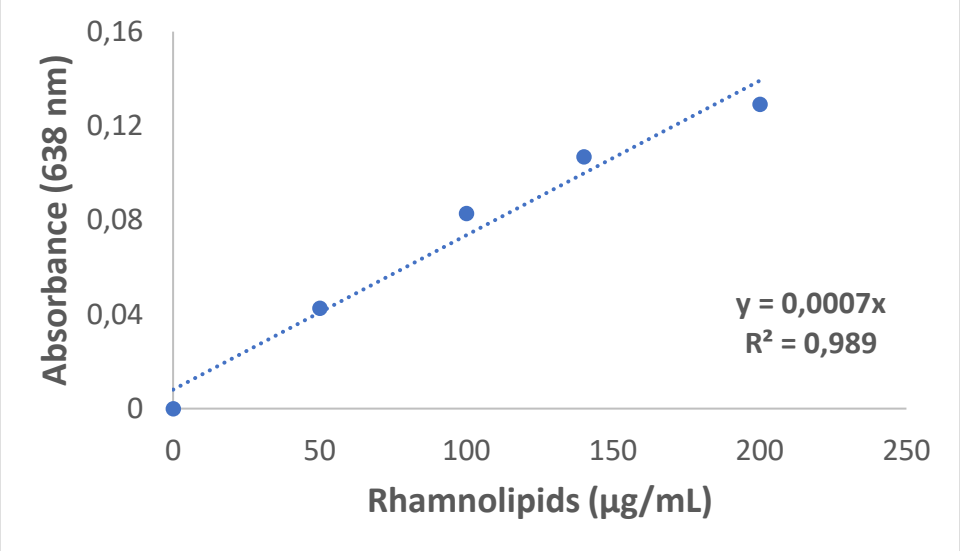

Figure A6: Standard calibration for rhamnolipids using methylene blue complexation assay for the estimation of rhamnolipids concentration in EPS.

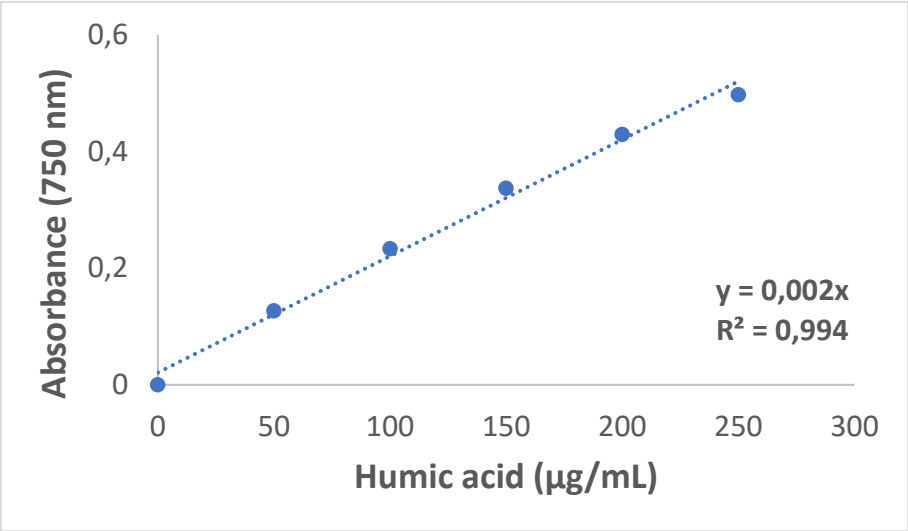

Figure A7: Standard calibration for humic acid using modified Lowry assay for the estimation of phenolic compounds in EPS.

Appendix B: Supplementary information for Chapter 3

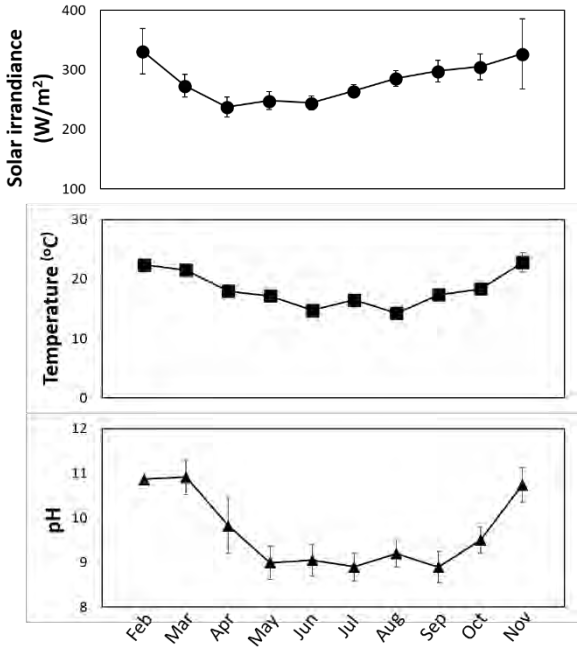

Figure B1: Average monthly solar radiation, atmospheric temperature and pond water pH during the period of study. Error bars represent S. E. of mean values.

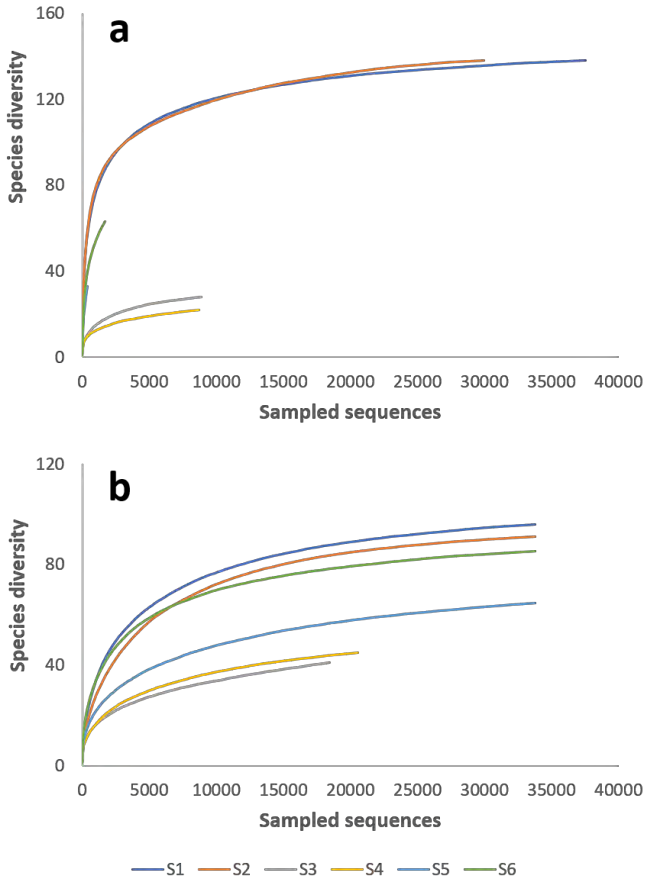

Figure B2: Rarefaction analysis showing species richness and diversity of bacteria (a) and eukaryotic population in HRAOP of an IAPS treating domestic sewage.

Table B1: Taxonomic classification of dominant OTUs of bacteria and eukaryotes found in HRAOP microbial population

Bacteria		Eukaryotes	
OTU ID	**Taxonomy**	**OTU ID**	**Taxonomy**
B_OTU001	*Thiothrix* sp.	OTU001	*Desmodesmus* sp.
B_OTU002	*Silanimonas* sp.	OTU002	*Desmodesmus* sp.
B_OTU003	*Mariniradius* sp.	OTU003	*Pseudopediastrum* sp.
B_OTU004	*SM1A02* sp.	OTU004	*Brachionus* sp.
B_OTU005	*Porphyrobacter* sp.	OTU005	*Sanchytrium* sp.
B_OTU006	*Porphyrobacter* sp.	OTU006	*Micractinium* sp.
B_OTU007	*Algoriphagus* sp.	OTU007	*Paraphysoderma* sp.
B_OTU008	*Ideonella* sp.	OTU008	*Chlorella* sp.
B_OTU009	*SM1A02* sp.	OTU009	*Desmodesmus* sp.
B_OTU010	*Gemmatimonas* sp.	OTU010	*Micractinium* sp.
B_OTU011	*Dokdonella* sp.	OTU011	*Scenedesmus* sp.
B_OTU012	uncultured Chitinophagaceae	OTU012	*Cephalodella* sp.
B_OTU013	*Malikia* sp.	OTU013	*Stenocypris* sp.
B_OTU014	uncultured Cyanobacterium	OTU014	*Desmodesmus* sp.
B_OTU015	*Rheinheimera* sp.	OTU015	*Moina* sp.
B_OTU016	*Roseomonas* sp.	OTU016	uncultured Choanoflagellate
B_OTU017	uncultured Cyanobacterium	OTU017	*Desmodesmus* sp.
B_OTU018	*Blastopirellula* sp.	OTU018	uncultured Chytridiomycota
B_OTU019	*Pseudohongiella* sp.	OTU019	*Hariotina* sp.
B_OTU020	*Tropicimonas* sp.	OTU020	*Desmodesmus* sp.
B_OTU022	*Pirellula* sp.	OTU021	*Telotrochidium* sp.
B_OTU031	*Hydrogenophaga* sp.	OTU022	*Amphileptus* sp.
B_OTU034	uncultured Cyanobacterium	OTU023	*Rhizophydium* sp.
B_OTU039	uncultured Rhodocyclaceae	OTU024	*Nitzschia* sp.
B_OTU040	*Polynucleobacter* sp.	OTU025	*Telotrochidium* sp.
B_OTU042	*Flavobacterium* sp.	OTU026	uncultured Chytridiomycota
B_OTU043	*Methylophilus* sp.	OTU027	*Chlorella* sp.
B_OTU044	*Pirellula* sp.	OTU028	*Desmodesmus* sp.
B_OTU046	*Flavobacterium* sp.	OTU031	*Pseudopediastrum* sp.
B_OTU047	*Phenylobacterium* sp.	OTU032	*Paraphysoderma* sp.
B_OTU051	*Rhodobaca* sp.	OTU033	*Brachionus* sp.
B_OTU052	*Sediminibacterium* sp.	OTU034	*Chlorella* sp.
B_OTU064	*Thauera* sp.	OTU035	*Micractinium* sp.
B_OTU066	*Gemmobacter* sp.	OTU038	*Scenedesmus* sp.
B_OTU068	uncultured Ignavibacteria	OTU039	*Desmodesmus* sp.
B_OTU080	*Kerstersia* sp.	OTU044	uncultured Eukaryote
B_OTU083	*Thiothrix* sp.	OTU052	*Brachionus* sp.
B_OTU086	*Thiothrix* sp.	OTU054	*Meyerozyma* sp.
B_OTU087	uncultured Rhizobiales	OTU088	*Peridinium* sp.
B_OTU0103	unultured Cyanobacterium		
B_OTU0108	uncultured Bacteroidia		
B_OTU0120	uncultured Cyanobacterium		
B_OTU0135	*Candidatus Halomonas phosphatis*		
B_OTU0136	*Algoriphagus* sp.		

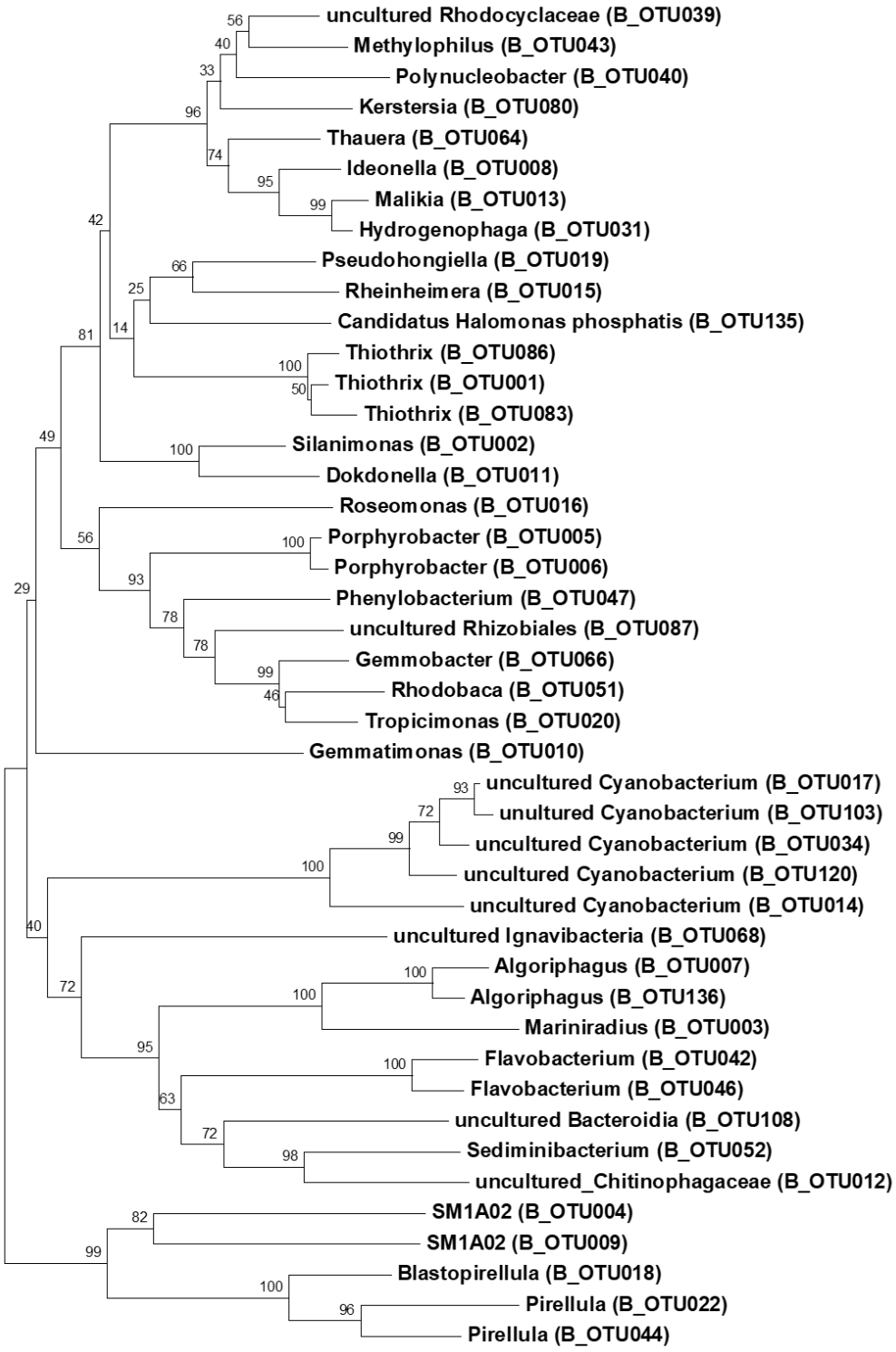

Figure B3: Phylogenetic relatedness of the dominant bacterial species in HRAOP of an IAPS treating domestic sewage using the Neighbour-Joining method.

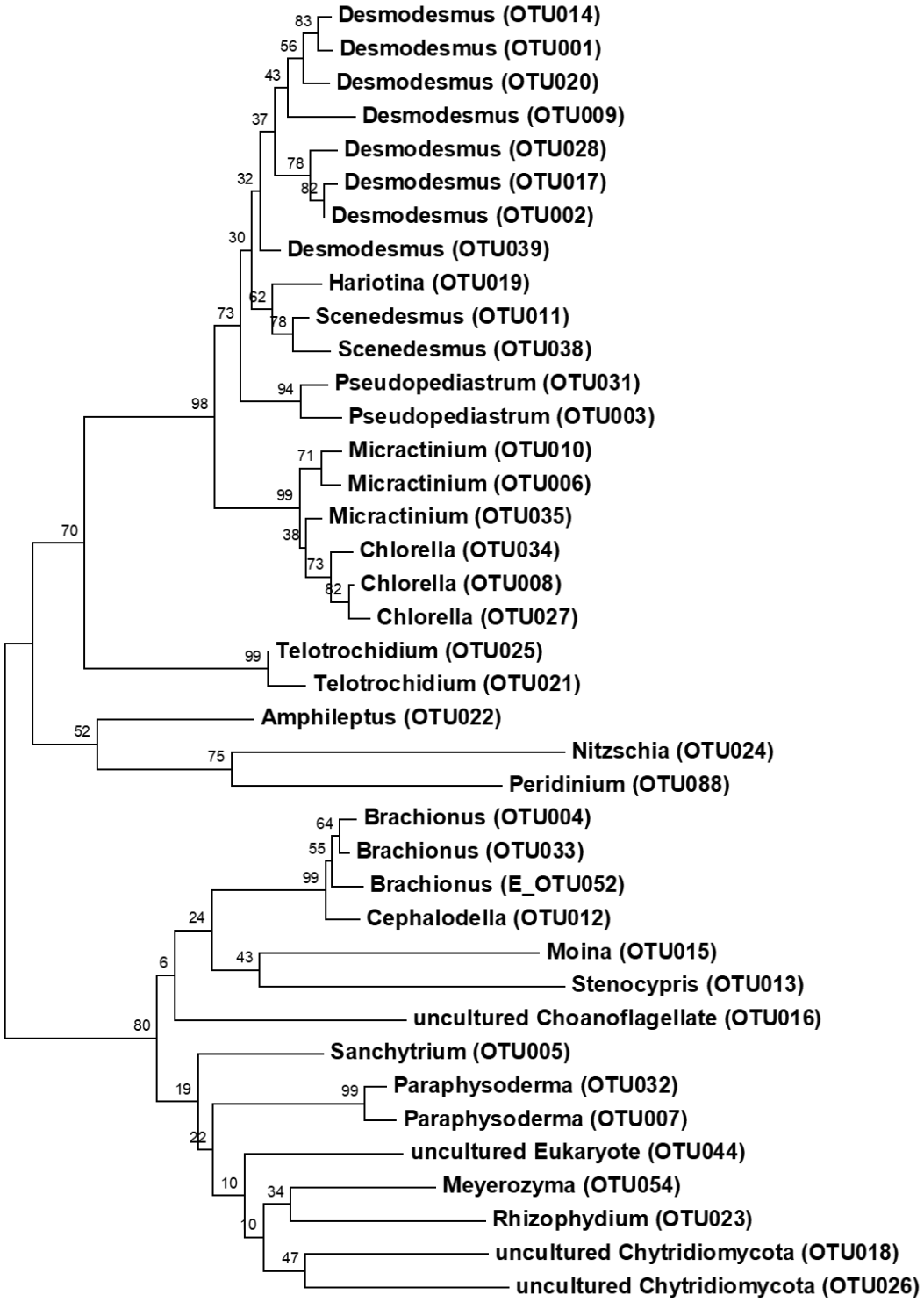

Figure B4: Phylogenetic relatedness of the dominant phytoplankton and zooplankton in HRAOP of an IAPS treating domestic sewage using the Neighbour-Joining method.

Table B2: The proportion of settleable to non-settleable biomass generated in high rate algal oxidation ponds over a period of one year. Values are mean ± S.E. of three replicates

Date	Total biomass (mg/L)	Non-settleable biomass (%)	Settleable: non-settleable ratio
21-Feb	190 ± 4	14 ± 3	6:1
12-Mar	123 ± 17	16 ± 1	5:1
20-Mar	138 ± 30	19 ± 2	4:1
09-Apr	104 ± 8	26 ± 1	3:1
24-Apr	71 ± 7	25 ± 0	3:1
14-May	80 ± 2	30 ± 3	2:1
24-May	70 ±2	60 ± 10	2:1
11-Jun	102 ± 0	64 ± 1	2:1
25-Jun	98 ± 2	57 ± 5	1:1
12-Jul	108 ± 0	55 ± 3	1:1
30-Jul	132 ± 2	58 ± 5	1:1
15-Nov	118 ± 4	31 ± 3	2:1
28-Nov	169 ± 15	14 ± 1	6:1
10-Dec	209 ± 11	6 ± 3	16:1

Appendix C: Supplementary information for Chapter 4

ECCN 40b identified as *Bacillus* strain (Accession No: MT705987)

TCATGGCTCAGGATGAACGCTGGCGGCGTGCCTAATACATGCAAGTCGAGCGAATGGATTAAGAGCTTGC
TCTTATGAAGTTAGCGGCGGACGGGTGAGTAACACGTGGGTAACCTGCCCATAAGACTGGGATAACTCCG
GGAAACCGGGGCTAATACCGGATAACATTTTGAACTGCATGGTTCGAAATTGAAAGGCGGCTTCGGCTGT
CACTTATGGATGGACCCGCGTCGCATTAGCTAGTTGGTGAGGTAACGGCTCACCAAGGCAACGATGCGTA
GCCGACCTGAGAGGGTGATCGGCCACACTGGGACTGAGACACGGCCCAGACTCCTACGGGAGGCAGCAGT
AGGGAATCTTCCGCAATGGACGAAAGTCTGACGGAGCAACGCCGCGTGAGGTGATGAAGGCTTTCGGGTC
GTAAAACTCTGTTGTTAGGGAAGAACAAGTGCTAGTTGAATAAGCTGGCACCTTGACGGTACCTAACCAG
AAAGCCACGGCTAACTACGTGCCAGCAGCCGCGGTAATACGTAGGTGGCAAGCGTTATCCGGAATTATTG
GGCGTAAAGCGCGCGCAGGTGGTTTCTTAAGTCTGATGTGAAAGCCCACGGCTCAACCGTGGAGGGTCAT
TGGAAACTGGGAGACTTGAGTGCAGAAGAGGAAAGTGGAATTCCATGTGTAGCGGTGAAATGCGTAGAGA
TATGGAGGAACACCAGTGGCGAAGGCGACTTTCTGGTCTGTAACTGACACTGAGGCGCGAAAGCGTGGGG
AGCAAACAGGATTAGATACCCTGGTAGTCCACGCCGTAAACGATGAGTGCTAAGTGTTAGAGGGTTTCCG
CCCTTTAGTGCTGAAGTTAACGCATTAAGCACTCCGCCTGGGGAGTACGGCCGCAAGGCTGAAACTCAAA
GGAATTGACGGGGGCCCGCACAAGCGGTGGAGCATGTGGTTTAATTCGAAGCAACGCGAAGAACCTTACC
AGGTCTTGACATCCTCTGAAAACCCTAGAGATAGGGCTTCTCCTTCGGGAGCAGAGTGACAGGTGGTGCA
TGGTTGTCGTCAGCTCGTGTCGTGAGATGTTGGGTTAAGTCCCGCAACGAGCGCAACCCTTGATCTTAGT
TGCCATCATTAAGTTGGGCACTCTAAGGTGACTGCCGGTGACAAACCGGAGGAAGGTGGGGATGACGTCA
AATCATCATGCCCCTTATGACCTGGGCTACACACGTGCTACAATGGACGGTACAAAGAGCTGCAAGACCG
CGAGGTGGAGCTAATCTCATAAAACCGTTCTCAGTTCGGATTGTAGGCTGCAACTCGCCTACATGAAGCT
GGAATCGCTAGTAATCGCGGATCAGCATGCCGCGGTGAATACGTTCCCGGGCCTTGTACACACCGCCCGT
CACACCACGAGAGTTTGTAACACCCGAAGTCGGTGGGGTAACCTTTTTGGAGCCAGCCGCCTAAGGGTGG
T

ECCN 41b identified as *Bacillus* strain (Accession No: MT706002)

TCATGGCTCAGGACGAACGCTGGCGGCGTGCCTAATACATGCAAGTCGAGCGGACAGATGGGAGCTTGCT
CCCTGATGTTAGCGGCGGACGGGTGAGTAACACGTGGGTAACCTGCCTGTAAGACTGGGATAACTCCGGG
AAACCGGGGCTAATACCGGATGGTTGTTTGAACCGCATGGTTCAGACATAAAAGGTGGCTTCGGCTACCA
CTTACAGATGGACCCGCGGCGCATTAGCTAGTTGGTGAGGTAACGGCTCACCAAGGCAACGATGCGTAGC
CGACCTGAGAGGGTGATCGGCCACACTGGGACTGAGACACGGCCMAGACTCYTACGGGAGGCAGGCAGTA
GGGAATCTTCCGCAATGGACGAAAGTCTGACSGAGCAWCGCCGCGTGAGTGATGAAGGTTTTCGGATCGT
AAAGCTCTGTTGTTAGGGAAGAACAAGTGCCGTYCAAAATAGGGCGGCACCTTGACGGTACCTAACCAGA
AAGCCACGGCTAACTACGTGCCAGCAGCCGCGGTAATACGTAGGTGGCAAGCGTTGTCCGGAATTATTGG
GCGTAAAGGGCTCGCAGGCGGTTTCTTAAGTCTGATGTGAAAGCCCCCGGCTCAACCGGGGAGGGTCATT
GGAAACTGGGGAACTTGAGTGCAGAAGAGGAGAGTGGAATTCCACGTGTAGCGGTGAAATGCGTAGAGAT
GTGGAGGAACACCAGTGGCGAAGGCGACTCTCTGGTCTGTAACTGACGCTGAGGAGCGAAAGCGTGGGGA
GCGAACAGGATTAGATACCCTGGTAGTCCACGCCGTAAACGATGAGTGCTAAGTGTTAGGGGGTTTCCGC
CCCTTAGTGCTGCAGCTAACGCATTAAGCACTCCCGSCTGGGGAGTACGGTCGCAAGACTGAAACTCAAA
GGAATTGACGGGGGCCCGCACAAGCGGTGGAGCATGTGGTTTAATTCGAAGCAACGCGAAGAACCTTACC
AGGTCTTGACATCCTCTGACAATCCTAGAGATAGGACGTCCCCTTCGGGGGCAGAGTGACAGGTGGTGCA
TGGTTGTCGTCAGCTCGTGTCGTGAGATGTTGGGTTAAGTCCCGCAACGAGCGCAACCCTTGATCTTAGT
TGCCAGCATTCAGTTGGGCACTCTAAGGTGACTGCCGGTGACAAACCGGAGGAAGGTGGGGATGACGTCA
AATCATCATGCCCCTTATGACCTGGGCTACACACGTGCTACAATGGACAGAACAAAGGGCAGCGAAACCG
CGAGGTTAAGCCAATCCCACAAATCTGTTCTCAGTTCGGATCGCAGTCTGCAACTCGACTGCGTGAAGCT
GGAATCGCTAGTAATCGCGGATCAGCATGCCGCGGTGAATACGTTCCCGGGCCTTGTACACACCGCCCGT
CACACCACGAGAGTTTGTAACACCCGAAGTCGGTGAGGTAACCTTTAGGAGCCAGCCGCCGAAGTGGAC

ECCN 45b identified as *Planococcus* strain (Accession No: MT706005)

TTATGGCTCAGGACGAACGCTGGCGGCGTGCCTAATACATGCAAGTCGAGCGGAACACTTGGAGCTTGCT
CCAAGCGTTTAGCGGCGGACGGGTGAGTAACACGTGGGCAACCTGCCCTGCAGATCGGGATAACTCCGGG
AAACCGGTGCTAATACCGAATAGTTTGAAGCCTCACCTGAGGCTTCACGGAAAGACGGTTTCGGCTGTCA
CTGCAGGATGGGCCCGCGGCGCATTAGCTAGTTGGTGGGGTAACGGCCCACCAAGGCCACGATGCGTAGC
CGACCTGAGAGGGTGACCGGCCACACTGGGACTGAGACACGGCCCAGACTCCTACGGGAGGCAGCAGTAG
GGAATCTTCCGCAATGGACGCAAGTCTGACGRAGCAACGCCGCGTGAGTGACGRAGGTTTTCGGATCGTA
AAACTCTGTTGTGAGGGAAGAACACGTACCAACTAACTATTGGTACCTTGACGGTACCTCACCAGAAAGC
CACGGCTAACTACGTGCCAGCAGCCGCGGTAATACGTAGGTGGCAAGCGTTGTCCGGAATTATTGGGCGT

AAAGCGCGCGCAGGCGGTTCCTTAAGTCTGATGTGAAAGCCCACCGGCTCAACCGTGGAGGGTCATTGGA
AACTGGGGAACTTGAGTGCAGAAGAGGAAAGTGGAATTCCACGTGTAGCGGTGAAATGCGTAGAGATGTG
GAGGAACACCAGTGGCGAAGGCGACTTTCTGGTCTGTAACTGACGCTGAGGCGCGAAAGCGTGGGGAGCA
AACAGGATTAGATACCCTGGTAGTCCACGCCGTAAACGATGAGTGCTAAGTGTTAGGGGGTTTCCGCCCC
TTAGTGCTGCAGCTAACGCATTAAGCACTCCCGCCWGGGGAGTACGGCCGCAAGGCTGAAACTCAAAGGA
ATTGACGGGGGCCCGCACAAGCGGTGGAGCATGTGGTTTAATTCGAAGCAACGCGAAGAACCTTACCAGG
TCTTGACATCCCGCTGCCCGCCTTGGAGACAAGGCTTTCCCTTCGGGGACAGCGGTGACAGGTGGTGCAT
GGTTGTCGTCAGCTCGTGTCGTGAGATGTTGGGTTAAGTCCCGCAACGAGCGCAACCCTTGATTTTAGTT
GCCAGCATTCAGTTGGGCACTTTAAGGTGACTGCCGGTGACAAACCGGAGGAAGGTGGGGATGACGTCAA
ATCATCATGCCCCTTATGACCTGGGCTACACACGTGCTACAATGGACGGTACAAAGGGCAGCCAACCCGC
GAGGGGGAGCCAATCCCAGAAAACCGTTCTCAGTTCGGATTGCAGGCTGCAACTCGCCTGCATGAAGCCG
GAATCGCTAGTAATCGTGGATCAGCATGCCACGGTGAATACGTTCCCGGGCCTTGTACACACCGCCCGTC
ACACCACGAGAGTTTGTAACACCCGAAGTCGGTGGGGTAACCCTTACGGGAGCCAGCCGCCGAAGTTGAA

ECCN 46b identified as *Exiguobacterium* strain (Accession No: MT706012)

TTCATGGCTCAGGACGAACGCTGGCGGCGTGCTTAATACATGCAAGTCGAGCGCAGGAAGCCGTCTGAAC
CCTTCGGGGGGACGACGGTGGAATGAGCGGCGGACGGGTGAGTAACACGTAAAGAACCTGCCCATAGGTC
TGGGATAACCACGAGAAATCGGGGCTAATACCGGATGTGTCATCGGACCGCATGGTCCGCTGATGAAAGG
CGCTCCGGCGTCGCCCATGGATGGCTTTGCGGTGCATTAGCTAGTTGGTGGGGTAACGGCCCACCAAGGC
GACGATGCATAGCCGACCTGAGAGGGTGATCGGCCACACTGRGACTGAGACACGGCCCAGACTCCTACGG
GARGCAGCAGTAGGGAATCTTCCACAATGGACGAAAGTCTGATGRAGCAACGCCGCGTGAACGATGAAGG
CTTTCGGGTCGTAAAGTTCTGTTGTAAGGGAAGAACAAGTGCCGCAGGCAATGGCGGCACCTTGACGGTA
CYTTGCGAGAAAGCCACGGCTAACTACGTGCCAGCAGCCGCGGTAATACGTAGGTGGCAAGCGTTGTCCG
GAATTATTGGGCGTAAAGCGCGCGCAGGCGGCCTCTTAAGTCTGATGTGAAAGCCCCCGGCTCAACCGGG
GAGGGCCATTGGAAACTGGGAGGCTTGAGTATAGGAGAGAAGAGTGGAATTCCACGTGTAGCGGTGAAAT
GCGTAGAGATGTGGAGGAACACCAGTGGCGAAGGCGACTCTTTGGCCTATAACTGACGCTGAGGCGCGAA
AGCGTGGGGAGCAAACAGGATTAGATACCCTGGTAGTCCACGCCGTAAACGATGAGTGCTAGGTGTTGGA
GGGTTTCCGCCCTTCAGTGCTGAAGCTAACGCATTAAGCACTCCCGCCCTGGGGAGTACGGTCGCAAGGC
TGAAACTCAAAGGAATTGACGGGGACCCGCACAAGCGGTGGAGCATGTGGTTTAATTCGAAGCAACGCGA
AGAACCTTACCAACTCTTGACATCCCCCTGACCGGTACAGAGATGTACCTTCCCCTTCGGGGGCAGGGGT
GACAGGTGGTGCATGGTTGTCGTCAGCTCGTGTCGTGAGATGTTGGGTTAAGTCCCGCAACGAGCGCAAC
CCTTGTCCTTAGTTGCCAGCATTTGGTTGGGCACTCTAGGGAGACTGCCGGTGACAAACCGGAGGAAGGT
GGGGATGACGTCAAATCATCATGCCCCTTATGAGTTGGGCTACACACGTGCTACAATGGACGGTACAAAG
GGCAGCGAAGCCGCGAGGTGGAGCCAATCCCAGAAAGCCGTTCTCAGTTCGGATTGCAGGCTGCAACTCG
CCTGCATGAAGTCGGAATCGCTAGTAATCGCAGGTCAGCATACTGCGGTGAATACGTTCCCGGGTCTTGT
ACACACCGCCCGTCACACCACGAGAGTTTGCAACACCCGAAGTCGGTGAGGTAACCGTAAGGAGCCAGCC
GCCGAAG

ECCN 20BG identified as *Leptolyngbya* strain (Accession No: MT723895)

GTCAGCAGCCGCGGTAATACGGAGGATGCAAGCGTTATCCGGAATTATTGGGCGTAAAGCGTCCGTAGGT
GGTTAATCAAGTCAGTTGTTAAAGCGTGGGGCTTAACCCCATAAAGGCGATTGAAACTGATTGACTAGAG
TTTCGTAGGGGTCAGGGGAATTCCCAGTGTAGCGGTGAAATGCGTTGATATTGGGAAGAACCCCGGTGGC
GAAAGCSCCTGACTGGGCCTGAACTGACMCTGAGGGACGAAAGCTAGGGGAGCGAAAGGGATTAGATWCC
CCTGTAGTCCTAGCTGTWAACGATGGAGWCTAGGTGTTKCCCGTATCGMCCCGGGCAGTKCCGTAGCTAA
CGCGTTAAGTWTCCCGCCTGGGGAGTACGCTCGCAAGAGTGAAACTTAAATAAATTGACGGCTGTCTCTT
ATAC

Figure C1: Sequences of isolated and identified bacterial and cyanobacterial strains.

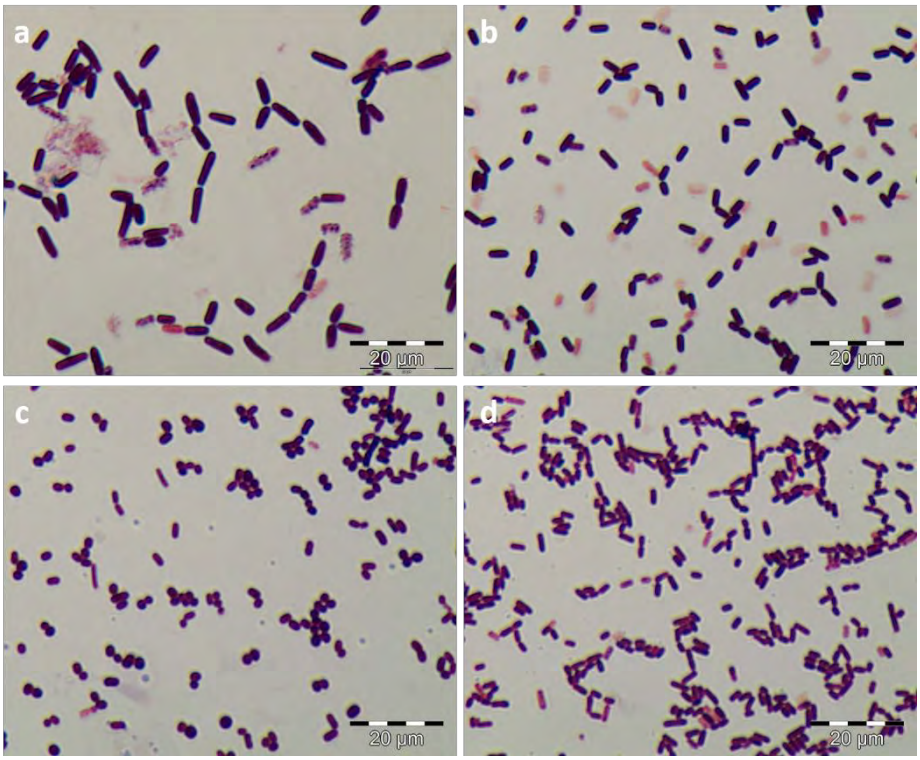

Figure C2: Gram staining images of the bacterial isolates used in the current study. Images were captured using an OLYMPUS BX50F-3 (Japan) light microscope equipped with a camera (OLYMPUS DP72). ECCN 40b (a), ECCN 41b (b), ECCN 45b (c) and ECCN 46b (d). Scale bar is 20 µm for all images.

Appendix D: Supplementary information for Chapter 7

Table D1: Performance of HRAOPs with and without mixing on MaB-floc and EPS production. Values are mean ± SE of three replicates

Parameter	Operation with paddlewheel*	Operation without paddlewheel*
MLSS (mg/L)	301.3 ± 2.4^{a}	100.0 ± 5.3^{b}
Settleability (%)	18.7 ± 2.9^{a}	66.3 ± 3.3^{b}
S-EPS (mg/L)	67.7 ± 1.5^{a}	108.7 ± 4.4^{b}
B-EPS (mg/L)	37.8 ± 3.1^{a}	74.5 ± 3.9^{b}

*Both ponds were operated in continuous mode at HRT of 2 d (pond with paddlewheel) and 4 d (pond without paddlewheel). Letters represent significant difference (*t*-test at 95% confidence level) between two samples paired (i.e. with and without paddlewheel) for each parameter.

Appendix E: Statistical analysis

Table E1: Analysis of variance (ANOVA) showing the significant difference in biomass production and settleability of ECCN 20BG after antibiotic treatment.

		SS	df	MS	F	Sig.
Biomass	Between Groups	5450.667	7	778.667	7.369	.000
	Within Groups	1690.667	16	105.667		
	Total	7141.333	23			
Settlelability	Between Groups	19566.165	7	2795.166	347.452	.000
	Within Groups	128.716	16	8.045		
	Total	19694.881	23			

Table F2: Analysis of variance (ANOVA) showing the significant difference in the flocculation activity of EPS fractions of MaB-flocs and some bacterial strains

		SS	df	MS	F	Sig.
2mg/ml	Between Groups	6466.856	8	808.357	148.525	.000
	Within Groups	97.966	18	5.443		
	Total	6564.822	26			
5mg/ml	Between Groups	8020.899	8	1002.612	153.501	.000
	Within Groups	117.569	18	6.532		
	Total	8138.468	26			
10g/ml	Between Groups	12781.294	8	1597.662	165.431	.000
	Within Groups	173.836	18	9.658		
	Total	12955.129	26			

Table F3: Table F1: Analysis of variance (ANOVA) showing the significant difference in the biochemical composition of S-EPS extracted from MaB-flocs in HRAOP over a period of one year.

		SS	df	M	F	Sig.
Carbs	Between Groups	346000.966	13	26615.459	37.368	.000
	Within Groups	19942.826	28	712.244		
	Total	365943.792	41			
Protein	Between Groups	929.977	13	71.537	12.958	.000
	Within Groups	154.582	28	5.521		
	Total	1084.558	41			
Amino N	Between Groups	430.142	13	33.088	25.304	.000
	Within Groups	36.613	28	1.308		
	Total	466.755	41			
Lipids	Between Groups	122300.324	13	9407.717	13.125	.000
	Within Groups	20070.516	28	716.804		
	Total	142370.839	41			
Phenolics	Between Groups	33892.081	13	2607.083	35.805	.000
	Within Groups	2038.801	28	72.814		
	Total	35930.882	41			
Uronic Acid	Between Groups	2913.763	13	224.136	48.032	.000
	Within Groups	130.659	28	4.666		
	Total	3044.422	41			
EPS	Between Groups	19123.768	13	1471.059	68.026	.000
	Within Groups	605.500	28	21.625		
	Total	19729.268	41			

Table F4: Analysis of variance (ANOVA) showing the significant difference in the biochemical composition of B-EPS extracted from MaB-flocs in HRAOP over a period of one year.

		SS	df	MS	F	Sig.
Carbs	Between Groups	2143187.695	13	164860.592	44.023	.000
	Within Groups	101111.767	27	3744.880		
	Total	2244299.461	40			
Protein	Between Groups	4303.344	13	331.026	11.681	.000
	Within Groups	793.495	28	28.339		
	Total	5096.840	41			
Amino N	Between Groups	1984.261	13	152.635	10.312	.000
	Within Groups	414.434	28	14.801		
	Total	2398.694	41			
Lipids	Between Groups	90416.352	13	6955.104	48.323	.000
	Within Groups	4030.059	28	143.931		
	Total	94446.411	41			
Phenolics	Between Groups	94227.173	13	7248.244	53.568	.000
	Within Groups	3788.638	28	135.309		
	Total	98015.811	41			
Uronic Aid	Between Groups	20684.636	13	1591.126	25.612	.000
	Within Groups	1739.497	28	62.125		
	Total	22424.133	41			
EPS	Between Groups	4103.138	13	315.626	14.753	.000
	Within Groups	599.051	28	21.395		
	Total	4702.190	41			

Table F5: Analysis of variance (ANOVA) showing the significant difference between the four bacterial isolates in terms of EPS production and its biochemical components

		SS	df	MS	F	Sig.
Carbs	Between Groups	4861.399	3	1620.466	11.086	.003
	Within Groups	1169.399	8	146.175		
	Total	6030.798	11			
Protein	Between Groups	563.679	3	187.893	6.313	.017
	Within Groups	238.106	8	29.763		
	Total	801.785	11			
Amino N	Between Groups	34.274	3	11.425	73.119	.000
	Within Groups	1.250	8	.156		
	Total	35.524	11			
Lipids	Between Groups	94.463	3	31.488	2.140	.173
	Within Groups	117.707	8	14.713		
	Total	212.170	11			
Humic Acid	Between Groups	3105.185	3	1035.062	7.505	.010
	Within Groups	1103.350	8	137.919		
	Total	4208.535	11			
Uronic Aid	Between Groups	313.400	3	104.467	128.883	.000
	Within Groups	6.484	8	.811		
	Total	319.884	11			
EPS	Between Groups	527676.563	3	175892.188	277.953	.000
	Within Groups	5062.500	8	632.813		
	Total	532739.063	11			